KWR 2024.090| October 2024

Modelling of OMPs removal in activated sludge and advanced oxidation systems

TKI Belissima

KWR

Bridging Science to Practice

Collaborating Partners

Report

Modelling of OMPs removal in activated sludge and advanced oxidation systems

TKI Belissima

KWR 2024.090 | October 2024

Project number
402715

Project manager
Frank Oesterholt

Client
TKI Water Technology

Authors
Maria Lousada Ferreira, Wolter Siegers, Johann Poinapen (Chapter 3), Bas Wols (Chapter 2.5 and 4) (KWR), Marlies van Hoeve (Waterschap Scheldestromen), Kaspar Groot Kormelinck (Van Remmen UV Techniek BV), Nelis De Rouck (PureBlue)

Quality Assurance
Emile Cornelissen

Sent to
TKI Belissima partners

This activity has been co-financed with PPP funding from the Top Consortia for Knowledge and Innovation (TKI) of the Ministry of Economic Affairs and Climate Change and the results are in the public domain.

Keywords

Wastewater; Organic micropollutants; Activated Sludge systems

Year of publishing
2024

More information
Dr.Eng Maria Lousada Ferreira
T 0031654295470
E Maria.Lousada.Ferreira@kwrwater.nl

PO Box 1072
3430 BB Nieuwegein
The Netherlands

T +31 (0)30 60 69 511
E info@kwrwater.nl
I www.kwrwater.nl

Summary

Wastewater treatment plants (WWTPs) play a significant role in the removal of Organic Micropollutants (OMPs). WWTPs usually rely on Conventional Activated Sludge (CAS) systems for removal of carbonaceous material and nutrients, which provides partial removal of OMPs. Additional removal of OMPs is obtained by a quaternary treatment level. However, potential synergies between CAS and quaternary technologies are often overlooked in the design phase of quaternary treatment. Furthermore possible optimization of the quaternary step, by optimizing CAS operation, is often not considered. To enable optimization studies, potentially leading to improved quality effluent discharges and cost savings, tools are required. In TKI Belissima we focused on the production of these tools, relying on modelling of the CAS and Advanced Oxidation Process (AOPs) technologies, namely UV peroxide (UV- H_2O_2) and single-stage Ozone (O_3). The core of the project was set on modelling of the water-line of WWTPs.

Initially, the TKI Belissima project focused on the removal of 11 OMPs, as proposed by the Dutch *Ministry of Infrastructure and Water management* (I&W) (RIVM, 2019), namely 4-5 methylbenzotriazole, benzotriazole, carbamazepine, clarithromycin, diclofenac, hydrochlorothiazide, metoprolol, propranolol, sotalol, sulfamethoxazole and trimethoprim. Since 2020, in the year the project started, additional OMPs were proposed as indicators (Stowa, 2021). Therefore, when possible in timing and budget, the list of researched OMPs was extended to include amisulpride, azithromycin, candesartan, citalopram, furosemide, gabapentine, irbesartan and venlafaxine, reaching a total of 19 OMPs.

The project included experimental testing at both laboratory and pilot scales, complemented with monitoring campaigns. Experimental materials (influent, activated sludge and secondary effluent) and monitoring campaigns, were provided/took place by/at the WWTP of Walcheren (Waterboard Scheldestromen). Two pilots were installed at Walcheren WWTP (from October 2023 to April 2024), namely a UV-H_2O_2 pilot (provided by Van Remmen UV Techniek) and a single-stage O_3 pilot (provided by PureBlue). The pilots were operated on an on-off basis; and a total of four measurement campaigns were conducted.

BioWin software (BioWin ASDM) was used to model the CAS system of the Walcheren WWTP. Notably, the BioWin software, which uses the Activated Sludge-Digestion Model (ASDM), does not include an OMP removal model by default (as developed by EnviroSim Associates Ltd, Canada). The TKI Bellissima project aimed to develop and integrate such a model within BioWin ASDM, utilizing data generated from the various project activities (batch tests and literature reviews). The resulting model was validated through a monitoring campaign. For AOP modelling, both UV-H_2O_2 and O_3 processes were modelled via a (photo)chemical kinetic model, describing all relevant reactions that occur in the wastewater matrix. These models were first calibrated and validated based on lab tests, followed by comparison and validation with pilot tests. Additionally, after sensitivity analysis, 4 (four) scenarios were tested, combining the CAS and AOP models, namely: 1- CAS + UV-H_2O_2 (average conditions: 600 mJ/cm^2 and 20 mg/L H_2O_2); 2- CAS + UV-H_2O_2 (high conditions: 1.200 mJ/cm^2 and 40 mg/L H_2O_2); 3- CAS + O_3 (average conditions: 5 mg/L O_3 at 10 mg/L DOC); and 4- CAS + O_3 (high conditions: 9 mg/L O_3 at 10 mg/L DOC).

The enhanced CAS ASDM model, equipped with OMP removal mechanisms and kinetic coefficients, successfully simulated the removal of the 11 tested OMPs, with results validated at full-scale. The removal efficiency of OMPs in CAS systems varies significantly, with compounds such as clarithromycin, propranolol and sulfamethoxazole showing high removal rates, while others such as carbamazepine, diclofenac, and hydrochlorothiazide exhibit poor removal. The model's simulated concentrations matched well with actual measured concentrations, demonstrating its validity and potential for optimizing OMP removal mechanisms alongside conventional pollutants.

Concerning the AOP technologies, both laboratory and pilot experiments at the WWTP, showed that UV-H_2O_2 as well as O_3 systems were able to achieve an average OMP removal of more than 80% for almost all tested compounds (19 OMPs). At the highest UV dose (about 1.000 mJ/cm^2 and higher) and higher H_2O_2 concentrations (around 40 mg/L) almost all compounds are removed by more than 90%; and at O_3 concentration of 0.6 g O_3 per g DOC most compounds are removed by 70% or more, and at O_3 concentration of 0.9 g O_3 per g DOC all but one compound are removed 80% or above. Walcheren secondary effluent has a high bromide content (on average 10 times higher than in other wastewater effluents in the Netherlands), therefore bromate formation becomes substantial at higher O_3 concentrations (10 µg/L BrO_3 or more). In practice, bromate can be better controlled by applying multiple stages and applying an ozone dose of about 0.6 g O_3 per g DOC.

The developed UV-H_2O_2 model accurately predicted both lab- and pilot-scale experiments for the 19 tested OMPs. Unfiltered secondary effluent is more difficult to predict possibly due to shadowing, light reflection or scavenging of radicals by the particles. Systems with a sand filtration step upstream to the UV-H_2O_2 provide more reliable model results. The developed O_3 model predicts accurately the lab-experiments results but is less accurate for the pilot-scale experiments, for compounds such as gabapentin, irbesartan, metoprolol and diclofenac; an explanation might be related to the ozone reactor using a side-stream ozone injection, which differs from lab conditions. As the hydrodynamics of the ozone reactor are not modelled here, spatial differences in ozone concentrations may lead to different OMP degradation compared to a perfectly mixed systems. Also the ozone model may be sensitive to the DOC composition as it was calibrated using the lab tests while the DOC composition during the pilot tests was different.

The sensitivity analysis (11 OMPs) showed that the most important secondary effluent quality parameters were DOC and NO_2-, and to a lesser extent (bi)carbonate and Br-. All these parameters scavenge OH radicals or react with ozone, so that less radicals or ozone are available for the oxidation of OMPs. Operational conditions such as O_3 concentration (for O_3 pilot); and UV dose and H_2O_2 concentration (for UV-H_2O_2 pilot) are important. The UV transmittance of the water, correlated with the DOC concentration, is incorporated in the kinetic model. The scenarios testing showed that in moderate AOP operational scenarios (600 mJ/cm^2 and 20 mg/L H_2O_2 or 5 mg/L O_3), for some OMPs with lower removal percentages (~60%) by the AOP, taking into account both CAS and AOP models can improve the degradation up to 80% . Also, for compounds such as benzotriazole and metoprolol, the removal percentage can be increased by combining both models. For other OMPs, the removal by the CAS is small, e.g. compounds that already have a high removal by the AOP or a small removal by the CAS.

In TKI Belissima, two tools were developed: 1- A CAS-post-treatment tool, integrating the removal of OMPs in CAS systems with known quaternary technologies (including other technologies than AOPs); 2- An AOP post-treatment tool, with QSAR models for UV-H_2O_2 and single-stage O_3, for secondary wastewater effluent. Tool 1 has been developed in BioWin, therefore it will require BioWin software to be able to use it. Regarding Tool 2, the models for UV-H_2O_2 and single-stage O_3, will be available through a KWR-owned tool, AquaPriori, upon request. The use of the developed models in other WWTPs will necessitate prior validation against wastewater quality parameters of the intended locations.

Table of contents

1 Introduction

1.1 Background information

Organic Micropollutants (OMPs) have been detected in all environmental compartments, air, water, and soil, with consequences for the ecosystems so far not completely understood. Emissions of OMPs to the aquatic environment, providing from discharges of municipal effluent, may reach drinking water abstraction areas, raising concerns about antimicrobial resistance (AMR) effects on human health. Eco-toxicological consequences with mutagenic effects for fish and animals, associated to the emissions of OMPs, have been measured. OMPs include a very wide variety of compounds such as pharmaceuticals, pesticides and herbicides, personal-care-products, industrial chemicals, that enter the aquatic environment by pinpoint and diffuse sources. Discharges of municipal effluent are examples of pinpoint sources, while trickling water from plantation fields or animal pastures are examples of diffuse sources. Municipal wastewater collects and concentrates pharmaceuticals and personal-care-products into a single stream, and therefore providing an unique opportunity for studying their removal in Wastewater Treatment Plants (WWTPs), preventing OMPs release into the aquatic environment. Currently, the discharge limits of municipal WWTPs in the Netherlands do not include OMPs. New discharge limits for urban wastewater, including OMP discharge restrictions, are pending on the approval of the European parliament. At present, in the terms of surface water regulations, there are no standards for single pharmaceutical compounds and only limited standards of other OMPs.

WWTPs play a significant role in the removal of OMPs, since most OMPs enter the water cycle via wastewater discharges. Existing WWTPs, mostly relying on conventional activated sludge systems (CAS) provide partial removal of OMPs. The total removal of OMPs can be increased by applying post-treatment technologies following CAS, which are also known as a quaternary treatment. Some WWTP already include a quaternary treatment step, such as activated carbon and/or ozone technologies. Additionally, there are other technologies able to provide OMP removal, such as Ultraviolet (UV) treatment and membrane-based technologies. Nevertheless, the possible synergies between CAS and quaternary treatment are often overlooked, namely: the contribution of the CAS to OMP removal is often underestimated on the quaternary technologies design phase; and possible optimization of the quaternary step, by optimizing CAS operation, is not considered. For the selection of quaternary technology, Stowa (2020) advises to consider a minimal OMP removal of 10% in the CAS, as an engineering security factor; however, the data shows 10 OMP compounds with CAS removal rates between 15 to 80%, with 9 (out of 10) compounds with removal rates above 20% (Stowa (2020)). Furthermore, to our knowledge, operational optimization of the quaternary technology by optimizing CAS operation is not yet applied.

Modelling approaches in wastewater have progressed immensely in the last decades, aiming to predict effluent discharges and improving WWTP design. Currently, the WWTPs in the Netherlands register in excel, operational conditions, flow rates and compositions of monitored streams. Based on the WWTP process flow diagrams (PFD's), the data is used on mass-balance equations, providing information about quantity and quality of other streams of the WWTP, closing the mass-balances, and allowing control of the operational conditions. However, this control system relies on regular measurements and analyses. Moreover, this control system does not include removal mechanisms, able to fully describe the processes and operations taking place at WWTP. Mechanistic or data models can fully represent processes and operations and have the added ability to, after proper validation, simulate scenarios with different operational conditions, without requiring full-scale experimental trials in an operating WWTPs. The modelling of the CAS effluent quality, without OMP removal, has been published (van Loosdrecht et al (2015)) and are included in software packages of commercial companies (van Loosdrecht et al (2015)). Quantitative structure-activity relationships (QSAR) models of effluent quality of quaternary level technologies are

currently being developed. Combined modelling of OMP removal, that is OMP effluent quality, in CAS and quaternary treatment, is, to our knowledge, still to be done.

In wastewater there are various OMPs present and not all are monitored and modelled. However, the QSAR models, which are statistical prediction models, can provide indications of the removal efficiencies of OMPs which are not measured. QSAR's are commonly applied in chemical toxicity assessments and have been previously developed at KWR for drinking water treatment technologies, such as UV-H_2O_2 (Wols et al, 2012) and nanomembrane filtration (Vries et al, 2013). The previously developed knowledge can be used to apply QSAR's to a wastewater matrix. To our knowledge QSAR's have so far not been applied to model quaternary level technology in WWTPs.

1.2 Project framework

The project TKI Belissima started in 2020 and finished in 2024. The project had a consortium of partners with the following roles:

- Technology partners: Van Remmen UV; and PureBlue water;
- End-users: Waterschap Brabantse Delta; Waterschap Scheldestromen; Waternet; Hoogheemraadschap de Stichtse Rijnlanden; and Aquafin;
- Knowledge institute: KWR water research institute.

In this project we focused on OMP removal in WWTPs, by combining the OMP removal performances of CAS and quaternary level technology. The quaternary level technologies addressed in this project are UV peroxide and Ozone, both classified as Advanced Oxidation Processes (AOP) technologies. Both technology suppliers participating in TKI Belissima supplied AOP technologies.
The core of the project consists on modelling OMP removal in WWTPs, combining removal of CAS systems with removal in AOP technologies as quaternary treatment. The project was divided into two parts, referring to industrial and fundamental research, on modelling of OMP removal in wastewater treatment (Figure 1). The industrial research focuses on the CAS system modelling and the fundamental research focuses on UV peroxide and Ozone modelling, The fundamental research part also focuses on the combined modelling of CAS and UV or AOP, given their innovative character.

Figure 1 shows how the activities in TKI Belissima were organized. Both the industrial and fundamental research started with a literature review (activity 2 and 3) focusing on OMP removal in the CAS and quaternary technology, respectively. Lab tests followed to support the modelling activities (activity 5 and 8). The CAS lab tests provided removal constants, required for the CAS modelling. The AOP lab-tests provided data for model calibration. The model of the CAS system with OMP removal included (activity 6), was validated by measurement campaigns at the WWTP of Walcheren (Waterboard Scheldestromen), where the UV peroxide (Van Remmen UV) and Ozone (PureBlue water) pilots were placed. The industrial research was complemented by a tool (activity 7), to be used as support decision on the selection of post-treatment technologies by the waterboards. Information about full-scale quaternary technology OMP removal rates, applied in activity 7, were obtained in activity 3.

The models of the UV peroxide and Ozone technologies (activity 9) were validated with results obtained at two pilots (activity 13). As aforementioned, two pilots, one from Van Remmen UV (UV peroxide) and one from PureBlue (single-stage ozone) were placed at Walcheren WWTP, Waterboard Scheldestromen. The fundamental part of the research was completed by combined modelling (activity 11). The combined modelling consisted of using the results of the validated CAS model, namely water quality results and OMP removal concentrations, as input parameters for the validated QSAR models, namely the UV peroxide and single-stage ozone pilots, obtaining the final quality of the treated effluent to be discharged into the aquatic environment (activity 11).

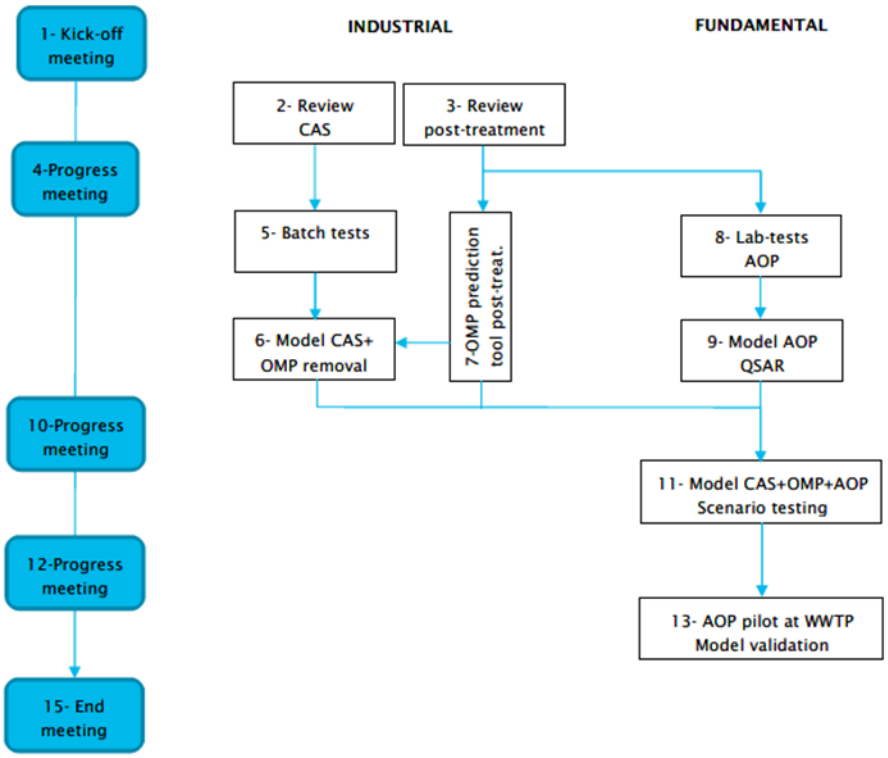

Figure 1- Schematics of the TKI Belissima activities. Additionally, Activity 14 for knowledge exchange is considered an transversal activity, taking place by default when interactions between partners are taking place.

1.3 Project objectives

The overall goal of the project is to produce tools, enabling the waterboards and technology suppliers to optimize OMP removal in WWTPs. The optimization of OMP removal can potentially lead to improved effluent quality; savings in design and operation of quaternary technology; in WWTPs with validated models, applying quaternary level technologies consisting of UV peroxide or Ozone. The tools rely on combining the modelling of both the CAS and UV peroxide/Ozone technologies.

To achieve the overall goal, the following research questions were identified:

CAS

1. Which OMPs are removed/converted in the CAS systems?
2. What are the removal mechanisms, and respective relevant parameters, of OMPs in CAS?
3. What are the design/operational values of the relevant parameters for the project partners ?
4. What are the optimal operational values of the relevant parameters to maximize OMP removal in CAS?

Quaternary Technologies (QT)

5. Which OMPs are removed in the post-treatment steps, according to the post-treatment technology?
6. What are the removal mechanisms, and respective relevant parameters, of OMPs in the post-treatment?
7. How is the post-treatment affected by the CAS effluent quality?
8. What are the optimal operational values of the relevant parameters to maximize OMP removal in post-treatment?

CAS+QT

9. What are the operational values of the relevant parameters, for CAS and post-treatment step combined, to optimize OMP removal? What are the operational savings?

QSARs modelling

10. Can the removal efficiency of other OMPs be predicted based on the properties of similar OMPs and applying the available information?
11. Which OMP properties affect post-treatment removal the most?
12. What is the removal rate of similar OMPs?

The research questions 1 to 4 were addressed in activity 2 (Figure 1), about which has been reported separately in the review report "*Fate of Organic Micropollutants in Activated sludge Systems"* was produced and published in 2022 (Lousada-Ferreira (2022), KWR 2022.090). The remaining research questions will be addressed in this report.

1.4 Organic Micropollutants (OMPs) addressed in TKI Belissima

The TKI Belissima project initially focused on the 11 OMPs proposed by the *Ministerie van Infrastructuur en Waterstaat* (I&W), namely 4-5 methylbenzotriazole, benzotriazole, carbamazepine, clarithromycin, diclofenac, hydrochlorothiazide, metoprolol, propranolol, sotalol, sulfamethoxazole and trimethoprim. The 11 OMP list was published by the *National Institute for Public Health and the Environment* (RIVM), executing the task at the request of the Ministry of Infrastructure and Water management (I&W) (RIVM 2019).

The TKI Belissima project was started in 2020 and, since then, other lists of OMPs indicators were published, namely by Stowa in the Netherlands. More recently, a new list of OMPs indicators is proposed by the EU, to be included in the new EU Urban Wastewater Directive (26-10-2022 proposal). The various lists are shown in Annex I.

Therefore, to produce more added value and when possible due to timing and budget, the experimental work and modelling activities of TKI Belissima were extended to a maximum of 19 OMPs. Therefore, adding to the 11 OMPs list proposed by RIVM, the following OMPs were also measured: gabapentin, amisulpride, azithromycin, venlafaxine, citalopram, irbesartan, candesartan and furosemide.

1.5 Report outline

The report is organized in three main chapters with project results. Chapter 2 describes all the experimental work performed in the project, used as base for the modelling of the CAS and UV peroxide/Ozone technologies. Chapter 2 refers to both lab and pilot experimental trials. Chapter 3 describes the CAS modelling, with integrated OMP removal models, per compound. Chapter 4 describes the QSAR modelling for UV peroxide and Ozone, for all OMP addressed in TKI Belissima. Chapter 4 also addresses the combined modelling of CAS and quaternary technologies, namely UV peroxide and single-stage ozone, obtaining OMP concentration results in the treated effluent of the WWTP, before being discharged into the aquatic environment. Chapter 5 lists the main conclusions of the project, and finally, chapter 6 addresses the tools produced in the TKI Belissima project, and how they can be used.

2 Experimental tests at lab- and pilot-scale

2.1 Introduction

In TKI Belissima the experimental tests included laboratory tests and pilot tests. The laboratory tests at KWR included batch-tests with activated sludge collected at Walcheren WWTP, to obtain biotransformation removal rates of the targeted OMPs, as support to the modelling activities of the activated sludge system (CAS); and advanced oxidation processes (AOP) tests, with ozone and UV, researching removal of OMP's by AOP from WWTP effluent under optimal circumstances. The lab tests for AOP modelling were performed with Mili-Q water, effluent from WWTP Walcheren and effluent from Horstermeer WWTP (Waternet). The pilot tests, aimed at removal of OMP's by AOP from WWTP effluent under practical circumstances, took place at Walcheren WWTP. The pilot tests for AOP modelling were performed on site with effluent from WWTP Walcheren. Two parallel pilots were placed at the WWTP, one with UV peroxide (UV Remmen) and another with single-stage Ozone (PureBlue). The influent of both pilots was effluent from the secondary clarifier of the WWTP. The pilot experimental period was from October 2023 to April 2024, with four sampling dates during the experimental period.

Section 2.2 to 2.3 provides general information about the Walcheren WWTP and the pilots. Section 2.4 and 2.5 describe the experimental tests performed addressing materials, methods, and results. Section 2.4 refers to lab-scale tests performed with activated sludge from WWTP Walcheren, to support the CAS modelling; section 2.5 describes the lab-scale and pilot-tests to support the AOP modelling.

2.2 Wastewater treatment plant (WWTP) of Walcheren

WWTP Walcheren is a municipal WWTP, operated by Waterboard Scheldestromen (WS). The plant is located at Ritthem and treats sewage from the area of Walcheren. It is a conventional activated sludge system (CAS) and includes a sludge digestion line, dewatering and treating sludge from local and external WWTPs.

2.2.1 Configuration and operational parameters

Table 1 provides design, operation and CAS configuration characteristics about Walcheren WWTP.

Table 1-Characteristics of the WWTP of Walcheren.

Design load [p.e.]	178.700
Max flow [m^3h^{-1}]	7.800
HRT [h]	6h at RWF, over 2 days at DWF
Influent- industrial %	20
Configuration CAS	PhoRedox
Primary clarifier	Yes
Anaerobic tank	Yes
Denitrification tank	Yes
Nitrification tank	Yes
Hydraulic regime	mixed
SRT [d]	18.5

2.2.2 Wastewater quality – influent and secondary effluent

In Figure 2 and Figure 3 the water quality of the influent and the effluent during the pilot testing period is provided for the main treatment parameters. The figures also include water quantity data for the influent. The concentrations of the different compounds in influent and effluent vary over time, following a normal behavior. The pilot testing period had quite some rain weather flow days (RWF). In general, the effect of dilution results in lower influent concentrations, which can be clearly seen in Figure 2 and Figure 3.

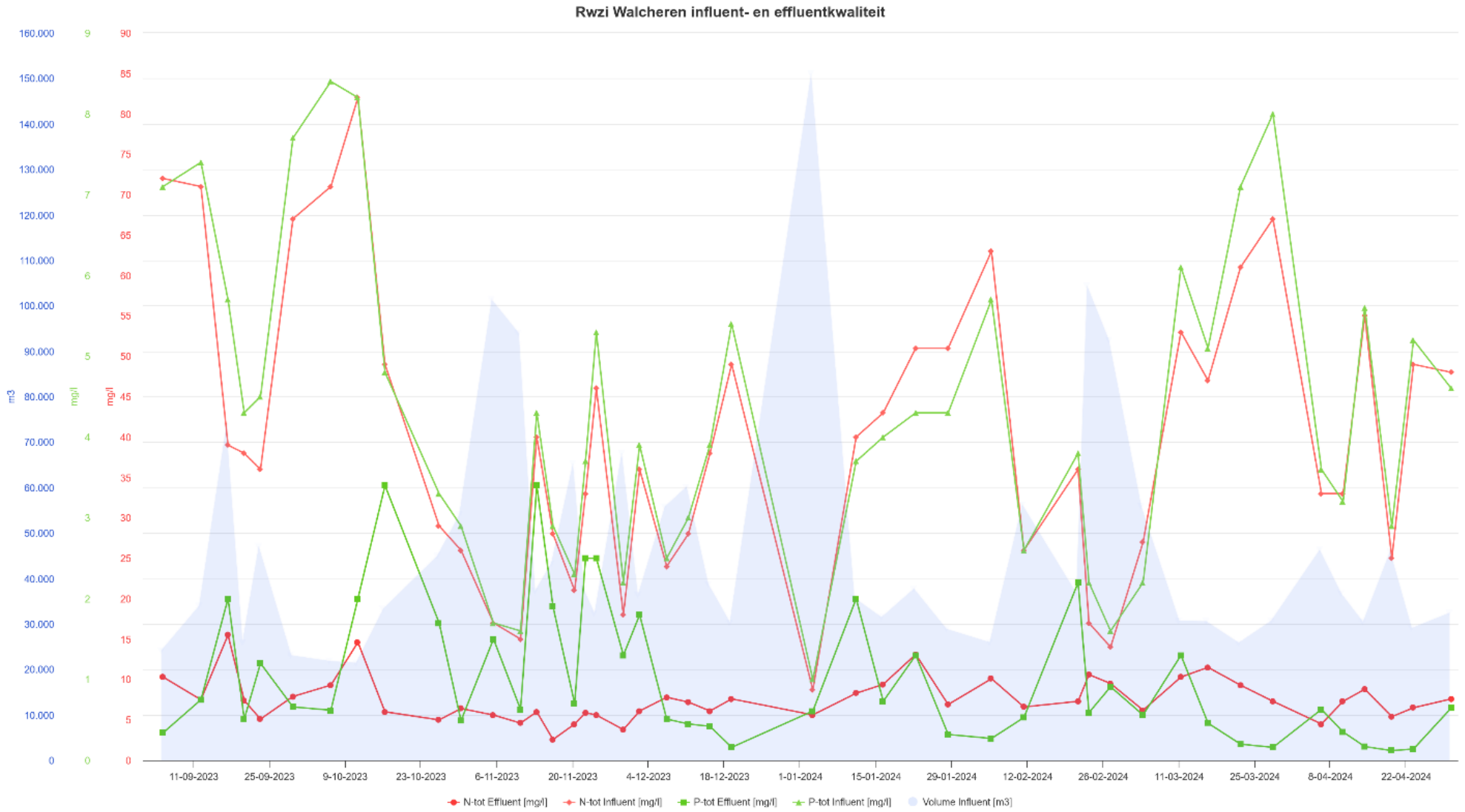

Figure 2- N-tot and P-tot in influent and effluent.

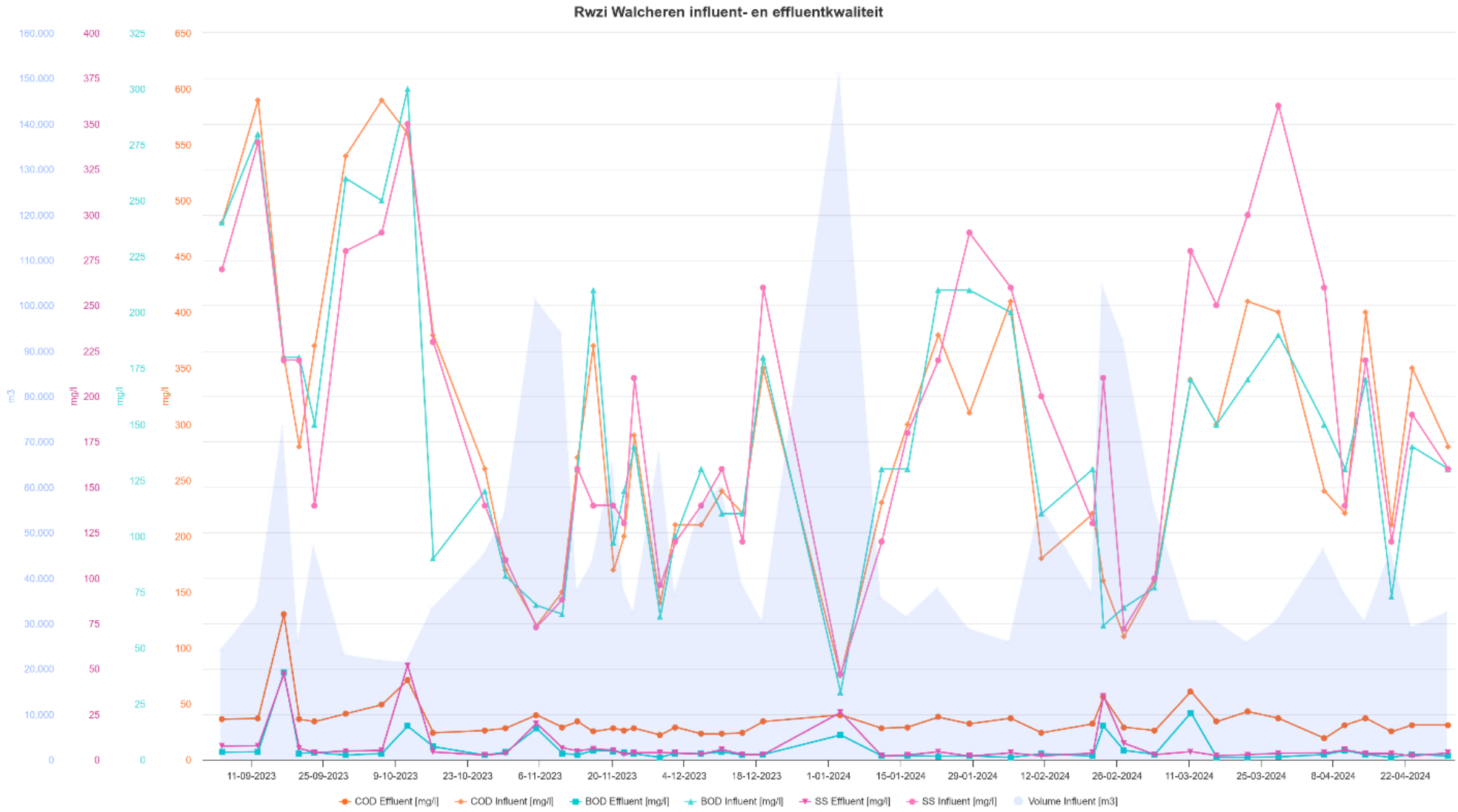

Figure 3- COD, BOD and SS in influent and effluent

2.3 Secondary effluent advanced oxidation pilot plants

2.3.1 Van Remmen UV Techniek - H_2O_2 UV pilot

An UV pilot of Van Remmen UV Techniek was available at the Walcheren WWTP, with a flow rate of approximately 2 m^3/h to remove the dosed OMP's. The pilot was operated and maintained by Van Remmen. The unit was placed close to the secondary clarifier of the WWTP; it was fed with secondary effluent from the WWTP, pumped out immediately before the secondary effluent collection tank.

A schematic overview of the UV pilot is shown in Figure 4. Figure 5 shows the UV-peroxide pilot placed at Walcheren WWTP.

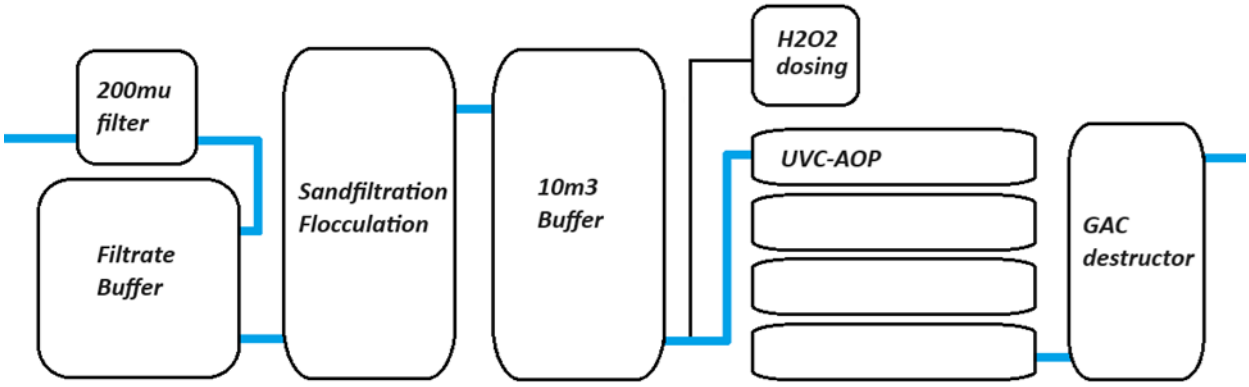

Figure 4- Schematics of the UV peroxide Van Remmen pilot.

Figure 5- Van Remmen UV pilot at Walcheren.

Due to the instant production of hydroxyl-radicals from hydrogen peroxide with the UVC lamps, the pilot was only operated on testing days (see section 2.5.3). During these sampling rounds the operational settings were kept stable, with corroborating on-site measurements like UV-absorbance and H_2O_2 concentration. A sufficient volume was flushed through the system between samples and experimental settings to avoid contamination between them. At minimum, 5 system volumes (the system volume was estimated at 40 L) were flushed between sampling points. The UVC system consisted of four individual Focus-130 Advanox UV reactors tailor made for the pilot. These reactors are flow controlled and number of lamps can be adjustable to yield the right UVC dose in combination with UV transmittance and flow. Hydrogen peroxide is injected and mixed in the full feed stream before entering the UVC reactors by a dosing pump maintaining a precise and stable hydrogen peroxide concentration as defined for the project (see Table 8). Residual hydrogen peroxide is removed with a short contact time (<2minutes) Granular Activated Carbon bed.

2.3.2 PureBlue Water O_3 pilot

A mobile ozone pilot of PureBlue Water (see Figure 6 and Figure 7) was available at the Walcheren location, with a hydraulic capacity of 7 m^3/h. The pilot was monitored, operated and maintained by PureBlue Water throughout the duration of the test period.

In Figure 6, a simplified Process Flow Diagram provides all major components of the ozone pilot. The pilot is equipped with a modular ozone generator with an adjustable ozone dosing rate between 8 and 60 g O_3/h at ozone concentrations between 100-300 g/Nm^3. The ozone is generated from pure oxygen and then injected using a self-developed ozone injection method by PureBlue Water. In comparison to conventional fine bubble diffuser columns, the self-developed injection method is suitable for smaller ozone reactors keeping the system mobile and transportable. The ozone generator is supported by a cooling system for optimal ozone production efficiency.

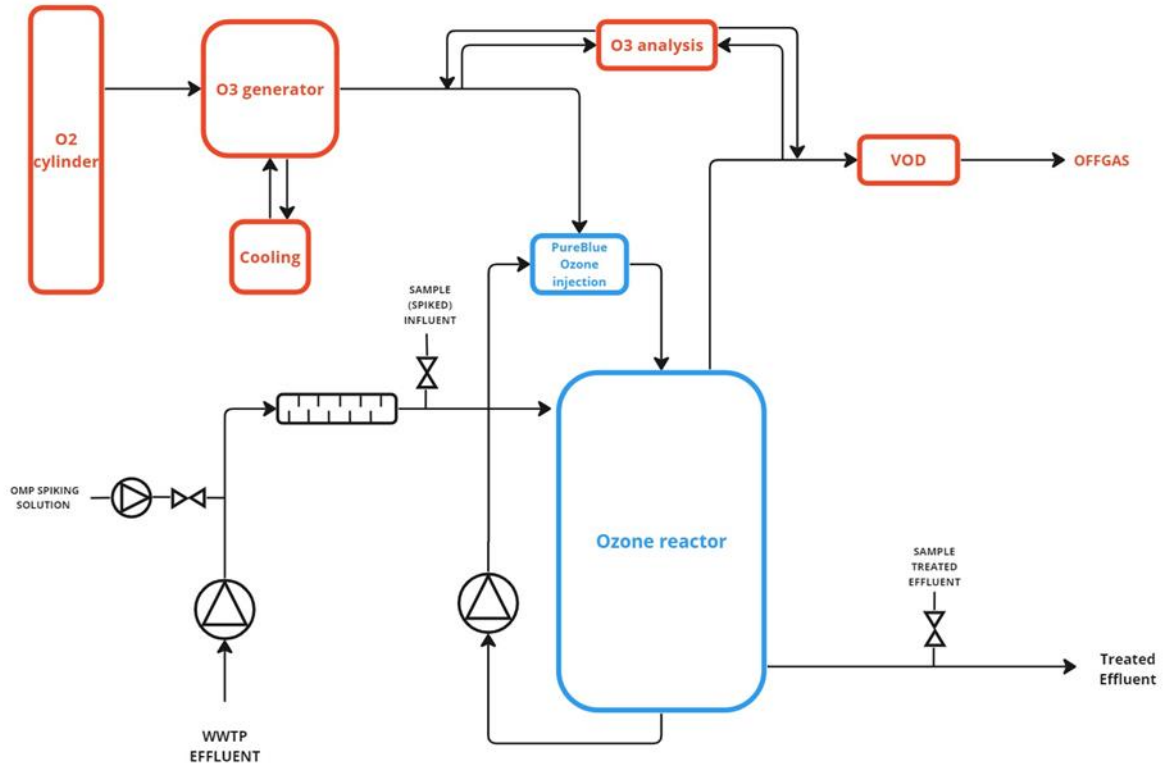

Figure 6- Process Flow Diagram of mobile ozone pilot provided by PureBlue Water.

The effluent is being pumped directly from the secondary clarifier to the ozone reactor. A dosing pump, injection nozzle and static mixer are in place in case of dosing/spiking OMP solutions to the raw effluent. The pilot is also

equipped with an ozone gas analyzer to monitor the ozone concentration in the feed gas, and to keep the remaining, undissolved ozone in the off-gas. This monitoring procedure allows for an accurate ozone transfer efficiency determination. Furthermore, the off-gas that might hold traces of ozone is further treated using a Vent Ozone Destruction module (VOD). This prevents any harmful gas emissions to the environment. Samples from the raw or spiked WWTP effluent (see 2.5.3) are taken from a sample valve upstream the ozone reactor, and the treated effluent can be sampled from a sample valve downstream the pilot. Safety measures are taken to operate the ozone pilot, including the use of a portable ambient ozone sensor and providing plenty of ventilation in the pilot unit during operation. Figure 7 shows the pilot at the WWTP of Walcheren, and at the PureBlue facilities.


a)

b)

Figure 7- PureBlue Ozone pilot at Walcheren with KWR dosing system (a); Ozone pilot at PureBlue facilities at Kapellebrug, 2022.

2.4 Lab-scale activated sludge experiments

The lab-scale activated sludge experiments were published in Martins et al, 2024 (see Annex II for the complete contents). The article provides a comprehensive description of the materials and methodologies applied, and results obtained, from CAS sludge batch tests, at different redox conditions, to obtain biotransformation rate constants for the targeted OMPs in TKI Belissima. A short description of materials applied and results obtained is provided in this section.

The biotransformation rates constants, required to model the removal of OMPs in CAS, were obtained by the experimental tests. Sorption rates, also required, were found in literature. Because biotransformation rates are a function of the redox conditions in the CAS tanks, sludge from the aerobic, anoxic and anaerobic CAS tanks of WWTP Walcheren, was transported to KWR and tested in batch tests. The results are shown in Table 2. Overall, the analyzed OMPs showed higher biotransformation rates under aerobic and anoxic conditions, however compounds such as clarithromycin bio-transformed faster under anaerobic conditions.

Table 2- Biotransformation rate constants (kbio) found for CAS in the literature, obtained results for the targeted micropollutants (In bold), and average sorption (distribution) coefficients (kd) calculated based on the values found in the literature (source Martins et al, 2024).

Micropollutants	k_{bio} [$L.gSS^{-1}.d^{-1}$]			K_d [$L.gSS^{-1}$]
	Aerobic	Anoxic	Anaerobic	
4-, 5-Methylbenzotriazole	**0,18***	**0,06***	**0,11***	0,168 (± 0,032) (n=6)

Azithromycin	<0,13[3]; 0,17[4]; 0,24[13], **1,48***		**1,27***	0,685 (±0,621) (n=3)
Benzotriazole	0,16[14]; 0,21[14]; 0,22[14]; 0,30[14]; 0,40[14]; 0,41[14]; **0,47***	0,23[14]; 0,24[14]; 0,25[14]; 0,32[14]; 0,33[14]; 0,34[14]; **0,58***	**0,14***	0,177 (± 0,081) (n=6)
Candesartan	**0,05***	**0,03***	**<0,00***	
Carbamazepine	**0,00***[13][10]; <0,01[3][4][10]; <0,10[5][7][9]; 0,10[2]; 0,70[15];	<0,03[7]; **0,07***	**<0,00***	0,123 (± 0,112) (n=20)
Clarithromycin	0,03[4]; 0,20[4]; ≤0,40[3]; 0,48[13]; <0,50[3]; **1,75***	**1,08***	**1,87***	0,395 (± 0,355) (n=7)
Diclofenac	**<0,00***; <0,02[4]; 0,02[10]; ≤0,10[3]; 0,10[9][10]; 0,30[15]; 0,40[2]; 0,50[15]; 0,70[15]; 0,80[2]; 0,90[15]; 1,20[7]	<0,04[7]; **0,07***	**<0,00***	0,087 (±0,173) (n=16)
Gabapentin	0,08[15]; 0,13[15]; 0,18[15]; **0,86***	**2,36***	**0,49***	
Hydrochlorothiazide	**0,05***	**0,09***	**<0,00***	
Irbesartan	0,10[15]; **0,33***; 0,50[15]; 0,90[15]	**0,25***	**0,45***	0,820 (±0,170) (n=2)
Metoprolol	0,13[11]; 0,20[15]; 0,35[15]; 0,40[5][15]; 0,60[15]; **0,92***	0,03[8]; **0,42***	**0,65***	0,340 (± 0,506) (n=4)
Propranolol	0,36[5]; 0,46[5]; **1,51***	**1,02***	**0,76***	0,332 (± 0,116) (n=7)
Sotalol	0,40[5][15]; 0,43[5]; **0,46***; 0,60[15]; 0,80[15]	**0,25***	**<0,00***	0,132 (± 0,197) (n=3)
Sulfamethoxazole	≤0,10[3][9]; 0,19[4]; 0,20[4]; 0,24[13]; 0,30[7][12]; 0,41[6]; **0,42***; 0,60[1][9]	0,41[6]; **2,02***	**0,42***	0,202 (± 0,149) (n=17)
Trimethoprim	0,05[10]; 0,09[10]; 0,15[7]; 0,22[4]; **0,23***; 0,24[13]; 0,65[9]	**0,12***; 0,67[8]	**1,07***	0,225 (± 0,106) (n=13)
Venlafaxine	**0,48***	**0,13***	**<0,00***	0,270 (± 0,151) (n=10)

(1) McArdell *et al.* (2003); (2) Clara *et al.* (2005); (3) Joss *et al.* (2006); (4) Abegglen *et al.* (2009); (5) Wick *et al.* (2009); (6) Plosz *et al.* (2010); (7) Suarez *et al.* (2010); (8) Xue *et al.* (2010); (9) Suarez *et al.* (2012); (10) Fernandez-Fontaina *et al.* (2013); (11) Pomies *et al.* (2013); (12) Fernandez-Fontaina *et al.* (2014); (13) Blair *et al.* (2015); (14) Mazioti *et al.* (2015); (15) Nolte *et al.* (2020); *This study (referring to Martins et al (2024)

2.5 Material and methods of advanced oxidation experiments

2.5.1 OMP Spiking solution

In Table 3 the OMP type and concentrations of the stock solution for the lab- and pilot experiments are shown. This stock solution was kept frozen at – 20 °C before every use, and diluted with Milli-Q water to achieve the desired dosing solution used for the experiments.

Table 3- Compounds and concentrations of the OMPs stock solution used for the experiments

Compounds	Concentration (mg/l) of the stock solution at the time of preparation
Gabapentine	1,00
Trimethoprim	0,98
Benzotriazole	0,99
Amisulpride	1,00
Metoprolol	1,00
Azithromycine	0,98
Tolytriazool	1,00
Venlafaxine	0,99
Sulfamethoxazool	1,00
Propranolol	1,00
Citalopram	0,99
Carbamazepine	1,00
Irbesartan	1,00
Candesartan	1,00
Diclofenac	0,99
Hydrochloorthiazide	1,01
Furosemide	0,50
Sotalol	1,00
Clarithromycin	1,00

2.5.2 Laboratory experiments

Ozone and UV lab-scale experiments

Different amounts of ozone or UV and peroxide were dosed to Walcheren WWTP effluent and ultrapure water (MilliQ water) with added OMPs, the generated data was required for the AOP model. Some experiments were

performed in combination with hydrogen peroxide. OMPs (Table 3) were dosed at about 100 times the lowest detection limit (ldl). In Table 4 the details of the laboratory experiments are given.
For the UV experiments with Milli-Q water, tertiary butyl alcohol (t-BuOH) (10 mg/L)was added as radical scavenger to mimic presence of DOC. For most experiments with Walcheren and Horstermeer WWTP effluent, the water was filtered by using 0,45 µm nitrocellulose filters. For some experiment the filtered effluents were diluted with Milli-Q water to achieve the same amount of DOC of the Milli-Q water with t-BuOH.
For the ozone experiments with Milli-Q water, it was decided later to use ethanol (5 and 50 mg/L) and buten-3-ol (1 and 5 mg/L) as a scavenger because of the high removal by ozone without scavenger in Milli-Q water. For the experiments with the Walcheren and Horstermeer WWTP effluent, the water was unfiltered.

Table 4- Details of the ozone and UV laboratory experiments

Parameter	Water type 1	Water type 2	Water type 3	Remarks
Water types	Walcheren WWTP effluent	Horstermeer WWTP effluent	Milli-Q water	Some follow-up experiments with quenching took place with Milli-Q water
Dosing of ozone (mg/L)	0-2-4-8	-	0-0.5-1-2	In duplicate
Dosing of UV (mJ/cm^2) / H_2O_2 (mg/L) / t-BuOH (mg/L)	0-100-300-600 / 10 and 20 / 0	0-100-300-600 / 20 / 0	0-100-300-600 / 10 and 20 / 8	With quenching of the hydrogen peroxide after the experiment for analysis, in duplicate
Performed analyses	OMPs	OMPs	OMPs	In duplicate
	Residual Ozone in water	-	Residual Ozone in water	After 15 min waiting time
	-	-	H_2O_2 in water	
	DOC, UV, HCO_3, pH, Turbidity, NH_4, NO_2, O-PO_4, SO_4, Br	DOC, UV, HCO_3, pH, Turbidity, NH_4, NO_2, O-PO_4, SO_4, Br	DOC, UV, Turbidity	In case of Ozone experiments only DOC, UV and BrO_3

The ozone experiments were carried out with a BMT laboratory setup, see Figure 8. This setup consists of an oxygen concentrator (Lenntech), ozone generator (BMT803 BT) , two ozone-in-gas analyzers (BMT 964) to measure the ozone concentration in the inflowing and outflowing gas of the reactor, a glass reactor (approx. 1 L), a recirculation pump and an ozone-in-gas destructor (all BMT Messtechnik GmbH, Stahnsdorf, Germany).

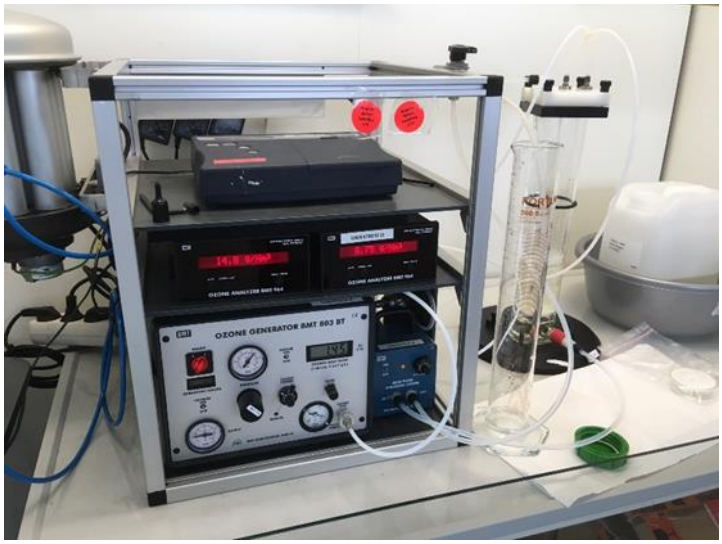

Figure 8- Picture of the BMT Ozone laboratory setup

Milli-Q water was cooled in the reactor, which was placed in crushed ice, to about 4 °C and recirculated in the reactor. Ozone gas was dosed to the recirculating Milli-Q water in the reactor at about 60 g/m^3 at a flow of 1 N-L/min for about 0,5 h until ca 20 mg/L of ozone was dissolved in the Milli-Q water. This ozonated water was dosed at the desired concentration to PE bottles containing specified volumes of Milli-Q or Walcheren WWTP effluent water with the OMPs and shaken for about 10 sec each. After about 15 min the residual ozone was measured to control the absence of ozone after the reaction.

The UV experiments were carried out in duplicate with 150 mL of water in the KWR UV collimated beam reactor using a Low Pressure (LP) lamp according to a standard procedure for measuring water samples, described in Harmsen [2004]. In Figure 9 a picture of the collimated beam setup is given. In case of MilliQ water a scavenger (t-BuOH) was added to mimic DOC. In case of the Walcheren WWTP effluent samples were UV irradiated either filtrated with 0,45 µm nitrocellulose membranes or irradiated with un-filtrated samples.

Figure 9- Picture of the collimated beam setup

2.5.3 Pilot- plant experiments at WWTP Walcheren

Sampling dates

The sampling dates on which the dosing experiments were performed were the 10th October and 22nd November of 2023; and 7th February and 17th April of 2024.

Pilot hydrogen peroxide UV (Van Remmen) and pilot single-stage Ozone (PureBlue)

At the four sampling dates(approximately every 2 months), a cocktail with OMPs was dosed (Table 3) for a few hours (depending on the residence time) at 20 times the lower analytical limit. Duplicate samples were taken at regular intervals for analysis for OMPs: after dosing and mixing, and or after the peroxide/UV step or after the single- stage ozone. The dosing unit with pump was supplied, installed and operated by KWR. The spiking solution was added just before the UV step/ozone dosing. OMPs were spiked at about 20 times the lowest detection limit (ldl). KWR took care of transport and analyses of the samples during the dosing days. N_{tot}, P_{tot} and COD were measured by Waterschap Scheldestromen (WS) or KWR; peroxide in water was measured at the location by Van Remmen; ozone in water was measured at the location by PureBlue.

The UV/peroxide dosages were set to 600/20 and 1.200/40 mJ/cm2. The desired ozone dosages were performed at zero, 0,3, 0,6 and 0,9 g O_3/ g DOC; the real applied dosages are found at the results section of this report.

Performed analysis

Table 5 summarises the analyses performed and methods applied.

Table 5- Performed analyses and methods

Analyses	Used methods
OMPs	KWR Specials 2
O_3 in water	Hach Lange LCK 310 (lab experiments) Macherey-Nagel Tube test NANOCOLOR Chlorine / Ozone 2 (0-17) https://www.mn-net.com/tube-test-nanocolor-chlorine/ozone-2-985017) (pilot experiments); Macherey-Nagel Tube test NANOCOLOR COD 160 (0-26) (https://www.mn-net.com/tube-test-nanocolor-cod-160-985026) (pilot experiments)
H_2O_2 in water	KWR LAM-048 (lab experiments) UVC Transmissie: P200 handheld transmittance meter (pilot experiments) Peroxide: Lovibond MD200 – H_2O_2 pH (pilot experiments)
pH, HCO_3^-	KWR LAM-043 and -042
UV-abs	KWR LAM-033
DOC	KWR LAM-068 (lab experiments) Macherey-Nagel COD testkit, calculation of DOC by 3/1 factor
Turbidity	KWR LAM-044
NH_4^+, NO_3^-, NO_2^-, O-PO_4^{3-} SO_4^{2-}	Aqualab Zuid AC1600
Br^-, BrO_3^-	Aqualab Zuid AC0122/AC0127
Suspended solids	Aqualab Zuid AC0225
BOD	Aqualab Zuid AC0501
N-tot, P-tot, CZV	Respectively Hach Lange LCK 238/338, LCK 349, LCK 314/514

2.6 Results and discussion of advanced oxidation experiments

2.6.1 Laboratory experiments

In Table 6 the measured water quality parameters are shown of the water used for the laboratory experiments.

Table 6- Measured water quality parameters

Water quality parameters	Milli-Q with tert-BuOH	Walcheren filtered	Horstermeer filtered
UV-absorption (E/m)	<0,3	32	29
pH (-)	6,4	7,3	7,6
DOC (mg C/L)	7,9	14	11
Bicarbonate (mg/L)	n.m.	315	210
Turbidity (FNE)	0,52	0,52	0,23
Ammonia (mg/L NH4)	n.m.	17	0,13
Nitrate (mg/L NO_3)	n.m.	52	1,4
Nitrite (mg/L NO2)	n.m.	2,4	0,087
Ortho-phosphate (mg/L P)	n.m.	0,041	< 0,02
Sulphate (mg/L SO4)	n.m.	150	27
Bromide (mg/L Br)	n.m.	1,8	0,29

n.m. means not measured.

The measured removal results of each ozone and UV laboratory experiments are given in Annex V.

In Figure 10 an overview is given of the total removal of the measured OMPs in relation to water type and amount of the ozone dosage. The figure shows that Milli-Q water (with ethanol) gave the highest removal, comparable with an ozone dosage of 4,2 mg/L with Walcheren water. While with the use of ethanol as a scavenger hardly lower removal was achieved, the use of buten-3-ol had significant effect on the removal of the OMPs. In Walcheren water, with a higher ozone dose, the removal of the OMPs also increased, as was expected. These data are used for the validation of the ozone model.

In Figure 11 an overview is given of the total removal of the measured OMPs in relation to water type and amount of the peroxide dosage. For each water type and peroxide dosage the removal at different UV doses (Annex V) were translated to a UV dose of 600 mJ/cm^2 (by fitting the concentration as exponential function of UV dose). The effect of the addition of and concentration of peroxide in Milli-Q water is very clear, showing that UV without peroxide hardly gave removal of the OMP's. Also with the Walcheren and Horstermeer water types the effect of the addition of peroxide is clear. Without peroxide the overall removal is relatively low, because only a few compounds are sensitive to direct UV photolysis (). When the water was diluted with Milli-Q, the removal also increased because the concentration of scavengers are decreased. Horstermeer water showed higher degradation results than Walcheren water, because the concentration of scavengers is lower. When unfiltered water is used, peroxide clearly had less effect on the removal of the OMPs. The measurement data are used for the validation of the UV/peroxide model.

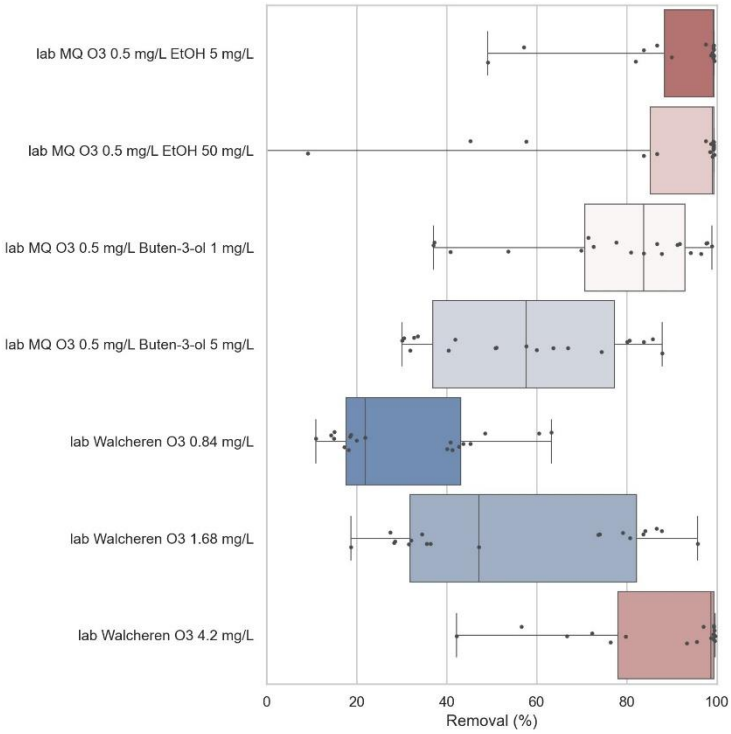

Figure 10: Overview of the removal of the measured OMPs in relation to water type and amount of ozone dosed

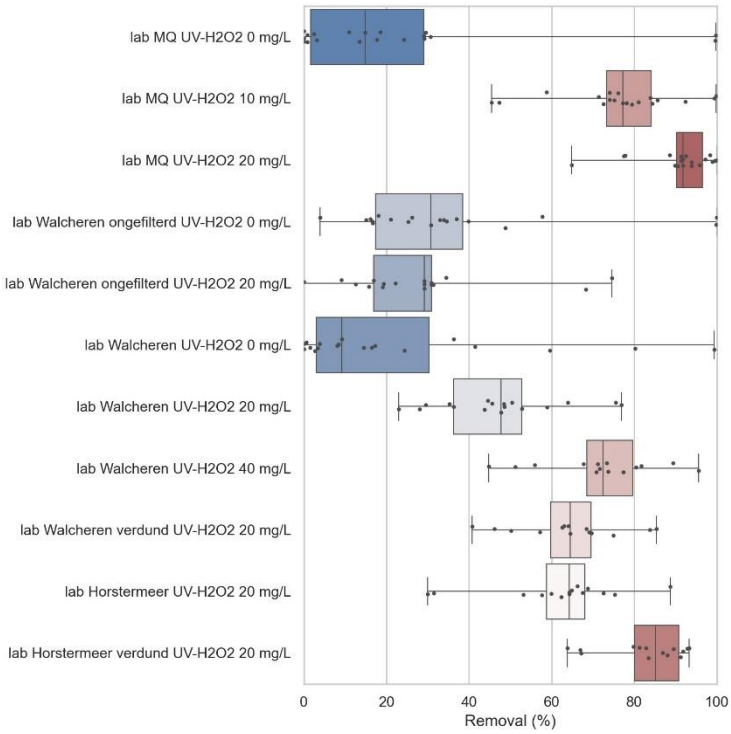

Figure 11: Overview of the removal of the measured OMPs in relation to water type and amount of peroxide dosed. Results were interpolated for a UV dose of 600 mJ/cm^2.

2.6.2 Pilot plant experiments

The water quality parameters of the wastewater effluent from Walcheren at the influent of both AOP pilots is given in Table 7 for the four rounds of testing. The water quality parameters influent of the ozone tests from the 3rd round show substantial lower values for HCO_3^-, DOC and UV-absorption, probably caused by dilution from precipitation. The ozone experiments were always performed in the afternoon. The UV/H_2O_2 experiments were performed at the same day, but in the morning and show less effect of the dilution. Some water quality parameters show a seasonal effect , like NO_3^-, NO_2^-, NH_4^+, Cl^-, Br^-, which is also visible in Figure 2 and Figure 3. In round 4, both pilots show a better effluent water quality (lower DOC, HCO_3^-, UV absorption). The UV/H_2O_2 influent in round 4 shows an even lower DOC due to the coagulation/filtration pre-treatment step that worked best in round 4 (in previous rounds it did not work very well due to issues with the filter).

Table 7: Water quality parameters measured from the influent of the AOP pilots (ozone and UV/H_2O_2).

Parameter	Round 1		Round 2		Round 3		Round 4	
	O_3	UV/H_2O_2	O_3	UV/H_2O_2	O_3	UV/H_2O_2	O_3	UV/H_2O_2
pH	7.1	7.0	7.1	7.1	7.2	7.2	7.0	6.8
HCO_3- (mg/L)	270	250	320	290	140	275	140	130
DOC (mg/L)	12.5	10	10	8	5.6	9.5	6.0	4.3
Turbidity (FNE)	2.0	2.4	1.1	1.2	4.5	2.1	1.7	1.7
UV-absorption (E/m)	36	28	30	23	16	27	18	11
Cl- (mg/L)	515	535	340	330	n.a.	n.a.	n.a.	n.a.
NO_3- (mg/L)	16.5	19	7.5	17	3.2	4.8	3.3	4.7
NO_2- (mg/L)	0.9	0.02	n.a.	n.a.	0.36	0.26	0.57	0.013
P-PO_4^{3-} (mg P/L)	1.25	0.04	2	0.6	0.12	1.3	0.08	0.02
NH_4^+ (mg/L)	2.0	1.8	2.2	0.2	4.6	13	4.3	4.0
BrO_3 (ug/L)	<0.1	n.a.	<0.1	n.a.	<0.1	n.a.	<0.1	<0.1
Br- (mg/L)	1.7	(1.7)	1.2	(1.2)	0.5	(0.5)	0.64	0.62
BZV5 (mg O_2/L)	2	1	2	1	4.5	3	3	<1
CZV (mg O_2/L)	38	45	18	21	28	32	23	22

UV pilot experiments

In the UV-peroxide pilot the secondary effluent is pre-filtered by a 200 micron screen before entering a sand filter. The original goal of the sand filter, with flocculation, was to increase the UV transmittance however due to operational constraints, the first three sampling moments were performed with the raw secondary effluent. The final sampling moment (April 2024) was performed including the sand filtration step which increased UV-transmittance from a raw value of 60,7% to 74,4% with 4 ppm powdered activated carbon (PAC) dosage. During the first three samplings moments, the sand filtration did not work optimal and the raw untreated transmittances over the UV-peroxide pilot were of : 39,9, 60,0 and 52,1%.

During the UV/H_2O_2 experiments, samples were taken from the influent and effluent of the UV/ H_2O_2 reactor. The influent sampling port is located after addition of H_2O_2. Both influent and effluent samples therefore contain H_2O_2. The H_2O_2 was not quenched, as in drinking water samples the experience is that quenching may interfere the analysis, whereas H_2O_2 has little influence on the results. However, for some OMP compounds the influent concentrations are lower than the desired concentration (see Annex IV) and because of analytical measuring ranges may even be too low to demonstrate sufficient degradation. The spiked concentration was set to 0.2 µg/L, which adds to the background concentrations of OMPs already present in the wastewater effluent. Little effect of the spiking could be found in the influent measurements (see Annex IV), in round 2 even lower concentrations were found after spiking, and for some compounds the concentration dropped to below detection limit. From round 3 onwards, therefore also influent samples without H_2O_2 were taken. In this case after the experiment, the H_2O_2 dosing was stopped, while the spiking of OMPs continued and an additional influent sample was taken. In round 3, the influent concentrations were closer to the desired spiked concentrations. Also, the difference between the influent samples with and without H_2O_2 were small for most compounds. Only at the highest H_2O_2 concentration, a few compounds (diclofenac, furosemide, propranolol, trimethoprim) show elevated influent concentrations. In round 4, again there was a larger difference in influent concentrations with and without H_2O_2. In round 3 and 4, the influent concentrations without H_2O_2 were used to calculate the removal.

For calculating removal rates, less removal can be shown for compounds with low influent concentrations. This is visualized by triangles in the removal figures (see Figure 12 and Annex VII). For compounds that have concentrations below detection limit, a value of 2/3 of the detection limit was chosen to calculate removal rates. The experimental settings of the UV reactor during the tests are given in Table 8. Depending on the UV-T of the influent water, the UV dose was set by changing the flow or number of lamps switched on. In the first 3 rounds, the UV-T was low (especially in round 1), because the pre-treatment did not work properly. This was improved in round 4. The removal percentages during UV/ H_2O_2 are shown in Figure 12 for round 4 and Annex VII for round 1-3, and a summary of all rounds is shown in Figure 13. The test with the higher UV dose and peroxide concentrations (1.300-1.400 mJ/cm2 and 40-50 mg/L H_2O_2) significantly showed the highest removal percentages: for most compounds 90% and higher. The moderate setting (500-600 mJ/cm2 and 20-25 mg/L H_2O_2) showed removal percentages between 60-80%, with a few exceptions that showed lower degradations (between 20-50%): Azithromycin, Chlarithromycin and Gabapentin. The increase in UV-T (Table 8) also confirms the effect of the UV dose and H_2O_2 concentration. In round 1 and 2 (Annex VII), a few compounds could not be measured accurately, as the influent concentration was too low (e.g. Furosemide, Trimethoprim, Propanolol, Carbemazepine). In round 2, the non-spiked experiment showed more accurate (meaning less compounds with too low influent concentrations) degradation results. In round 3, for all 19 compounds accurate removal results were obtained, because the influent samples without H_2O_2 were taken to calculate the removal. Except for azithromycin and clarithromycin, there is no significant difference in removal percentages between spiking and non-spiking of OMPs. For the tests in round 4 (Figure 12), also at the lower UV setting (674 mJ/cm^2 and 21 mg/L H_2O_2) high degradations are observed (above 90% for most of the compounds, and above 80% for Azithromycin, Chlarithromycin and Gabapentin). The better performance of the UV/H_2O_2 process in round 4 can be attributed to the better pre-treatment by the coagulation/sand filtration. In the previous experiments, the filtration did not work properly, but in this round the UV-T and DOC were improved so that less competition for OH radicals is present and higher degradation could be

obtained. At the higher UV setting (1.370 mJ/cm^2 and 44 mg/L H_2O_2) all compounds were removed with 90-95% or higher.

Table 8: Settings of the UV/H_2O_2 experiments for the four rounds. H_2O_2 concentrations are given before the UV reactor.

Setting (intended UV dose and H_2O_2 dose)	Flow (L/h)	# lamps	Actual UV dose (mJ/cm^2)	Actual H_2O_2 (mg/L)	UV-T (%)	
					Before	After
Round 1, 600-20 (no spike)	900	4	478	19	36.9	41
Round 1, 600-20	900	4	474	19	36.4	39.9
Round 1, 1200-40	450	4	960	38	38.3	44.2
Round 2, 600-20 (no spike)	540	2	645	25	56	61.7
Round 2, 600-20	540	2	659	25	56.1	62.7
Round 2, 1200-40	540	4	1319	54	54.1	69.5
Round 3, 600-20 (no spike)	900	4	571	21	47.4	50.8
Round 3, 600-20	900	4	547	20	49.8	53.8
Round 3, 1200-40	470	4	1452	36	51.6	61.8
Round 4, 600-20 (no spike)	770	2	674	26	70.4	77.0
Round 4, 600-20	770	2	674	21	71.1	76.9
Round 4, 1200-40	770	4	1370	44	69.0	81.7

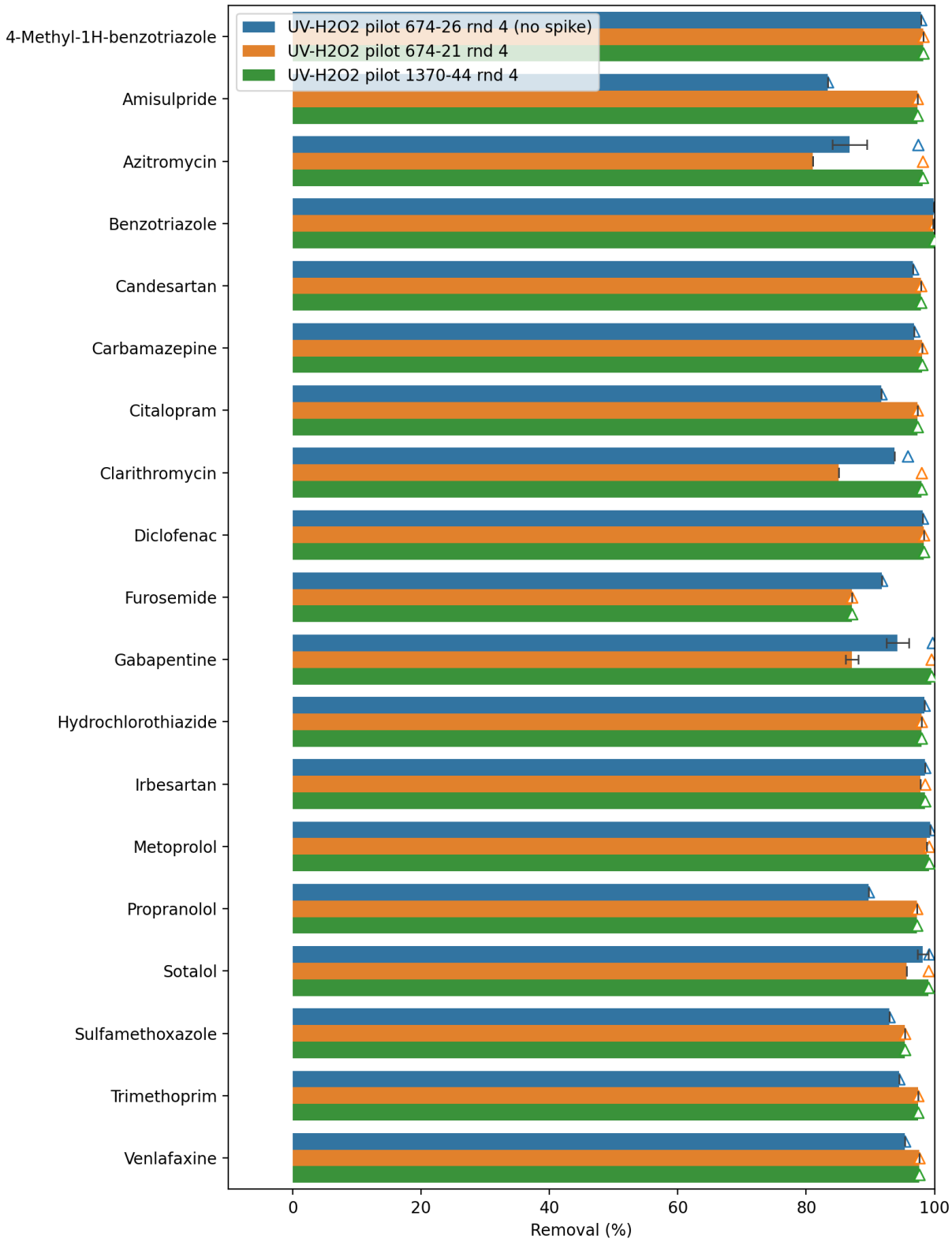

Figure 12: Removal percentages of micropollutants during UV/H_2O_2 treatment for round 4. The first number in the legend represents the UV dose (mJ/cm^2), the second number represents the H_2O_2 concentration (mg/L). The triangles show the maximum degradation that can be demonstrated given the influent concentration and limit of detection. The error range is calculated from the standard deviation of the duplicate samples.

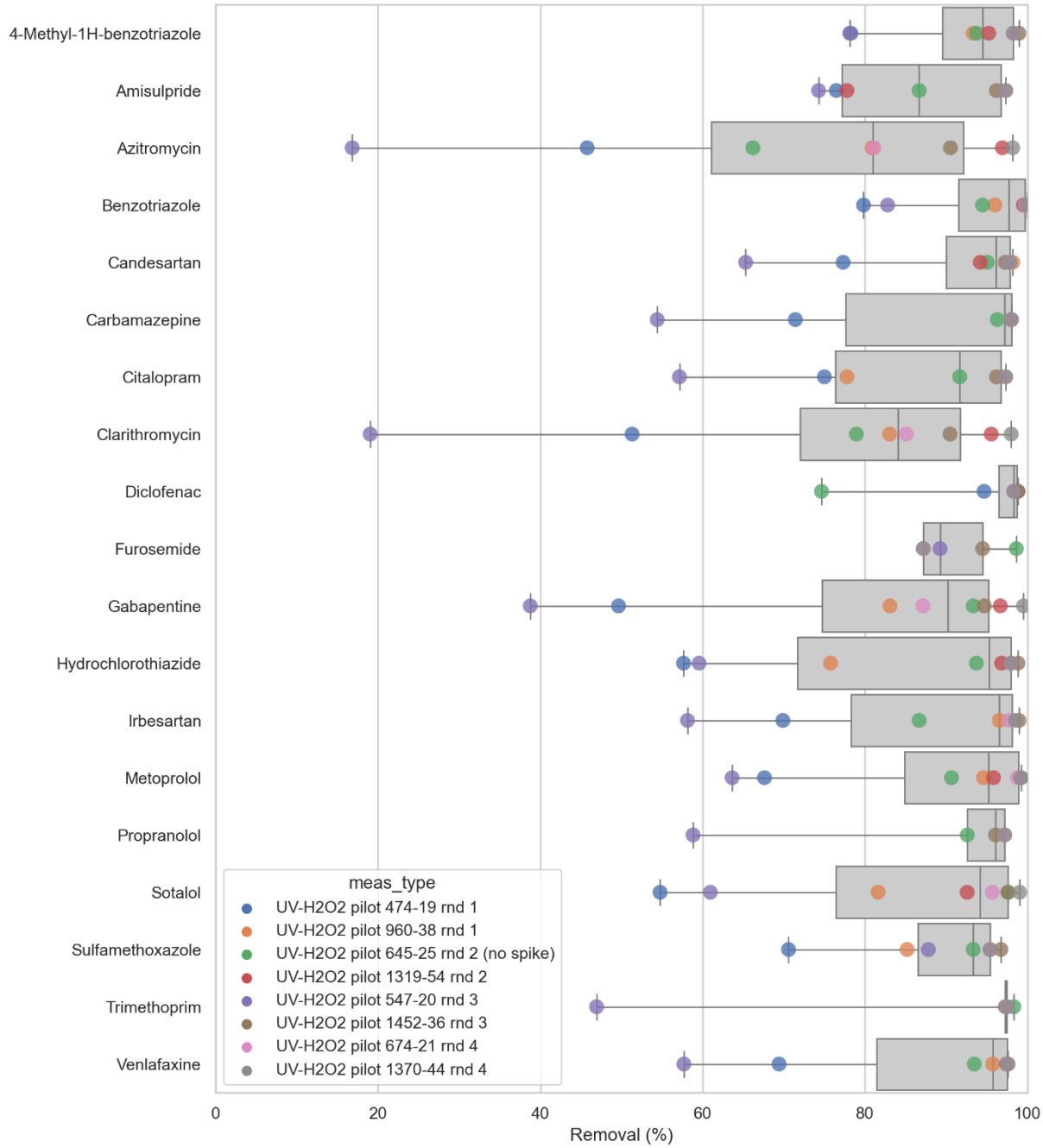

Figure 13: Summary of UV/H_2O_2 pilots, removal percentage for each OMP under different conditions during the four rounds of tests. Results are only shown if more than 75% removal can be demonstrated calculated from influent concentrations and limit of detection.

Ozone pilot experiments

Next to UV/H_2O_2, experiments were conducted in the ozone pilot. The influent concentrations of the OMPs are given in Annex VI. Here the influent concentrations for all OMPs remained stable and the increase of 0.2 µg/L from the spiking can be clearly seen in the results. For round 3, there is a larger error bar on the influent concentrations, caused by differences in the duplicates due to the rainfall during and before the experiments. In round 4 the concentration of benzotriazole in the background is much higher, up to 16 µg/L (compared to between 1 and 4 µg/L in the other rounds).

The experimental settings of the ozone reactor are given in Table 9. In round 1 and 2 the highest ozone dosages (O_3/DOC ratio of 0.9) could not be reached in all cases mostly because of technical issues in the field. The ozone dose was set according to an onsite measurement of DOC, which could sometimes differ from the laboratory measurements of DOC (that was done afterwards). The O_3/DOC dose was calculated according to the DOC measurement of the laboratory. Therefore, in round 3 and 4, where the laboratory DOC results were almost 2 times lower than the on-site measured results, the actual O_3/DOC ratio was higher than expected.

Table 9: Settings of the ozone pilot experiments for the four rounds. Ozone concentrations are given before the ozone reactor, DO and BrO_3 are given after the ozone reactor.

Setting	O_3 (mg/L)	O_3/DOC	DO (mg/L)	T (°C)	BrO_3 (µg/L)
Round 1, influent	0	0	4.4	19.7	<0.1
Round 1, 0.6 O_3/DOC (no spike)	6.8	0.52	12.8	19.6	8.8
Round 1, 0.3 O_3/DOC	3.4	0.26	10.2	20.3	<0.1
Round 1, 0.6 O_3/DOC	6.8	0.53	13.2	21.2	6.4
Round 1, 0.9 O_3/DOC	8.6	0.66	15.9	22.2	21
Round 2, influent	0	0	5.1	12.3	<0.1
Round 2, 0.6 O_3/DOC (no spike)	5.5	0.55	18.0	12.7	18
Round 2, 0.3 O_3/DOC	3.0	0.3	14.0	14.3	<0.1
Round 2, 0.6 O_3/DOC	5.8	0.58	17.6	13.6	18
Round 2, 0.9 O_3/DOC	7.4	0.74	19.7	13.7	n.g.
Round 3, influent	0	0	5.5	10.7	<0.1
Round 3, 0.6 O_3/DOC (no spike)	6.1	1.10	16.5	10.8	10
Round 3, 0.3 O_3/DOC	3.1	0.56	14.1	10.7	4.6
Round 3, 0.6 O_3/DOC	5.8	1.04	16.5	10.5	11
Round 3, 0.8 O_3/DOC	5.5	0.98	16.9	10.1	15
Round 4, influent	0	0	5.7	12.8	<0.1
Round 4, 0.6 O_3/DOC (no spike)	5.4	0.90	17.6	13.6	14
Round 4, 0.3 O_3/DOC	3.1	0.52	11.9	13.5	1.5
Round 4, 0.6 O_3/DOC	5.5	0.92	17.4	13.2	15
Round 4, 0.9 O_3/DOC	7.9	1.32	20.5	13.8	26

The results of the OMP degradation by ozone are shown in Figure 14 for round 4 and in Annex VII for round 1-3. A higher ozone dosage clearly results in a higher degradation of OMPs. At the highest ozone dose in round 3 and 4 (Annex VII and Figure 14), most of the OMPs can be degraded around 90% and more, except for Gabapentin, Irbesartan and Benzotriazole because these compounds slowly react with ozone. At a moderate ozone dosage of 0.5-0.6*DOC, a large portion of OMPs can be degraded 70% and more, except for Benzotriazole, 4-Methyl-1H-Benzotriazole and Gabapentin. At the lowest ozone dosage of 0.3*DOC, most of the compounds are removed between 40% and 50%.

Bromate formation becomes high at the highest ozone/DOC dosage varying from 10 to 26 µg/L. At the lowest ozone dosage (0.3*DOC), bromate formation remains low (<0.1 µg/L). As Walcheren is located close to the sea, the bromide concentration is high compared to other wastewater treatment locations, resulting in high bromate concentrations. In practice, bromate can be controlled by using multiple stages of lower ozone dosages.

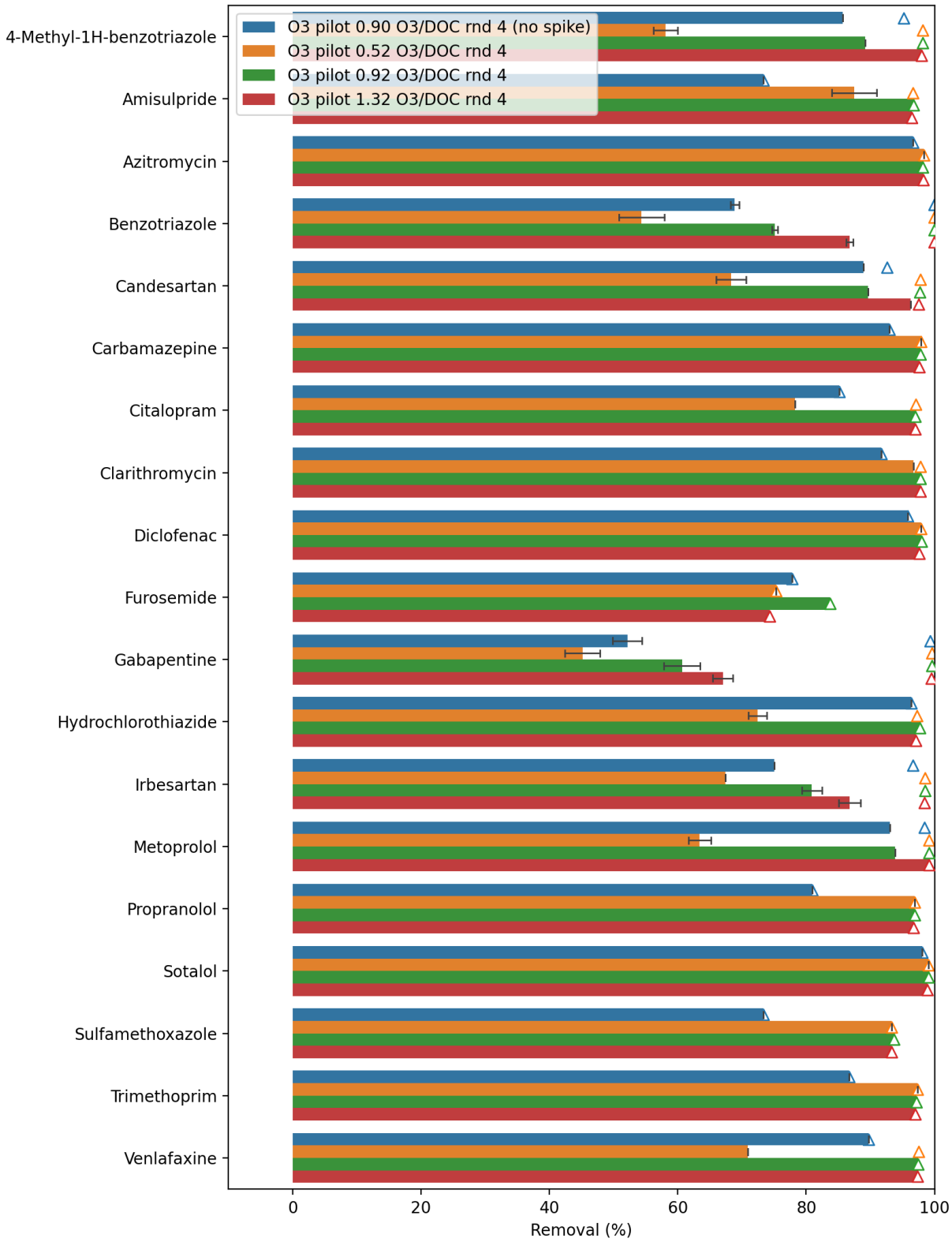

Figure 14: Removal percentages of micropollutants during ozone treatment for round 4. The triangles show the maximum degradation that can be demonstrated given the influent concentration and limit of detection. The error range is calculated from the standard deviation of the duplicate samples.

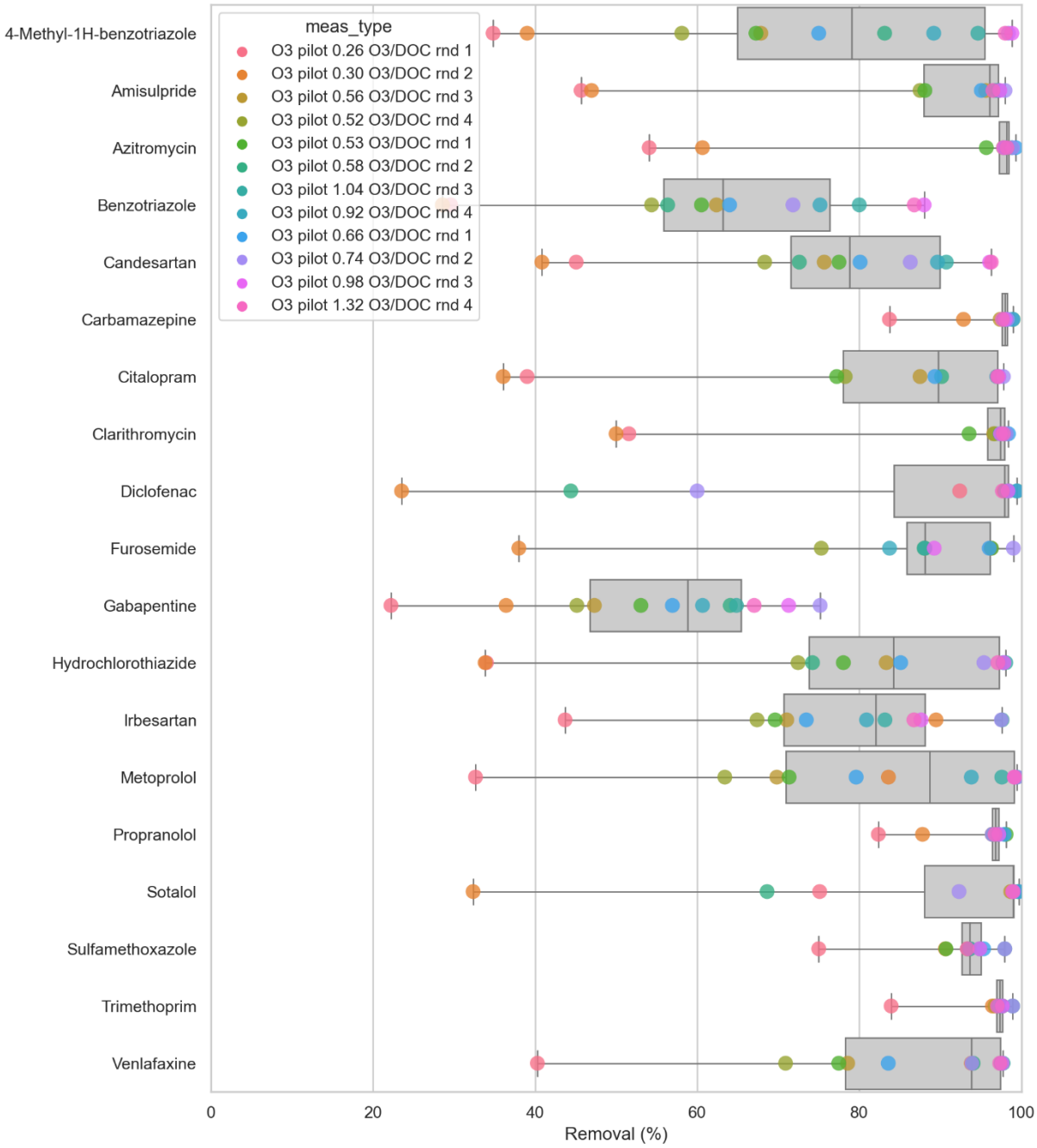

Figure 15: Summary of ozone pilots, removal percentage for each OMP under different conditions during the four rounds of tests. Results are only shown if more than 75% removal can be demonstrated calculated from influent concentrations and limit of detection.

2.6.3 Synthesis

Figure 16 summarizes and compares the degradation results of all conditions and OMPs in both pilots. The effect of operating conditions (UV dose, H_2O_2 and O_3 concentration) can be clearly seen: if more energy (UV dose) or oxidants (H_2O_2 or O_3) are supplied, a higher removal will be obtained. For the higher UV dose (at around 1.000 mJ/cm^2 and higher) and higher H_2O_2 concentration, almost all compounds are degraded more than 80%. For O_3, at a O_3 concentration of 0.6 of the DOC, most compounds are removed by 70% or more, and at a O_3 concentration of 0.9 of the DOC and higher, all but one compounds are removed 80% or higher. However, bromate formation will be substantial (more than 10 µg/L). This can be explained by the high bromide concentrations in the effluent (~10

times higher than average in Dutch wastewater effluents). Also, measures could be taken to reduce bromate formation, for example applying multiple stages of low ozone dosages.

There are differences between the experimental rounds. For O_3, the differences can largely be explained by the differences in DOC and therefore O_3/DOC ratio. For UV/H_2O_2, the degradations at moderate UV settings (500-600 mJ/cm^2 and 20 mg/L) show variations between the different rounds, which can only partly be explained by differences in operating conditions. Also, differences in water quality (UVT, DOC, etc.) may cause differences in degradation results. Especially lowering DOC concentrations will result in higher removal rates for both AOPs (a pre-treatment step such as a biological sand filter may also degrade some of the OMPs). In the modelling of the AOP processes, these water quality parameters will be taken into account.

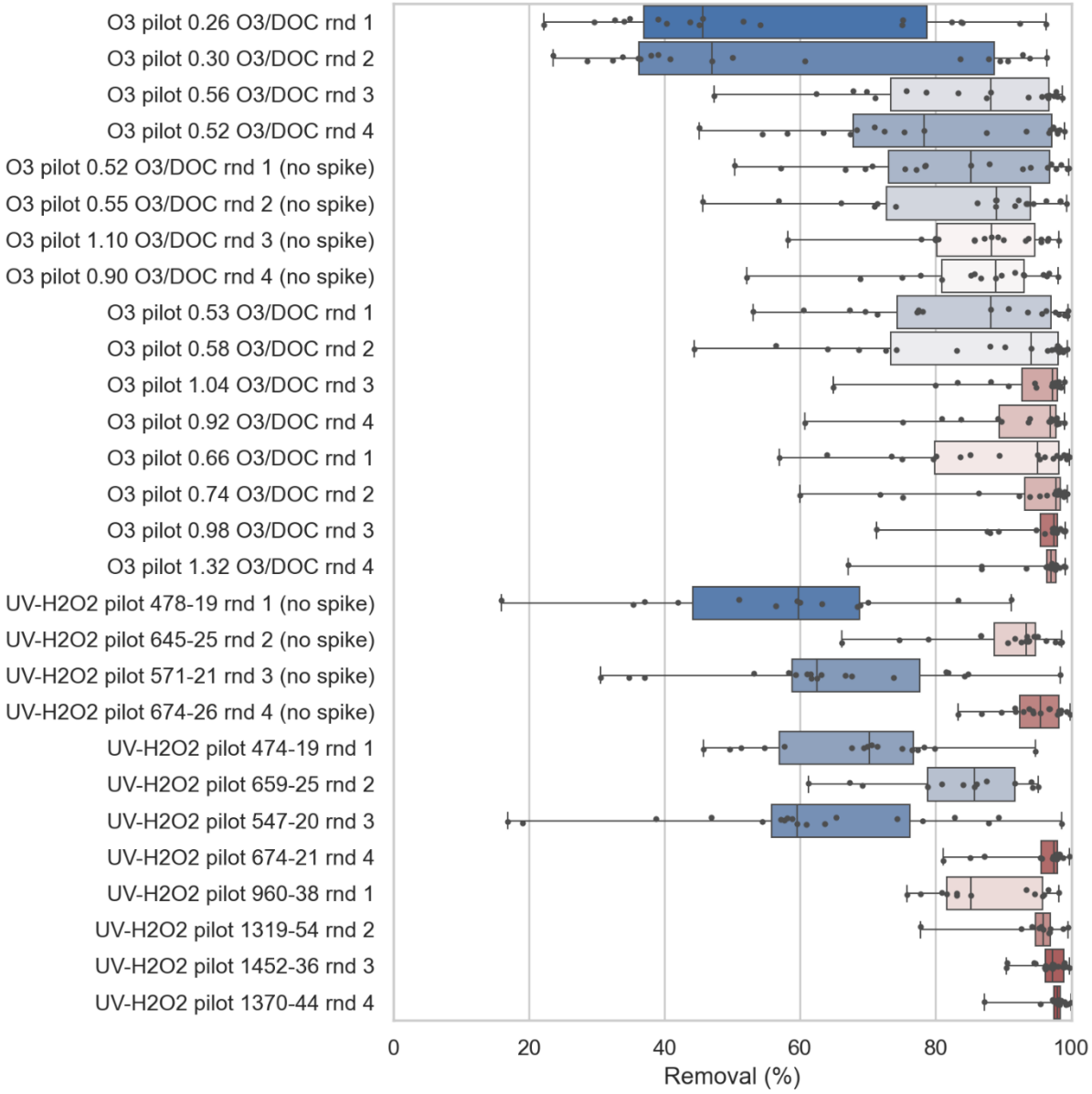

Figure 16: Removal percentages for different conditions at O_3 pilot and UV/ H_2O_2 pilot. The boxplot shows the minimum, first quartile, median, third quartile and maximum degradation for the 19 OMPs. The black dots show the individual degradation of each OMP. Results are only shown if more than 75% removal can be demonstrated calculated from influent concentrations and limit of detection. The colors show the average removal per experiment (blue to red: lower to higher removal).

3 Activated sludge modelling

3.1 Introduction

Activated sludge systems are among the most commonly used biological treatment processes for removing organic matter and nutrients from wastewater. Activated sludge relies on biological activity to remove carbonaceous material, nitrogen and phosphorus, depending on the design configuration and applied operational parameters. The removal efficiency of OMPs in these systems can vary widely depending on factors such as compound properties, system configuration, and operating conditions.

Given the complexity of micropollutant behavior in activated sludge systems, mathematical modelling has emerged as a valuable tool for understanding and predicting their fate within these treatment systems. Modelling approaches can help elucidate the underlying mechanisms governing OMP removal processes, optimize system performance, and design treatment strategies to enhance OMP removal efficiency. Many of these mechanisms are not well understood. Accordingly, there is a need to extend the activated sludge models to include OMP mechanisms, namely biotransformation, sorption, desorption and retransformation processes.

Some attempts have been made to develop mathematical models to describe OMP behavior in activated sludge systems, ranging from simple empirical models to more complex mechanistic models based on mass balance equations and reaction kinetics. However, only a limited number OMPs have been thoroughly modelled in these systems. Significant gaps remain in our understanding and data regarding the biokinetics of many OMPs across various mechanisms.

3.2 OMP removal processes in Activated Sludge systems

In activated sludge systems, the removal of organic micropollutants (OMPs) involves four key processes (Plosz et al., 2012):

1. Biotransformation (Biodegradation):

This process involves the metabolic conversion of OMPs by microorganisms present in the activated sludge. The microorganisms either completely mineralize the OMPs into carbon dioxide, water, and biomass or transform them into intermediate products that may be further degraded. Biotransformation rates (K_{bio}) can vary depending on the chemical structure of the OMPs and the environmental conditions within the treatment system, such as oxygen levels, temperature, and nutrient availability.

2. Sorption (Adsorption and Absorption):

Sorption refers to the attachment of OMPs to sludge particle surfaces (adsorption) or their incorporation into the sludge matrix itself (absorption). These process are influenced by the hydrophobicity and charge of the OMPs, as well as the characteristics of the sludge, including its composition and surface area. The solid-liquid partition coefficient (K_d) is a crucial parameter that quantifies the extent of sorption.

3. Desorption:

Desorption is the reverse process of sorption, where OMPs detach from sludge particle surfaces or internal structure and re-enter the aqueous phase. This can occur due to changes in environmental conditions, such as pH, temperature, ionic strength, hydraulic shear, or the presence of competing substances. Desorption is important

because it can affect the bioavailability of OMPs for biodegradation and their overall removal efficiency. The desorption rate constant (K_{des}) helps in understanding and modelling this process.

4. Chemical Transformation and Retransformation (Abiotic Processes):

Besides biotransformation, OMPs can undergo chemical transformations through abiotic processes such as hydrolysis, photolysis, and redox reactions. These processes can either directly degrade OMPs or transform them into other compounds that may or may not be more easily biodegradable. In some cases, retransformation can occur, where intermediate transformation products revert to the parent compounds or other related substances. The retransformation rate constant (q_C) captures the dynamics of these conversions.

Each of the above mentioned processes plays a crucial role in the overall removal of OMPs in activated sludge systems, and understanding their interactions and relative contributions is essential for optimizing wastewater treatment plant performance. Advanced modelling approaches as developed in this study integrate these processes to simulate the fate of specific OMPs and support the design and operation of more effective treatment systems.

3.2.1 ASDM Model

Activated sludge models (ASMs) are widely used for process modelling (Sin & Al, 2021). The objectives of ASMs are to simulate and predict the performance of activated sludge systems in wastewater treatment, optimize biological processes for contaminant removal, and assist in the design and scaling of treatment plants. They aim to improve operational efficiency, ensure regulatory compliance, evaluate different operational strategies, support process control decisions, and facilitate the development of advanced treatment technologies. The ASMs have evolved over the years with the inclusion of specific wastewater treatment unit process models, thereby leading to newer versions, from ASM1 evolving to Activated Sludge Digestion Model (ASDM).

In this investigation, the simulation software BioWin was used to modelling the removal of OMPs in activated sludge systems. BioWin comprises a general Activated Sludge/Anaerobic Digestion model (ASDM) which is divided into six main parts that cover the main processes in wastewater treatment: activated sludge modelling, anaerobic digestion model, settling models, chemical precipitation modelling, pH modelling, and an aeration and gas transfer model (Elawwad et al., 2019).

The OMP removal mechanisms, with their corresponding process rates, were added to the ASDM model to create an uncalibrated model. Subsequently, the kinetic and stoichiometric coefficients were obtained from the batch experiments conducted in this project supplemented with values extracted from the literature (Plósz et al. ,2012) to develop and calibrate the OMP model in this project (see Annex IV).

3.2.2 Model development, implementation and parameter values

In the TKI Belissima project, the BioWin software was used to model the CAS system of WWTP Walcheren. The CAS configuration at Walcheren, comprises an anaerobic, anoxic and aerobic process reactors. In Biowin ASDM, no OMP removal model is included by the software developer (EnviroSim Associates Ltd, Canada) due to the lack of sufficient and validated kinetic parameters and removal mechanisms with regard to OMPs. As mentioned before, there is still a lack of understanding and data regarding the biokinetics of many OMPs across various mechanisms to develop a robust OMP model. This project aimed to develop and integrate such a model in BioWin ASDM, utilizing data generated from the various project activities (batch tests and literature review).

In developing the OMP model in this project, the removal mechanisms of the 11 target OMPs were integrated into the ASM section of the Biowin ASDM. The structured approach of the Peterson Matrix was used in the development of the model for the 11 OMPs. The Petersen matrix is a pivotal tool in modelling activated sludge

systems, and is a comprehensive framework that integrates stoichiometric coefficients and kinetic rates to describe and quantify the biochemical transformations and reactions occurring within the wastewater treatment processes. Petersen matrices are particularly useful for complex models with several processes and variables and are used a lot in literature (Gujer and Henze, 1991). The biotransformation rates (K_{bio}) vary with redox conditions of the CAS tanks, sludge from the aerobic, anoxic and anaerobic CAS tanks of WWTP Walcheren. Accordingly, batch tests were conducted to determine these rates as well as sorption coefficients for each of the 11 targeted OMPs. These were supplemented with coefficient values for other removal mechanisms found in the literature as reported by Martins et al. (2024) as summarized in Table 2. The biotransformation and sorption values used in the ASDM model development for OMP removal mechanisms are listed in Table 17 below. Retransformation (to parent compound) rates were available for only 2 OMPs, namely Diclofenac and Carbamazepine, obtained from Plósz et al. (2012), and hence retransformation modelling was not possible for the remaining 9 OMPs. This is an area of future work that needs to be conducted.

Table 10: Biotransformation rates and sorption coefficients used in the ASDM OMP model development.

		Biotransformation rate, Kbio (L/gSS/d)			Sorption coefficient, Kd (L/gSS)
No.	Micropollutants	Anaerobic	Anoxic	Aerobic	All
1	4- and 5-methylbenzotriazole	0.11	0.06	0.18	0.168
2	Benzotriazole	0.14	0.58	0.47	0.177
3	Carbamazepine	0.00	0.07	0.00	0.123
4	Clarithromycin	1.87	1.08	1.75	0.395
5	Diclofenac	0.00	0.07	0.00	0.087
6	Hydrochlorothiazide	0.00	0.09	0.05	N/A
7	Metoprolol	0.65	0.42	0.92	0.34
8	Propranolol	0.76	1.02	1.51	0.332
9	Sotalol	0.00	0.25	0.46	0.132
10	Sulfamethoxazole	0.42	2.02	0.42	0.202
11	Trimethoprim	1.07	0.12	0.23	0.225

The Petersen Matrix describing the model structures of the 11 OMPs added to ASDM are shown in Table 11 .

Table 11:Petersen Matrix describing the model structures of the 11 OMPs added to ASDM in BioWin.

Compound (Micropollutant)	***Process rate description***	***Micropollutant and its metabolite components***			***Process rate***
		UD1 (C_{LI})	***UD2 (C_{CJ})***	***UD3 (C_{SL})***	
Sulfamethoxazole	***Aerobic processes***				
	Biodegradation of OMP	*1*			$K_{Bio,Ox} * UD1 * \frac{K_S \eta_{Bio}}{(K_S \eta_{Bio} + S_S)} * \frac{S_O}{(K_O + S_O)} * Z_B$
	Parent compound transformation		*1*		$K_{Dec,Ox} * UD2 * \frac{K_S \eta_{Dec}}{(K_S \eta_{Dec} + S_S)} * \frac{S_O}{(K_O + S_O)} * Z_B$
	Sorption	*1*			$K_{Des} * K_{D,Ox} * UD1 * \frac{S_O}{(K_O + S_O)} * Xss$
	Anoxic processes				
	Biodegradation of OMP	*1*			$K_{Bio,Ax} * UD1 * \frac{K_S \eta_{Bio}}{(K_S \eta_{Bio} + S_S)} * \frac{K_O}{(K_O + S_O)} * Z_B$
	Parent compound transformation		*1*		$K_{Dec,Ax} * UD2 * \frac{K_S \eta_{Dec}}{(K_S \eta_{Dec} + S_S)} * \frac{K_O}{(K_O + S_O)} * Z_B$
	Sorption	*1*			$K_{Des} * K_{D,Ax} * UD1 * \frac{K_O}{(K_O + S_O)} * Xss$
	Anaerobic process				
	Biodegradation of OMP	*1*			$K_{Bio,An} * UD1 * \frac{K_S}{(K_S + S_S)} * \frac{K_O}{(K_O + S_O)} * Z_B$
	Sorption	*1*			$K_{Des} * K_{D,An} * UD1 * \frac{K_O}{(K_O + S_O)} * Xss$
Diclofenac and Carbamazepine	***Aerobic processes***				
	Biodegradation of OMP	*1*			$q_{C,Ox} * \frac{S_S}{(K_S + S_S)} * K_{Bio,Ox} * UD1 * \frac{S_O}{(K_O + S_O)} * Z_B$
	Parent compound transformation		*1*		$K_{Dec,Ox} * \frac{S_S}{(K_S + S_S)} * UD2 * \frac{S_O}{(K_O + S_O)} * Z_B$
	Sorption	*1*			$K_{Des} * K_{D,Ox} * UD1 * \frac{S_O}{(K_O + S_O)} * Xss$
	Anoxic processes				
	Biodegradation of OMP	*1*			$q_{C,Ax} * \frac{S_S}{(K_S + S_S)} * K_{Bio,Ax} * UD1 * \frac{K_O}{(K_O + S_O)} * Z_B$
	Parent compound transformation		*1*		$K_{Dec,Ax} * \frac{S_S}{(K_S + S_S)} * UD2 * \frac{K_O}{(K_O + S_O)} * Z_B$
	Sorption	*1*			$K_{Des} * K_{D,Ax} * UD1 * \frac{K_O}{(K_O + S_O)} * Xss$
	Anaerobic process				
	Biodegradation of OMP	*1*			$K_{Bio,An} * UD1 * \frac{K_S}{(K_S + S_S)} * \frac{K_O}{(K_O + S_O)} * Z_B$
	Sorption	*1*			$K_{Des} * K_{D,An} * UD1 * \frac{K_O}{(K_O + S_O)} * Xss$
4- and 5-methylbenzotriazole; Benzotriazole; Clarithromycin; Hydrochlorothiazide; Metoprolol; Propranolol; Sotalol; Trimethoprim	***Aerobic processes***				
	Biodegradation of OMP	*1*			$K_{Bio,Ox} * UD1 * \frac{K_S}{(K_S + S_S)} * \frac{S_O}{(K_O + S_O)} * Z_B$
	Sorption	*1*			$K_{Des} * K_{D,Ox} * UD1 * \frac{S_O}{(K_O + S_O)} * Xss$
	Anoxic processes				
	Biodegradation of OMP	*1*			$K_{Bio,Ax} * UD1 * \frac{K_S}{(K_S + S_S)} * \frac{K_O}{(K_O + S_O)} * Z_B$
	Sorption	*1*			$K_{Des} * K_{D,Ax} * UD1 * \frac{K_O}{(K_O + S_O)} * Xss$
	Anaerobic process				
	Biodegradation of OMP	*1*			$K_{Bio,An} * UD1 * \frac{K_S}{(K_S + S_S)} * \frac{K_O}{(K_O + S_O)} * Z_B$
	Sorption	*1*			$K_{Des} * K_{D,An} * UD1 * \frac{K_O}{(K_O + S_O)} * Xss$
All 11 Micropollutants	***Desorption (same for all reactor processes)***			*1*	$K_{Des} * UD3$

where:

UD1: User Defined parameter in BioWin for parent OMP in liquid (C_{Ll})
UD2: User Defined parameter in BioWin for retransformation (C_{Cl}) back to parent OMP (C_{Ll})
UD3: User Defined in BioWin for parent OMP adsorbed in Sludge (C_{SL})
Z_B: Masses of OHOs, AOB, NOB and PAOs
X_{SS}: Mixed liquor suspended solids (MLSS)

Kinetic model parameters
kDes (/d): De-sorption rate coefficient for C_{SL} = 100[c] (applied for all OMPs)
K_S (mg/L): Half-saturation coefficient for S_S (substrate) = 10[f]
K_O (mg/L): Half-saturation coefficient for dissolved oxygen = 0.2[f]

Aerobic process parameters
$K_{D,Ox}$ (L/gXss): Aerobic solids-liquid sorption coefficient
$K_{Dec,Ox}$ (L/g/d): Aerobic biotransformation rate coefficient for C_{Cl} = 5[e]
$q_{C,Ox}$ (L/g/d): Aerobic maximum specific co-metabolic substrate biotransformation rate in the presence of growth substrates for C_{Ll} = 1.6[d] and 2[d]
$K_{Bio,Ox\ SRT=16d}$ (L/g/d): Aerobic biotransformation rate coefficient for C_{Ll}

Anoxic process parameters
$K_{D,Ax}$ (L/gXss): Anoxic solids-liquid sorption coefficient
$K_{Dec,Ax}$ (L/g/d): Anoxic biotransformation rate coefficient for C_{Cl} = 5[e]
$q_{C,Ax}$ (L/g/d): Anoxic maximum specific co-metabolic substrate biotransformation rate in the presence of growth substrates for C_{Ll} = 0.96[d] and 1.2[d] for Diclofenac and Carbamazepine respectively.
$K_{Bio,Ax\ SRT=16d}$ (L/g/d): Anoxic biotransformation rate coefficient for C_{Ll}

[a]Diclofenac consumption data is presented by Grung et al. (2008).
[b]More information on the flow boundary conditions are shown by (Plósz et al., 2010c).
[c]Parameter value derived from literature (Ternes and Joss, 2006; Plósz et al., 2010a).
[d]Parameter values estimated using the measured batch experimental data and simulation for Diclofenac and Carbamazepine only.
[e]Parameter values estimated using the full-scale experimental data.
[f]ASM1 parameter values according to Spanjers et al. (1998).

3.2.3 Case study - Walcheren WWTP

The OMP model developed was applied to the CAS system of the Walcheren WWTP. The Walcheren WWTP has as a biological nutrient removal configuration (Figure 17) designed for 178,700 population equivalent and an average capacity of 1460 m3/h. Apart from predominantly municipal wastewater, the WWTP also receives around 20% industrial wastewater flows.

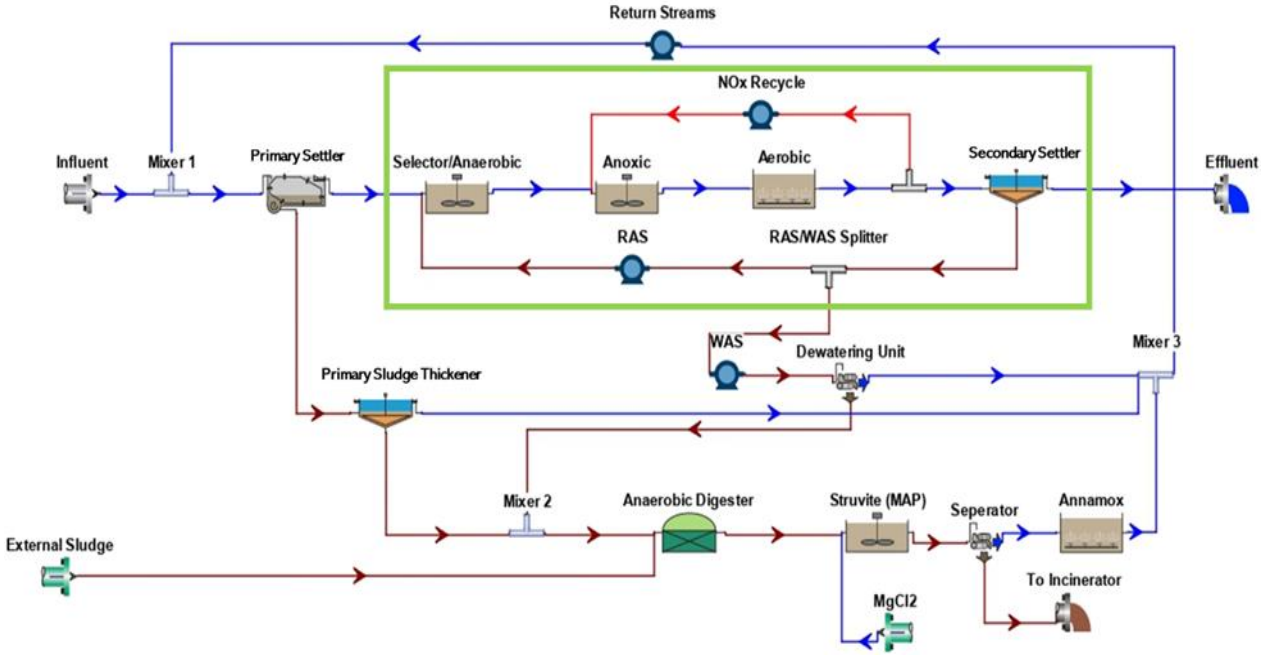

Figure 17- Walcheren WWTP configuration as represented in BioWin.

The WWTP consists of the following treatment steps - pre-treatment (for screening, grease, and sand removal), primary clarifier (for solid particles removal), selector (for controlling the activated sludge processes), anaerobic tank, anoxic tank, aerobic tank, and secondary clarifier (for biological sludge separation). This line also includes an anammox process that treats the remaining water from the sludge separator before being sent to the beginning of the water line. The sludge treatment line comprises thickeners, a dewatering unit, anaerobic digestion, struvite production, and anammox. As shown in Figure 17, this system possesses both internal and external circulation routes to maximize nutrient removal and guarantee the desired sludge age and mixed liquor suspended solids (MLSS) concentration.

3.2.4 Model calibration and validation

Comprehensive sampling campaigns were conducted to characterize the Walcheren influent wastewater parameters and their fractions, the activated sludge (taken from the tanks under the different redox conditions), and the effluent. The model was calibrated using design (e.g. volumes, areas and loadings) and operational data (e.g. Dissolved Oxygen (DO), flows and temperature), as well as water quality parameters (influent, effluent and activated sludge characteristics) from the Walcheren WWTP (Table 12 and Table 13). Initially, the process configuration of the treatment process was represented in BioWin by using the physical dimensions of the process units. The influent quality data measured from the sampling campaign was entered into the influent specifier function of BioWin, providing the characterization of the physical and chemical components of the influent wastewater. This provided a list of the wastewater fractions specific to the Walcheren wastewater which can then be mapped into the BioWin ASDM inputs. Laboratory and online sensor data were inserted into the biokinetic model. Data quality control was performed on the datasets. The data was filtered to identify any extreme anomalous/unfeasible values which were then removed. Figure 18 shows the various locations of the sampling conducted at Walcheren WWTP.

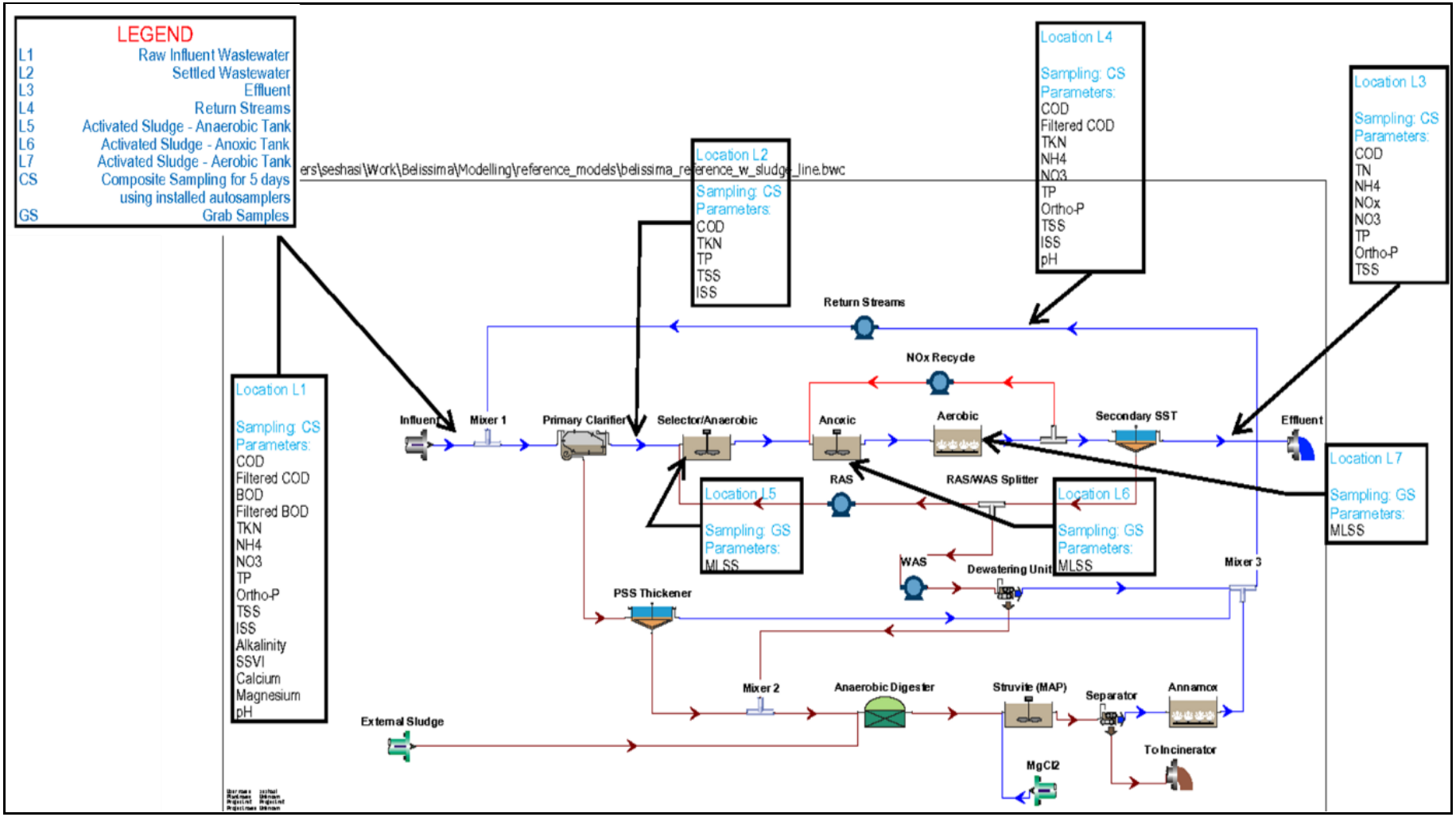

Figure 18- Walcheren WWTP sampling locations.

The average values of the influent parameters at Walcheren WWTP are shown in Table 12.

Table 12- Walcheren WWTP influent parameter values.

Influent	Unit	Values
Flow	m^3/h	1460
COD	mg/L	572.7
TKN	mg/L	59.46
TP	mg/L	6.58
ISS	mg/L	31.3
Ca	mg/L	85
Mg	mg/L	37
pH	-	7.64

For the operating conditions, online sensor data for key process parameters were used, namely - the influent flowrate, return streams flowrate, internal recycle flowrates, DO concentrations in the different reactors, temperature of the mixed liquor, and the return activated sludge (RAS) flowrates. The physical and operational parameters are listed in Table 13 below.

Table 13- Walcheren WWTP physical and operational parameters.

Description	Unit	Values
Influent flow rate	m3/d	35057
RAS flow rate	m3/d	18624
Wastage flow rate	m3/d	456
SRT	d	19
Anaerobic reactor volume	m3	5920
Anoxic reactor volume	m3	7600
Aerobic reactor volume	m3	11400
Total bioreactor HRT	hr	17
Secondary Clarifier surface area	m2	12120
Average DO concentration in Aerobic reactor	mg/L	1.0
Average Temperature	°C	20

The online and laboratory measurements on the effluent quality were used to compare the predictions from the model to perform the calibration procedure. The model was calibrated to field data representing the operating conditions and system performance of the Walcheren WWTP. A steady-state modelling was conducted where the processing units were fine-tuned. The simulations were conducted using the default kinetic and stoichiometric

parameters as available in BioWin. Additionally, the sludge retention time (SRT), and hence the wasting of sludge, was controlled. The SRT was calculated by the model based on the predicted MLSS concentrations which were very close to the observed values. The actual and simulated data are shown in Table 14.

Table 14- Effluent and bioreactor actual and simulated values.

Effluent parameters	Unit	Measured (Actual)	Simulated (ASDM)
COD	mg/L	45.5	40.1
TKN	mg/L	5.02	4.74
NH4	mg/L	2.4	2.2
NO_3	mg/L	4.14	4.58
NOx	mg/L	4.49	5.42
TN	mg/L	9.51	10.16
TP	mg/L	1.05	1.16
OP	mg/L	0.71	0.77
TSS	mg/L	10.5	11.0
Bioreactor			
MLSS	mg/L	4164	4162

The very good corroboration between the actual (measured) and the simulated effluent quality parameters provided evidence that the model was properly calibrated. This was further ascertained by the close reactor MLSS concentration between the actual and simulated values.

3.3 Simulation results and discussion

After the development of the OMP fate model and its integration into ASDM, the simulation of the OMP removal mechanisms in the Walcheren activated sludge system was performed for all the 11 targeted OMPs.
Screenshots of the modelling of Benzotriazole (represented as UD1) are shown below in Figure 19 to Figure 21 to illustrate the removal of this OMP in the various zones of the activated sludge system and other treatment steps. The effluent concentration of Benzotriazole is also shown. All concentrations are reported in mg/L.

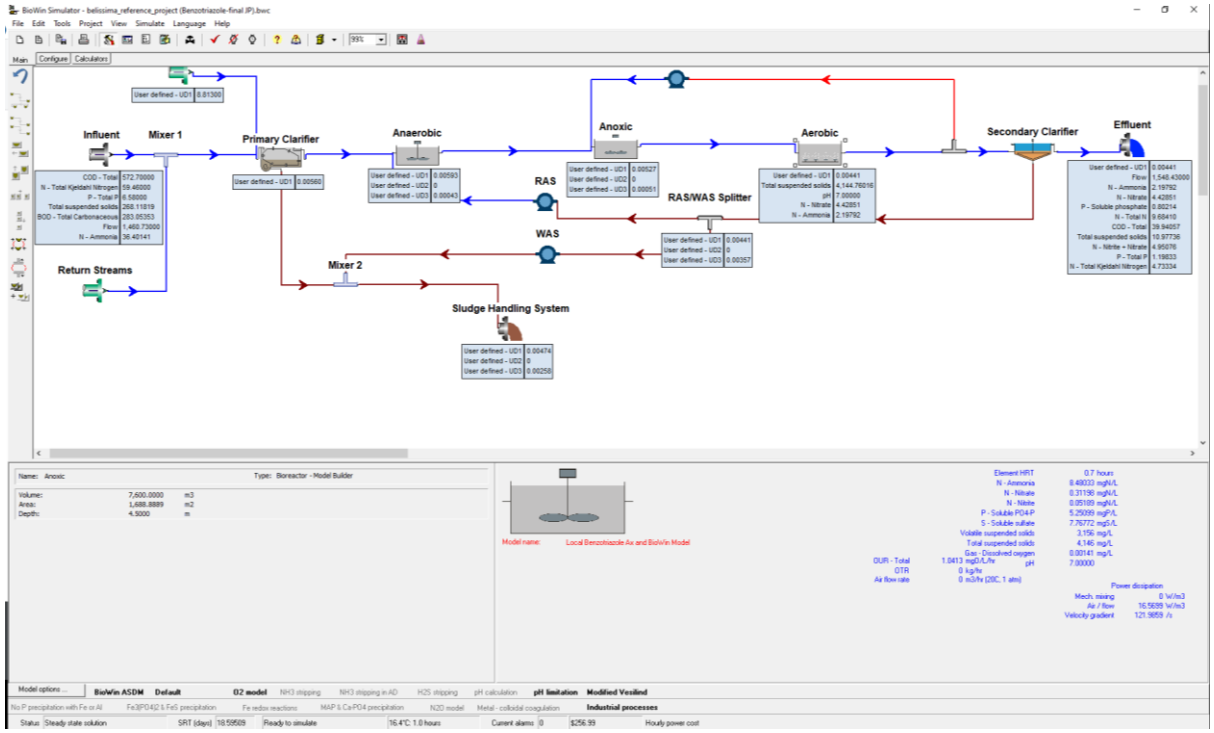

Figure 19- Screenshot of the simulation of Benzotriazole in BioWin ASDM integrated with the developed OMP fate model for Walcheren WWTP (where UD1: Parent Benzotriazole; UD2: Retransformed Benzotriazole; UD3: Sorbed Benzotriazole)

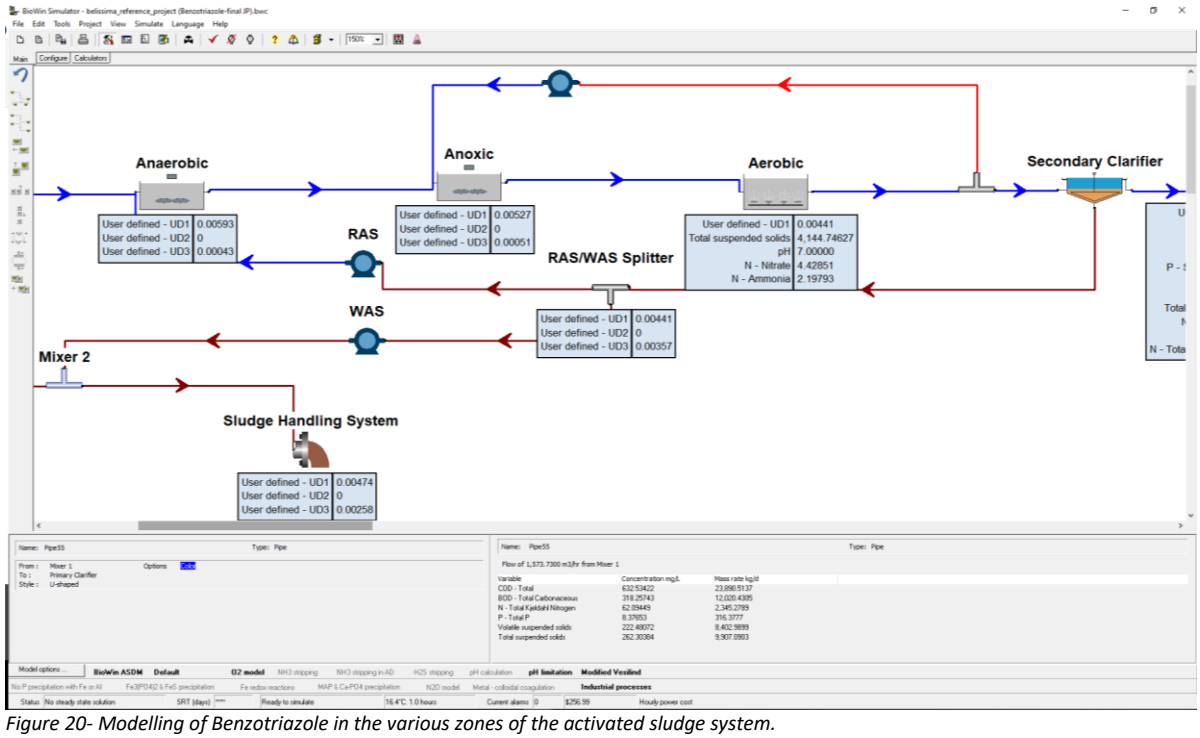

Figure 20- Modelling of Benzotriazole in the various zones of the activated sludge system.

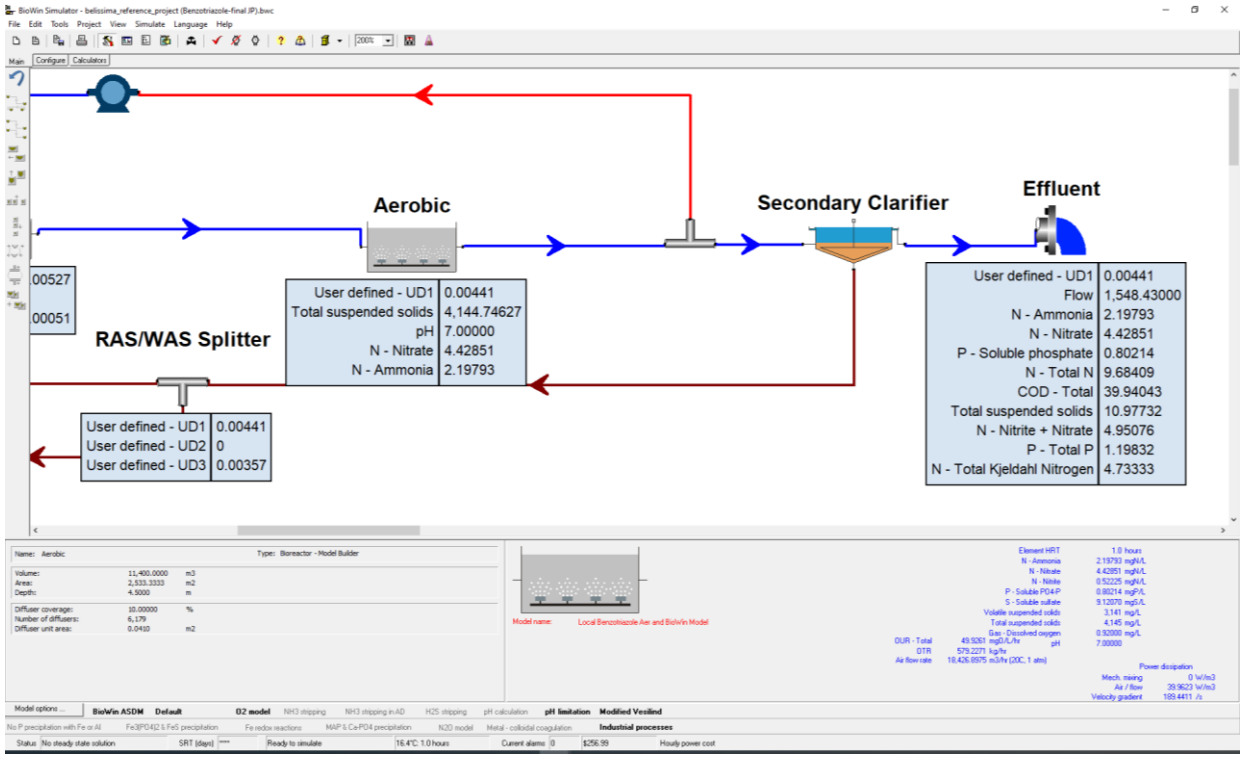

Figure 21- Modelling of Benzotriazole in the various zones of the activated sludge system.

The simulated effluent OMP concentrations (after the activated sludge system) are compared with the measured concentrations in Table 15. The influent OMP concentrations are also shown.

Table 15- OMP concentrations of influent and effluent (measured vs simulated).

		Concentration (µg/L)				
No.	**Micropollutants**	**Influent**	**Effluent (Batch test results)**	**Effluent (Simulation)**	**Model Removal Efficiency (%)**	**Walcheren Removal Efficiency (%)**
1	4- and 5-methylbenzotriazole	0,92 ± 0,17	1,01 ± 0,13	**0.85**	7.6%	11.3%
2	Benzotriazole	5,60 ± 0,95	4,45 ± 1,20	**4.41**	21.3%	20.5%
3	Carbamazepine*	0,37 ± 0,09	0,40 ± 0,01	**0.36**	2.7%	-2.7%
4	Clarithromycin	0,09 ± 0,04	0,08 ± 0,01	**0.04**	55.6%	58.9%
5	Diclofenac*	0,71 ± 0,29	0,74 ± 0,04	**0.69**	2.8%	-1.4%
6	Hydrochlorothiazide	1,76 ± 0,59	1,95 ± 0,07	**1.73**	1.7%	5.1%
7	Metoprolol	1,60 ± 0,70	1,70 ± 0,07	**1.12**	30.0%	24.4%
8	Propranolol	0,02 ± 0,01	0,02 ± 0,01	**0.01**	50.0%	0.0%
9	Sotalol	1,61 ± 0,68	1,70 ± 0,07	**1.31**	18.6%	25.3%
10	Sulfamethoxazole*	0,38 ± 0,19	0,18 ± 0,08	**0.21**	44.7%	52.6%
11	Trimethoprim	0,10 ± 0,04	0,10 ± 0,01	**0.09**	10.0%	0.0%

**** Denotes complex model with all 4 processes (Biotransformation, retransformation, sorption and desorption).***

The unmarked micropollutants are modelled with biotransformation, sorption and desorption processes. No retransformation process kinetics exist for these OMPs.

The negative Walcheren removal efficiency can be assumed to be 0%, meaning no net removal of these OMPs (Carbamazepine and Diclofenac) was observed.

From Table 15, the model simulated OMP effluent concentrations closely match the effluent values observed at the Walcheren WWTP. This indicates that the simulation model developed and integrated in ASDM is robust and accurately reflects the real-world performance of the activated sludge treatment processes for these specific compounds. In addition, it can be seen that the removal efficiency of organic micropollutants (OMPs) varies significantly in activated sludge systems. Some OMPs have high removal efficiencies, namely Clarithromycin (~56%), Propranolol (50%) and Sulfamethoxazole (~45%), while others (such as Carbamazepine, Diclofenac and Hydrochlorothiazide) have poor removal pointing to the need for additional treatment steps or alternative methods to enhance removal. Another observation is that even though some OMPs are fairly well removed in activated sludge systems, their concentrations still remain quite high in the effluent suggesting that these substances are not being efficiently removed by the biological treatment processes. This is particularly the case for OMPs Benzotriazole (4.41 µg/L) and Hydrochlorothiazide (1.73 µg/L). From the model, it can also be deduced that the primary removal mechanisms for most OMPs were biotransformation, followed by sorption. While biotransformation is a critical removal mechanism for many OMPs, it is not universally the dominant process. The removal efficiency and predominant mechanism depend on the specific properties of the OMPs, the design and operation of the treatment system, and the prevailing environmental conditions. Thus, a combination of biotransformation, sorption, desorption, and retransformation typically contributes to the overall removal of OMPs in activated sludge systems.

Overall, while some compounds are effectively biodegraded and removed, others persist, posing challenges for wastewater treatment processes. Understanding the removal mechanisms and their rates is crucial for optimizing treatment methods and improving the removal efficiency of persistent pollutants. The use of complex models as developed in this study, incorporating biotransformation, retransformation, sorption, and desorption processes, provides a more comprehensive understanding of the fate of certain OMPs, but still indicates that additional or improved treatment methods are needed for effective removal of some persistent compounds.

3.4 Sensitivity analysis

The operation of wastewater treatment plants varies widely based on process configuration and effluent requirements. Accordingly, a sensitivity analysis was conducted by varying two key parameters, namely sludge age (Rs) and temperature (T). Simulations were run to investigate the effect of different sludge ages and temperatures on the removal of Benzotriazole. Table 16 below shows the concentrations of Benzotriazole under these changing operating conditions.

Table 16- Effect of changing sludge age and temperatures on the removal of Benzotriazole in activated sludge system

Sensitivity analysis on Benzotriazole				
Sludge age (d)	15	18.5*	20	25
Temperature (°C)	16.4	16.4	16.4	16.4
MLSS	3531	4162	4361	5136
Effluent (µg/L)	4.49	4.41	4.39	4.32
Conc. sorbed (µg/L)	3.34	3.57	3.64	3.85
Temperature (°C)	10	16.4*	20	25
Sludge age (d)	18.5	18.5	18.5	18.5
MLSS (mg/L)	4532	4162	4055	3953
Effluent (µg/L)	4.27	4.41	4.46	4.53
Conc. sorbed (µg/L)	4.05	3.57	3.40	3.18

*Walcheren current operational conditions

From the sensitivity analysis reported in Table 16 above, some deductions can be made, namely:

1. Increase in SRT (sludge age) enhances removal of Benzotriazole, due to increase in mixed liquor suspended solids (MLSS) and biomass, which enhances the biotransformation and sorption activities. Although, this increase in removal efficiency will tend to plateau at much longer sludge ages.
2. Changing the SRT from 15d to 20d reduced Benzotriazole effluent concentration by 0.10 µg/L, while increasing the SRT from 20d to 25d reduced the concentration by 0.07 µg/L. This shows that increasing the SRT to a longer value has a diminishing removal efficiency, hence an optimum SRT for the removal of OMPs can be found using the model.
3. Decreasing the operating temperature reduces the effluent Benzotriazole concentration. This is due to the fact that a decrease in temperature in the activated sludge systems increases the MLSS which in turn increases the biomass available for the OMP removal mechanisms, namely biotransformation and sorption.
4. Understanding the sensitivity of these 2 parameters and other key parameters by plant operators/engineers is vital to be able to tune them to improve OMPs removal efficiency. The developed OMP fate model in activated sludge allows for such sensitivity analysis to be made before adjusting any process operations on-site.

3.5 Conclusions

3.5.1 Activated sludge modelling

A complex fate model has been developed to enhance the understanding and optimization of OMPs removal mechanisms alongside conventional pollutant removal in wastewater treatment plants. The removal mechanisms of the model incorporated kinetic rates and coefficients in ASDM and simulated removal using the software BioWin. The model was applied to the Walcheren WWTP and calibrated with the design and operational values of the plant. The developed and calibrated model successfully simulated the removal efficiency of 11 OMP compounds and their concentrations align with actual (measured) concentrations.

3.5.2 Model limitations, applicability and further developments

Although the results of the OMP modelling at Walcheren WWTP showed great promise of the validity of the model developed, it should be acknowledged that understanding the complex removal mechanisms for each OMP in models still remains a challenge. Moreover, the limited availability of both influent and effluent OMP data is often a drawback when it comes to validation of the model and making it robust. Rigorous and regular OMP analysis is expensive and not often done in WWTPs. OMP concentrations in wastewater influent can fluctuate widely over time and vary spatially within treatment plants. Modelling these variations accurately requires detailed data which unfortunately is not available.

Improvements of the presented OMP fate model as developed in this study are to include retransformation kinetic for all OMPs. At present, out of the 11 targeted OMPs investigated and modelled, only retransformation rate constants (q_C) of Diclofenac and Carbamazepine exist and have been included in the model. Studies on investigating and finding the retransformation rates of the remaining OMPs need to be conducted and added to the developed model. Moreover, the model can be extended to include other OMPs of interest. This will require the determination of the removal kinetic rates and coefficients of these additional OMPs in all redox conditions (anaerobic, anoxic and aerobic conditions) before including the reactions in the Peterson Matrix and in the ASDM in BioWin. Furthermore, additional investigation needs to be performed in the anaerobic zone of the bioreactor and

the sludge line to better understand the relevant removal mechanisms active in these processes. This will necessitate further batch tests experiments and validation on-site.

This study offers significant knowledge and advancement in understanding the fate of OMPs in activated sludge systems and how their fate impact the design of advanced treatment systems (such as advanced oxidation processes) downstream wastewater treatment plants. Activated sludge systems serve as the primary stage for biological treatment in WWTPs. Therefore, effective degradation of OMPs in this stage reduces the load and complexity of contaminants for downstream treatment processes, such as advanced oxidation processes (AOPs), membrane filtration, or activated carbon adsorption. This not only improves the efficiency and effectiveness of these downstream processes but also reduces operational costs and energy consumption.

4 Advanced oxidation modelling and scenarios testing

4.1 Introduction

For advanced oxidation post-treatment steps, UV/ H_2O_2 and O_3 are considered as options. Both processes were modelled via a (photo)chemical kinetic model, describing all relevant (photo)chemical reactions that occur in the wastewater matrix when treated by the advanced oxidation. The model is first calibrated and validated based on laboratory tests. Thereafter the model is compared and validated with the pilot tests. Finally, different scenarios are tested combining the results of the activated sludge model and the AOP model.

4.2 Advanced oxidation modelling

4.2.1 Model description

UV/ H_2O_2 model

During the UV/H_2O_2 process, the UV radiation splits the H_2O_2 into highly reactive OH radicals. The OH radicals react non-selectively with all kinds of constituents in the water, including OMPs. Besides reactions with OH radicals, an OMP can also directly be degraded by UV radiation, in a process called direct photolysis. The water matrix plays an important role in the efficiency of UV/ H_2O_2 processes, as water matrix components can block UV radiation and can also compete for the available OH radicals.

The UV/ H_2O_2 model consists of a (photo)kinetic model that contains all the relevant (photo)chemical reactions that occur in the water matrix during the UV/ H_2O_2 treatment. The UV/ H_2O_2 model was initially developed for drinking water treatment processes (Hofman-Caris and Wols, 2020; Wols et al., 2024), and included reaction of OH radicals with (bi)carbonate (depending on pH), phosphate, H_2O_2 and DOC competing for the reaction of OH radicals with OMPs. In the current project, this model is extended to wastewater effluent, allowing chemical reactions of OH radicals with Br^-, NO_3^-, NO_2^-, NH_4^+ and DOC (specific for wastewater effluent). The reaction of OH radicals with effluent DOC is an important factor in the model and this reaction rate constant may vary depending on the DOC composition. In literature values between 1E8 and 8E8 $M_C^{-1}s^{-1}$ ($L \cdot mol^{-1} \cdot s^{-}1$) are reported (Wols and Hofman-Caris., 2012). (M_C indicates that for the molar mass of DOC moles of C are taken). In the model, the OH radical reaction rate constant with DOC is determined from the laboratory scale experiments (see 4.2.3).

Ozone model

During ozonation, the ozone can directly degrade the OMPs, but also the highly reactive OH radical can be formed. This occurs in the reaction of ozone with OH- and in the reaction of ozone with a part of the DOC. Similar as in the UV/ H_2O_2 process, the OH radicals react non-selectively with background components and with OMPs. All the reactions of OH radicals with background components that are in the UV/ H_2O_2 model are also included in the ozone model. The ozone model was initially developed for drinking water treatment processes (Hofman-Caris and Wols, 2020; Wols et al., 2024) and extended to wastewater effluent. The background components in the water matrix included in the model that directly react with ozone are (bi)carbonate, OH-, NO_2^-, Br^- and DOC. DOC is split into a fast reacting part generating OH radicals (via the ozone radical $O_3^{\cdot-}$, Buffle and von Gunten, 2006) and a slower reacting part only consuming O_3. The reaction rate constants of ozone with both parts of DOC are calibrated from the laboratory scale experiments (see 4.2.3).

4.2.2 Model implementation and parameter values

The model is built into a Python scripts that solves a system of ordinary differential equations (using the module *odeint* from the Python package *scipy*, Virtanen et al. (2020)) for each water matrix component (including the OMPs) that is included. The model is solved over a time frame in which the process takes place (for collimated beam experiments: 2-10 minutes, for ozone laboratory experiments: 20 minutes), so that for each component the concentration is calculated as a function of time.

A stochiometric matrix *N* is used containing all reactions and all compounds. The system of differential equations that needs to be solved reads (see Wols et al., 2014):

$$\frac{d\boldsymbol{C}}{dt} = N\boldsymbol{v}$$

Where v is the reaction rate, that consist of a photolysis part and a part for the other chemical reactions. The photolysis reactions are first order (see Wols et al., 2014):

$$v_{photo,i} = \ln(10)\, \varepsilon_i \Phi_i C_i E_p$$

Where ε_i is the molar extinction (m^2/mol) and Φ_i the quantum yield (mol/Einstein) of compound i, E_p the fluence rate (Einstein/m^2/s). The other chemical reactions are second order reactions (see Wols et al., 2014):

$$v_{reac,i} = k_{ij} C_i C_j$$

Where k_{ij} the reaction rate constant between compound i and j.

Initial concentrations of the water matrix components in the model were set according to the water quality measurements of the treated water.

For the UV/H_2O_2 model the (mean) irradiation needs to be set, so that the UV dose (fluence) is equal to the irradiation multiplied with the residence time. The irradiation in W/m^2 is divided by the energy of a photon (J/Einstein) to get the fluence rate in Einstein/m^2/s.

Reaction constants OMPs

The reaction rate constants of the 19 OMPs used in the model were obtained from (Table 17 and Table 18):

1. Literature data if constants are available from literature.
2. Fitted from collimated beam data performed in MQ water (see 2.6 and Annex III). This was only possible for UV/H_2O_2 constants (quantum yield, molar extinction and OH radical reaction rate constant). The photolysis constants quantum yield and molar extinction can only be fitted as their mutual product (and are also used in this way in the model), so that the fitted values of quantum yield in Table 18 are set to 1.
3. If no literature and no fit was possible, values were obtained from QSPRs. These are statistical models that can predict reaction rate constants based upon the molecular structure. These QSPRs were developed in another project, see Hofman-Caris and Wols, 2020 and Wols et al., 2024.

Table 17: Reaction rate constants used in model for different OMPs. If no literature data was available, data was fitted from laboratory experiments, and if no fit was possible, data was obtained from QSPR.

Compound	OH. Reaction rate constants ($M^{-1}s^{-1}$ or $L \cdot mol^{-1} \cdot s^{-1}$)		O_3 reaction rate constant ($M^{-1}s^{-1}$ or $L \cdot mol^{-1} \cdot s^{-1}$)	
	Value	Reference	Value	Reference
4-Methyl-1H-benzotriazole	8.6E0E+9	Lee et al. (2014)	5.89E+03	Lee et al. (2014)
Amisulpride	5.88E+09	Fit (current data)	1.50E+05	Bourgin et al., (2018)
Azithromycin	4.13E+09	QSPR	1.10E+05	Dodd et al. (2006)
Benzotriazole	7.60E+09	Naik et al. (1995)	2.09E+02	Benitez et al. (2015), Lutze et al. (2005)
Candesartan	9.12E+09	Fit (current data)	5.60E+02	Bourgin et al. (2018)
Carbamazepine	8.30E+09	Wols et al. (2014), Wols et al. (2012), Pereira et al., (2007)	2.93E+05	Huber et al. (2003), Lee et al. (2014)
Citalopram	6.25E+09	Fit (current data)	5.4E+04	QSPR
Clarithromycin	5.00E+09	Lee et al. (2014)	4.0E+05	Lee et al. (2014)
Diclofenac	8.03E+09	Wols et al. (2014), Wols et al. (2012), Lee et al., (2013)	7.08E+05	Zimmerman et al. (2011), Lee et al. (2014), Bourgin et al. (2017)
Furosemide	1.10E+10	Wols et al. (2014)	6.80E+04	Lee et al. (2014)
Gabapentin	3.82E+09	Fit (current data)	2.2E+02	Lee et al. (2014) (pH=7)
Hydrochlorothiazide	5.70E+09	Real et al. (2010)	1.26E+05	Borowska et al. (2006), Bourgin et al. (2017)
Irbesartan	7.89E+09	Fit (current data)	2.40E+01	Bourgin et al., (2018)
Metoprolol	7.907+09	Wols et al. (2014), Wols et al. (2012)	2.49E+03	Javier Rivas et al., (2011)
Propranolol	1.10E+10	Wols et al. (2014)	1.25E+05	Mathon et al. (2021)
Sotalol	7.90E+09	Wols et al. (2014)	1.38E+05	Mathon et al. (2021)
Sulfamethoxazole	5.96E+09	Wols et al. (2014), Wols et al. (2012)	5.68E+05	Lee et al. (2014), Bourgin et al. (2017)
Trimethoprim	7.15E+09	Wols et al. (2014), Wols et al. (2012)	3.07E+05	Hubner et al. (2013), Bourgin et al. (2017)
Venlafaxine	8.80E+09	Wols et al. (2014)	4.39E+04	Lee et al. (2013), Lee et al. (2014)

Table 18: Quantum yield values and molar absorption values used in model for different OMPs. If no literature data was available, data was fitted from laboratory experiments (where quantum yield was set to 1), and if no fit was possible, data was obtained from QSPR.

Compound	Quantum yield (mol.Einstein^{-1})		Molar absorption ($M^{-1}cm^{-1}$)	
	Value	Reference	Value	Reference
4-Methyl-1H-benzotriazole	2.39E-02	QSPR	2.22E+03	QSPR
Amisulpride	1.00E+00	Fit (current data)	1.51E+02	Fit (current data)
Azithromycin	5.23E-02	QSPR	1.43E+03	QSPR
Benzotriazole	1.60E-02	Miklos et al. (2018)	6.14E+02	Miklos et al. (2018)
Candesartan	1.00E+00	Fit (current data)	7.88E+01	Fit (current data)
Carbamazepine	1.50E-03	Wols et al. (2014), Wols et al. (2012), Pereira et al. (2007)	5.97E+03	Wols et al. (2014), Pereira et al. (2007), Vogna et al. (2004)
Citalopram	1.00E+00	Miklos et al. (2018)	1.19E+02	Miklos et al. (2018)
Clarithromycin	1.00E+00	Fit (current data)	5.92E+01	Fit (current data)
Diclofenac	2.98E-01	Wols et al. (2014), Canonica et al. (2008), Meite et al. (2010)	5.17E+03	Wols et al. (2014), Kim et al. (2009), Canonica et al. (2008), Meite et al. (2010)
Furosemide	2.20E-02	Wols et al. (2014)	6.70E+03	Wols et al. (2014)
Gabapentin	1.00E+00	Fit (current data)	6.99E+01	Fit (current data)
Hydrochlorothiazide	1.88E-02	Real et al. (2010)	6.65E+03	Real et al. (2010)
Irbesartan	1.00E+00	Fit (current data)	4.89E+01	Fit (current data)
Metoprolol	5.04E-02	Wols et al. (2014), Wols et al. (2012)	4.48E+02	Wols et al. (2014), Wols et al. (2012)
Propranolol	3.20E-02	Wols et al. (2014)	1.30E+03	Wols et al. (2014)
Sotalol	3.90E-01	Wols et al. (2014)	3.70E+02	Wols et al. (2014)
Sulfamethoxazole	6.09E-02	Wols et al. (2014), Wols et al. (2012)	1.31E+04	Wols et al. (2014), Wols et al. (2012)
Trimethoprim	1.04E-03	Wols et al. (2014), Wols et al. (2012)	9.47E+03	Wols et al. (2014), Wols et al. (2012)
Venlafaxine	9.70E-02	Wols et al. (2014)	3.80E+02	Wols et al. (2014)

4.2.3 Model calibration and validation for laboratory experiments

UV/ H_2O_2 model

For the UV/H_2O_2 model, the reaction rate constant of OH radicals with DOC was initially set to 2.0E+08 $M_C^{-1}s^{-1}$ (M_C indicates that for the molar mass of DOC moles of C are taken), which is in the range of DOC scavenging values used in literature (Wols et al., 2012). No further calibration was needed to improve the model.

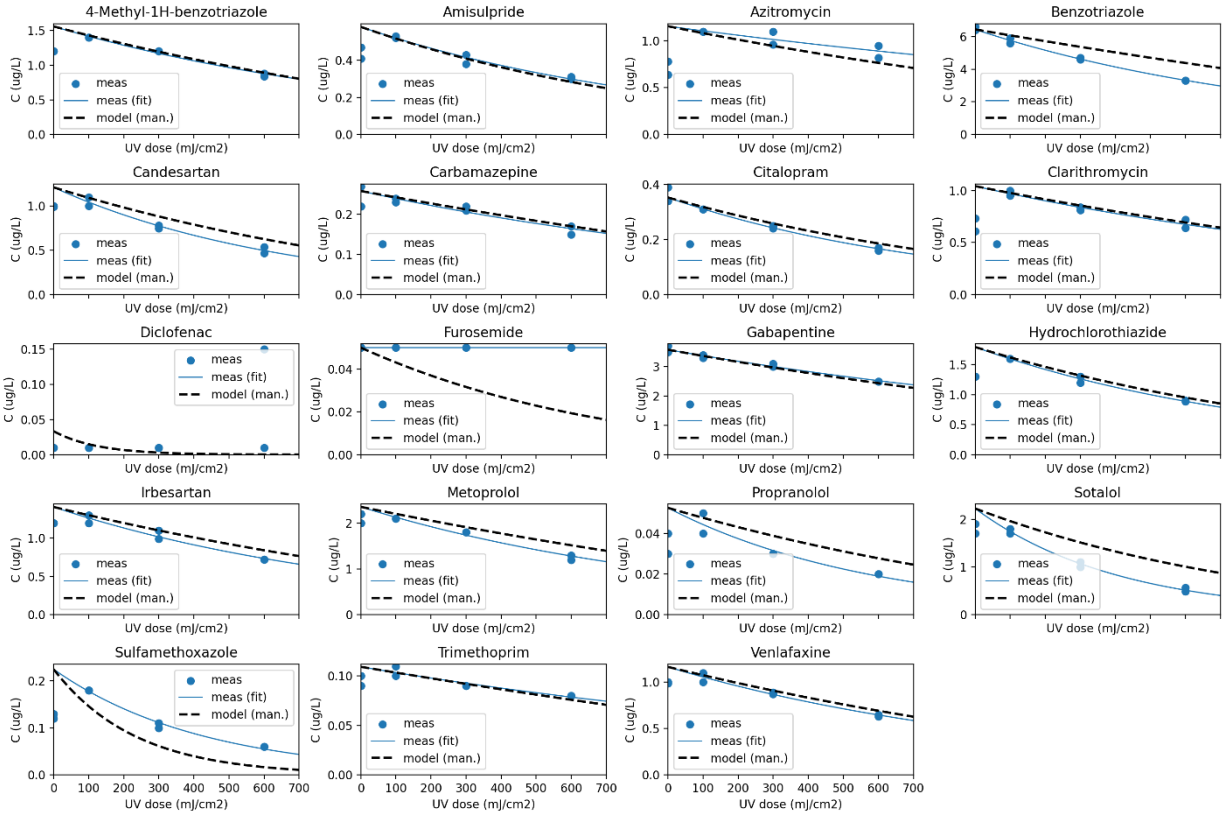

Figure 22: Comparison between model and measurements for the laboratory experiments (collimated beam). Each subfigure shows the concentration of OMP as a function of UV dose.

The model was validated for various water types and experimental conditions from the collimated beam tests. The modelled and measured degradation for the 19 compounds at each experimental condition are shown in Annex VII. Figure 23 provides a summary of the absolute error in removal percentage between model and measurement for the different conditions. For most conditions a good agreement between model and measurement can be found (within 10% difference between model and measurement), only the unfiltered Walcheren water is more difficult to model. Scattering and or shielding of UV light by particles may be an explanation for these differences. Figure 24 summarizes the differences between model and measurements for each of the 19 compounds. Most of the compounds are well predicted over the range of water types and conditions. Compounds with the largest differences are sotalol, benzotriazole (under prediction) and azithromycin and clarithromycin (over prediction). Although the model was calibrated for DOC of Walcheren, the models also worked well for Horstermeer effluent without additional calibration.

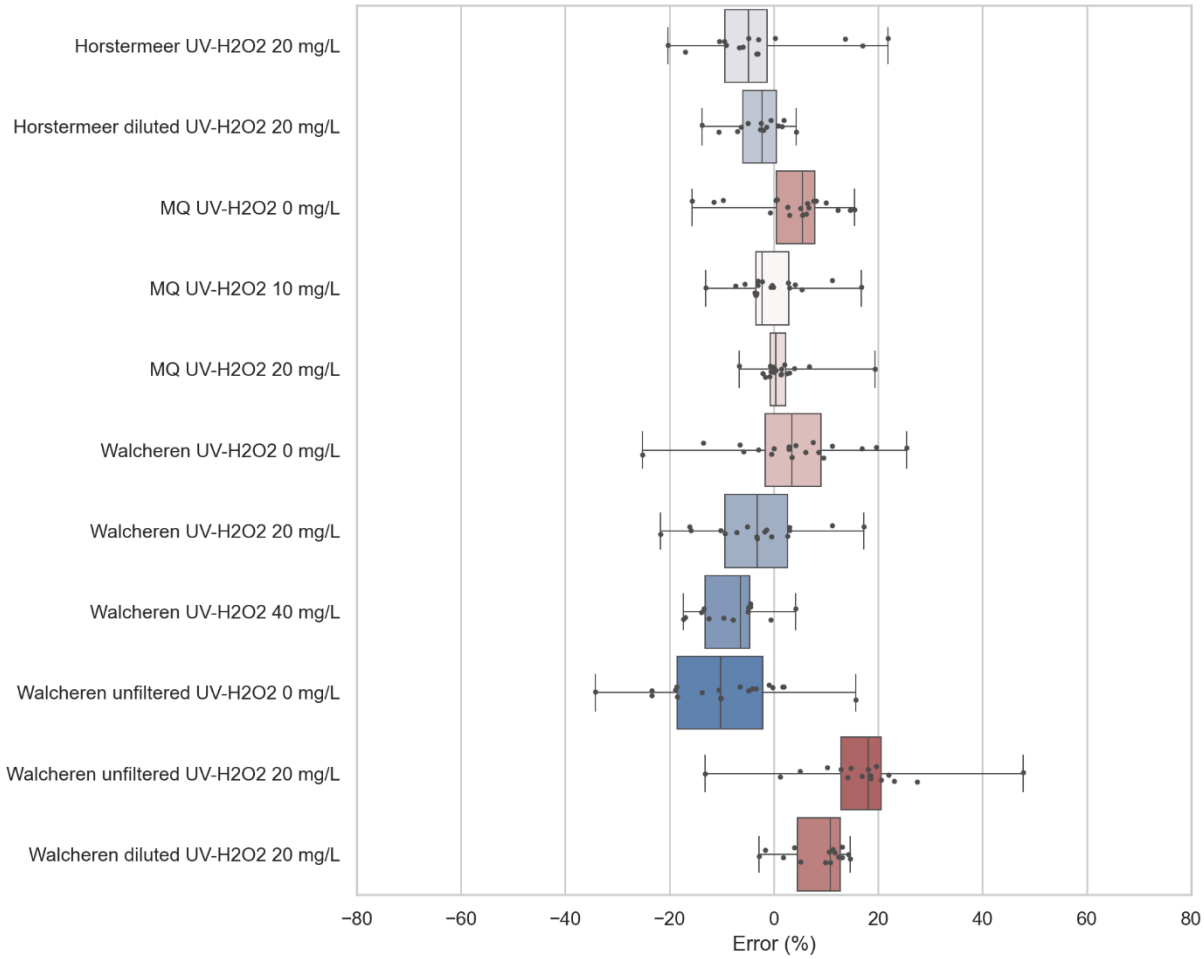

Figure 23: Absolute error (%) between predicted and measured removal percentage for the laboratory UV/H_2O_2 experiments for the different conditions and water types (a negative value means under prediction of the model). The boxplot shows the minimum, lower quartile, median, upper quartile and maximum error in degradation for the 19 OMPs. The black dots show the individual error in degradation of each OMP.

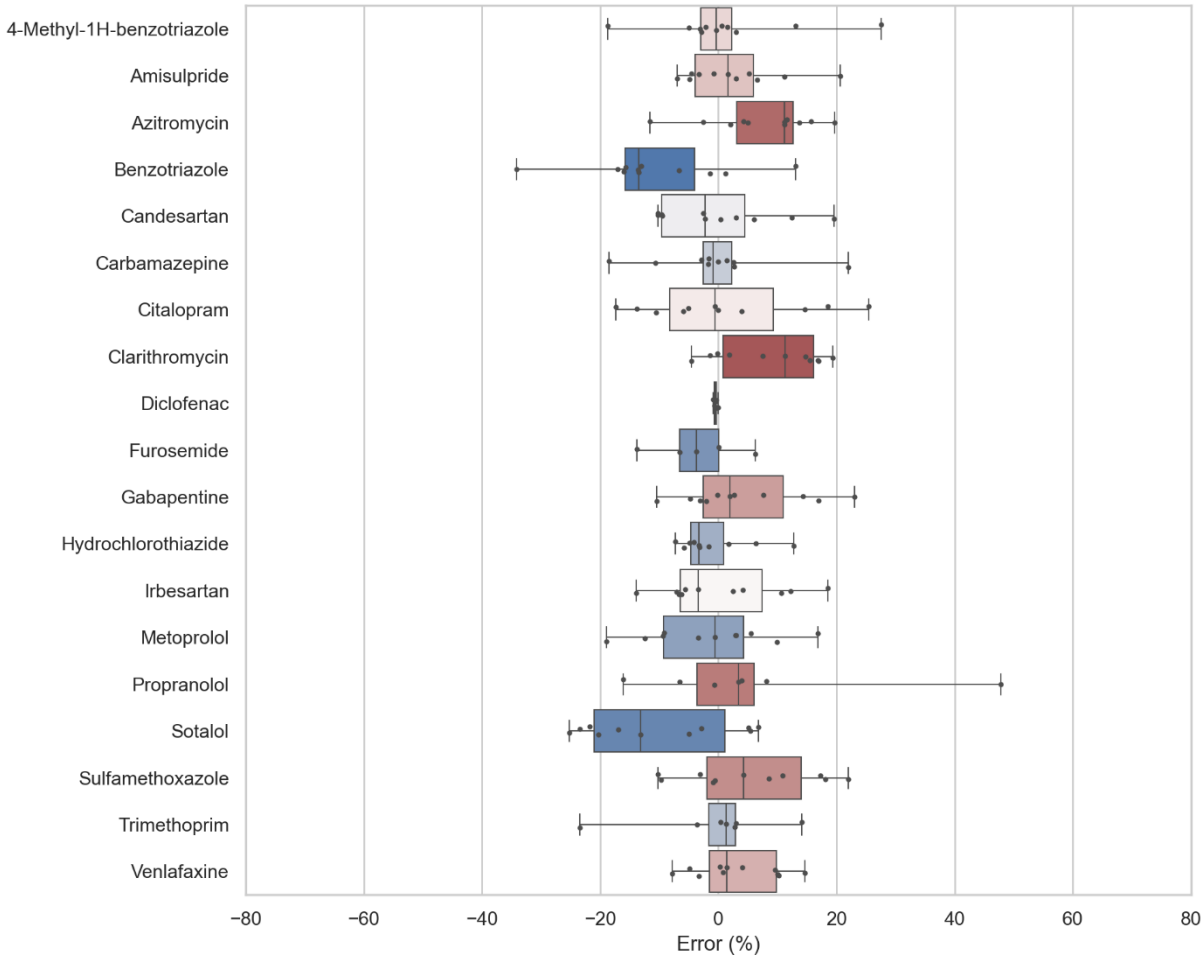

Figure 24: Absolute error (%) between predicted and measured removal percentage for the laboratory UV/H_2O_2 experiments for the different OMPs (a negative value means under prediction of the model). The boxplot shows the minimum, lower quartile, median, upper quartile and maximum error in degradation for the different conditions and water types. The black dots show the individual error in degradation of each condition or water type.

Ozone model

The ozone model in Walcheren wastewater effluent is calibrated for four compounds varying in O_3 and OH radical reaction rate constants (OH radical reaction rate constant ranges between 6E9 and 11E9 $M^{-1}s^{-1}$, O_3 reaction rate constants ranges between 2.5E3 and 5.7E5 $M^{-1}s^{-1}$, see Table 17). About 10% of the DOC is marked as fast reacting DOC and the remaining 90% is marked as slower reacting DOC. The fast reacting DOC reacts with ozone with a reaction rate constant of 2E5 L/mol/s and the slow reacting DOC reacts with a reaction rate constant of 1.5E3 L/mol/s. The fast reacting DOC gives O_3-. radicals with a stochiometric factor of 0.33 that react with H_2O to form OH. radicals. The slow reacting DOC does not result in other radicals. The reaction of DOC with OH radicals is similar as in the UV/H_2O_2 model. The above mentioned factors can be different depending on the composition of the DOC and may need to be calibrated for a specific wastewater effluent (in Buffle and von Gunten (2006) some of these factors are determined for specific NOM moieties). For Walcheren effluent, the above mentioned factors were calibrated and the modelled degradation for the four compounds closely matched the measurements (see Figure 25).

Furthermore, all the 19 compounds for the three laboratory scale settings were modelled using the ozone model. The modelled and measured degradation for the 19 compounds at each experimental condition are shown in Annex VII. An overview of the absolute errors (difference in percentage removal between model and measurements) is given in Figure 26 (summarizing over the three conditions) and Figure 27 (summarizing over the 19 compounds). In general, the absolute errors are small (on average for all compounds within 10% absolute difference). As expected, metoprolol, sulfamethoxazole, trimethoprim and venlafaxine show a good agreement, as

they were used for the calibration. Also, most of the other compounds show a good agreement between model and measurement. Only azithromycin, furosemide and hydrochlorothiazide show some deviations between the model and measurements. A possible explanation could be that the reaction rate constants used for these compounds are less accurate, or for compounds that show an underprediction (azithromycin, furosemide) addition pathways (e.g. with other radicals) occur that are not in the model.

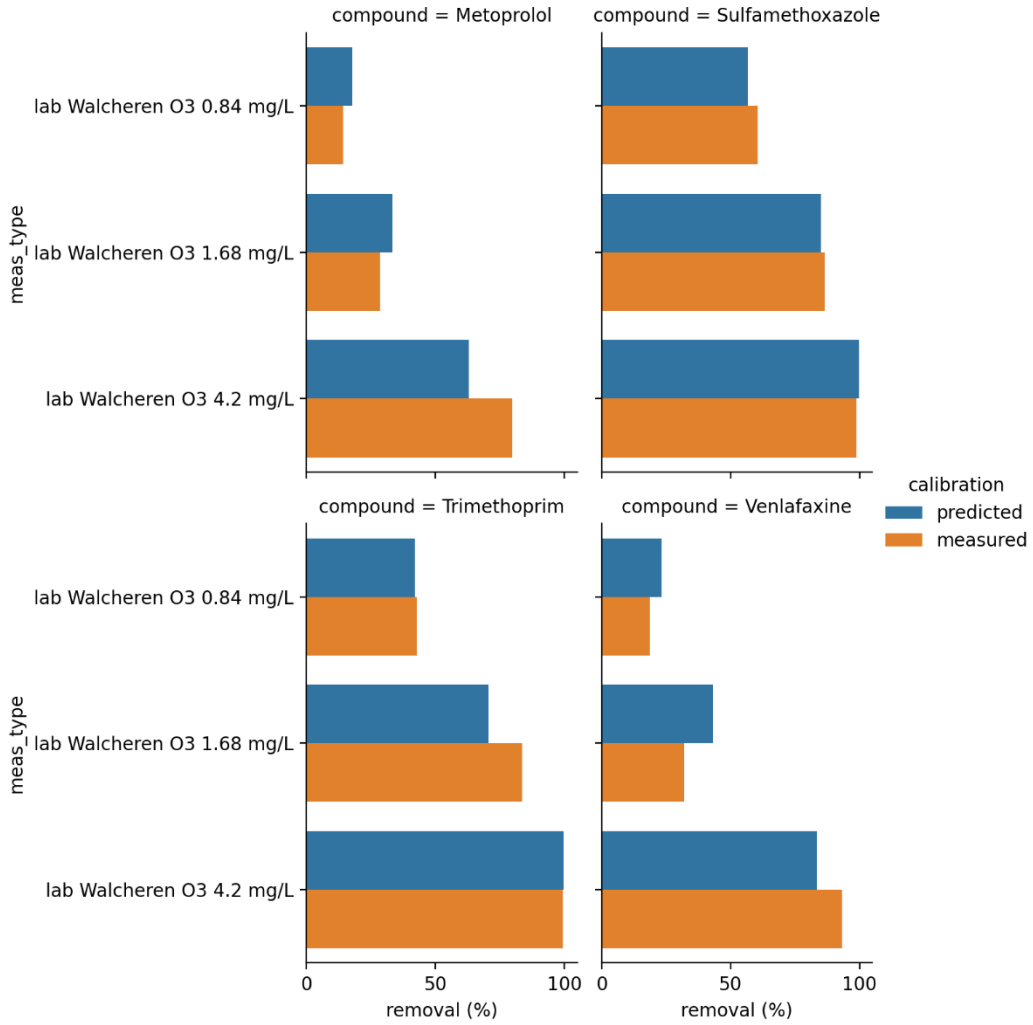

Figure 25: Calibration of ozone model for compounds Metoprolol, Sulfamethoxazole, Trimethoprim and Venlafaxine.

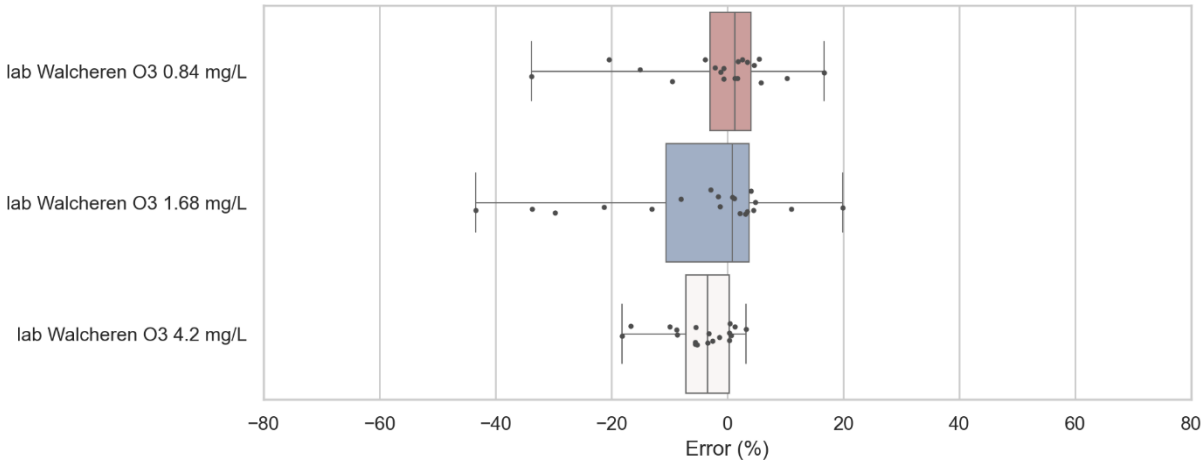

Figure 26: Absolute error (%) between predicted and measured removal percentage for the laboratory O_3 experiments for the different conditions and water types (a negative value means under prediction of the model). The boxplot shows the minimum, lower quartile, median, upper quartile and maximum error in degradation for the 19 OMPs. The black dots show the individual error in degradation of each OMP.

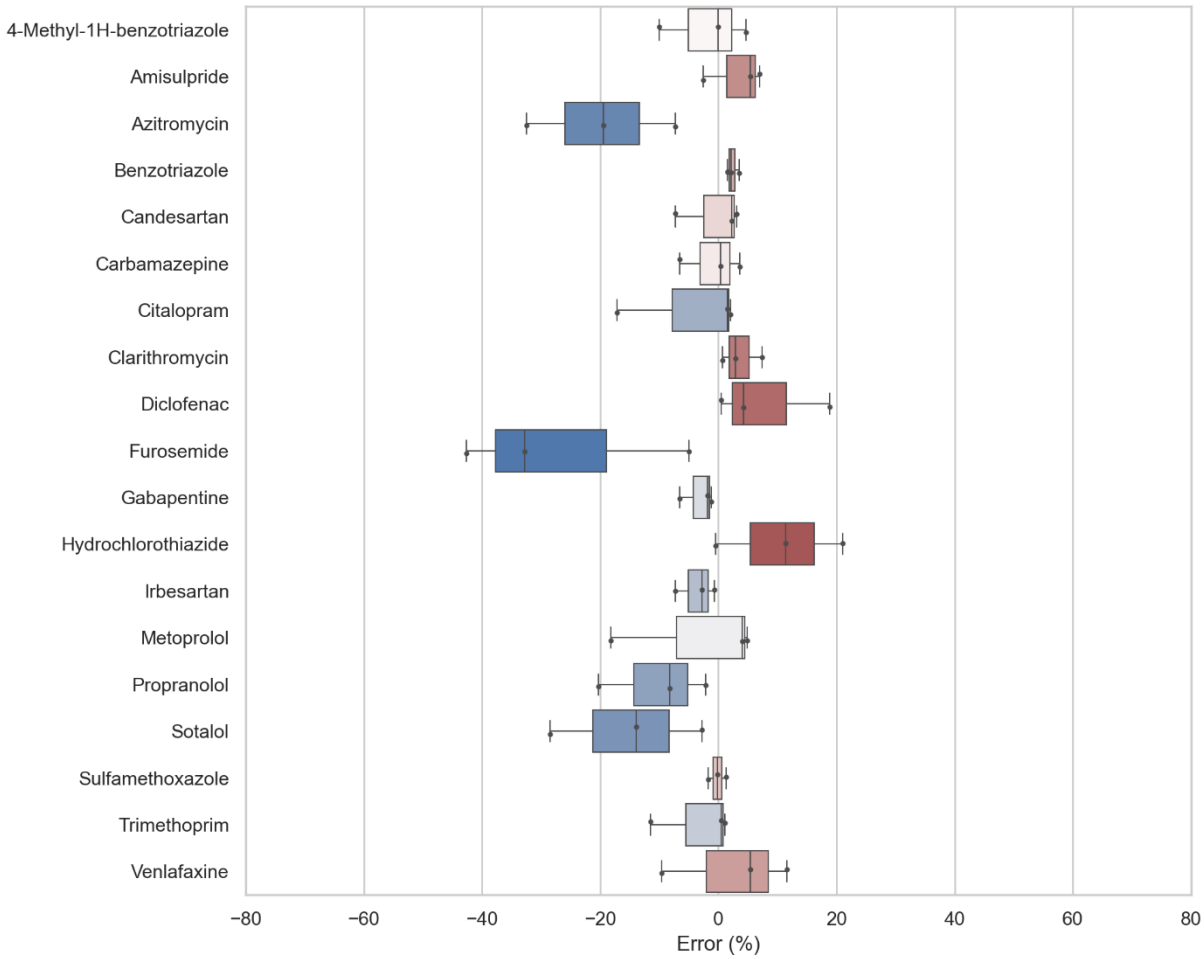

Figure 27: Absolute error (%) between predicted and measured removal percentage for the laboratory O_3 experiments for the different OMPs (a negative value means under prediction of the model).. The boxplot shows the minimum, lower quartile, median, upper quartile and maximum error in degradation for the different conditions and water types. The black dots show the individual error in degradation of each condition or water type.

4.2.4 Model validation for pilot experiments

UV/ H_2O_2 model

The kinetic UV/H_2O_2 model, calibrated and validated using the laboratory tests is used to predict degradation during pilot trials. Interactions between hydrodynamics and the photochemical reactions are not considered in the model, as this would require a computational extensive CFD model, which is beyond the scope of the project. Also, for AOP processes, the effect of the hydraulics on the performance of the reactors is less critical, as the removal levels are lower (typically between 60-90%) compared to disinfection processes (more than 99%)[1]. For the UV/H_2O_2 model, the UV dose calculated by Van Remmen UV Techniek is used, which is based upon interpolation of former CFD calculations of the reactor using the UV transmittance, number of lamps switched on and flow rate. So, CFD calculations are only used to determine the mean UV dose, but not to model the interactions between the hydrodynamics and photochemical reactions.

The UV/H_2O_2 model gives on average accurate predictions (within 10% absolute difference of removal percentage) of the removal of OMPs in the pilot systems, see Figure 28. The comparison between measured and modelled removal for each of the 19 OMPs at experimental condition is shown in Annex IX, and a summary per OMP is given in Figure 29. Diclofenac and sulfamethoxazole are a bit overpredicted by the model (20%), whereas trimethoprim is underpredicted (+/- 20 %). For diclofenac and sulfamethoxazole, which are known to be very sensitive to UV/ H_2O_2, the measurements in round 1 were bound by the initial concentrations and detection limits (in reality a higher degradation could have occurred) and the measurements in round 1 seem to have an unrealistic low degradation. Trimethoprim also had issued with low influent concentrations, so that not for all rounds measurement results could be used.

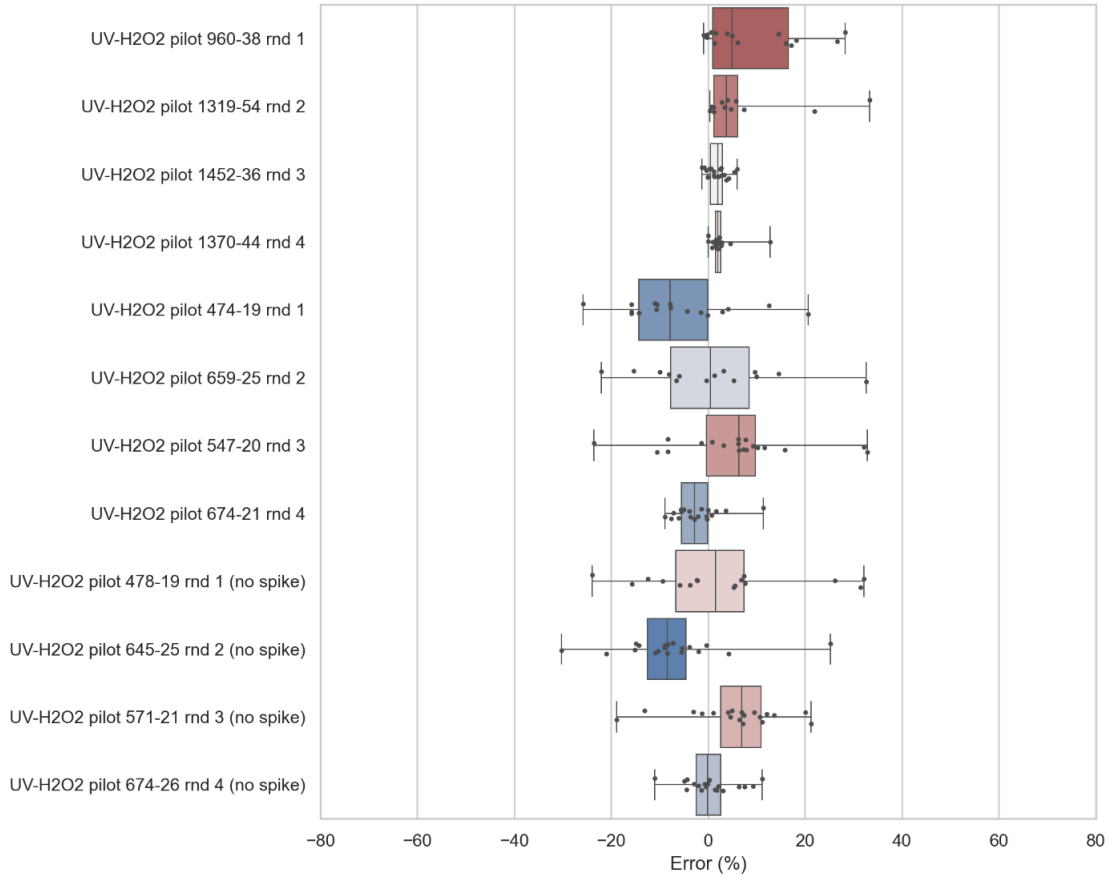

Figure 28: Absolute error (%) between predicted and measured removal percentage for the laboratory UV/H_2O_2 experiments for the different conditions and water types (a negative value means under prediction of the model).. The boxplot shows the minimum, lower quartile, median, upper quartile and maximum error in degradation for the 19 OMPs. The black dots show the individual error in degradation of each OMP.

[1] E.g. if 1% of the UV reactor is not irradiated because of non-ideal hydraulics, no more disinfection than 99% can be obtained.

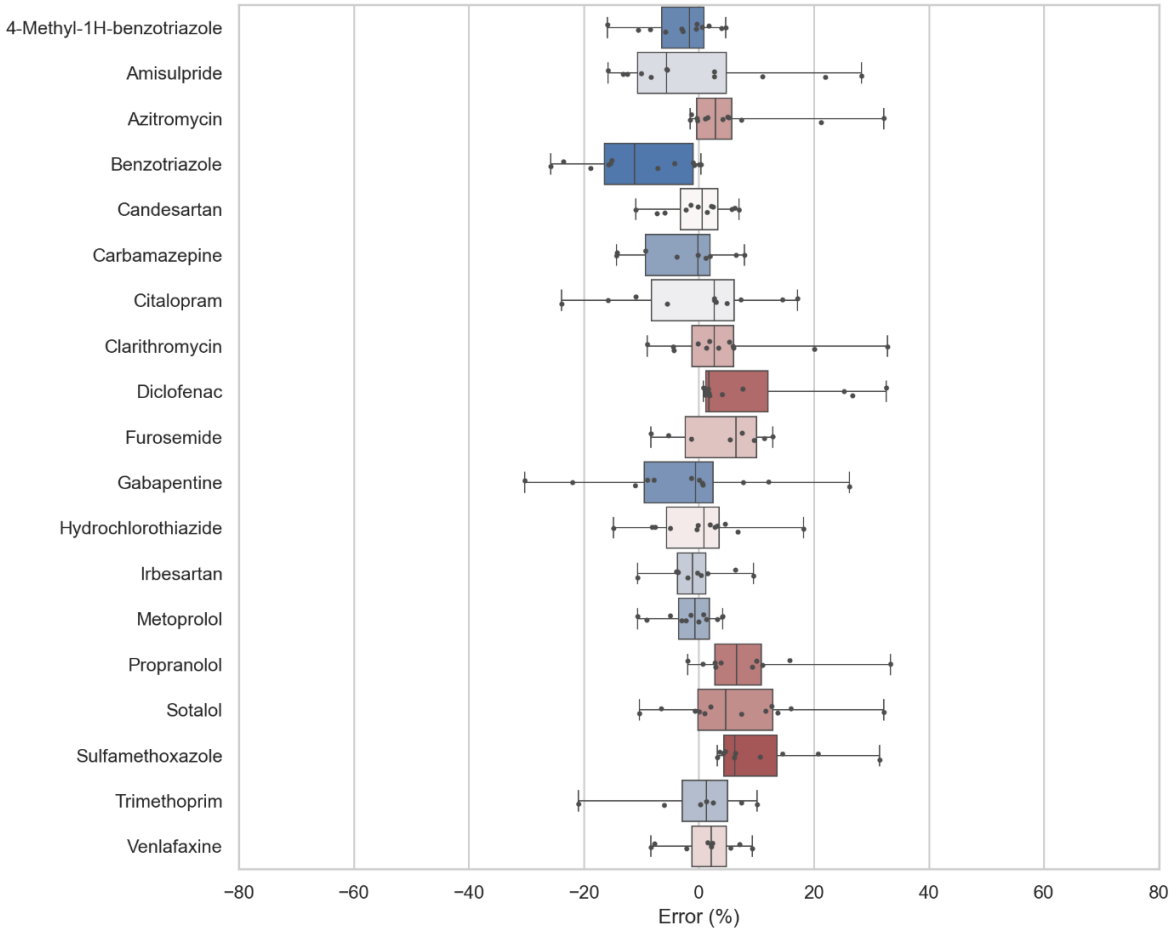

Figure 29: Absolute error (%) between predicted and measured removal percentage for the pilot UV/H_2O_2 experiments for the different OMPs (a negative value means under prediction of the model). The boxplot shows the minimum, lower quartile, median, upper quartile and maximum error in degradation for the different conditions and water types. The black dots show the individual error in degradation of each condition or water type.

Ozone model

The kinetic ozone model, calibrated and validated using the laboratory tests is used to predict the degradation in the pilot trials. The hydraulics and ozone bubbles are not considered in the model, as this would require a computational extensive multiphase CFD model, which is beyond the scope of the project. Only the dissolved ozone concentration is used in the model, that is calculated by PureBlue using the incoming gas flow and ozone gas concentration, and outcoming gas flow and ozone gas concentration, from which the ozone gas transfer efficiency from gas to water can be determined.

The comparison between measured and modelled removal for each of the 19 OMPs at each experimental condition is shown in Annex IX, and an overview per experimental condition and round is shown in Figure 30. The ozone model is less accurate than the UV/ H_2O_2 model, some compounds seem to show substantial deviations from the measurements (Figure 31). Benzotriazole, candersartan, gabapentin, irbesartan and metoprolol seem to be under predicted and diclofenac (for some conditions) and hydrochlorothiazide seem to be over predicted. Interestingly, these compounds, except for hydrochlorothiazide, were well predicted in the laboratory experiments. For diclofenac, similar as in UV/ H_2O_2 the degradation results in round 2 seem to be unrealistic low. Benzotriazole, candersartan, gabapentin, irbesartan and metoprolol have the lowest O_3 reaction rate constant (Table 17), so possibly omitting the ozone injection via bubbles in the model, where locally high concentrations of ozone and of OH radicals may occur, may lead to these under predictions. An other explanation may be that the ozone model is

more sensitive to the DOC composition. The reaction parameters with DOC were calibrated using the laboratory tests and the DOC composition during the pilot tests may have been different from the laboratory tests (the DOC concentrations were also lower in some test).

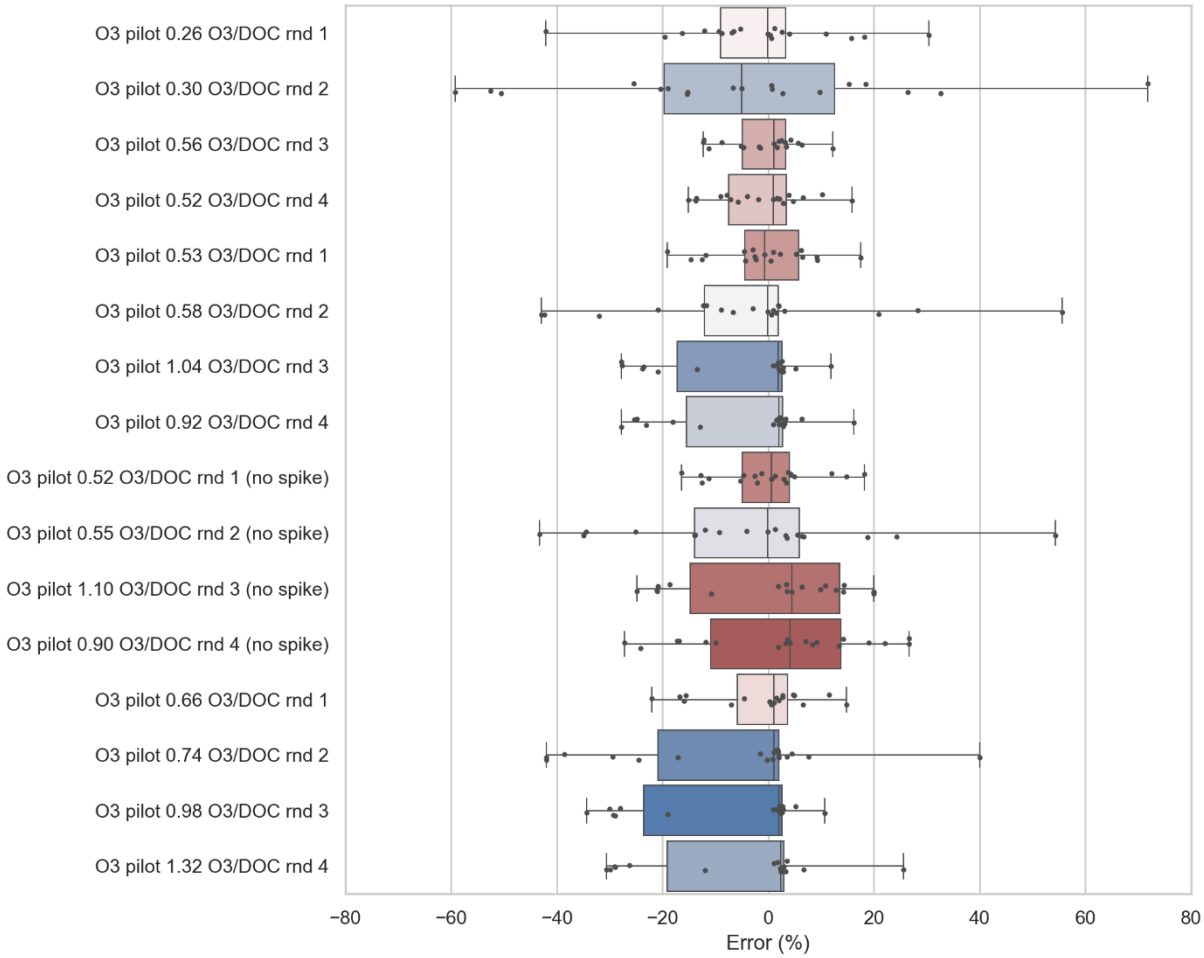

Figure 30: Absolute error (%) between predicted and measured removal percentage for the pilot O_3 experiments for the different conditions and water types (a negative value means under prediction of the model). The boxplot shows the minimum, lower quartile, median, upper quartile and maximum error in degradation for the 19 OMPs. The black dots show the individual error in degradation of each OMP.

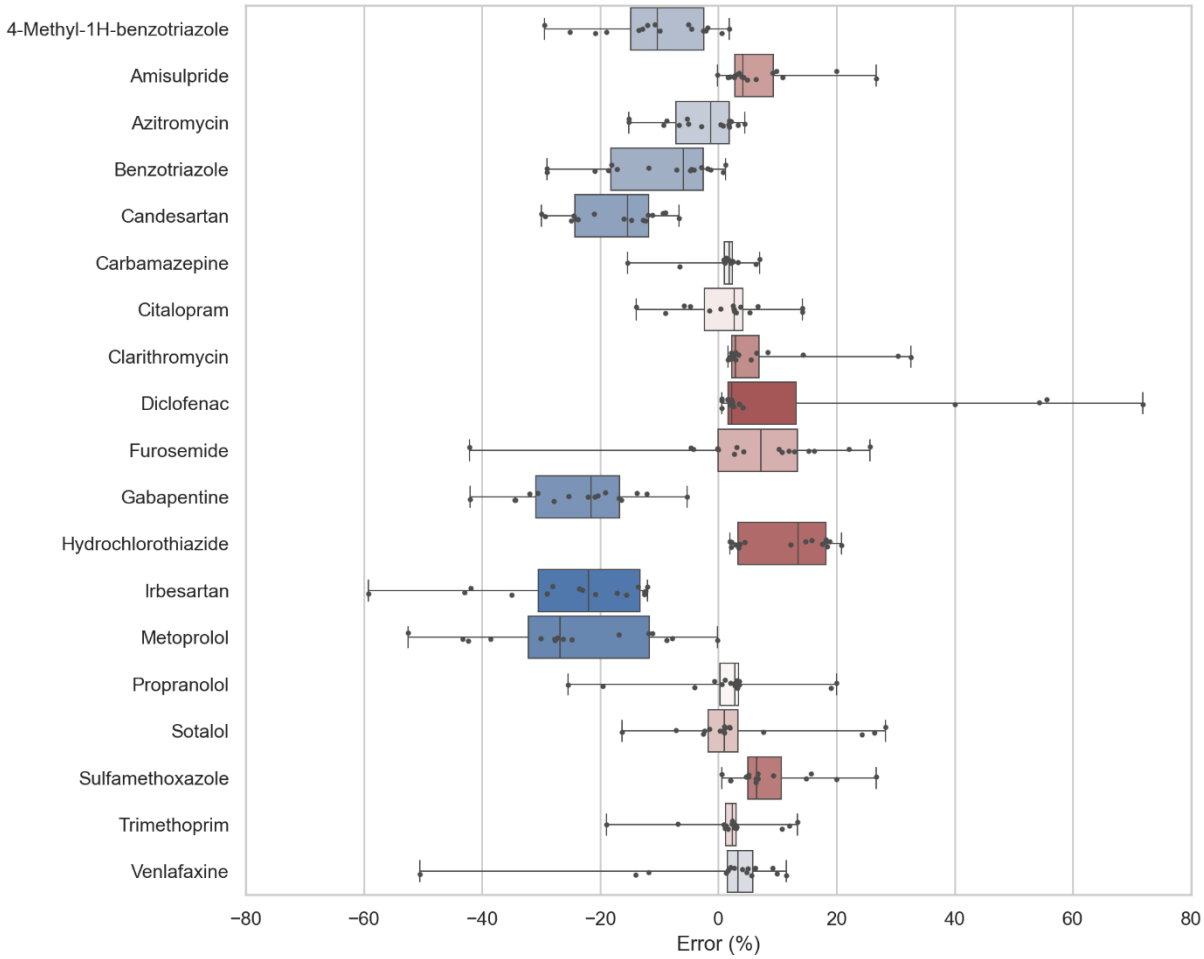

Figure 31: Absolute error (%) between predicted and measured removal percentage for the pilot O_3 experiments for the different OMPs (a negative value means under prediction of the model). The boxplot shows the minimum, lower quartile, median, upper quartile and maximum error in degradation for the different conditions and water types. The black dots show the individual error in degradation of each condition or water type.

4.3 Activated sludge and advanced oxidation models-scenario's testing

4.3.1 Concept description

The CAS model predicts the removal of 11 OMPs by the CAS (Chapter 3). For the AOP treatment, first a sensitivity analysis with respect to the water quality parameters of the wastewater effluent is performed for four compounds that differ in terms of direct UV photolysis and sensitivity towards OH radical and O_3 reaction rate constants to demonstrate which parameters are most important for the removal of OMPs. Then the AOP model is combined with the CAS model to predict the total removal of 11 OMPs for four scenarios:

- CAS + UV/ H_2O_2 (average conditions: 600 mJ/cm^2 and 20 mg/L H_2O_2)
- CAS + UV/ H_2O_2 (high conditions: 1200 mJ/cm^2 and 40 mg/L H_2O_2)
- CAS + O_3 (average conditions: 5 mg/L O_3 at 10 mg/L DOC)
- CAS + O_3 (high conditions: 9 mg/L O_3 at 10 mg/L DOC)

For each scenario, the removal is predicted for the AOP with and without CAS. For the water quality parameters, typical concentrations for Walcheren effluent were taken:

- pH: 7.2
- DOC: 10 mg/L
- Dissolved inorganic carbon: 250 mg/L
- NO_3^-: 10 mg/L
- NO_2^-: 0.2 mg/L
- NH_4^+: 5 mg/L
- Phosphate: 0.037 mg/L
- Br^-: 1 mg/L

4.3.2 Results and discussion

The effect of water quality and process conditions on the performance of the AOP is shown in Figure 32 for UV/H_2O_2 and in Figure 33 for the O_3 process. As already shown by the pilot experiments, the UV dose and H_2O_2 concentration are very important parameters for the performance of the UV/H_2O_2 process. The most important water quality parameters are concentrations of DOC and NO_2^-, and to a lesser extent (bi)carbonate and Br^-. The higher the concentrations of these parameters are, the lower the degradation of micropollutants. All these parameters scavenge OH radicals, so that less radicals are available for the oxidation of OMPs.
For the O_3 process, obviously the O_3 concentration itself is an important process parameter. Similar as for the UV/H_2O_2 process, the most important water quality parameters are DOC and NO_2^-, and to a lesser extent (bi)carbonate and Br^-.
Note that UV transmittance of the water is also an important parameter for the performance of the UV/H_2O_2 process, which is incorporated in the UV dose. So if the water has a low UV transmittance, more energy is required to obtain the same UV dose. But the UV transmittance is also inversely correlated to DOC concentrations, so that at a low UV transmittance more OH radicals will be scavenged by DOC and less OH radicals are available to degrade organic micropollutants. This is incorporated in the kinetic model. Also, UV reactors can be more efficient at higher UVT (better distribution of UV radiation). A pre-treatment step in addition to the treatment of the CAS (for example a sand filtration step, as installed in the pilot set-up) can therefore significantly reduce the energy consumption of the UV/H_2O_2 process. Tertiary treatment, using for instance sand filters, is common in WWTPs and having this treatment step before the AOP is important in reducing the OPEX.

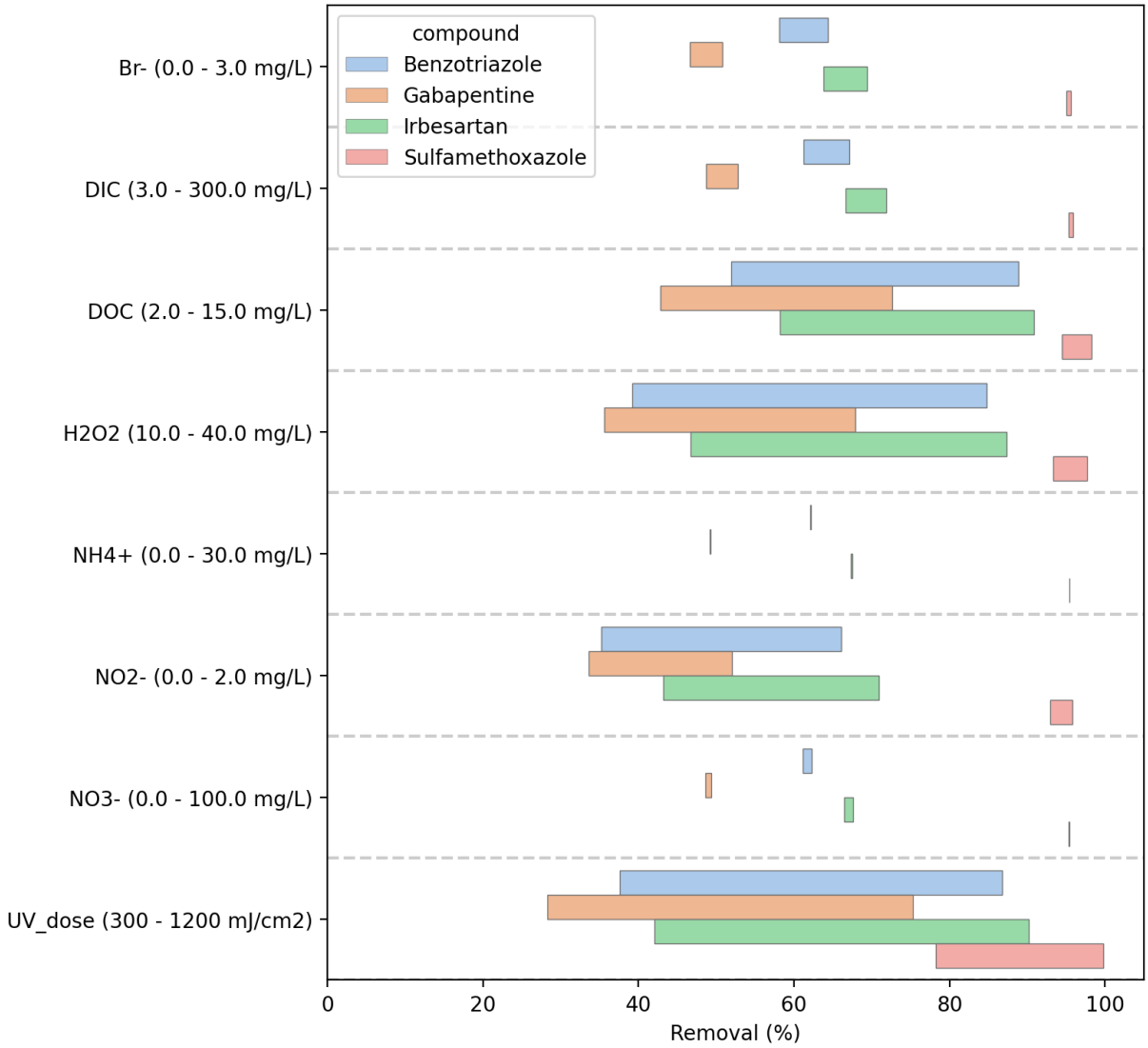

Figure 32: Sensitivity study of process conditions and water quality parameters for UV/H_2O_2 model. The predicted removal percentage for four OMPs is plotted over the range of each parameter given.

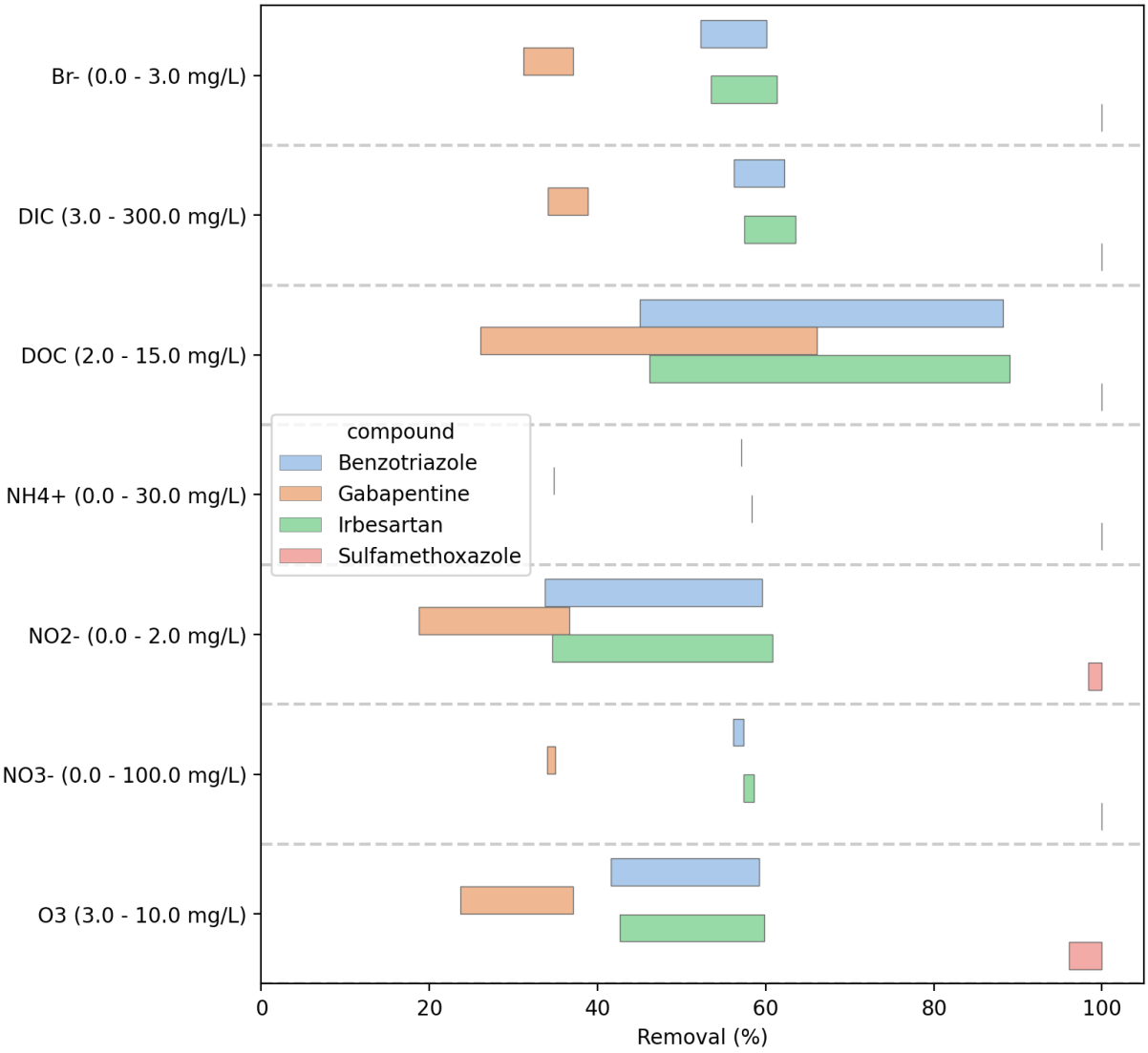

Figure 33: Sensitivity study of process conditions and water quality parameters for O_3 model. The predicted removal percentage for four OMPs is plotted over the range of each parameter given.

For the four selected AOP scenarios, the removal of 11 OMPs is shown in Figure 34, predicting the removal using only the AOP model and the removal using both CAS and AOP models. For the moderate AOP scenarios (600 mJ/cm^2 and 20 mg/L H_2O_2 or 5 mg/L O_3), the removal percentage of some OMPs is around 60% and can be improved by the combination of CAS + AOP models up to about 80%. For compounds that are more recalcitrant to ozone and are also more difficult to remove at higher ozone dosages, such as benzotriazole and metoprolol, the predicted removal is higher by the combination of CAS + AOP. For other OMPs, the predicted removal of the combination of CAS + AOP is not much higher than the removal of only the AOP.. Depending on the influent concentrations of OMPs and the required effluent concentration after AOP, taking into account the removal of the CAS may assist in obtaining the desired removal percentage or to lower the energy consumption of the AOP. This is demonstrated in Figure 35, where it shows the concentrations of 11 OMPs after the four AOP scenarios with and without taking into account the removal by the CAS. For the influent concentrations, typical concentrations that are encountered in Walcheren water were used. The results show that for some compounds (metoprolol, benzotriazole) the concentration after the AOP is substantially lower by accounting the effect of the CAS. If these compounds are critical for the juridical targets, accounting for the CAS removal can reduce the energy demand of the AOP.

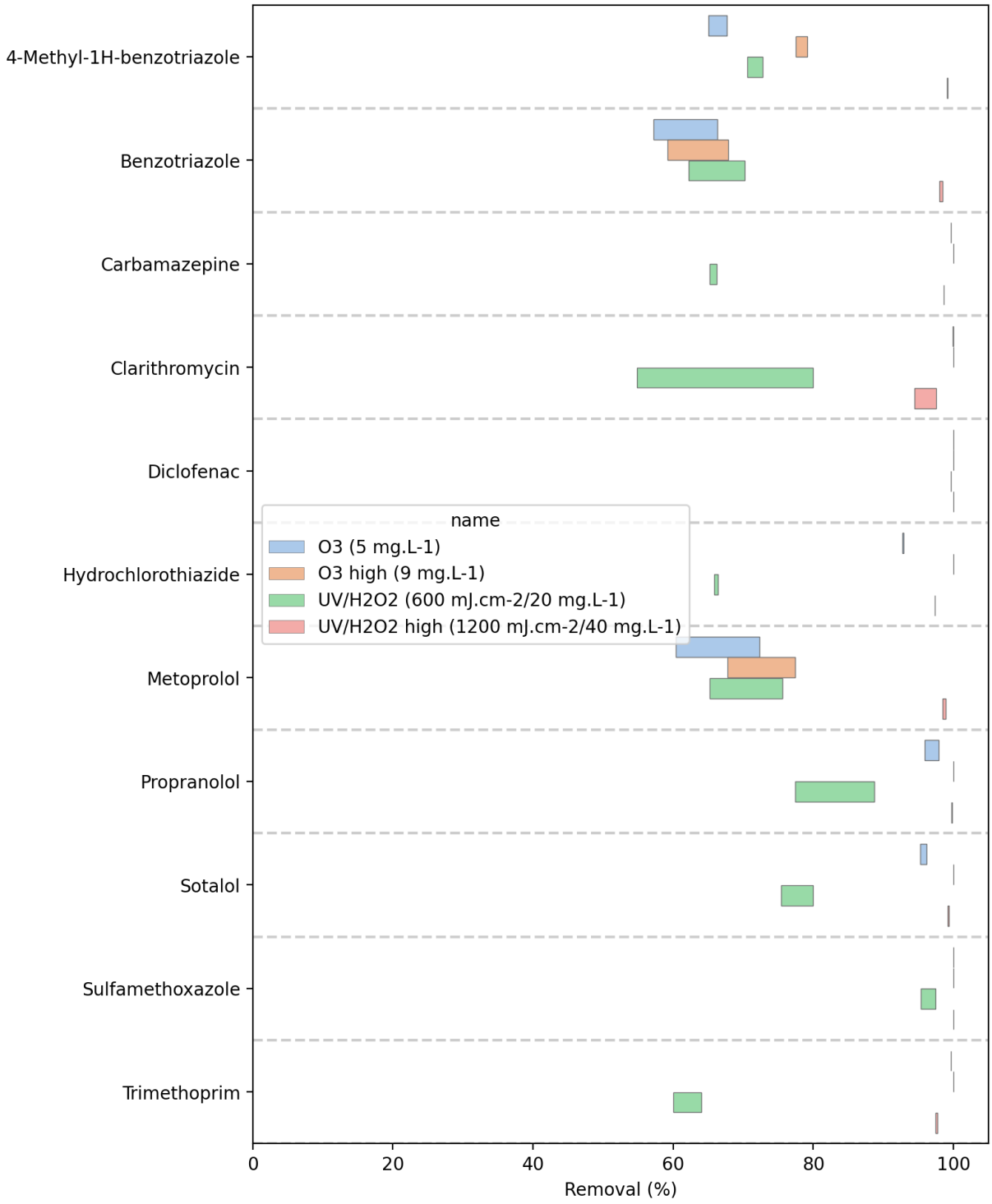

Figure 34: Removal scenario's for 11 OMPs with and without CAS. De left side of the bar is the removal percentage of the AOP, and the right side of the bar is the removal percentage of both CAS and AOP.

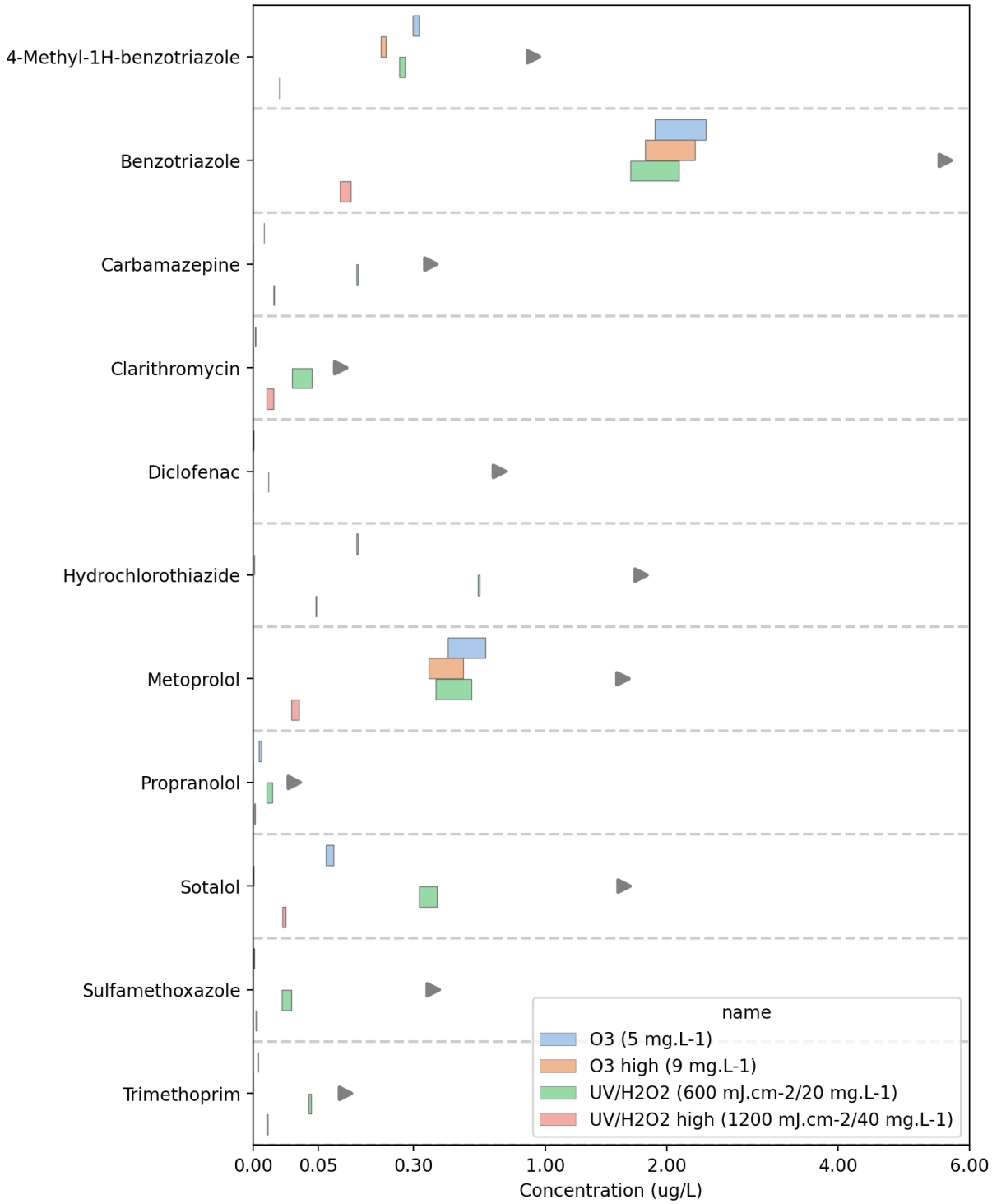

Figure 35: Removal scenarios for 11 OMPs with and without CAS removal. The left side of the bar is the predicted effluent concentration after the CAS and AOP , and the right side of the bar is the predicted effluent concentration after AOP without the removal of the CAS. The triangles represent the influent concentrations. Note that the x-axis is not equidistant.

4.4 Conclusions and recommendations

For the UV/H_2O_2 model, 19 OMPs can be accurately predicted both at laboratory scale as in the pilot scale experiments. On average, predictions of the model are within 10% of the measured data (Table 19), and none of the 19 OMPs showed large deviations between model and measurements (Figure 36). Only unfiltered Walcheren water is difficult to predict by the UV/ H_2O_2 model, possibly due to shadowing, light reflection or scavenging of radicals by the particles. In practice the water will be filtered by for example a coagulation/ sand filter upstream of the UV/ H_2O_2 treatment.

For the O_3 model, in general good results can be obtained for the laboratory experiments, but for the pilot experiments the model is less accurate (for some conditions, deviations are higher than 15%, see Table 19). A few compounds are more difficult to predict (e.g. Gabapentin, Irbersartan, Metoprolol, Diclofenac), see Figure 36. A possible explanation is that the local effects at the ozone inlet system (via a side-stream) in the pilot are not incorporated into the model (in the laboratory the ozone is dissolved first before the OMPs are added).

The AOP models can be applied to scenario studies, design studies and model predictive control. In scenario studies, the effect of the AOP on the effluent quality can be predicted for different scenarios (e.g. operational conditions of the AOP, seasonal effects or changes in water quality parameters). In design studies, the operational parameters and energy consumptions can be estimated from the model results to meet the required effluent quality . The models can also be used to control full-scale systems to match the desired effluent quality or reduce energy consumption. Due to the large variations in effluent water quality, the models can be used to set the UV, H_2O_2 or O_3 dose based upon incoming water quality parameters in order to obtain a specific effluent OMP concentration.

The model has been built for Walcheren water. For use in other wastewater effluents, first the water quality parameters (pH, DOC, HCO_3^-, NO_2^-, Br^-, etc.) need to be set. In addition the most important parameter that needs to be tuned in the model is the DOC reaction rate constant with OH. radicals and/or ozone. These constants were calibrated for Walcheren water, but also worked well for Horstermeer water in the UV/H_2O_2 lab-scale tests. But for other effluents, these constants may need to be set from additional laboratory experiments for a particular effluent.

For drinking water purposes, the AOP models are built into a webtool called AquaPriori, that calculates AOP removal percentages for an arbitrary organic micropollutant using the combination of QSPR models (statistical models that predict the relevant kinetic parameters based upon molecular structure) and AOP models. This tool can be used to make a quick assessment of how the AOP system would remove a new micropollutant. The AOP models developed in the current project for wastewater effluent can be added to the AquaPriori tool by adding the reaction scheme described in this report.

The formation of by-products and specifically bromate during ozone treatment could be added to the model in the future. In the experiments high bromate concentrations were formed at high ozone dosages, however experience from practice learn that ozone dosage of around 0.6 g O_3/DOC are often sufficient to reach juridical targets, and applying multi-staging ozonation and other measures are still possible to control bromate formation. Using a model that predict bromate formation could also help in finding an optimization between bromate formation and OMP removal.

Table 19: Overview of average modelled removal and mean absolute error (MAE) between measured and modelled removal percentage for all conditions in laboratory experiments and pilot experiments for UV/H_2O_2 and O_3 process.

Process	Condition	Removal (%)	MAE (%)	Process	Condition	Removal (%)	MAE (%)
Lab UV/H_2O_2 (600 mJ/cm^2)	MQ 0 mg/L H_2O_2	25.8	7.5	Lab O_3	Walcheren 0.84 mg/L O_3	29.6	7.4
	MQ 10 mg/L H_2O_2	76.3	4.9		Walcheren 1.68 mg/L O_3	50.8	11.0
	MQ 20 mg/L H_2O_2	92.3	2.9		Walcheren 4.2 mg/L O_3	83.4	5.3
	Walcheren 0 mg/L H_2O_2	25.8	9.1				
	Walcheren 20 mg/L H_2O_2	48.0	7.8	Pilot O_3	Round 1, 0.26 O_3/DOC	53.6	11.1
	Walcheren 40 mg/L H_2O_2	66.5	8.4		Round 2, 0.30 O_3/DOC	53.2	23.6
	Walcheren ongefilterd 0 mg/L H_2O_2	25.9	12.6		Round 3, 0.56 O_3/DOC	83.3	5.5
	Walcheren ongefilterd 20 mg/L H_2O_2	48.0	17.9		Round 4, 0.52 O_3/DOC	78.5	6.8
	Walcheren verdund 20 mg/L H_2O_2	75.6	9.2		Round 1, 0.53 O_3/DOC	82.8	7.0
	Horstermeer 20 mg/L H_2O_2	62.1	9.7		Round 2, 0.58 O_3/DOC	81.7	15.5
	Horstermeer verdund 20 mg/L H_2O_2	81.7	4.3		Round 3, 1.04 O_3/DOC	88.1	9.3
					Round 4, 0.92 O_3/DOC	84.2	12.5
Pilot UV/H_2O_2	Round 1, 960 mJ/cm^2-38 mg/L H_2O_2	95.2	6.6		Round 1, 0.66 O_3/DOC	86.1	7.1
	Round 2, 1319 mJ/cm^2-54 mg/L H_2O_2	99.6	3.1		Round 2, 0.74 O_3/DOC	85.5	13.8
	Round 3, 1452 mJ/cm^2-36 mg/L H_2O_2	98.6	2.2		Round 3, 0.98 O_3/DOC	87.9	11.0
	Round 4, 1370 mJ/cm^2-44 mg/L H_2O_2	100.0	2.5		Round 4, 1.32 O_3/DOC	88.3	10.6
	Round 1, 474 mJ/cm^2-19 mg/L H_2O_2	62.3	10.7		Round 1, 0.52 O_3/DOC (no spike)	82.6	7.1
	Round 2, 659 mJ/cm^2-25 mg/L H_2O_2	83.0	10.3		Round 2, 0.55 O_3/DOC (no spike)	80.5	16.6
	Round 3, 547 mJ/cm^2-20 mg/L H_2O_2	67.0	11.0		Round 3, 1.10 O_3/DOC (no spike)	88.2	13.3
	Round 4, 674 mJ/cm^2-21 mg/L H_2O_2	92.8	4.1		Round 4, 0.90 O_3/DOC (no spike)	87.1	12.0
	Round 1, 478 mJ/cm^2-19 mg/L (no spike)	62.5	12.4				
	Round 2, 645 mJ/cm^2-25 mg/L (no spike)	82.6	10.8				
	Round 3, 571 mJ/cm^2-21 mg/L (no spike)	69.8	9.3				
	Round 4, 674 mJ/cm^2-26 (no spike)	95.2	4.0				

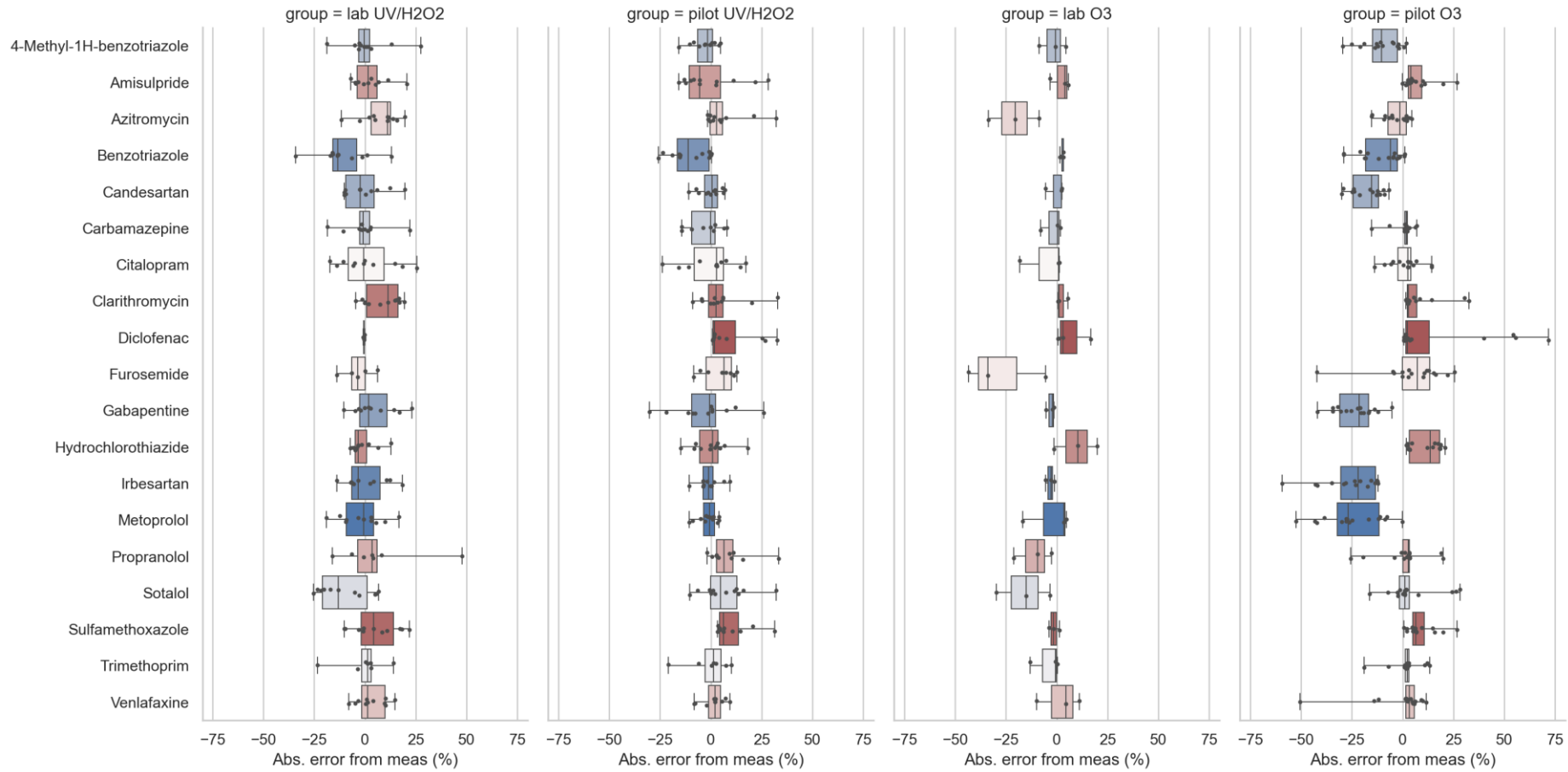

Figure 36: Overview of differences between modelled and measured degradation percentage for the 19 compounds in laboratory and pilot experiments for UV/H_2O_2 and O_3.

5 Conclusions

The overall conclusions of TKI Belissima are summarized as follows:

- The CAS ASDM model, enhanced with OMP removal mechanisms and kinetic coefficients, was able to successfully simulate the removal of the 11 tested OMPs, with results validated by measurements at the full-scale Walcheren WWTP. The model's simulated concentrations matched well with actual measured concentrations, demonstrating its validity and potential for optimising OMP removal mechanisms alongside conventional pollutants.
- The removal efficiency of OMPs in activated sludge (CAS) systems varies significantly, with some compounds like Clarithromycin, Propranolol and Sulfamethoxazole showing high removal rates, while others such as Carbamazepine, Diclofenac, and Hydrochlorothiazide exhibit poor removal. This suggests the need for additional or alternative treatment steps to enhance the removal of persistent compounds, as even those with relatively high removal efficiencies can still be present at significant concentrations in the effluent.
- Laboratory and pilot experiments at the WWTP, showed that both UV-H_2O_2 and O_3 systems are able to achieve an average OMPs removal of more than 80% for almost all tested compounds (19 OMPs); at the highest UV dose (about 1.000 mJ/cm^2 and higher) and high H_2O_2 concentrations (around 40 mg/L) almost all compounds are removed more than 90%; and at O_3 concentration of 0.6 g O_3 per g DOC most compounds are removed by 70% or more, and at O_3 concentration of 0.9 g O_3 per g DOC all but one compound are removed 80% or above. But for Walcheren effluent with high bromide content (on average 10 times higher than in other wastewater effluents in the Netherlands) bromate formation becomes substantial at these higher O_3 concentrations in a single-stage system (forming 10 µg/L BrO_3 or more). In practice, bromate can be better controlled by applying multiple stages and an ozone dose of about 0.6 g O_3 per g DOC.
- The developed UV-H_2O_2 model can accurately predict both lab- and pilot-scale experiments for the 19 tested OMPs. Unfiltered secondary effluent is more difficult to predict possibly due to shadowing, light reflection or scavenging of radicals by the particles. Therefore more reliable model results are obtained for systems with a sand filtration step upstream to the UV-H_2O_2.
- The developed O_3 model predicts accurately the lab-experiments results but is less accurate for the pilot-scale experiments, for compounds such as gabapentin, irbesartan, metoprolol and diclofenac; an explanation might be related with the side-stream ozone injection, which differs from the lab conditions. Also the ozone model may be more sensitive to the DOC composition, it was calibrated using the lab tests, but the DOC composition may be different during the pilot tests.
- In the combined scenario testing (enhanced CAS ASDM model with AOP models), the most relevant secondary effluent quality characteristics are DOC, NO_2^- and to a lesser extent (bi)carbonate and Br^-. A pre-treatment step (coagulation/sand filtration) can be applied to reduce DOC concentrations, resulting in a more efficient degradation. UV transmittance is also relevant for the energy consumption of the UV-H_2O_2 and can be improved by applying the same pre-treatment step. A techno-economical comparison would be needed to judge if an additional pre-treatment would be beneficial.
- The scenario testing of combined modelling showed that the contribution of the CAS is relevant for the removal of some OMPs (i.e. OMPs with lower removal percentages by the AOP (~60%), benzotriazole and metoprolol), when the AOP apply moderate operational conditions (600 mJ/cm^2 and 20 mg/L H_2O_2 or 5 mg/L O_3). For other OMPs, the removal by the CAS is small, e.g. compounds that already have a high removal by the AOP.
- Depending on the influent concentrations of OMPs and the required effluent concentration after AOP, combining the prediction of both the CAS and AOP models may assist in obtaining the desired removal percentage or to lower the energy consumption or chemical dosing of the AOP. Regarding summer and winter

seasons, the influence of temperature in the AOPs is small. Biological systems, such as the CAS, are affected by temperature, therefore seasonal effects are expected.

Implications for further research, practice and policy development

- Despite promising results, capturing the complex removal mechanisms in the CAS for each OMP remains challenging. The limited availability of detailed influent and effluent OMP data hinders model validation and robustness. Regular and rigorous OMP analysis, which is often costly and infrequent, is essential for accurate modelling, especially given the fluctuations in OMP concentrations.
- Enhancing the OMP fate model should include incorporating retransformation kinetics for all targeted OMPs, as currently, only Diclofenac and Carbamazepine are fully integrated in the CAS modelling. Further research is needed to determine removal kinetic rates and coefficients for other OMPs under varying redox conditions.
- The QSAR AOP models were built for Walcheren water. To use the QSAR AOP models in other wastewater effluents, requires measurement of the water quality parameters (pH, DOC, HCO_3-, NO_2-, Br-, etc.). The most important parameter is the DOC reaction rate constant with OH-radicals and/or ozone. In TKI Bellissima these constants were calibrated for Walcheren water, but also worked well for Horstermeer water in the UV/H_2O_2 lab-scale tests. Nevertheless, for other effluents, these constants may need to be set, requiring additional laboratory experiments.
- The QSAR O_3 AOP model could be extended with the formation of by-products and specifically bromate. In the experiments, high bromate concentrations were formed at high ozone dosages, however practice shows that ozone dosage of around 0.6 g O_3/DOC is often enough to reach legal targets. Applying multi-staging ozonation and other measures are still possible to control bromate formation. Using a model that predicts bromate formation can also help in finding an optimization between bromate formation and OMP removal.
- In practice, the validated models can be used by WWTP operators to optimize treatment processes, reduce operational costs, and enhance the removal efficiency of OMPs, ultimately leading to better environmental protection.
- This research can lead to the development of more comprehensive models and innovative treatment technologies.
- Policymakers can leverage these findings to implement regulations that require detailed and regular monitoring of OMPs in wastewater, ensuring more robust data for model validation and operational improvements.

Extended conclusions can be found in sections 2.6.3; 3.5 and 4.4.

6 Produced tools and how to use them

The TKI Belissima project goal was to develop tools that enable the project partners to optimize OMP removal in WWTPs. The tools created are based on modelling the CAS system and AOP post-treatment technologies, specifically UV-H_2O_2 and single-stage O_3. In both modelling exercises, existing models and knowledge were used, followed by calibration and validation using wastewater samples (influent, sludge and secondary effluent) from the Walcheren WWTP.

Modelling of operations and processes in WWTPs is complex, thus, the success of TKI Belissima relied on prior relevant knowledge - both from wastewater treatment processes modelling (in the case of the CAS model) and drinking water modelling (in the case of UV-H_2O_2 and single-stage O_3). Calibration and validation are essential steps, using historical data from WWTPs to calibrate the integrated model and ensure it accurately represents biological, physical and chemical processes. Validation with actual plant data ensures the model reliably predicts OMP removal under various operational conditions. Practitioners can use the tools developed in this project to design more effective treatment systems that combine biological and chemical processes, leading to improved OMP removal.

In this project, two tools were developed:

1- A CAS-post-treatment tool: This tool integrates the removal of OMPs in the CAS with known post-treatment technologies (referring to Activity 7, in Figure 1) – Tool 1
2- An AOP post-treatment tool: This tool includes QSAR models and kinetic models for UV-H_2O_2 and single-stage O_3 applied for secondary wastewater effluent – Tool 2

Regarding Tool 1, integrating the OMP removal model in Conventional Activated Sludge (CAS) systems with post - treatment technologies, into a single tool can enhance the ability of waterboards, end-users and practitioners to design, operate, and optimise wastewater treatment plants (WWTPs) for OMP removal. In TKI Belissima, this integration was done using the comprehensive commercial wastewater modelling software BioWin, which supports many other models, like ASM, ADM, pH model and N_2O model. Using the model builder functions in BioWin helped to code and input the four (4) processes of OMP removal in activated sludge systems (Section 3.2). The model builder function of Biowin also allowed to include post-treatment removal efficiencies as a white box. The removal efficiencies, as fixed percentages of removal, can be derived from various data sources, such as literature, experimental or modelling exercises (such as kinetic models with QSAR, as applied in tool 2). Data integration involved merging datasets required for CAS and post-treatment technologies, ensuring consistent data formats and units, including influent characteristics, design and operational parameters, and kinetic data. The CAS and post-treatment processes should be sequentially linked within the model, such as simulating the activated sludge process first to predict the effluent OMP concentrations, which are then used as input for the post-treatment tool.

An illustration of the CAS post-treatment tool is shown in Figure 37, in this case for the CAS-AOP combination. Figure 37 shows the removal of OMP 4-5-methylbenzotriazole using a combination of activated sludge and advanced oxidation processes. In this example, the OMP fate model in CAS is combined with the AOP removal efficiency (set at 80% for 4-5-methylbenzotriazole) and integrated into the BioWin ASDM. Users can adjust the removal percentage for each OMP within the tool, tailoring it to reflect the specific removal efficiencies achieved by the post-treatment. As aforementioned the removal percentages can be obtained from literature, experiments or modelling. This integration allows for more precise modelling and optimization of OMP removal processes in wastewater treatment using a combination of activated sludge systems and post-treatment technologies, in this example the advanced oxidation processes. In summary, the influent 4-5-methylbenzotriazole concentration is 0.92

µg/L, after the CAS, the treated effluent 4-5-methylbenzotriazole concentration is 0.85 µg/L and after the AOP, the final concentration in the effluent is 0.17 µg/L.

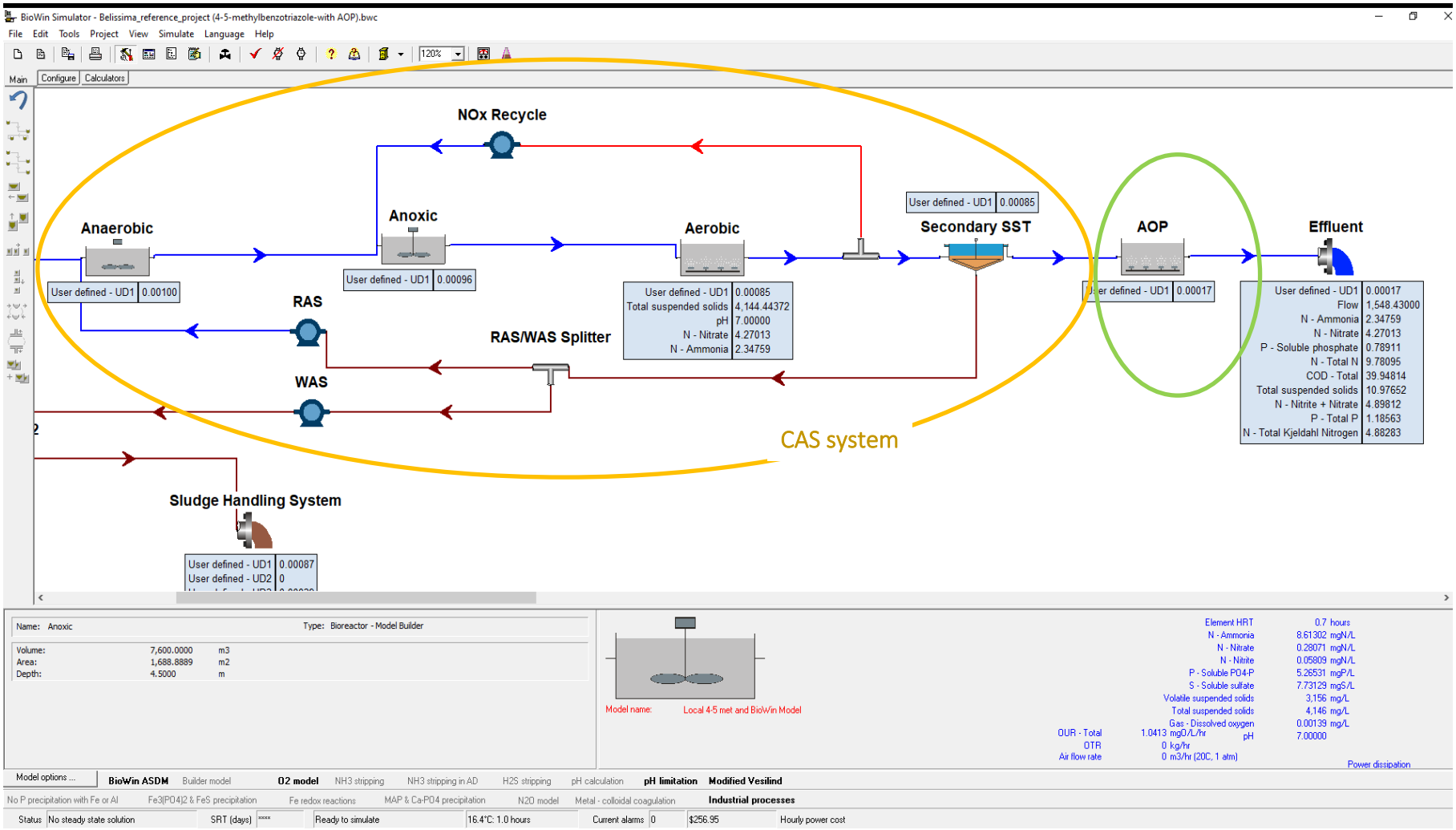

Figure 37: Integration of CAS and AOP processes in BioWin to be used as a combined tool for OMP removal

Concerning other post-treatment technologies, Table 20 shows OMP removal efficiencies, obtained in literature, than can be used as a reference. As previously mentioned, users can adjust the removal percentage for each OMP within the tool, in order to reflect the specific removal efficiencies achieved by the post-treatment.

Table 20- Removal rates of OMPs per post-treatment technology [%] obtained in full-scale WWTP campaigns. Sources: [(1)] Bourgin, Beck et al. (2018), 0.54±005 gO_3/g DOC as recommended ozone dosage, removal rates excluding conventional activated sludge removal; [(2)] several references referred by Mulder, Antakyali et al. (2015), PAC added to the effluent in a dosage of 1,1 g PAC/g DOC; contact time 35 min for effluent DOC of 11 mgL^{-1}; [(3)]several references referred by Mulder, Antakyali et al. (2015); GAC 30 min of empty bed contact time, standing time of 6 months, bed volumes of 8.800.

OMP	Ozone [(1)]	PAC [(2)]	GAC [(3)]
benzotriazole	74 ± 3	> 80	93
Clarithromycin	> 95 ± 1	> 80	> 80
Carbamazepine	> 98 ± 1	> 80	90
diclofenac	100 ± 1	60-80	79
metoprolol	94 ± 1	> 80	91
Hydrochlorothiazide	> 98 ± 2		
4- and 5-methylbenzotriazole	89± 4	> 80	95
propranolol			
sotalol			46
Sulfamethoxazole	> 97±1	60-80	30-60
Trimethoprim	> 61± 15		

Tool 1 has been developed in BioWin, therefore it will require BioWin software to be able to use it. BioWin is owned by EnviroSim Associates Ltd and the licence can be purchased by contacting them. All the BioWin files produced for the removal of the 11 target OMPs can be made available to the partners of this project on request.

Tool 2, relying on QSAR models and kinetic models for UV-H_2O_2 and single-stage O_3, for secondary effluent, will provide more accurate results about AOP performance, than through the use of fixed removal percentages obtained in literature, as applied in tool 1. In tool 2, changes in water quality of the secondary effluent (such as DOC, bicarbonate, etc.) can be used to update the removal percentages of the AOPs. As for Tool 2, the QSAR models and kinetic models for UV-H_2O_2 and single-stage O_3, for secondary wastewater effluent, developed within TKI Belissima, can be integrated into a KWR-owned web-tool AquaPriori. AquaPriori is designed primarily for drinking water companies and estimates the removal of organic micropollutants in membrane filtration, activated carbon filtration, advanced oxidation and soil passage. The web-tool AquaPriori can also be made available to the partners of this project, upon request, for a yearly subscription fee.

References

Benitez, F.J., Acero, J.L., Real, F.J., Roldán, G. and Rodríguez, E. 2015. Ozonation of benzotriazole and methylindole: Kinetic modeling, identification of intermediates and reaction mechanisms. Journal of Hazardous Materials 282, 224-232.

Borowska, E., Bourgin, M., Hollender, J., Kienle, C., McArdell, C.S., von Gunten, U. 2016. Oxidation of cetirizine, fexofenadine and hydrochlorothiazide during ozonation: Kinetics and formation of transformation products. Water Research, Volume 94, 350-362.

Bourgin, M., Borowska, E., Helbing, J., Hollender, J., Kaiser, H.-P., Kienle, C., McArdell, C.S., Simon, E. and von Gunten, U. 2017. Effect of operational and water quality parameters on conventional ozonation and the advanced oxidation process O_3/H2O2: Kinetics of micropollutant abatement, transformation product and bromate formation in a surface water. Water Research 122, 234-245.

Bourgin, M., Beck, B., Boehler, M., Borowska, E., Fleiner, J., Salhi, E., Teichler, R., von Gunten, U., Siegrist, H., McArdell, C.S. 2018. Evaluation of a full-scale wastewater treatment plant upgraded with ozonation and biological post-treatments: Abatement of micropollutants, formation of transformation products and oxidation by-products. Water Research, Volume 129, 486-498, https://doi.org/10.1016/j.watres.2017.10.036.

Buffle, M.-O. and von Gunten, U. 2006. Phenols and Amine Induced HO• Generation During the Initial Phase of Natural Water Ozonation. Environmental Science & Technology 40(9), 3057-3063.

Canonica, S., Meunier, L., von Gunten, U. 2008. Phototransformation of selected pharmaceuticals during UV treatment of drinking water. Water Research 42 (1-2), 121–128.

Dodd, M.C., Buffle, M.-O. and von Gunten, U. 2006. Oxidation of Antibacterial Molecules by Aqueous Ozone: Moiety-Specific Reaction Kinetics and Application to Ozone-Based Wastewater Treatment. Environmental Science & Technology, 40(6), 1969-1977.

Elawwad, A., Matta, M., Abo-Zaid, M., & Abdel-Halim, H. 2019. Plant-wide modeling and optimization of a large-scale WWTP using BioWin's ASDM model. Journal of Water Process Engineering, 31, 100819, https://doi.org/10.1016/J.JWPE.2019.100819

Grung, M.,Ka¨llqvist, T.; Sakshaug, S.; Skurtveit, S., Thomas, K. V. 2008. Environmental assessment of Norwegian priority pharmaceuticals based on the EMEA guideline. Ecotoxic. Environ. Safety,71 (2), 328–340.

Gujer, W., Henze, M. 1991. Activated sludge modeling and simulation. Water Science & Technology, 23 (4-6), 1011-1023.

Harmsen, D. J. H. 2004. Protocol collimated beam UV. KWR rapport BTO 2004.014

Hofman-Caris, C. H. M. ,Wols, B.A. 2020. Voorspelling en validatie van de verwijdering van organische microverontreinigingen uit water; deel 2: oxidatieve processen, BTO 2020.063, KWR Water Research Institute, Nieuwegein, The Netherlands.

Huber, M.; Canonica, S. 2003. Oxidation of pharmaceuticals during ozonation and advanced oxidation processes. Environ. Sci. Technol. 37, 1016–1024.

Hübner, U., S. Keller, Jekel, M. 2013. Evaluation of the prediction of trace organic compound removal during ozonation of secondary effluents using tracer substances and second order rate kinetics. Water Research, Volume 47, 17, 6467-6474.

Javier Rivas, F., Sagasti, J., Encinas, A., & Gimeno, O. 2011. Contaminants abatement by ozone in secondary effluents. Evaluation of second-order rate constants. Journal of Chemical Technology & Biotechnology, 86(8), 1058–1066.

Joss, A., Zabczynski, S., Gobel, A., Hoffmann, B., Loffler, D., McArdell, C. S., Ternes, T. A., Thomsen, A., Siegrist, H. 2006. Biological degradation of pharmaceuticals in municipal wastewater treatment: proposing a classification scheme. Water Res, 40(8), 1686-1696, doi:10.1016/j.watres.2006.02.014

Kim, I., Yamashita, N., Tanaka, H. 2009. Photodegradation of pharmaceuticals and personal care products during UV and UV/H2O2 treatments. Chemosphere, 77 (4), 518–525

Lee, Y., Gerrity, D., Lee, M., Bogeat, A. E., Salhi, E., Gamage, S., Von Gunten, U. 2013. Prediction of micropollutant elimination during ozonation of municipal wastewater effluents: Use of kinetic and water specific information. Environmental Science and Technology, 47(11), 5872–5881.

Lee, Y., Kovalova, L., McArdell, C. S., & von Gunten, U. 2014. Prediction of micropollutant elimination during ozonation of a hospital wastewater effluent. Water Research, 64, 134–148.

Lousada-Ferreira, M. 2022. Fate of Organic Micropollutants in Activated Sludge Systems. KWR 2022.090. TKI Belissima. 49 pages. August. Nieuwegein. The Netherlands.

Lutze, H., 2005. Ozonung von Benzotriazolen. Bachelor Thesis, Universität Duisburg, Essen.

Martins, T.A.E., Munoz Sierra, J., Nieuwlands, J.A., Lousada-Ferreira, M., Amaral, L. 2024. Micropollutant biotransformation under different redox conditions in *PhoRedox* conventional activated sludge systems. Environmental Technology & Innovation, 35, doi: 10.1016/j.et.2024.103639

Mathon, B., Coquery, M., Liu, Z., Penru, Y., Guillon, A., Esperanza, M., Choubert, J. M. 2021. Ozonation of 47 organic micropollutants in secondary treated municipal effluents: Direct and indirect kinetic reaction rates and modelling. Chemosphere, 262, 127969.

Meite, L., Szabo, R., Mazellier, P., De Laat, J., 2010. Kinetics of phototransformation of emerging contaminants in aqueous solution. Revue des Sciences de l'Eau 23 (1), 31–39.

Miklos, D.B., Hartl, R., Michel, P., Linden, K.G., Drewes, J.E. and Hübner, U. 2018. UV/H2O2 process stability and pilot-scale validation for trace organic chemical removal from wastewater treatment plant effluents. Water Research 136, 169-179.

Mulder, M., D. Antakyali and Ante S. 2015. Costs of Removal of Micropollutants from Effluents of Municipal Wastewater Treatment Plants-General Costs Estimates for the Netherlands based on Implemented Full Scale Post Treatments of Effluents of Wastewater Treatment Plants in Germany and Switzerland. The Netherlands, Stowa Waterboard the Dommel.

Naik, D.B., Moorthy, P.N. 1995. Studies on the transient species formed in the pulse-radiolysis of benzotriazole, Radiat. Phys. Chem., 46 (3), 353-357

Pereira, V.J., Weinberg, H.S., Linden, K.G., Singer, P.C. 2007. UV degradation kinetics and modeling of pharmaceutical compounds in laboratory grade and surface water via direct and indirect photolysis at 254 nm. Environ. Sci. Technol. 41, 1682–1688. https://doi.org/10.1021/es061491b

Plósz, B.G., Leknes, H., Thomas, K.V. 2010. Impacts of competitive inhibition, parent compound formation and partitioning behaviour on antibiotic trace chemicals removal in activated sludge: measurements and modelling. Environ. Sci. Technol. 44 (2), 734-742

Plósz, B.G., Langford, K.H., Thomas, K.V. 2012. An activated sludge modeling framework for xenobiotic trace chemicals (ASMX): assessment of diclofenac and carbamazepine. Biotechnol Bioeng., 109(11),2757–69.

Polesel, F., Andersen, H.R., Trapp, S. & Plósz, B.G. 2016. 2016. Removal of Antibiotics in Biological Wastewater Treatment Systems-A Critical Assessment Using the Activated Sludge Modeling Framework for Xenobiotics (ASM-X). https://pubs.acs.org/doi/10.1021/acs.est.6b01899

Real, F. J., Acero, J. L., Benitez, F. J., Roldan, G., Fernandez, L. C., 2010. Oxidation of hydrochlorothiazide by UV radiation, hydroxyl radicals and ozone: Kinetics and elimination from water systems. Chemical Engineering Journal 160 (1), 72–78

RIVM 2019. Informatieblad- Nut en noodzaak van normen voor medicijnresten in oppervlaktewater. W. e. S. Rijksinstituut voor Volksgezondheid en Milieu; Ministerie van Volksgezondheid. Bielthoven, Nederland, Opdracht van het Ministerie van Infrastructuur en Waterstaat.

Sin, G., Al, R. 2021. Activated sludge models at the crossroad of artificial intelligence—A perspective on advancing process modeling. Npj Clean Water, 4(1), 1–7.

Spanjers, H., Vanrolleghem, P., Nguyen, K., Vanhooren, H., Patry, G. G. 1998. Towards a simulation-benchmark for evaluating respirometry-based control strategies. Water Sci. Technol., 37 (12), 219–226

Ternes, T. A.; Joss, A. 2006. Human Pharmaceuticals, Fragrances - The Challenge of Micropollutants Management. IWA Publishing, London

Virtanen, P., Gommers, R., Oliphant, T.E., Haberland, M., Reddy, T., Cournapeau, D., Burovski, E., Peterson, P., Weckesser, W., Bright, J., van der Walt, S.J., Brett, M., Wilson, J., Millman, K.J., Mayorov, N., Nelson, A.R.J., Jones, E., Kern, R., Larson, E., Carey, C.J., Polat, İ., Feng, Y., Moore, E.W., VanderPlas, J., Laxalde, D., Perktold, J., Cimrman, R., Henriksen, I., Quintero, E.A., Harris, C.R., Archibald, A.M., Ribeiro, A.H., Pedregosa, F., van Mulbregt, P., Vijaykumar, A., Bardelli, A.P., Rothberg, A., Hilboll, A., Kloeckner, A., Scopatz, A., Lee, A., Rokem, A., Woods, C.N., Fulton, C., Masson, C., Häggström, C., Fitzgerald, C., Nicholson, D.A., Hagen, D.R., Pasechnik, D.V., Olivetti, E., Martin, E., Wieser, E., Silva, F., Lenders, F., Wilhelm, F., Young, G., Price, G.A., Ingold, G.-L., Allen, G.E., Lee, G.R., Audren, H., Probst, I., Dietrich, J.P., Silterra, J., Webber, J.T., Slavič, J., Nothman, J., Buchner, J., Kulick, J., Schönberger, J.L., de Miranda Cardoso, J.V., Reimer, J., Harrington, J., Rodríguez, J.L.C., Nunez-Iglesias, J., Kuczynski, J., Tritz, K., Thoma, M., Newville, M., Kümmerer, M., Bolingbroke, M., Tartre, M., Pak, M., Smith, N.J., Nowaczyk, N., Shebanov, N., Pavlyk, O., Brodtkorb, P.A., Lee, P., McGibbon, R.T., Feldbauer, R., Lewis, S., Tygier, S., Sievert, S., Vigna, S., Peterson, S., More, S., Pudlik, T., Oshima, T., Pingel, T.J., Robitaille, T.P., Spura, T., Jones, T.R., Cera, T.,

Leslie, T., Zito, T., Krauss, T., Upadhyay, U., Halchenko, Y.O., Vázquez-Baeza, Y. and SciPy, C. 2020. SciPy 1.0: fundamental algorithms for scientific computing in Python. Nature Methods 17(3), 261-272.

Vries, D., Wols, B.A., Voogt, W.P. 2013. Removal efficiency calculated beforehand: QSAR enabled predictions for nanofiltration and advanced oxidation. Water Science & Technology: Water Supply, 13 (6), 1425-1436.

Vogna, D., Marotta, R., Napolitano, A., Andreozzi, R. and d'Ischia, M. 2004. Advanced oxidation of the pharmaceutical drug diclofenac with UV/H2O2 and ozone. Water Research, 38(2), 414-422.

Wols, B. A., Hofman-Caris, C. H. M. 2012. Review of photochemical reaction constants of organic micropollutants required for UV advanced oxidation processes in water. Water Research 46(9), 2815-2827.

Wols, B.A., Harmsen, D.J.H., Beerendonk, E.F. and Hofman-Caris, C.H.M. 2014. Predicting pharmaceutical degradation by UV (LP)/H2O2 processes: A kinetic model. Chemical Engineering Journal 255, 334-343.

Wols, B.A., J. Immink, Hofman-Caris. C.H.M. 2024, Voorspellingsmodellen voor de verwijdering van OMV's, BTO 2024.014, KWR Water Research Institute, Nieuwegein, The Netherlands.

Zimmermann, S. G., Wittenwiler, M., Hollender, J., Krauss, M., Ort, C., Siegrist, H., von Gunten, U. 2011. Kinetic assessment and modeling of an ozonation step for full-scale municipal wastewater treatment: Micropollutant oxidation, by-product formation and disinfection. Water Research, 45(2), 605–617.

I Annex – Organic Micropollutants (OMPs) Indicators Lists

OMPs indicators list- I&V (RIVM, 2019)

1. 4-5 Methylbenzotriazole,
2. Benzotriazole
3. Carbamazepine,
4. Clarithromycin,
5. Diclofenac,
6. Hydrochlorothiazide,
7. Metoprolol,
8. Propranolol,
9. Sotalol,
10. Sulfamethoxazole
11. Trimethoprim

OMPs indicators list- Stowa- 2021

1. 4-5 methylbenzotriazole (addition of the 2 compounds)
2. Amisulpride
3. Azithromycin
4. Benzotriazole
5. Candesartan
6. Carbamazepine
7. Citalopram
8. Clarithromycin
9. Diclofenac
10. Furosemide
11. Gabapentine
12. Hydrochlorothiazide
13. Irbesartan
14. Metoprolol
15. Propranolol
16. Sotalol
17. Sulfamethoxazole
18. Trimethoprim
19. Venlafaxine

OMPs indicators list – new EU Urban Wastewater Directive (26-10-2022 proposal)[2]

1. 4- and 6- methylbenzotriazole (mixture of the 2 compounds) (category 2)
2. Amisulpride (category 1)
3. Benzotriazole (category 2)
4. Candesartan (category 2)

[2] The new EU Urban Wastewater Directive (26-10-2022 proposal) divides the OMP substances in the 2 categories: category 1 as substances that can be easily treated; category 2 as substances that can be easily disposed of. The 80% average percentage removal, proposed in the new law, is calculated for at least 6 substances, with category 1 substances being twice the number of substances of category 2.

5. Citalopram (category 1)
6. Clarithromycin (category 1)
7. Diclofenac (category 1)
8. Hydrochlorothiazide (category 1)
9. Irbesartan (category 2)
10. Metoprolol (category 1)
11. Venlafaxine (category 1)

II Annex- Biotransformation constant rates

Environmental Technology & Innovation 35 (2024) 103639

Contents lists available at ScienceDirect

Environmental Technology & Innovation

journal homepage: www.elsevier.com/locate/eti

Micropollutant biotransformation under different redox conditions in *PhoRedox* conventional activated sludge systems

Tiago A.E. Martins [a,d], Julian D. Muñoz Sierra [a,b,*], Jo A. Nieuwlands [c], Maria Lousada-Ferreira [a], Leonor Amaral [d]

[a] KWR Water Research Institute, Groningenhaven 7, Nieuwegein 3433 PE, the Netherlands
[b] Section Sanitary Engineering, Department of Water Management, Delft University of Technology, Stevinweg 1, Delft 2628 CN, the Netherlands
[c] Water Authority Scheldestromen, Middelburg 4330 ZW, the Netherlands
[d] CENSE (Center for Environmental and Sustainability Research) & CHANGE (Global Change and Sustainability Institute), Department of Environmental Engineering Sciences, NOVA School of Science and Technology, Caparica 2829-516, Portugal

ARTICLE INFO

Keywords:
Micropollutants
Activated sludge
Redox conditions
Biotransformation rate
Kinetics

ABSTRACT

The ecotoxicological safety of the water bodies relies on the reduction of micropollutant emissions from wastewater treatment plants (WWTP). The ecotoxicological safety of the water bodies relies on the reduction of micropollutant emissions from wastewater treatment plants (WWTP). Quantification of micropollutant removal at full-scale WWTP is scarce. To our knowledge, the anaerobic conversion rates determined at conventional activated sludge processes are, so far, scarcely available in the literature for most of the micropollutants. In this research, we quantified the biotransformation rate constants and the removal efficiencies of 16 micropollutants (4,5-methylbenzotriazole, azithromycin, benzotriazole, candesartan, carbamazepine, clarithromycin, diclofenac, gabapentin, hydrochlorothiazide, irbesartan, metoprolol, propranolol, sotalol, sulfamethoxazole, trimethoprim, and venlafaxine), under aerobic, anoxic, and anaerobic redox conditions; using as inoculum wastewater and biomass from a full-scale conventional activated sludge (CAS) system in the Netherlands. Clarithromycin was the compound that exhibited the highest aerobic (76%) and anaerobic (78%) removal efficiencies, while gabapentin showed the highest removal under anoxic conditions (91%). A preference for cometabolic biotransformation of the targeted micropollutants was observed. The highest biotransformation rate constants obtained were: at aerobic conditions clarithromycin with 1.46 $L.g_{SS}^{-1}.d^{-1}$; at anoxic conditions, gabapentin with 2.36 $L.g_{SS}^{-1}.d^{-1}$; and at anaerobic redox conditions clarithromycin with 1.87 $L.g_{SS}^{-1}.d^{-1}$. The obtained results of biotransformation rates will allow further modelling of micropollutant removal in CAS systems, under various redox conditions. These biotransformation rates can be added to extended ASM models to predict effluent concentration and optimize targeted advanced oxidation processes allowing savings in the operational costs and increasing the process viability.

1. Introduction

Many chemical compounds are used daily in households and industries, entering, therefore, the municipal sewage (e.g., through

* Corresponding author at: KWR Water Research Institute, Groningenhaven 7, Nieuwegein 3433 PE, the Netherlands.
E-mail address: julian.munoz@kwrwater.nl (J.D. Muñoz Sierra).

https://doi.org/10.1016/j.eti.2024.103639
Received 7 January 2024; Received in revised form 10 April 2024; Accepted 13 April 2024
Available online 15 April 2024

body excretions), and ending up in the wastewater treatment plants (WWTP) (Kennes-Veiga et al., 2022). The existent wastewater treatment plants are mainly based on biological treatments that were not designed to remove micropollutants, leading to their presence in the effluent (Kennes-Veiga et al., 2021). Nevertheless, activated sludge-based wastewater treatments have shown some extent of micropollutant removal (Bourgin et al., 2018).

The micropollutants may be removed from wastewater by biotransformation, sorption, or stripping (Joss et al., 2006). Biotransformation is the process by which microorganisms transform, degrade, or remove chemicals and according to the literature is usually the major removal mechanism, together with sorption (Kennes-Veiga et al., 2022). This mechanism is mainly affected by the WWTP parameters - hydraulic retention time (HRT) (Ruas et al., 2022), sludge concentration (Gusmaroli et al., 2020), sludge retention time (SRT) (Suarez et al., 2012), and redox condition (Falas et al., 2016). The redox condition is defined by the main electron acceptor available, which can oxidize other substances. The electron acceptors' nature and availability affect the biotransformation, as well as the microbial community, meaning that the redox condition will favour the enzymatic activity to biotransform the compounds (Kennes-Veiga et al., 2022). Three redox conditions are mainly present in conventional activated sludge (CAS) systems: aerobic, anoxic, and anaerobic. Falas et al. (2016) observed that coupling the aerobic and anaerobic conditions in the wastewater treatment processes could allow the removal of persistent micropollutants like venlafaxine and its metabolites.

Besides the WWTP design parameters, the micropollutant physicochemical characteristics also influence their biotransformation. Compounds with Log K_{ow} values lower than 3.2 are considered hydrophilic and it's expected for them to have a low sorption potential, on the other side, Log K_{ow} values greater than 4.0 indicate hydrophobic behaviour and that sorption may be the main removal mechanism (Gusmaroli et al., 2020). Nevertheless, compounds that are positively charged and with a refractory nature (e.g., atenolol) will mostly be removed by sludge sorption (Wirenfeldt Jensen et al., 2022). Similarly, compounds with a solid-water distribution coefficient (K_d) lower than 2.5 are more likely to stay in the aqueous phase while compounds with a K_d greater than 3.2 are more likely to sorb to solids (Golovko et al., 2021). The removal of micropollutants is expected to be higher at greater sludge concentrations, due to higher sorption potential and biomass to biotransform the compounds (Gobel et al., 2005).

To improve micropollutant biotransformation, the kinetic data is of the foremost importance, mainly to develop design and removal prediction models. Nevertheless, this information is still scarce. Some studies have been carried out to analyze the biotransformation of micropollutants in CAS systems, and which parameters affect that (Falas et al., 2016). However, most of them only determine micropollutant removal efficiencies without looking at the kinetics. Due to the increasing list of micropollutants present in wastewater, many have not been studied or identified yet. To get better insights, the EU created a Watch list with 297 key micropollutants aimed to be monitored and better studied (Mutzner et al., 2022). In the Netherlands, the Dutch Ministry of Infrastructure and Water Management proposed a selection of 11 from the 19 micropollutants proposed by the Dutch Foundation for Applied Water Management Research – STOWA (Moermond et al., 2019), to be monitored in the WWTP.

To the best of our knowledge, based on a performed literature review (see Table 5), no biotransformation rate constants of these 16 key micropollutants were found under anaerobic conditions nor determined in CAS systems. Few studies (Mazioti et al., 2015; Plosz et al., 2010; Suarez et al., 2010; Xue et al., 2010) have determined the biotransformation rates of some of these targeted micropollutants under anoxic conditions, while several studies focused only on determining them under aerobic conditions. Moreover, there was not any biotransformation rate constant found for the targeted compounds 4-,5-methylbenzotriazole, candesartan, hydrochlorothiazide, and venlafaxine. Nevertheless, many other studies have reported the removal efficiencies of these micropollutants under different redox conditions in CAS systems, as summarized in Table S1.

This study aims to determine the biotransformation rates of 16 targeted micropollutants (14 pharmaceuticals and 2 industrial chemicals – see Table 1) under aerobic, anoxic, and anaerobic conditions present in a PhoRedox activated sludge system. The obtained values were compared and looked over according to the metabolic/cometabolic pathway and correlation with physicochemical properties. Furthermore, the removal efficiencies of each compound under the different redox conditions were assessed.

2. Materials and methods

2.1. Sampling

To determine the biotransformation kinetics, batch experiments were conducted with wastewater from a Dutch WWTP, with a PhoRedox CAS configuration (Figure S1). The WWTP was designed for a maximum flow of 8 015 m^3/h, with an HRT of 6.2 h and an SRT of 25 days.

A sample campaign was conducted weekly to this WWTP, to minimize as much as possible the storage time, and guarantee new samples to feed the bioreactors. This campaign was made for five consecutive weeks in March and April. During the sampling campaign, the maximum temperature was 11 (±2) °C, the minimum temperature 5 (±1) °C and the precipitation 1.7 (±0,6) mm. The samples were taken from the influent, the activated sludge (taken from the tanks under the different redox conditions), and the effluent. Both influent and effluent were collected with 24 h samples with WWTP OMY *Efcon®* autosamplers (*Efcon B.V, Utrecht, The Netherlands*) to obtain representative samples. After collection, samples were transported and stored at 4 °C in a cold room before the experiments were conducted, never for more than 48 h.

2.2. Bioreactor set-up

The set-up consisted of two bioreactors of 2.5 L each, operated in batch mode in parallel. A total of 15 batch tests were carried out for 48 h. The reactors were equipped with a stirrer (200 rpm), a sampling system, online sensors (dissolved oxygen, pH, redox,

conductivity, and temperature), and an aeration/pH/stirring control system (*Applikon EZ-Control*) (Fig. 1). The bioreactors were placed against direct exposure to sunlight to minimize any photodegradation.

2.3. Operation

To mimic the WWTP environment, the dissolved oxygen was kept at 3.5 (±0.4) mg O_2/L (aerobic conditions); 0.2 mg O_2/L (anoxic conditions); 0.0 mg O_2/L (anaerobic conditions). Under anaerobic conditions, the concentration was kept by sparging nitrogen at a flow rate of 1 L N_2/h. The temperature during the experiment was regulated through room temperature control at 18.7 (±0.5)° C. pH was not corrected due to potential interferences of the reagents in the biotransformation rate (Table 2). Sludge solids concentration was set to about 0.50 (±0.05) g_{SS}/L to increase the experimental resolution, mainly of compounds with high biotransformation rates.

Batch experiments were carried out in duplicates per redox condition: I) the control batch, only with effluent; II) a batch with sludge diluted in the effluent; III) a batch with sludge diluted in the effluent and fed with primary influent (substrate) following the methodology proposed by Joss et al. (2006). The control tests were only performed once since no major changes were observed. The difference between batches II and III allows us to infer the influence of metabolic and cometabolic processes in the compound biotransformation (Edefell et al., 2021). Table 3 presents the wastewater characterization as well as the volume used per batch.

The batches were spiked with 5 mL of the stock solution to ensure a minimum analysis concentration of each compound. A stock solution prepared with *Mili-Q®* ultrapure water (*MilliporeSigma, Massachusetts, USA*), that contains all the targeted compounds was used. Table S2 shows the concentration of each compound in the stock solution as well as the theoretical oxygen demand of each.

Samples of 20 mL were taken from each batch at the times 0 min, 15 min, 40 min, 2 h, 6 h, 12 h, 24 h, and 48 h. Controls were only sampled at the beginning and end of the experiment (0 min and 48 h).

2.4. Analysis

After collection, the samples were filtered through an NC45 nitrocellulose membrane (*Whatman, Maidstone, UK*), stored in glass vials, and then preserved at −20 °C until analysis. All wastewater samples (influent, activated sludge, and effluent) were characterized. The suspended solids were analysed following the Standard Methods N° 2540, while the chemical oxygen demand (COD), total organic carbon (TOC), ammonium, nitrate, nitrite, and phosphate were determined using Cuvette Hach Test Kits.

To quantify the micropollutants, it was used direct injection of the sample on a C18 column in combination with mass spectrometry. Internal standards were first added to the wastewater sample, after which it was filtered through a 0.20 µm filter. After this, 100 µL of the sample was applied to the C18 analytical column. The analysis was performed using a *Shimadzu Nexera X2 HPLC* system coupled to a triple quadrupole *SCIEX 6500+* mass spectrometer. The mass spectrometer was equipped with a heated electrospray ionization interface (H-ESI) and measured according to the selected reaction monitoring (SRM) principle. The analysis was performed in positive ionization mode. For the chromatographic separation, a *Phenomenex Luna Omega Polar C18 column* (100 mm × 2.1 mm I.D., particle size 1.6 m) was used in combination with a *Phenomenex SecurityGuard Ultra precolumn*. The concentration was calculated based on an external calibration curve, whereby correction is made for the internal standards. The method's detection limit depends on the matrix and can vary between 0.0 and 0.1 µg/L.

2.5. Biotransformation rate constants determination

To determine the biotransformation rate constant a pseudo-first-order kinetics was used as shown in Eq. 1 and proposed by Joss

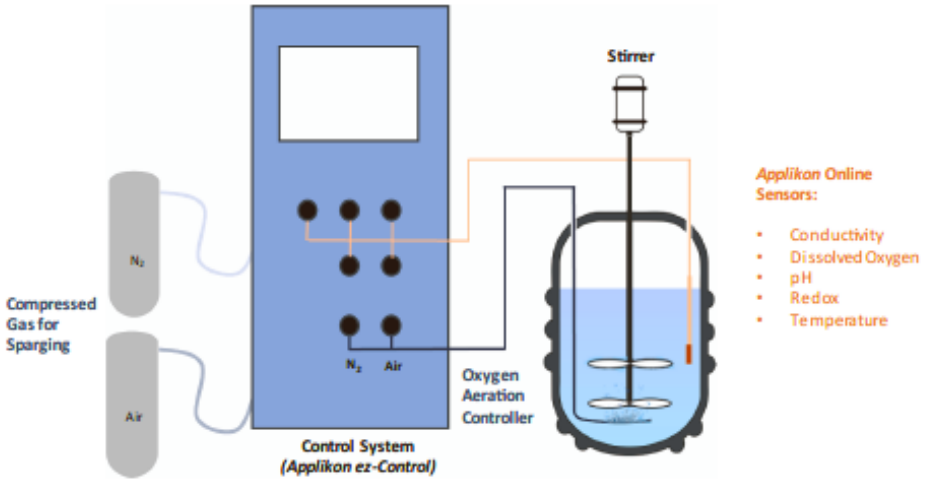

Fig. 1. Bioreactor set-up scheme for biotransformation batch tests.

Table 2
Operational conditions of the batch experiments under different redox conditions.

Parameter	Unit	Anaerobic	Anoxic	Aerobic	Average
Conductivity	mS/cm	1.26 ± 0.47	1.87 ± 0.10	2.05 ± 0.22	1.7 ± 0.5
Dissolved Oxygen	g O_2/L	0.0 ± 0.0	0.2 ± 0.1	3.5 ± 0.4	-
pH	-	9.1 ± 0.2	7.9 ± 0.5	7.9 ± 0.2	8.3 ± 0.7
Solids	g SS/L	0.46 ± 0.01	0.48 ± 0.01	0.49 ± 0.03	0.48 ± 0.02
Temperature	°C	18.5 ± 0.7	18.7 ± 0.3	19.1 ± 0.2	18.7 ± 0.5
Redox	mV	-161.3 ± 84.1	N.D	118.6 ± 23.2	-

N.D: Non Determined

Table 3
Composition of the batch experiments.

Parameters	Units	Effluent	Aerobic Activated Sludge	Anoxic Activated Sludge	Anaerobic Activated Sludge	Primary Influent (substrate)
Suspended Solids	g/L	0.03 ±0.02	4.50 ± 0.08	4.37 ± 0.08	4.93 ± 0.51	0.38 ± 0.39
Total Chemical Oxygen Demand	mg O_2/L	70 ± 34	5825 ± 460	5220	5885 ± 870	562 ± 216
Total Organic Carbon	mg C/L	70 ± 22	86 ± 4	61	65 ± 23	135 ± 26
Ammonia	mg NH_4/L	5 ± 3	7 ± 5	14	26 ± 19	41 ± 15
Nitrite	mg NO_2/L	0.17 ± 0.04	0.10 ± 0.04	0.02	0.02 ± 0.01	0.11 ± 0.06
Nitrate	mg NO_3/L	17 ± 5	3 ± 1	2	2 ± 0	3 ± 1
Phosphorous	mg PO_4/L	0.2 ± 0.1	2.9 ± 5.2	0.6	19.0 ± 11.2	9.4 ± 6.7
Batch I – Control: Volume	L	2.50	0.00			0.00
Batch II – AS: Volume	L	2.25	0.25			0.00
Batch III – AS+Substrate: Volume	L	2.00	0.25			0.25

et al. (2006) and Mazioti et al. (2015). This determination was carried out using K_d values from the literature (see Table S5), similar to what has been performed by Falas et al. (2016).

$$\frac{dC}{dt} = \frac{C_{t+dt} - C_t}{dt} = \frac{-k_{bio} \times X_{SS} \times C}{1 + K_d \times X_{SS}} \tag{1}$$

To simplify the determination, the equation was linearized using the natural logarithmic. First, the equation was organized in order of dC/C and reduced to a constant (k). Eq. 2 shows the process.

$$\frac{dC}{dt} = \frac{-k_{bio} \times X_{SS} \times C}{1 + K_d \times X_{SS}} \Leftrightarrow \quad \frac{dC}{C} = \frac{-k_{bio} \times X_{SS}}{1 + K_d \times X_{SS}} dt \Rightarrow \frac{dC}{C} = k \quad dt \tag{2}$$

Once simplified, Eq. 3 indicates the final linearized form.

$$\ln C = kt \quad dt \quad \Rightarrow \quad \ln C = \frac{-k_{bio} \times X_{SS}}{1 + K_d \times X_{SS}} t \tag{3}$$

After linearization of the equation, it was possible to obtain the biotransformation rate constant from the slope of Eq. 3, according to Eq. 4.

$$k_{bio} = -\frac{slope}{X_{SS}} \times (1 + K_d \times X_{SS}) \tag{4}$$

If in the batch test, for a compound, $K_d \times X_{SS}$ is lower than 0,1 this term was neglected meaning that less than 10% of the compound was sorped. Therefore, the constant can be determined by Eq. 5.

$$k_{bio} = -\frac{slope}{X_{SS}} \tag{5}$$

From the 16 micropollutants analysed, seven showed Kd x Xss $\leq$ 0,1: azithromycin, clarithromycin, metoprolol, propranolol, irbesartan, trimethoprim, and venlafaxine. For both candesartan and gabapentin, the distribution coefficient values in activated sludge were not found. However, this value was found for other matrixes, observing distribution coefficients lower than the one observed for clarithromycin (Berthod et al., 2017). Therefore, it was considered that the sorped fraction is lower than 10% for both candesartan and gabapentin and therefore negligible for the k_{bio} determination.

2.6. Correlation between biotransformation rate constants and micropollutant physicochemical properties

An attempt to correlate the biotransformation rate constants and the physicochemical properties was carried out. For that, the compounds were first grouped by their physicochemical properties (hydrophobicity, polarity, and solubility). Then, the average biotransformation constant per group was used to analyse hydrophobicity and polarity correlation. The solubility's linear correlation was analysed through the square-R of the obtained line after plotting the solubility and removal efficiency of each micropollutant.

3. Results and discussion

3.1. Control batch tests

The control experiments showed no substantial removal for the most of micropollutants However, gabapentin and irbesartan appeared to have some consistent degradation above the analytical error margin. Under anoxic conditions, both gabapentin and irbesartan showed to suffer some type of degradation, of about 20%. These degradations may be due to the chemical instability of the compounds (Jansook et al., 2022).

3.2. Biotransformation rate constants under different redox conditions

The obtained results of biotransformation rate constants for the targeted micropollutants were presented in Table S3 and Table S4 and synthesized in Table 4. These values were determined using the average distribution coefficients (K_d) obtained from previous studies (Table S5). The coefficient of determination for first-pseudo-kinetics linear correlation can be observed in Table S6. Average values of 0.91, 0.93 and 0.93 were obtained for aerobic, anoxic, and anaerobic conditions, respectively.

The substrate addition impact was not as substantial as expected since the effluent used had not undergone advanced treatment processes presenting still a high COD [70 (±34) mgO_2/L] (Table 3). Kennes-Veiga et al. (2022) inferred that COD highly influences micropollutant biotransformation mainly due to the general cometabolic removal pathway.

Following Joss et al. (2006) categorization, it can be concluded that candesartan, carbamazepine, diclofenac, and hydrochlorothiazide have low biotransformation constant rates (K_{bio}<0.1 $L.g_{SS}^{-1}.d^{-1}$; <20% of removal) under all the redox conditions. On the contrary, 4-,5-methylbenzotriazole, azithromycin, benzotriazole, clarithromycin, gabapentin, irbesartan, metoprolol, propranolol, trimethoprim, and sulfamethoxazole exhibited moderate values under all the redox conditions (0.1<K_{bio}<10 $L.g_{SS}^{-1}.d^{-1}$; removal between 20% and 90%). Sotalol and venlafaxine showed moderate biotransformation under all the redox conditions besides anaerobic conditions, in which negative values were obtained. Moreover, none of the compounds exhibited high biotransformation since they are all below 10 $L.g_{SS}^{-1}.d^{-1}$.

Table 5 points out our contribution under anoxic and anaerobic conditions. Besides, for aerobic conditions, it also fulfilled the K_{bio} gap for 4-,5-methylbenzotriazole, candesartan, hydrochlorothiazide, and venlafaxine. Additionally, under aerobic conditions, azithromycin, clarithromycin, gabapentin, and propranolol exhibited K_{bio} with a substantial difference when compared to the literature. Under anoxic conditions, a substantial difference has been shown in metoprolol, sulfamethoxazole, and trimethoprim. These differences may be attributed to the operation parameters (e.g., HRT, SRT), sludge concentrations and matrix used among the different studies.

Table 4
Biotransformation rates for the sixteen targeted compounds in the three main redox conditions, with and without the addition of influent.

Micropollutants	Aerobic ($L.g_{SS}^{-1}.d^{-1}$)		Anoxic ($L.g_{SS}^{-1}.d^{-1}$)		Anaerobic ($L.g_{SS}^{-1}.d^{-1}$)	
	Without Influent	With Influent	Without Influent	With Influent	Without Influent	With Influent
4-, 5-Methylbenzotriazole	0.09 ± 0.02	0.18 ± 0.01	0.13 ± 0.03	0.06 ± 0.02	0.20 ± 0.03	0.11 ± 0.05
Azithromycin	0.95 ± 0.34	1.48 ± 0.31	0.32 ± 0.20	N.D.	0.99 ± 0.12	1.27 ± 0.17
Benzotriazole	0.30 ± 0.01	0.47 ± 0.06	0.52 ± 0.01	0.58 ± 0.10	-0.09 ± 0.05	0.14 ± 0.18
Candesartan	0.04 ± 0.03	0.05 ± 0.03	0.03 ± 0.03	0.03 ± 0.04	-0.17 ± 0.11	-0.05 ± 0.03
Carbamazepine	0.00 ± 0.00	-0.10 ± 0.14	0.03 ± 0.03	0.07 ± 0.05	0.03 ± 0.08	-0.07 ± 0.03
Clarithromycin	1.45 ± 0.12	1.75 ± 0.59	1.26 ± 0.02	1.08 ± 0.23	1.42 ± 0.17	1.87 ± 0.14
Diclofenac	0.00 ± 0.00	0.00 ± 0.00	0.10 ± 0.06	0.07 ± 0.04	0.00 ± 0.00	0.00 ± 0.00
Gabapentin	0.51 ± 0.02	0.86 ± 0.01	1.52 ± 0.14	2.36 ± 0.30	0.04 ± 0.01	0.49 ± 0.19
Hydrochlorothiazide	0.10 ± 0.08	0.05 ± 0.01	0.08 ± 0.04	0.09 ± 0.05	0.06 ± 0.07	-0.06 ± 0.05
Irbesartan	0.29 ± 0.00	0.33 ± 0.06	0.20 ± 0.06	0.25 ± 0.08	0.49 ± 0.02	0.45 ± 0.04
Metoprolol	0.90 ± 0.11	0.92 ± 0.39	0.52 ± 0.02	0.42 ± 0.08	0.02 ± 0.07	0.65 ± 0.01
Propranolol	1.79 ± 0.39	1.51 ± 0.21	1.42 ± 0.09	1.02 ± 0.09	0.83 ± 0.22	0.76 ± 0.16
Sotalol	0.46 ± 0.02	0.46 ± 0.05	0.32 ± 0.01	0.25 ± 0.02	-0.11 ± 0.01	-0.03 ± 0.22
Sulfamethoxazole	0.27 ± 0.04	0.42 ± 0.00	1.63 ± 0.32	2.02 ± 0.33	0.09 ± 0.02	0.42 ± 0.03
Trimethoprim	0.40 ± 0.12	0.23 ± 1.21	0.17 ± 0.06	0.12 ± 0.05	1.75 ± 0.03	1.07 ± 0.03
Venlafaxine	0.17 ± 0.02	0.48 ± 0.18	0.30 ± 0.06	0.13 ± 0.08	0.00 ± 0.07	-0.04 ± 0.15

N.D.: Not Determined

Table 5
Biotransformation rate constants (k_{bio}) found for CAS in the literature and obtained results in this study for the targeted micropollutants. and average sorption (distribution) coefficients (k_d) calculated based on the values found in the literature.

Micropollutants	k_{bio} [L.gSS^{-1}.d^{-1}]			K_d [L.gSS^{-1}]
	Aerobic	Anoxic	Anaerobic	
4-. 5-Methylbenzotriazole	**0.18***	**0.06***	**0.11***	0.168 (± 0.032) (n=6)
Azithromycin	<0.13[3]; 0.17[4]; 0.24[12]. **1.48***		**1.27***	0.685 (±0.621) (n=3)
Benzotriazole	0.16[14]; 0.21; 0.22[14]; 0.30[14]; 0.40; 0.41[14]; **0.47***	0.23[14]; 0.24[14]; 0.25[14]; 0.32[14]; 0.33[14]; 0.34[14]; **0.58***	**0.14***	0.177 (± 0.081) (n=6)
Candesartan	**0.05***	**0.03***	**<0.00***	
Carbamazepine	**0.00***[,13,10]; <0.01[3,4,10]; <0.10[5,7,9]; 0.10[2]; 0.70[15];	<0.03[7]; **0.07***	**<0.00***	0.123 (± 0.112) (n=20)
Clarithromycin	0.03[4]; 0.20[4]; ≤0.40[3]; 0.48[13]; <0.50[5]; **1.75***	**1.08***	**1.87***	0.395 (± 0.355) (n=7)
Diclofenac	**<0.00***; <0.02[4]; 0.02[10]; ≤0.10[3]; 0.10[9,10]; 0.30[15]; 0.40[2]; 0.50[15]; 0.70[15]; 0.80[2]; 0.90[15]; 1.20[7]	<0.04[7]; **0.07***	**<0.00***	0.087 (±0.173) (n=16)
Gabapentin	0.08[15]; 0.13[15]; 0.18[15]; **0.86***	**2.36***	**0.49***	
Hydrochlorothiazide	**0.05***	**0.09***	**<0.00***	
Irbesartan	0.10[15]; **0.33***; 0.50[15]; 0.90[15]	**0.25***	**0.45***	0.820 (±0.170) (n=2)
Metoprolol	0.13[11]; 0.20[15]; 0.35[15]; 0.40[5,15]; 0.60[15]; **0.92***	0.03[8]; **0.42***	**0.65***	0.340 (± 0.506) (n=4)
Propranolol	0.36[5]; 0.46[5]; **1.51***	**1.02***	**0.76***	0.332 (± 0.116) (n=7)
Sotalol	0.40[5,15]; 0.43[5]; **0.46***; 0.60[15]; 0.80[15]	**0.25***	**<0.00***	0.132 (± 0.197) (n=3)
Sulfamethoxazole	≤0.10[3,9]; 0.19[4]; 0.20[4]; 0.24[12]; 0.30[7,12]; 0.41[6]; **0.42***; 0.60[1,9]	0.41[6]; **2.02***	**0.42***	0.202 (± 0.149) (n=17)
Trimethoprim	0.05[10]; 0.09[10]; 0.15[7]; 0.22[4]; **0.23***; 0.24[13]; 0.65[9]	**0.12***; 0.67[8]	**1.07***	0.225 (± 0.106) (n=13)
Venlafaxine	**0.48***	**0.13***	**<0.00***	0.270 (± 0.151) (n=10)

[1] McArdell et al. (2003): shi
[2] Clara et al. (2005)
[3] Joss et al. (2006)
[4] Abegglen et al. (2009)
[5] Wick et al. (2009)
[6] Plosz et al. (2010)
[7] Suarez et al. (2010)
[8] Xue et al. (2010);
[9] Suarez et al. (2012)
[10] Fernandez-Fontaina et al. (2013)
[11] Pomies et al. (2013)
[12] Fernandez-Fontaina et al. (2014)
[13] Blair et al. (2015)
[14] Mazioti et al. (2015)
[15] Nolte et al. (2020)
* This study

3.3. Removal efficiencies under different redox conditions

The experiments with influent addition (Batch III) represent the normal WWTP situation. Therefore, the experiment without influent addition (Batch II) was carried out to determine the impact of less available carbon sources on the targeted micropollutant biotransformation. The influent addition showed a variable impact on the removal efficiencies of the micropollutants under different redox conditions (See Figure S2 and Table S7). For example, gabapentin showed the highest removal efficiency increase (20%) under aerobic conditions when the influent was added (Fig. 2.A and Fig. 2.B). On the contrary, the influent addition allowed trimethoprim to exhibit the highest decrease in removal efficiency (19%) (Fig. 2.A and Fig. 2.B). Under anoxic conditions, the influent addition allowed gabapentin to show the highest removal efficiency increase (13%) while venlafaxine exhibited the highest decrease of 10% (Fig. 2.A and Fig. 2.B). The influent addition, under anaerobic conditions, led to the highest removal efficiency increase (39%) for metoprolol, while led to the highest decrease (21%) for trimethoprim (Fig. 2.A and Fig. 2.B).

Of the 16 targeted compounds, only 8 (aerobic), 6 (anoxic), and 7 (anaerobic) exhibited removal efficiencies of over 30% when influent was added (Fig. 2. A). Yet, when influent wasn't added only 6 (aerobic), 6 (anoxic), and 4 (anaerobic) exhibited removals of more than 30%. Overall, only 2 compounds (clarithromycin and propranolol) showed to be removed over 50% under all redox conditions. Gabapentin was the only compound that exhibited removal efficiencies higher than 80%, achieving 91% under anoxic

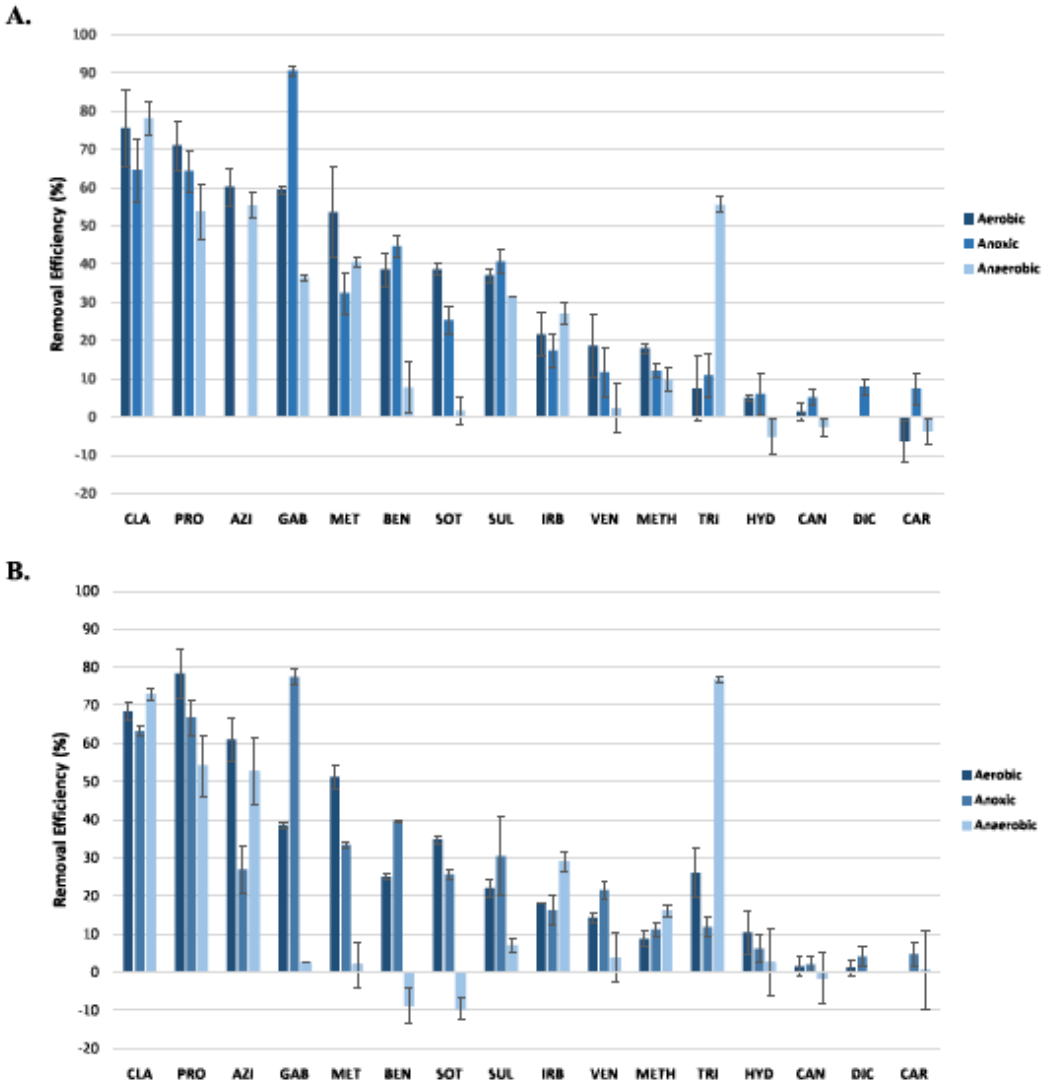

Fig. 2. Removal efficiencies of targeted micropollutants after 48 h, under aerobic, anoxic, and anaerobic redox conditions: A. with influent addition; B. without influent addition.

conditions, with influent addition.

Aerobic and anoxic conditions generally exhibited higher removals compared to anaerobic conditions (Fig. 2. A), with average removals of 31%, 28%, and 24%, respectively. These observations are aligned with previous research that highlighted the importance of oxygen availability for micropollutant biotransformation (Di Marcantonio et al., 2020). Under aerobic conditions, the presence of dissolved oxygen facilitates the activity of nitrifying bacteria that have a big role in micropollutant biotransformation (Kennes-Veiga et al., 2022). Furthermore, the high removal efficiencies observed under anoxic redox conditions might be attributed to alternated aerobic and anaerobic moments. This allows a more diverse microbial community, leading to enhanced micropollutant degradation (Di Marcantonio et al., 2020). Results confirmed that specific redox conditions offering the best removal efficiency varied depending on the micropollutant.

Among the targeted micropollutants, clarithromycin, propranolol, and gabapentin were highly removed with 73%, 63%, and 62% average removals, respectively, inferring to be easily removed in CAS systems. On the other hand, carbamazepine, diclofenac, hydrochlorothiazide, and candesartan exhibited low removal efficiencies, meaning potential adsorption onto sludge, or indicating their recalcitrant nature. 4-,5-methylbenzotriazole, azithromycin, metoprolol, propranolol, sotalol, and venlafaxine were primarily degraded under aerobic conditions, with removals of 18%, 60%, 54%, 71%, 39%, and 19%, respectively. Whereas under anoxic conditions benzotriazole, candesartan, carbamazepine, diclofenac, gabapentin, hydrochlorothiazide, and sulfamethoxazole were predominantly removed, achieving removal percentages of 45%, 5%, 7%, 8%, 91%, 6% and 41%, respectively. Clarithromycin, irbesartan, and trimethoprim showed higher removal efficiencies under anaerobic conditions, with removals of 78%, 27%, and 56%, respectively. Karthikraj and Kannan (2017), and Voutsa et al. (2006) also observed CAS removals in the range of 20–90% (Table S1) for 4-,5-methylbenzotriazole. However, Weiss et al. (2006) observed an 11% removal for 5-methylbenzotriazole and a −6% removal for 4-methylbenzotriazole. Previous studies showed removal efficiencies from 0% to 79% (Table S1) for the macrolide azithromycin (Blair et al., 2015; Pan & Yau, 2021; Yan et al., 2014), which are in line with the ones observed in this study.

Benzotriazole exhibited its higher removal efficiency under anoxic conditions (45%) as also observed by Mazioti et al. (2015) and other studies (see Table S1). For this compound, the influent addition impacted positively its removal (≈15%) under aerobic and anaerobic conditions (Fig. 2.A).

Due to its recalcitrancy, candesartan exhibited low removal, reaching a maximum of 5% under anoxic conditions with influent addition. Gurke et al. (2015) reported removal efficiencies in the range of −10–10%. In the same way, carbamazepine recalcitrancy has been known and may be due to its heterocyclic N-containing aromatic ring that provides molecular stability and difficult biotransformation (Kennes-Veiga et al., 2022).

Clarithromycin is the compound that appeared to have greater removal on CAS systems, according to the obtained removals. Clarithromycin exhibited removal efficiencies higher than 50% under all redox conditions, which match the ones observed in the literature (see Table S1).

Similarly, to carbamazepine and candesartan, diclofenac showed no substantial removal under any redox conditions, as also stated by Grandclement et al. (2017). Nonetheless, Suarez et al. (2010) reported small removals (≈2%) under anoxic conditions, which infer that denitrifying bacteria mechanisms may be responsible for its biotransformation. According to the literature, CAS removal efficiencies of diclofenac varied from a range between −143–77% (Lishman et al., 2006), suggesting that it doesn't have a redox condition where it is clearly removed.

The highest removal efficiency of 91% for gabapentin was obtained under anoxic conditions. This compound was the most influenced by the influent addition leading to increases of 21%, 13%, and 34% under aerobic, anoxic, and anaerobic conditions, respectively. Kasprzyk-Hordern et al. (2009) reported similar removal efficiencies of about 80–90% in CAS.

Hydrochlorothiazide did not show a removal higher than 10% under any redox condition. The addition of influent led to a non-substantial variation (<10%) only under aerobic and anaerobic conditions, which is in line with Radjenovic et al. (2009). Likewise, irbesartan exhibited an average removal of 20% in each determined redox condition without substantial impact when influent was added. Previous research reported irbesartan removals between 10% and 40% (Bayer et al., 2014; Gurke et al., 2015).

The beta-blocker metoprolol showed its higher removal efficiency (53%) under aerobic conditions. The influent addition led to a substantial increase (39%) in the removal efficiency under anaerobic conditions. The observed range of values is within the one observed by both Kasprzyk-Hordern et al. (2009) (38%), and Lin et al. (2009) (67%), in CAS systems (Table S1). The observed values for propranolol were higher than the ones observed in the literature (Table S1). Nonetheless, lower values (≈60%) may be linked to the scale-down of the process and matrix differences. The removal efficiency of this beta-blocker had no substantial variation with influent addition. Similarly, to the other beta-blockers, sotalol, also exhibited its highest removal efficiency (39%) under aerobic conditions with influent addition. Like metoprolol, this compound had a removal increase (11%) under anaerobic conditions after influent addition. Vieno et al. (2007) observed removal efficiencies of 48% at CAS systems, which are following the expected values of this study for a CAS.

According to the literature, the range of values obtained for sulfamethoxazole in real and lab-scale CAS is between 65% and 96% (Di Marcantonio et al., 2020; Radjenovic et al., 2009). Falas et al. (2016) also observed the high biotransformation of this compound under anaerobic conditions. However, our study observed higher removal under anoxic conditions, like Arias et al. (2018).

Ghosh et al. (2009) and Ruas et al. (2022) observed removal efficiencies in the range of 35% and 88%, in real WWTP and pilots, which followed the obtained values for trimethoprim (77% under anaerobic conditions). The influent addition decreased the removal by about 19% and 21% under aerobic and anaerobic conditions, respectively. Falas et al. (2016) and Arias et al. (2018) determined that trimethoprim is susceptible to anaerobic biotransformation which may be explained by the substitution of the pyrimidine ring functional group by the carboxyl group, at this redox condition.

Lastly, venlafaxine exhibited its higher removal (22%) under anoxic conditions, without influent addition. Both Castaño-Trias et al.

(2020) and Tiwari et al. (2021) obtained similar removal efficiencies in real CAS WWTP (see Table S1).

Micropollutants can undergo various transformation reactions, leading to the formation of new compounds with potentially different environmental behaviours and toxicities. Therefore, some micropollutants exhibited negative removals (e.g., benzotriazole, candesartan, carbamazepine) that may be attributed to higher congener and precursor retransformations to the parent compound (Kotowska et al., 2021; Wu et al., 2017), or the release of sorbed compounds during organic matter degradation. Nonetheless, the low solubility at time zero of some compounds can also mistakenly give the idea of compound retransformation (Jansook et al., 2022). Consequently, the influence of redox conditions on the formation and fate of transformation products warrants further investigation to ensure the comprehensive assessment of micropollutant removal in WWTP.

Our results showed that antibiotics (azithromycin, clarithromycin, trimethoprim, and sulfamethoxazole) exhibited higher biotransformation under different redox conditions, with removal efficiencies varying from 7% to 78%. Differently, the anticonvulsants (carbamazepine and gabapentin) exhibited higher removal efficiency under anoxic conditions. However, gabapentin presented a substantially higher removal efficiency when compared to carbamazepine, which may be correlated to its structural similarity to the neurotransmitter gamma-aminobutyric acid (GABA) (Tony et al., 2023). Likewise, metoprolol, propranolol, and sotalol (antihypertensives/beta-blockers) also exhibited the highest removal efficiencies under anoxic conditions. The lab batch tests showed higher micropollutant removal efficiencies than the Dutch WWTP from where the samples were taken (See Table S8), which may be attributed to the different HRT.

Overall, the removal efficiencies of micropollutants varied depending on the redox condition and the specific compound. While aerobic and anoxic conditions generally showed higher average removals, the most favourable redox conditions varied for each targeted micropollutant.

3.4. *Potential biotransformation route*

Micropollutant biotransformation can take place via metabolism or cometabolism. Usually, cometabolism is predominant in WWTP processes due to the lack of enzymes and cofactor specificity (Criddle, 1993). Compounds consisting of strong electron acceptors functional groups are less prone to be used as a substrate being therefore cometabolically degraded (Granatto et al., 2021; Wei et al., 2018).

However, this is just an indication since biotransformation rates can be affected by various factors (e.g., active biomass, micropollutant concentration, enzymes) (Kennes-Veiga et al., 2022). Therefore, further research is needed to prove the actual route by linking the biotransformation rates with concentration of specific enzymes mediating the micropollutants conversion; or by molecular sequencing data demonstrating growth of specific microorganisms when using the micropollutants as substrate.

Fig. 3 summarizes the inferred preferred cometabolic or metabolic route of the targeted micropollutants based on the obtained biotransformation rates (Table 5). Table S9 compile the observed difference in the determined biotransformation rates due to the effect of substrate concentration increased (with addition of influent). Increased biotransformation rate upon influent addition indicates cometabolism, relying on enzymatic processes in the presence of easily degradable organics. Conversely, a decreased rate upon influent addition implies metabolism dominance, with the compound serving as the main energy and carbon source for microorganisms (Angelidaki & Sanders, 2004). Only variations greater than 5% when influent (substrate) was added were considered relevant. However, this is just an indication since biotransformation rates can be affected by various factors (e.g., active biomass, micropollutant concentration, enzymes) (Kennes-Veiga et al., 2022). Therefore, further research is needed to prove the actual route by linking the biotransformation rates with concentration of specific enzymes mediating the micropollutants conversion; or by molecular sequencing data demonstrating growth of specific microorganisms when using the micropollutants as substrate.

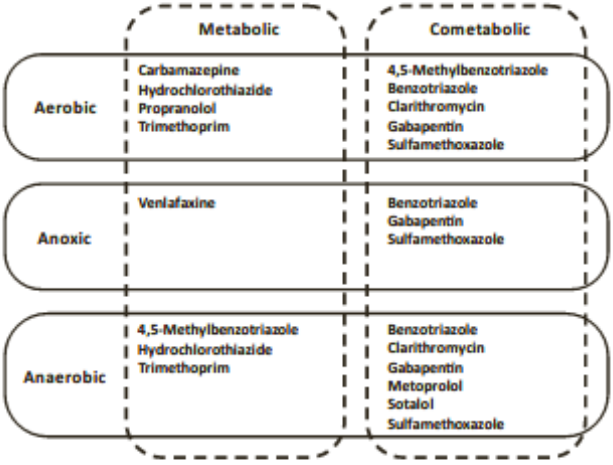

Fig. 3. Inferred metabolic or cometabolic biotransformation of the targeted micropollutants under different redox conditions.

According to the results, cometabolic biotransformation appears to be predominant for the majority of the targeted micropollutants, as expected (Fischer & Majewsky, 2014). Three compounds i.e., benzotriazole, gabapentin, and sulfamethoxazole, are biotransformed by cometabolism under all redox conditions. Only 4-,5-methylbenzotriazole exhibited metabolic and cometabolic biotransformation depending on the redox condition. Under anoxic conditions, it was not possible to infer the potential biotransformation route from different compounds. The sufficient COD present in the effluent may have also interfered with the results to be able to see a more substantial difference with and without the addition of influent (substrate).

3.5. Physicochemical properties

An attempt to correlate the obtained biotransformation constant rates with the physicochemical properties (hydrophobicity, polarity, and solubility) of the micropollutants was carried out (Table 6). Hydrophilic compounds (e.g., clarithromycin, gabapentin) were shown to have an average biotransformation 15% greater than hydrophobic compounds (e.g., diclofenac, candesartan). This difference may be explained by the fact that hydrophobic compounds are more prone to sorption which inhibits biotransformation processes (Phan et al., 2018). Yet, since most enzyme active sites are hydrophobic, it was expected hydrophobic substrates to easily bind because interactions between hydrophobes are spontaneous (Li et al., 2016). The greatest difference occurred under anoxic conditions, where hydrophilic compounds exhibited a biotransformation 61% greater than hydrophobic compounds.

Overall, polar compounds exhibited an average biotransformation 36% higher than non-polar ones, which can be explained by their increased reactivity, being, therefore, more prone to degrade (Niaounakis, 2015). However, under anaerobic conditions, non-polar compounds exhibited a 55% biotransformation increase over polar compounds. Since polar compounds are more prone to biotransformation, the presence of extremozymes may also have been a mechanism to improve their biotransformation (Sharma & Debnath, 2022). It was not possible to observe any difference between polar and non-polar compounds biotransformation under aerobic conditions, while under anoxic conditions the greatest difference (71%) was observed for polar compounds.

Lastly, the solubility and removal of the compound showed no linear correlation at any redox condition, being the maximum squared-R obtained of 0.51 (under aerobic conditions) – see Table 6.

3.6. Future outlook

Future research should focus on tackling the challenge of closing the mass balance by analysing the micropollutants both in the liquid and solid phases in similar experiments to trace the compounds and guarantee that they were biotransformed or sorped. A higher micropollutant spike dose must be studied in batch tests to verify if they minimize the concentration variations associated with analytical errors and detection limits. Although, this may lead to unrealistic kinetic values caused by high concentrations, which should be verified. Moreover, seasonal variations must also be studied since temperature and flow rate may change the wastewater characteristics and micropollutant concentrations.

There is still a lack of knowledge about the biotransformation kinetics and removal pathways of several micropollutants in wastewater treatment. Most of the studies were carried out under aerobic conditions with CAS or MBR, yet there are currently other technologies (e.g., MBBR, AGS), that operate with different redox conditions. For example, MBBR exhibited high removals of micropollutants, mostly at high-loaded reactors (Edefell et al., 2021), while Margot et al. (2016) have pointed out that AGS achieved higher removals of 40%, 15%, 75%, and 20% for compounds like benzotriazole, diclofenac, gabapentin, and metoprolol, correspondingly. However, Burzio et al. (2022) observed that AGS was less effective in biotransforming some micropollutants compared to CAS. Therefore, future studies should aim to explore further these technologies and how the biotransformation of micropollutants might be improved.

The results indicated that the presence of co-substrates and competing electron acceptors in the wastewater influent can impact biodegradation. Therefore, it is recommended to use effluent that has undergone an advanced treatment to minimize the present COD and determine more clearly whether metabolic or cometabolic biotransformation is preferred. Furthermore, future studies could explore chemical properties, such as molecular structure and stability to develop a comprehensive understanding of the relationships between micropollutant characteristics, redox conditions, and biotransformation rates. This information will therefore allow the future incorporation of the biotransformation rates into ASM models or software-simulating tools, to predict the effluent concentrations and promote more targeted advanced oxidation processes.

4. Conclusions

The micropollutant biotransformation rates varied substantially under different redox conditions. On average, aerobic, and anoxic conditions favour higher average biotransformation rates. Nevertheless, compounds such as clarithromycin had a higher biotransformation rate under anaerobic conditions (1.87 $L.g_{SS}^{-1}.d^{-1}$). Additionally, gabapentin exhibited the highest biotransformation rate constant of 2.36 $L.g_{SS}^{-1}.d^{-1}$ under anoxic conditions. Candesartan, carbamazepine, diclofenac, and hydrochlorothiazide were shown to be persistent, and under the three redox conditions, they exhibited low biotransformation rates (<0.1 $L.g_{SS}^{-1}.d^{-1}$). Under anaerobic conditions, candesartan, carbamazepine, hydrochlorothiazide, sotalol, and venlafaxine showed negative rates that may be associated with higher congeners and precursor retransformations to the parent compound. Antibiotics and beta-blockers are the micropollutant classes with greater biotransformation constants. The beta-blockers and anticonvulsants exhibited their higher removal efficiencies under anoxic conditions.

Under aerobic conditions, the average removal efficiency was 31%, while under anoxic and anaerobic conditions, it was 28% and

Table 6
Correlation between the biotransformation rate constants of the micropollutants and their physicochemical properties.

	Hydrophobicity Percentual difference	Polarity	Solubility Square-R
General	15%[a]	36%	0.33
Aerobic conditions	19%	0%	0.51
Anoxic conditions	61%[a]	71%	0.09
Anaerobic Conditions	6%[a]	55%[b]	0.18

[a] Hydrophilic compounds exhibited greater biotransformation
[b] Non-polar compounds exhibited greater biotransformation

24%, respectively. Overall, only clarithromycin and propranolol showed removal efficiencies of over 50% under all redox conditions. Other compounds, such as carbamazepine, diclofenac, and hydrochlorothiazide, exhibited low removal efficiencies, demonstrating their recalcitrant nature. Cometabolic biotransformation was inferred to be predominant for most compounds, where the presence of co-substrates and competing electron acceptors influenced the degradation processes. Only 4-,5-methylbenzotriazole exhibited both metabolic and cometabolic biotransformation at different redox conditions. Hydrophilic and polar compounds generally exhibited higher biotransformation rates compared to hydrophobic and non-polar compounds.

Future research should aim to close the mass balance by analysing micropollutants in both the liquid and solid phases. The findings of this study provide valuable insights into the biotransformation kinetics of micropollutants in CAS. They can help the development of more effective wastewater treatment strategies to mitigate their environmental impact.

CRediT authorship contribution statement

Tiago A. E. Martins: Writing – original draft, Visualization, Methodology, Investigation, Data curation. **Julian David Muñoz Sierra:** Writing – review & editing, Writing – original draft, Supervision, Methodology, Investigation, Formal analysis, Conceptualization. **Jo A. Nieuwlands:** Resources. **Maria Lousada-Ferreira:** Writing – review & editing, Project administration, Funding acquisition. **Leonor Amaral:** Writing – review & editing, Supervision.

Declaration of Competing Interest

The authors declare that they have no known competing financial interests or personal relationships that could have appeared to influence the work reported in this paper.

Data availability

Data will be made available on request.

Acknowledgements

This work was performed within the TKI Belissima project at KWR Water Research Institute. This research was co-financed with PPS-funding from the Top consortia for Knowledge & Innovation (TKI's) of the Dutch Ministry of Economic Affairs and Climate Policy. The authors would like to thank the KWR Water Treatment and Resource Recovery team, and the KWR Materials Research and Chemical Analysis Laboratory for their cooperation and fruitful discussions. The authors would also like to thank the Dutch project partners who facilitated the sampling campaign and data sharing for performing the lab tests. Finally, Tiago Martins would like to express his gratitude to everyone not abovementioned who contributed to this research with knowledge, advice, and emotional support.

Appendix A. Supporting information

Supplementary data associated with this article can be found in the online version at doi:10.1016/j.eti.2024.103639.

References

Abegglen, C., Joss, A., McArdell, C.S., Fink, G., Schlusener, M.P., Ternes, T.A., Siegrist, H., 2009. The fate of selected micropollutants in a single-house MBR. Water Res. 43 (7), 2036–2046. https://doi.org/10.1016/j.watres.2009.02.005.

Angelidaki, I., Sanders, W., 2004. Assessment of the anaerobic biodegradability of macropollutants. Rev. Environ. Sci. Bio/Technol. 3 (2), 117–129. https://doi.org/10.1007/s11157-004-2502-3.

Arias, A., Alvarino, T., Allegue, T., Suarez, S., Garrido, J.M., Omil, F., 2018. An innovative wastewater treatment technology based on UASB and IFAS for cost-efficient macro and micropollutant removal. J. Hazard Mater. 359, 113–120. https://doi.org/10.1016/j.jhazmat.2018.07.042.

Bayer, A., Asner, R., Schussler, W., Kopf, W., Weiss, K., Sengl, M., Letzel, M., 2014. Behavior of sartans (antihypertensive drugs) in wastewater treatment plants, their occurrence and risk for the aquatic environment. Environ. Sci. Pollut. Res. Int. 21 (18), 10830–10839. https://doi.org/10.1007/s11356-014-3060-z.
Berthod, L., Whitley, D.C., Roberts, G., Sharpe, A., Greenwood, R., Mills, G.A., 2017. Quantitative structure-property relationships for predicting sorption of pharmaceuticals to sewage sludge during waste water treatment processes. Sci. Total Environ. 579, 1512–1520. https://doi.org/10.1016/j.scitotenv.2016.11.156.
Blair, B., Nikolaus, A., Hedman, C., Klaper, R., Grundl, T., 2015. Evaluating the degradation, sorption, and negative mass balances of pharmaceuticals and personal care products during wastewater treatment. Chemosphere 134, 395–401. https://doi.org/10.1016/j.chemosphere.2015.04.078.
Bourgin, M., Beck, B., Boehler, M., Borowska, E., Fleiner, J., Salhi, E., Teichler, R., von Gunten, U., Siegrist, H., McArdell, C.S., 2018. Evaluation of a full-scale wastewater treatment plant upgraded with ozonation and biological post-treatments: Abatement of micropollutants, formation of transformation products and oxidation by-products. Water Res. 129, 486–498. https://doi.org/10.1016/j.watres.2017.10.036.
Burzio, C., Ekholm, J., Modin, O., Falås, P., Svahn, O., Persson, F., van Erp, T., Gustavsson, D.J.I., Wilén, B.-M., 2022. Removal of organic micropollutants from municipal wastewater by aerobic granular sludge and conventional activated sludge. J. Hazard. Mater. https://doi.org/10.1016/j.jhazmat.2022.129528.
Castaño-Trias, M., Brienza, M., Tomei, M.C., Buttiglieri, G., 2020. Fate and Removal of Pharmaceuticals in CAS for Water and Sewage Sludge Reuse. Remov. Degrad. Pharm. Act. Compd. Wastewater Treat. 23–51.
Clara, M., Kreuzinger, N., Strenn, B., Gans, O., Kroiss, H., 2005. The solids retention time-a suitable design parameter to evaluate the capacity of wastewater treatment plants to remove micropollutants. Water Res. 39 (1), 97–106. https://doi.org/10.1016/j.watres.2004.08.036.
Criddle, C., 1993. The Kinectics of Cometabolism. Biotechnol. Bioeng. 41 (11), 1048–1056. https://doi.org/10.1002/bit.260411107.
Das, S., Ray, N.M., Wan, J., Khan, A., Chakraborty, T., Ray, M.B., 2017. Micro Wastewater.: Fate Remov. Process.
Di Marcantonio, C., Chiavola, A., Bains, A., Singhal, N., 2020. Effect of oxic/anoxic conditions on the removal of organic micropollutants in the activated sludge process. Environ. Technol. Innov. 20 https://doi.org/10.1016/j.eti.2020.101161.
Edefell, E., Falas, P., Torresi, E., Hagman, M., Cimbritz, M., Bester, K., Christensson, M., 2021. Promoting the degradation of organic micropollutants in tertiary moving bed biofilm reactors by controlling growth and redox conditions. J. Hazard. Mater. 414, 125535 https://doi.org/10.1016/j.jhazmat.2021.125535.
Falas, P., Wick, A., Castronovo, S., Habermacher, J., Ternes, T.A., Joss, A., 2016. Tracing the limits of organic micropollutant removal in biological wastewater treatment. Water Res. 95, 240–249. https://doi.org/10.1016/j.watres.2016.03.009.
Fernandez-Fontaina, E., Carballa, M., Omil, F., Lema, J.M., 2014. Modelling cometabolic biotransformation of organic micropollutants in nitrifying reactors. Water Res. 65, 371–383. https://doi.org/10.1016/j.watres.2014.07.048.
Fernandez-Fontaina, E., Pinho, I., Carballa, M., Omil, F., Lema, J.M., 2013. Biodegradation kinetic constants and sorption coefficients of micropollutants in membrane bioreactors. Biodegradation 24 (2), 165–177. https://doi.org/10.1007/s10532-012-9568-3.
Fischer, K., Majewsky, M., 2014. Cometabolic degradation of organic wastewater micropollutants by activated sludge and sludge-inherent microorganisms. Appl. Microbiol. Biotechnol. 98 (15), 6583–6597. https://doi.org/10.1007/s00253-014-5826-0.
Ghosh, G.C., Okuda, T., Yamashita, N., Tanaka, H., 2009. Occurrence and elimination of antibiotics at four sewage treatment plants in Japan and their effects on bacterial ammonia oxidation. Water Sci. Technol. 59 (4), 779–786. https://doi.org/10.2166/wst.2009.067.
Gobel, A., Thomsen, A., McArdell, C.S., Joss, A., Giger, W., 2005. Occurrence and sorption behavior of sulfonamides, macrolides, and trimethoprim in activated sludge treatment. Environ. Sci. Technol. 39 (11), 3981–3989. https://doi.org/10.1021/es048550a.
Golovko, O., Orn, S., Sorengard, M., Frieberg, K., Nassazzi, W., Lai, F.Y., Ahrens, L., 2021. Occurrence and removal of chemicals of emerging concern in wastewater treatment plants and their impact on receiving water systems. Sci. Total Environ. 754, 142122 https://doi.org/10.1016/j.scitotenv.2020.142122.
Granatto, C.F., Grosseli, G.M., Sakamoto, I.K., Fadini, P.S., Varesche, M.B.A., 2021. Influence of cosubstrate and hydraulic retention time on the removal of drugs and hygiene products in sanitary sewage in an anaerobic Expanded Granular Sludge Bed reactor. J. Environ. Manag. 299, 113532 https://doi.org/10.1016/j.jenvman.2021.113532.
Grandclement, C., Seyssiecq, I., Piram, A., Wong-Wah-Chung, P., Vanot, G., Tiliacos, N., Roche, N., Doumenq, P., 2017. From the conventional biological wastewater treatment to hybrid processes, the evaluation of organic micropollutant removal: A review. Water Res. 111, 297–317. https://doi.org/10.1016/j.watres.2017.01.005.
Gurke, R., Rossler, M., Marx, C., Diamond, S., Schubert, S., Oertel, R., Fauler, J., 2015. Occurrence and removal of frequently prescribed pharmaceuticals and corresponding metabolites in wastewater of a sewage treatment plant. Sci. Total Environ. 532, 762–770. https://doi.org/10.1016/j.scitotenv.2015.06.067.
Gusmaroli, L., Mendoza, E., Petrovic, M., Buttiglieri, G., 2020. How do WWTPs operational parameters affect the removal rates of EU Watch list compounds? Sci. Total Environ. 714, 136773 https://doi.org/10.1016/j.scitotenv.2020.136773.
Jansook, P., Hnin, H.M., Praphanwittaya, P., Loftsson, T., Stefansson, E., 2022. Effect of salt formation on γ-cyclodextrin solubilization of irbesartan and candesartan and the chemical stability of their ternary complexes. J. Drug Deliv. Sci. Technol. 67 https://doi.org/10.1016/j.jddst.2021.102980.
Joss, A., Zabczynski, S., Gobel, A., Hoffmann, B., Loffler, D., McArdell, C.S., Ternes, T.A., Thomsen, A., Siegrist, H., 2006. Biological degradation of pharmaceuticals in municipal wastewater treatment: proposing a classification scheme. Water Res. 40 (8), 1686–1696. https://doi.org/10.1016/j.watres.2006.02.014.
Karthikraj, R., Kannan, K., 2017. Mass loading and removal of benzotriazoles, benzothiazoles, benzophenones, and bisphenols in Indian sewage treatment plants. Chemosphere 181, 216–223. https://doi.org/10.1016/j.chemosphere.2017.04.075.
Kasprzyk-Hordern, B., Dinsdale, R.M., Guwy, A.J., 2009. The removal of pharmaceuticals, personal care products, endocrine disruptors and illicit drugs during wastewater treatment and its impact on the quality of receiving waters. Water Res. 43 (2), 363–380. https://doi.org/10.1016/j.watres.2008.10.047.
Kennes-Veiga, D.M., Gonzalez-Gil, L., Carballa, M., Lema, J.M., 2022. Enzymatic cometabolic biotransformation of organic micropollutants in wastewater treatment plants: A review. Bioresour. Technol. 344 (Pt B)), 126291 https://doi.org/10.1016/j.biortech.2021.126291.
Kennes-Veiga, D.M., Vogler, B., Fenner, K., Carballa, M., Lema, J.M., 2021. Heterotrophic enzymatic biotransformations of organic micropollutants in activated sludge. Sci. Total Environ. 780, 146564 https://doi.org/10.1016/j.scitotenv.2021.146564.
Kim, S., Chen, J., Cheng, T., Gindulyte, A., He, J., He, S., Li, Q., Shoemaker, B.A., Thiessen, P.A., Yu, B., Zaslavsky, L., Zhang, J., Bolton, E.E., 2021. PubChem in 2021: new data content and improved web interfaces. Nucleic Acids Res. 49 (D1), D1388–D1395. https://doi.org/10.1093/nar/gkaa971.
Kotowska, U., Struk-Sokolowska, J., Piekutin, J., 2021. Simultaneous determination of low molecule benzotriazoles and benzotriazole UV stabilizers in wastewater by ultrasound-assisted emulsification microextraction followed by GC-MS detection. Sci. Rep. 11 (1), 10098 https://doi.org/10.1038/s41598-021-89529-1.
Li, S., Piletsky, S.A., Cao, S., Turner, A.P.F., 2016. Molecularly Imprinted Catalysts: Principles, Syntheses, and Applications. Elsevier.
Lin, A.Y., Yu, T.H., Lateef, S.K., 2009. Removal of pharmaceuticals in secondary wastewater treatment processes in Taiwan. J. Hazard. Mater. 167 (1-3), 1163–1169. https://doi.org/10.1016/j.jhazmat.2009.01.108.
Lishman, L., Smyth, S.A., Sarafin, K., Kleywegt, S., Toito, J., Peart, T., Lee, B., Servos, M., Beland, M., Seto, P., 2006. Occurrence and reductions of pharmaceuticals and personal care products and estrogens by municipal wastewater treatment plants in Ontario, Canada. Sci. Total Environ. 367 (2-3), 544–558. https://doi.org/10.1016/j.scitotenv.2006.03.021.
Margot, J., Lochmatter, S., Barry, D.A., Holliger, C., 2016. Role of ammonia-oxidizing bacteria in micropollutant removal from wastewater with aerobic granular sludge. Water Sci. Technol. 73 (3), 564–575. https://doi.org/10.2166/wst.2015.514.
Mazioti, A.A., Stasinakis, A.S., Gatidou, G., Thomaidis, N.S., Andersen, H.R., 2015. Sorption and biodegradation of selected benzotriazoles and hydroxybenzothiazole in activated sludge and estimation of their fate during wastewater treatment. Chemosphere 131, 117–123. https://doi.org/10.1016/j.chemosphere.2015.03.029.
McArdell, C.S., Molnar, E., Suter, M.J., Giger, W., 2003. Occurrence and fate of macrolide antibiotics in wastewater treatment plants and in the Glatt Valley watershed, Switzerland. Environ. Sci. Technol. 37 (24), 5479–5486. https://doi.org/10.1021/es034368i.
Lousada-Ferreira, M. (2022). Fate of Organic Micropollutants in Activated Sludge Systems: Work package 1. Report TKI Belissima. KWR - Water Research Institute. Retrieved from https://library.kwrwater.nl/:
Moermond, C. a, Montforts, M., & Smit, E. (2019). Informatieblad - nut en noodzaak van normen voor medicijnresten in oppervlaktewater. RIVM - Rijksinstituut voor Volksgezondheid en Milieu; Ministerie van Volksgezondheid. Bielthoven, Nederland, Opdracht van het Ministerie van Infrastructuur en Waterstaat. Retrieved from www.rivm.nl:

Mutzner, L., Furrer, V., Castebrunet, H., Dittmer, U., Fuchs, S., Gernjak, W., Gromaire, M.C., Matzinger, A., Mikkelsen, P.S., Selbig, W.R., Vezzaro, L., 2022. A decade of monitoring micropollutants in urban wet-weather flows: What did we learn? Water Res. 223, 118968 https://doi.org/10.1016/j.watres.2022.118968.
Niaounakis, M. (2015). Biopolymers: Processing and Products: Plastics Desing Library.
Nolte, T.M., Chen, G., van Schayk, C.S., Pinto-Gil, K., Hendriks, A.J., Peijnenburg, W., Ragas, A.M.J., 2020. Disentanglement of the chemical, physical, and biological processes aids the development of quantitative structure-biodegradation relationships for aerobic wastewater treatment. Sci. Total Environ. 708, 133863 https://doi.org/10.1016/j.scitotenv.2019.133863.
Pan, M., Yau, P.C., 2021. Fate of Macrolide Antibiotics with Different Wastewater Treatment Technologies. Water Air Soil Pollut. 232 (3), 103. https://doi.org/10.1007/s11270-021-05053-y.
Phan, H.V., Wickham, R., Xie, S., McDonald, J.A., Khan, S.J., Ngo, H.H., Guo, W., Nghiem, L.D., 2018. The fate of trace organic contaminants during anaerobic digestion of primary sludge: A pilot scale study. Bioresour. Technol. 256, 384–390. https://doi.org/10.1016/j.biortech.2018.02.040.
Plosz, B.G., Leknes, H., Thomas, K.V., 2010. Impacts of competitive inhibition, parent compound formation and partitioning behavior on the removal of antibiotics in municipal wastewater treatment. Environ. Sci. Technol. 44 (2), 734–742. https://doi.org/10.1021/es902264w.
Pomies, M., Choubert, J.M., Wisniewski, C., Coquery, M., 2013. Modelling of micropollutant removal in biological wastewater treatments: a review. Sci. Total Environ. 443, 733–748. https://doi.org/10.1016/j.scitotenv.2012.11.037.
Radjenovic, J., Petrovic, M., Barcelo, D., 2009. Fate and distribution of pharmaceuticals in wastewater and sewage sludge of the conventional activated sludge (CAS) and advanced membrane bioreactor (MBR) treatment. Water Res. 43 (3), 831–841. https://doi.org/10.1016/j.watres.2008.11.043.
Ruas, G., Lopez-Serna, R., Scarcelli, P.G., Serejo, M.L., Boncz, M.A., Munoz, R., 2022. Influence of the hydraulic retention time on the removal of emerging contaminants in an anoxic-aerobic algal-bacterial photobioreactor coupled with anaerobic digestion. Sci. Total Environ., 154262 https://doi.org/10.1016/j.scitotenv.2022.154262.
Sharma, P., & Debnath, M. (2022). Impact of extremozymes on the removal of pollutants for industrial wastewater treatment. Paper presented at the Conference on Cutting Edge Research in Materials and Sustainable Chemical Technologies (CRMSCT-2022), Jaipur, India.
Suarez, S., Lema, J.M., Omil, F., 2010. Removal of pharmaceutical and personal care products (PPCPs) under nitrifying and denitrifying conditions. Water Res. 44 (10), 3214–3224. https://doi.org/10.1016/j.watres.2010.02.040.
Suarez, S., Reif, R., Lema, J.M., Omil, F., 2012. Mass balance of pharmaceutical and personal care products in a pilot-scale single-sludge system: influence of T, SRT and recirculation ratio. Chemosphere 89 (2), 164–171. https://doi.org/10.1016/j.chemosphere.2012.05.094.
Tiwari, B., Ouarda, Y., Drogui, P., Tyagi, R.D., Vaudreuil, M.A., Sauvé, S., Buelna, G., Dubé, R., 2021. Fate of Pharmaceuticals in a Submerged Membrane Bioreactor Treating Hospital Wastewater. Front. Water 3. https://doi.org/10.3389/frwa.2021.730479.
Tony, R.M., El Hamd, M.A., Gamal, M., Saleh, S.F., Maslamani, N., Alsaggaf, W.T., El-Zeiny, M.B., 2023. Green Bio-Analytical Study of Gabapentin in Human Plasma Coupled with Pharmacokinetic and Bioequivalence Assessment Using UPLC-MS/MS. Separations 10 (4). https://doi.org/10.3390/separations10040234.
Vieno, N., Tuhkanen, T., Kronberg, L., 2007. Elimination of pharmaceuticals in sewage treatment plants in Finland. Water Res. 41 (5), 1001–1012. https://doi.org/10.1016/j.watres.2006.12.017.
Voutsa, D., Hartmann, P., Schaffner, C., Giger, W., 2006. Benzotriazoles, alkylphenols and bisphenol A in municipal wastewaters and in the Glatt River, Switzerland. Environ. Sci. Pollut. Res. Int. 13 (5), 333–341. https://doi.org/10.1065/espr2006.01.295.
Wei, C.-H., Wang, N., HoppeJones, C., Leiknes, T., Amy, G., Fang, Q., Hu, X., Rong, H., 2018. Organic micropollutants removal in sequential batch reactor followed by nanofiltration from municipal wastewater treatment. Bioresour. Technol. 268, 648–657. https://doi.org/10.1016/j.biortech.2018.08.073.
Weiss, S., Jakobs, J., Reemtsma, T., 2006. Discharge of three benzotriazole corrosion inhibitors with municipal wastewater and improvements by membrane bioreactor treatment and ozonation. Environ. Sci. Technol. 40 (23), 7193–7199. https://doi.org/10.1021/es061434i.
Wick, A., Fink, G., Joss, A., Siegrist, H., Ternes, T.A., 2009. Fate of beta blockers and psycho-active drugs in conventional wastewater treatment. Water Res. 43 (4), 1060–1074. https://doi.org/10.1016/j.watres.2008.11.031.
Wirenfeldt Jensen, N., Faraji, T., Gonzalez Ospina, A., Guillosso, R., Petitpain Perrin, F., Krøyer Kristensen, P., Hove Hansen, S., Jørgensen, M.K., Boel Overgaard Andersen, M., Tranekær, C., & Lind-Frendsen, M. (2022). Removal of micropollutants by application of multiple point ozonation and powder activated carbon. The Danish Environmental Protection Agency. ISBN:978-87-7038-412-4. Retrieved from https://www2.mst.dk/Udgiv/publications/2022/04/978-87-7038-412-4.pdf.
Wishart, D.S., Feunang, Y.D., Guo, A.C., Lo, E.J., Marcu, A., Grant, J.R., Sajed, T., Johnson, D., Li, C., Sayeeda, Z., Assempour, N., Iynkkaran, I., Liu, Y., Maciejewski, A., Gale, N., Wilson, A., Chin, L., Cummings, R., Le, D., Pon, A., Knox, C., Wilson, M., 2018. DrugBank 5.0: a major update to the DrugBank database for 2018. Nucleic Acids Res. 46 (D1), D1074–D1082. https://doi.org/10.1093/nar/gkx1037.
Wu, Q., Lam, J.C.W., Kwok, K.Y., Tsui, M.M.P., Lam, P.K.S., 2017. Occurrence and fate of endogenous steroid hormones, alkylphenol ethoxylates, bisphenol A and phthalates in municipal sewage treatment systems. J. Environ. Sci. (China) 61, 49–58. https://doi.org/10.1016/j.jes.2017.02.021.
Xue, W., Wu, C., Xiao, K., Huang, X., Zhou, H., Tsuno, H., Tanaka, H., 2010. Elimination and fate of selected micro-organic pollutants in a full-scale anaerobic/anoxic/aerobic process combined with membrane bioreactor for municipal wastewater reclamation. Water Res. 44 (20), 5999–6010. https://doi.org/10.1016/j.watres.2010.07.052.
Yan, Q., Gao, X., Huang, L., Gan, X.M., Zhang, Y.X., Chen, Y.P., Peng, X.Y., Guo, J.S., 2014. Occurrence and fate of pharmaceutically active compounds in the largest municipal wastewater treatment plant in Southwest China: mass balance analysis and consumption back-calculated model. Chemosphere 99, 160–170. https://doi.org/10.1016/j.chemosphere.2013.10.062.

III Annex – Fitted (photo)chemical constants

For the 19 OMPs, (photo)chemical constants that were performed in the laboratory set-up (collimated beam) in MQ with different H2O2 dosages (0, 10 and 20 mg/L) were fitted (minimizing least-squares errors). Two constants were fitted:

- The product of quantum yield and molar extinction of an OMP (k_UV), which represents the direct photolysis degradation pathway.
- The reaction rate constants of an OMP with OH radicals, which represents the oxidative degradation pathway.

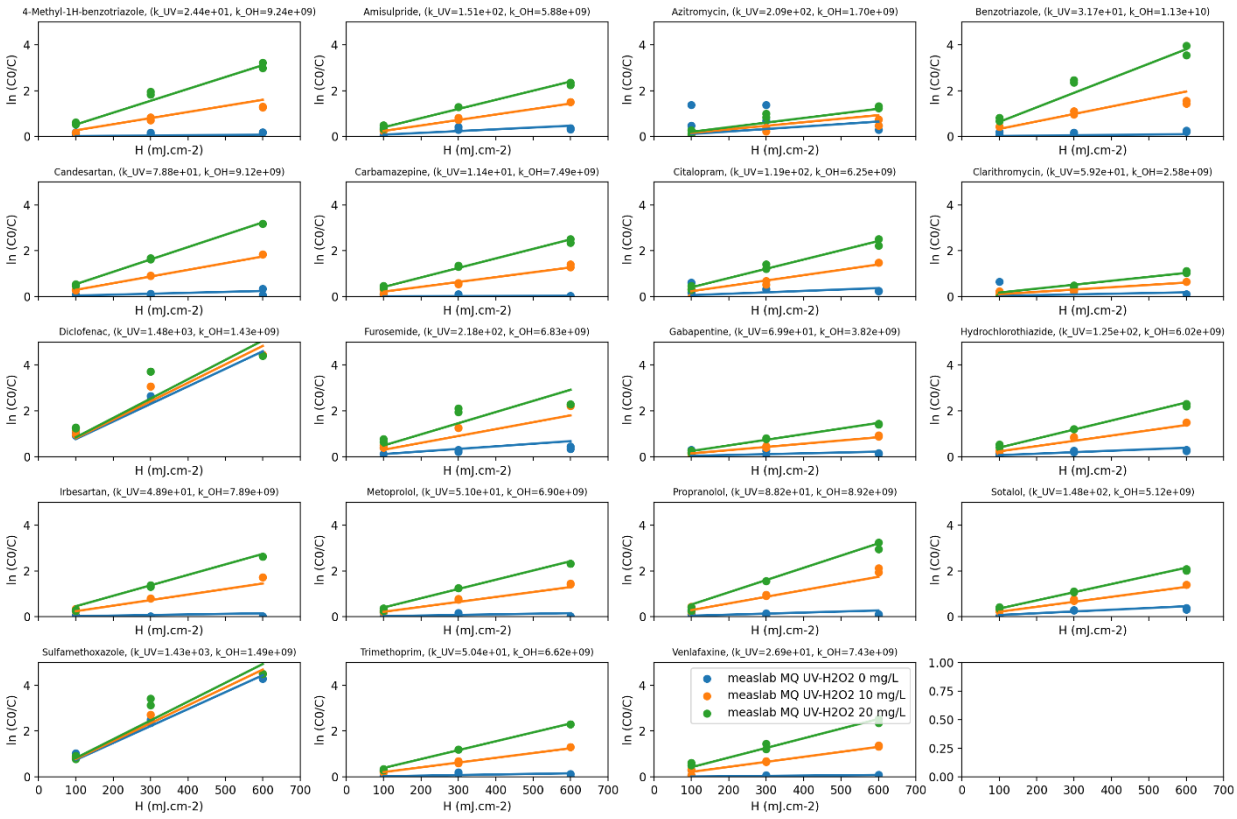

IV Annex – ASM-X model parameter values

Reproduction of Table II, as published by Plósz, B.G., Langford, K.H., Thomas, K.V. 2012. An activated sludge modeling framework for xenobiotic trace chemicals (ASMX): assessment of diclofenac and carbamazepine. Biotechnol Bioeng., 109(11),2757–69, presenting the information on diclofenac and carbamazepine, and model parameter values, applied to simulate the ASM-X and ASM1 models.

Symbol	Definition	Unit	Compound	
			Diclofenac	Carbamazepine
	CAS registry #		105307-86-5	298-46-4 85756-57-6
	Annual consumption (Norway)	$kg\,year^{-1}$	1588[a]	3619
	Average daily influent C_{LI} load measured	$mg\,day^{-1}\ 1{,}000\,PE^{-1}$	58 ± 14	192 ± 48
	Average daily influent C_{CJ} load calculated	$mg\,day^{-1}\ 1{,}000\,PE^{-1}$	65 ± 15	77 ± 18
Kinetic model parameters				
k_{Des}	De-sorption rate coefficient for C_{SL}	day^{-1}	100[c]	100[c]
K_S	Half-saturation coefficient for S_S	$mg\,L^{-1}$	10[f]	10[f]
K_O	Half-saturation coefficient for dissolved oxygen	$mg\,L^{-1}$	0.2[f]	0.2[f]
Aerobic process parameters				
$K_{D,Ox}$	Aerobic solids-liquid sorption coefficient	$L\,g\,X_{SS}^{-1}$	0.019[c], 0.09[e]	0.0012[c]
$k_{Dec,Ox}$	Aerobic biotransformation rate coefficient for C_{CJ}	$L\,g^{-1}\,day^{-1}$	5[e]	5[e]
$q_{C,Ox}$	Aerobic maximum specific cometabolic substrate biotransformation rate in the presence of growth substrates for C_{LI}	$L\,g^{-1}\,day^{-1}$	1.6[d]	2[d]
$k_{Bio,Ox,SRT=16\ days}$	Aerobic biotransformation rate coefficient under growth substrate limiting conditions for C_{LI}	$L\,g^{-1}\,day^{-1}$	0.14[d]	0.01[d]
Anoxic process parameters				
$K_{D,Ax}$	Anoxic solids-liquid sorption coefficient	$L\,g\,X_{SS}^{-1}$	0.019[c]	0.0012[c]
$k_{Dec,Ax}$	Anoxic biotransformation rate coefficient for C_{CJ}	$L\,g^{-1}\,day^{-1}$	5[e]	5[e]
$q_{C,Ax}$	Anoxic maximum specific cometabolic substrate biotransformation rate in the presence of growth substrates for C_{LI}	$L\,g^{-1}\,day^{-1}$	0.96[d]	1.2[d]
$k_{Bio,Ax,SRT=16\ days}$	Anoxic biotransformation rate coefficient under growth substrate limiting conditions for C_{LI}	$L\,g^{-1}\,day^{-1}$	0.1[d]	0.01[d]
$k_{Bio,SRT>20\ days}$	Aerobic/anoxic biotransformation rate coefficients at SRT > 20 days	$L\,g^{-1}\,day^{-1}$	1.04[g]	—
Parameters for the dynamic input time-series				
$C_{LI,Inf}/C_{CJ,Inf}$	Ratio of the pre-clarified influent C_{LI} and C_{CJ} concentration values for the three daily inflow regimes[b]			
10:00–18:00 h	Parameter value for the morning increased inflow	—	0.85[e]	2.5[e]
18:00–02:00 h	Parameter value for the daily peak inflow	—	0.85[e]	2.5[e]
02:00–10:00 h	Parameter value for the midnight low inflow	—	0.85[e]	2.5[e]
$C_{SL,I,Inf}/C_{LI,Inf}$	Ratio of the pre-clarified influent C_{LI} and $C_{SL,I}$ concentration values	%	2.2[e]	1
$C_{LI,0,ss}$	Steady-state concentration value used in the dynamic WWTP simulations as initial condition for influent xenobiotic concentration	$ng\,L^{-1}$	100[e]	375[e]

[a]Diclofenac consumption data is presented by Grung et al. (2008).
[b]More information on the flow boundary conditions are shown by (Plósz et al., 2010c).
[c]Parameter value derived from literature (Ternes and Joss, 2006; Plósz et al., 2010a).
[d]Parameter values estimated using the measured batch experimental data.
[e]Parameter values estimated using the full-scale experimental data.
[f]ASM1 parameter values according to Spanjers et al. (1998).
[g]Estimated model parameter values used in approximating literature data with the full-scale input and WWTP data of this study (Fig. 3a).

V Annex – Laboratory AOP results

UV/peroxide laboratory results

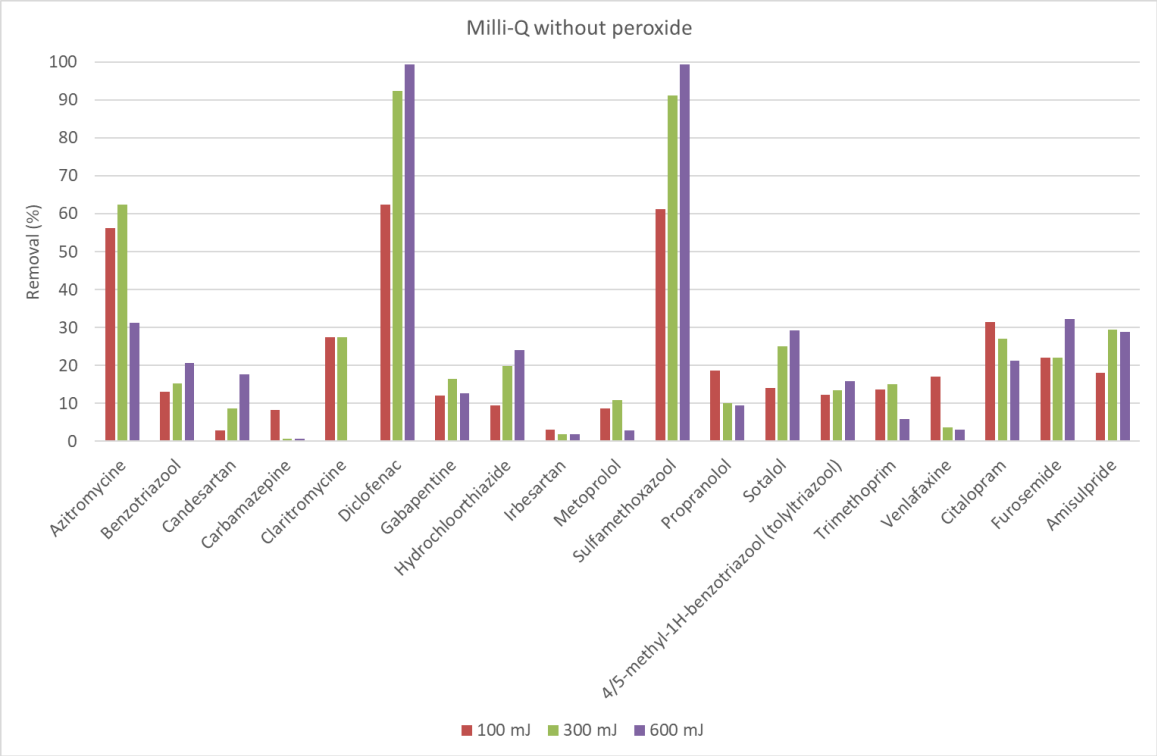

Removal (%) of the dosed compounds in Milli-Q water with t-BuOH with UV without peroxide

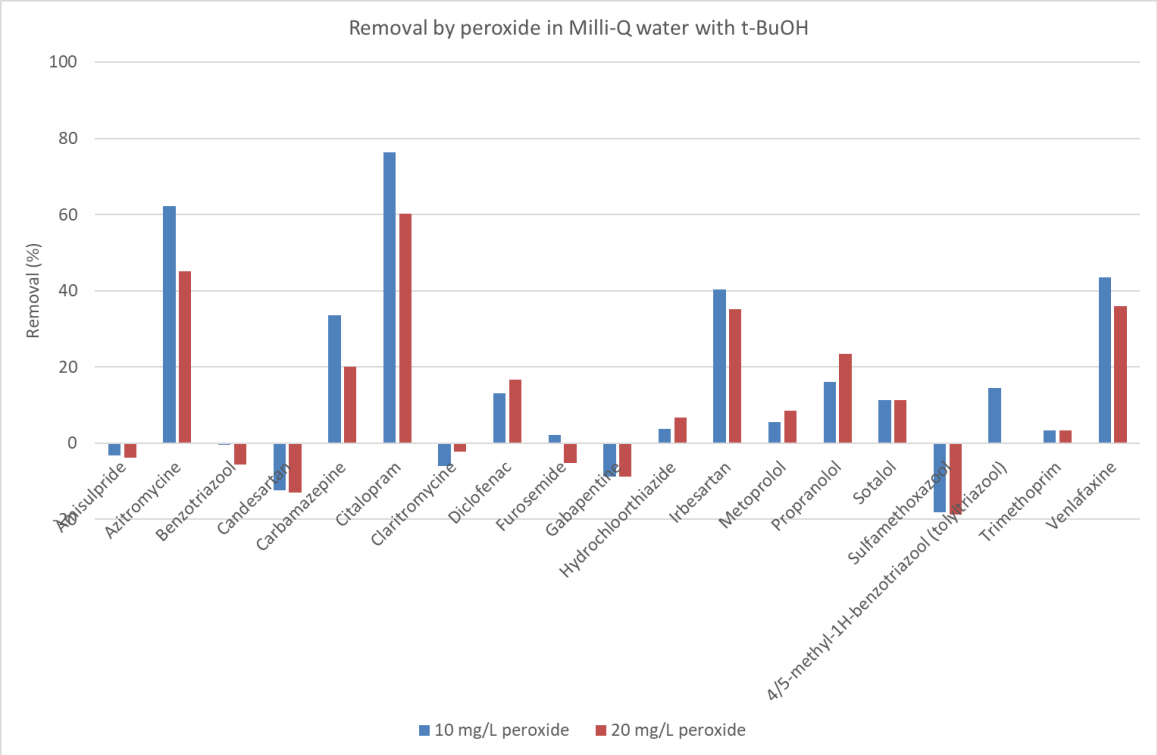

Removal of the compounds by 10 mg/L of peroxide in Milli-Q water with t-BuOH

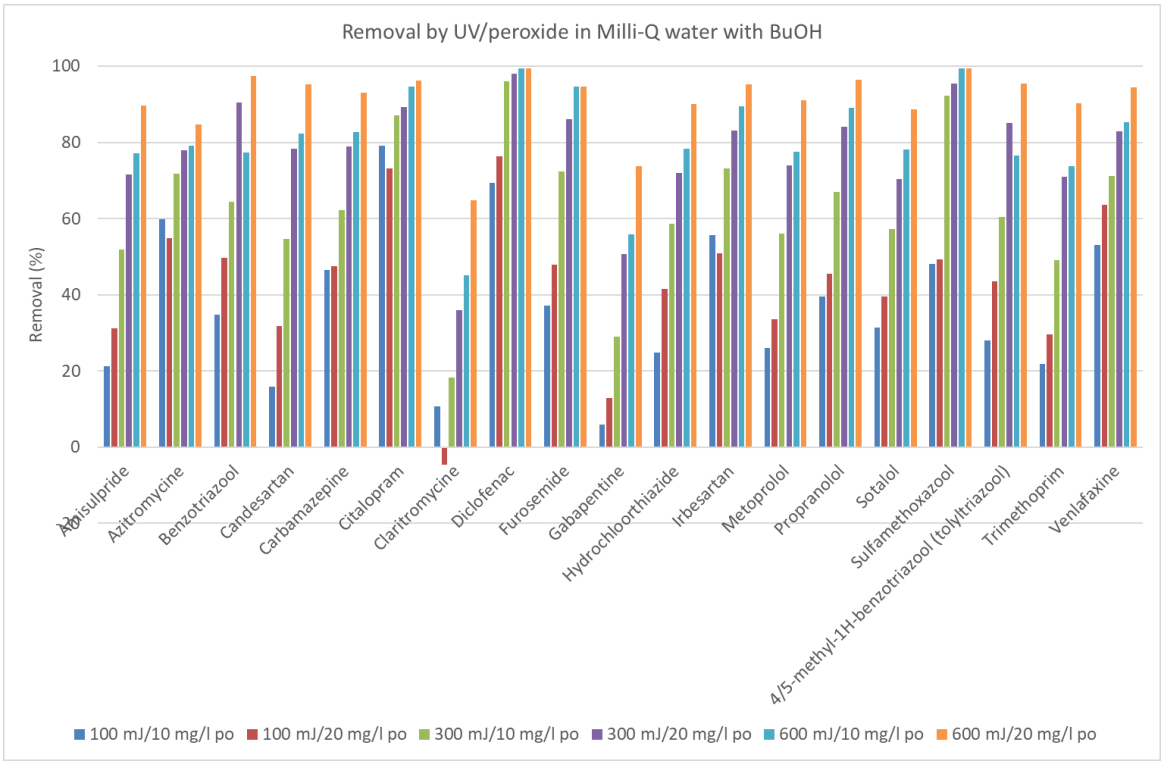

Removal of compounds by UV/peroxide with Milli-Q water with t-BuOH

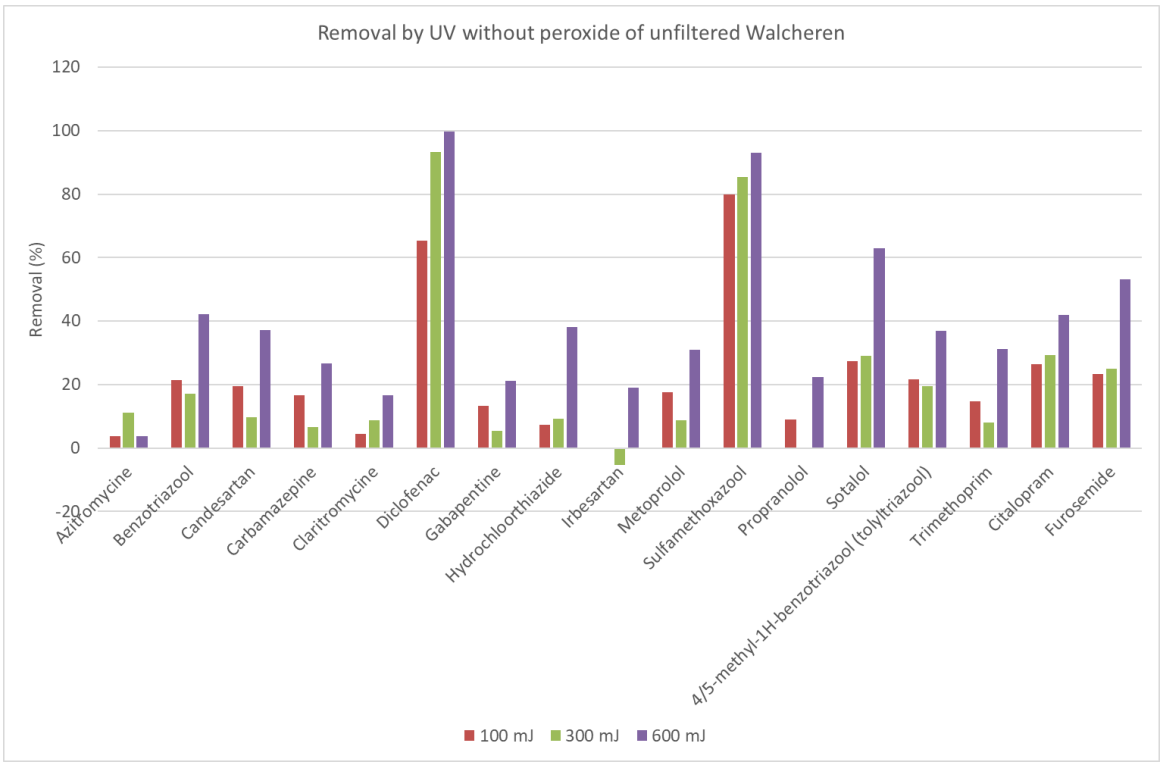

Removal of the compounds by UV without peroxide in unfiltered Walcheren WWTP effluent

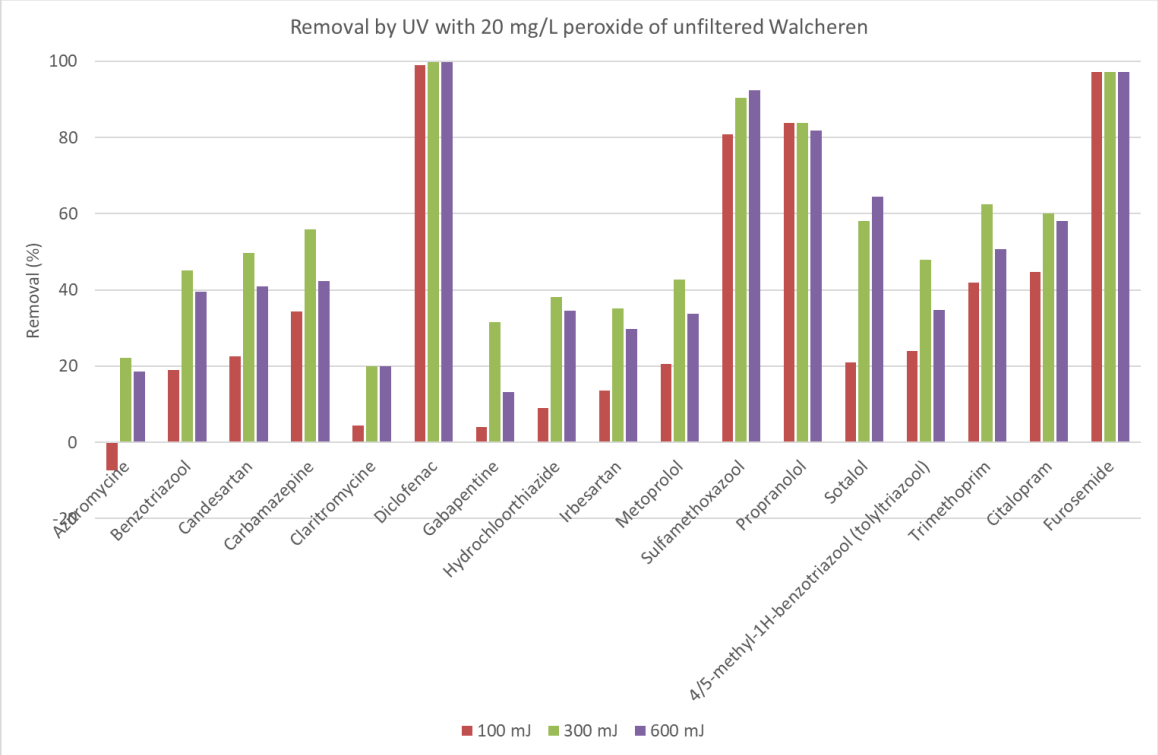

Removal of the compounds by UV with 20 mg/L peroxide in unfiltered Walcheren WWTP effluent

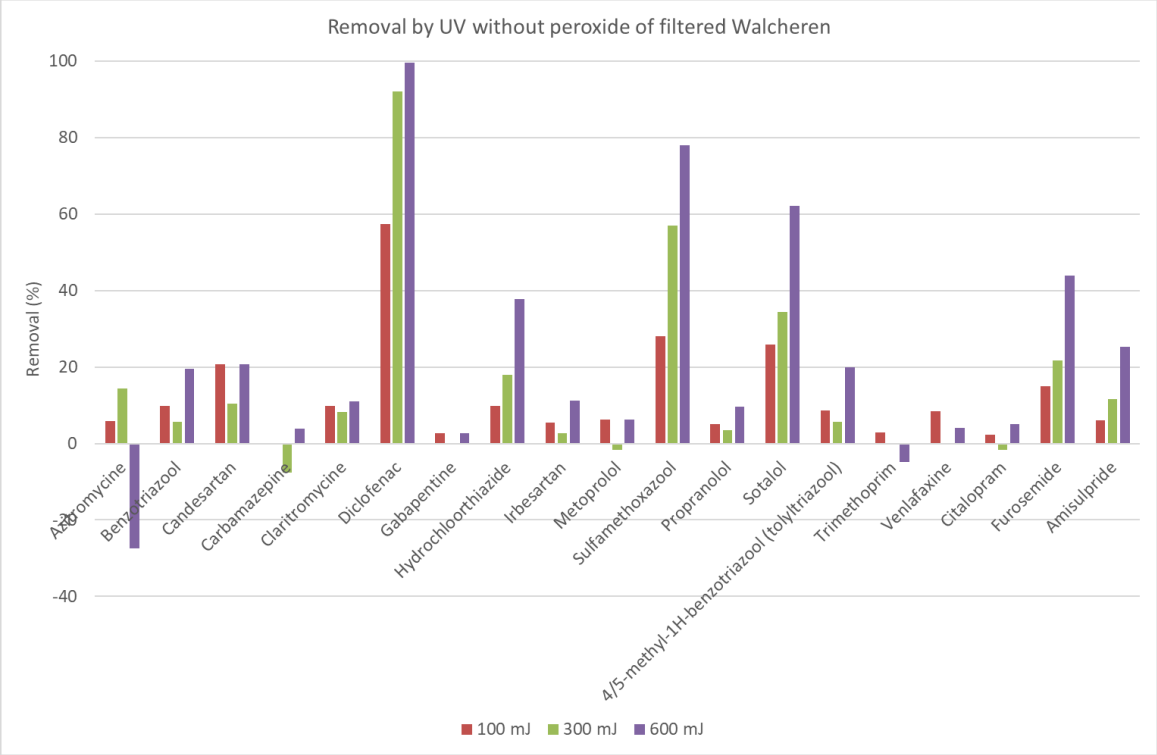

Removal of the compounds by UV without peroxide in filtered Walcheren WWTP effluent

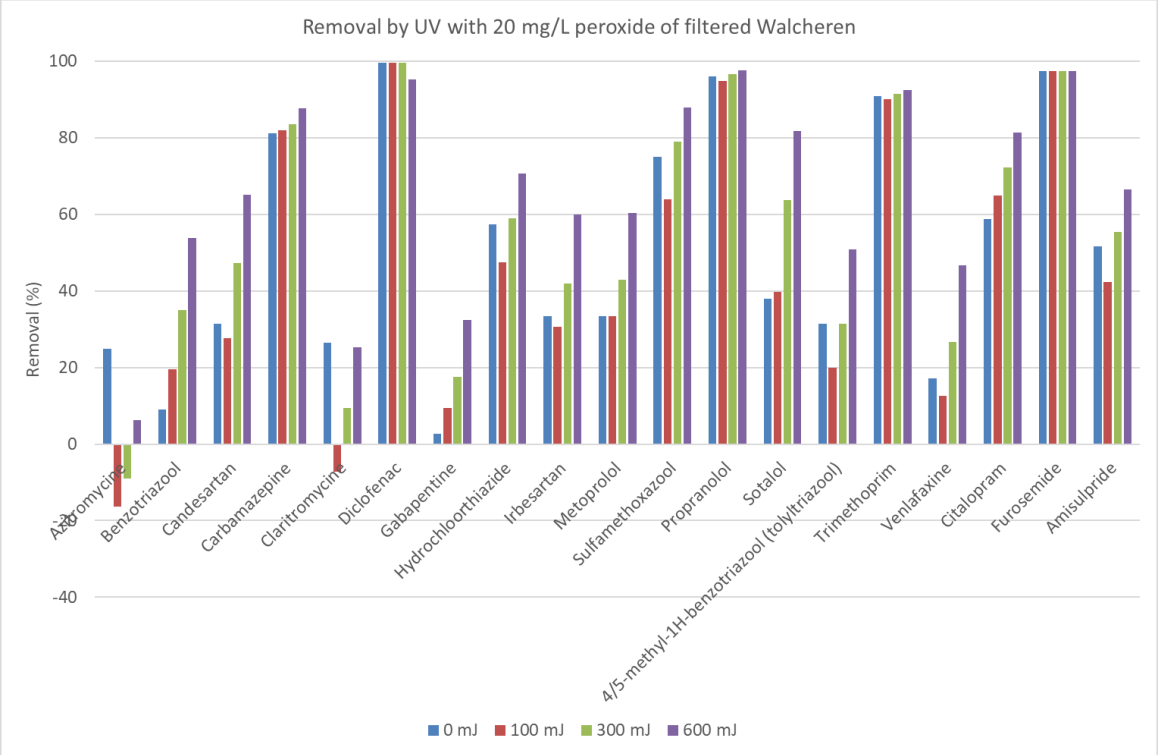

Removal of the compounds by UV with 20 mg/L peroxide in filtered Walcheren WWTP effluent

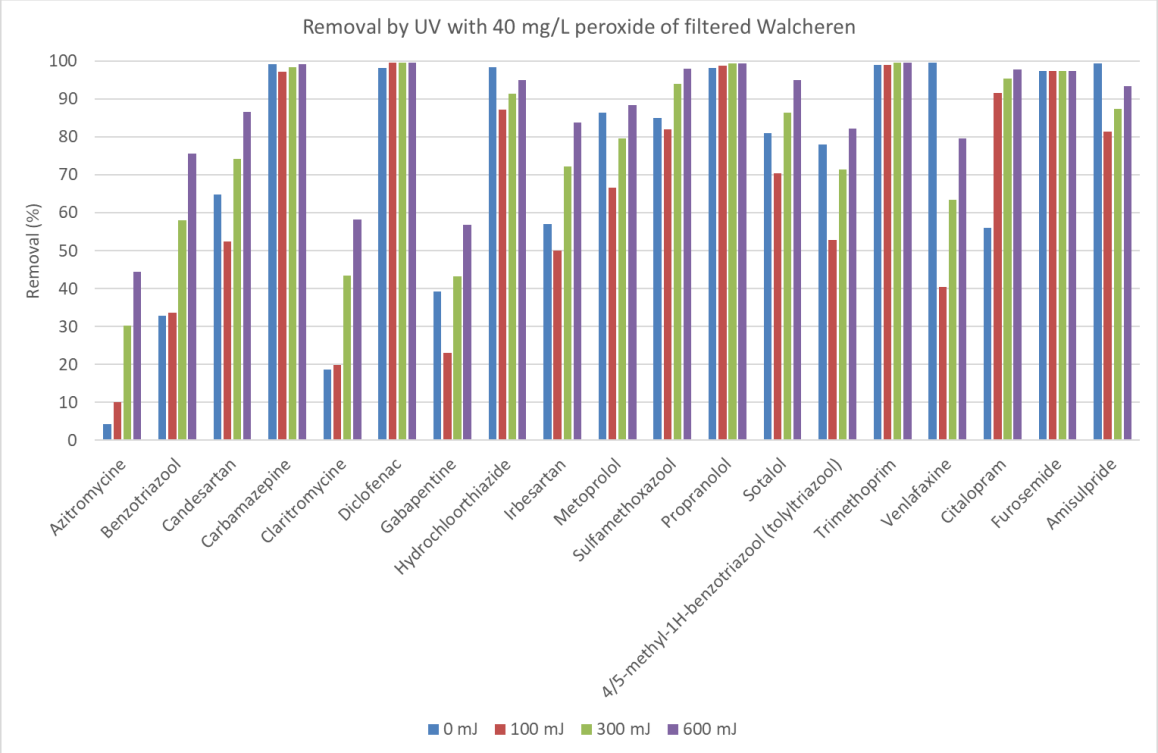

Removal of the compounds by UV with 40 mg/L peroxide in filtered Walcheren WWTP effluent

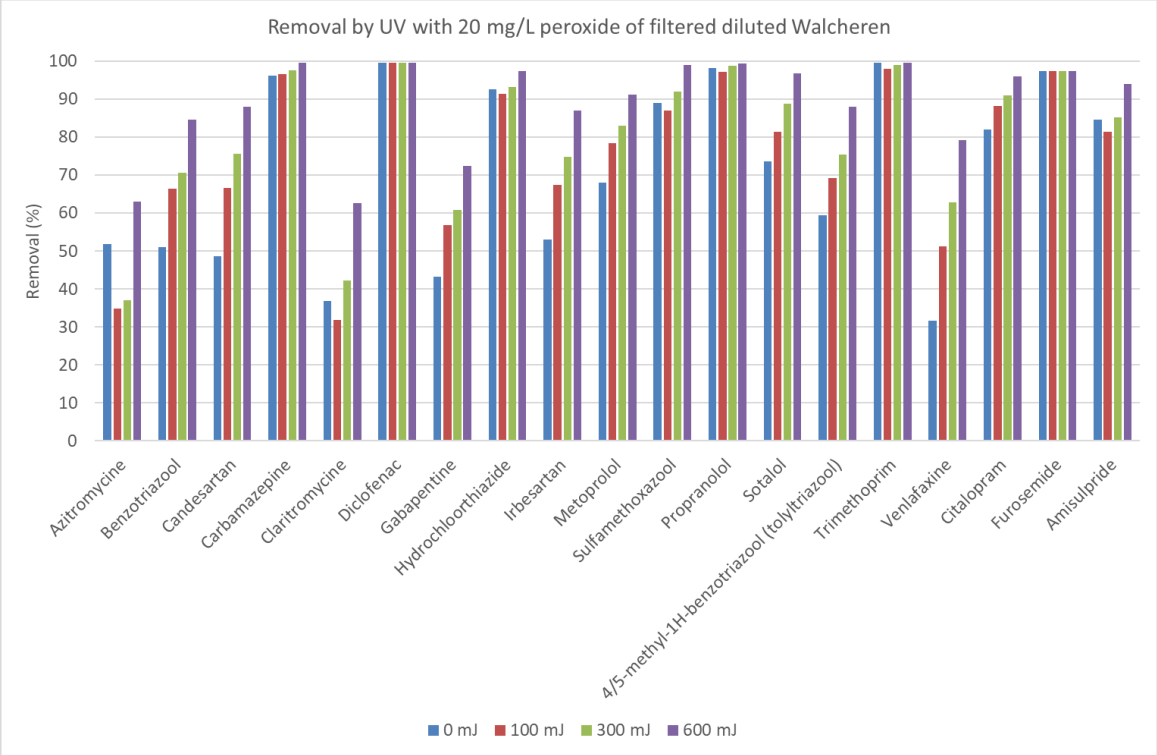

Removal of the compounds by UV with 20 mg/L peroxide in filtered diluted Walcheren WWTP effluent

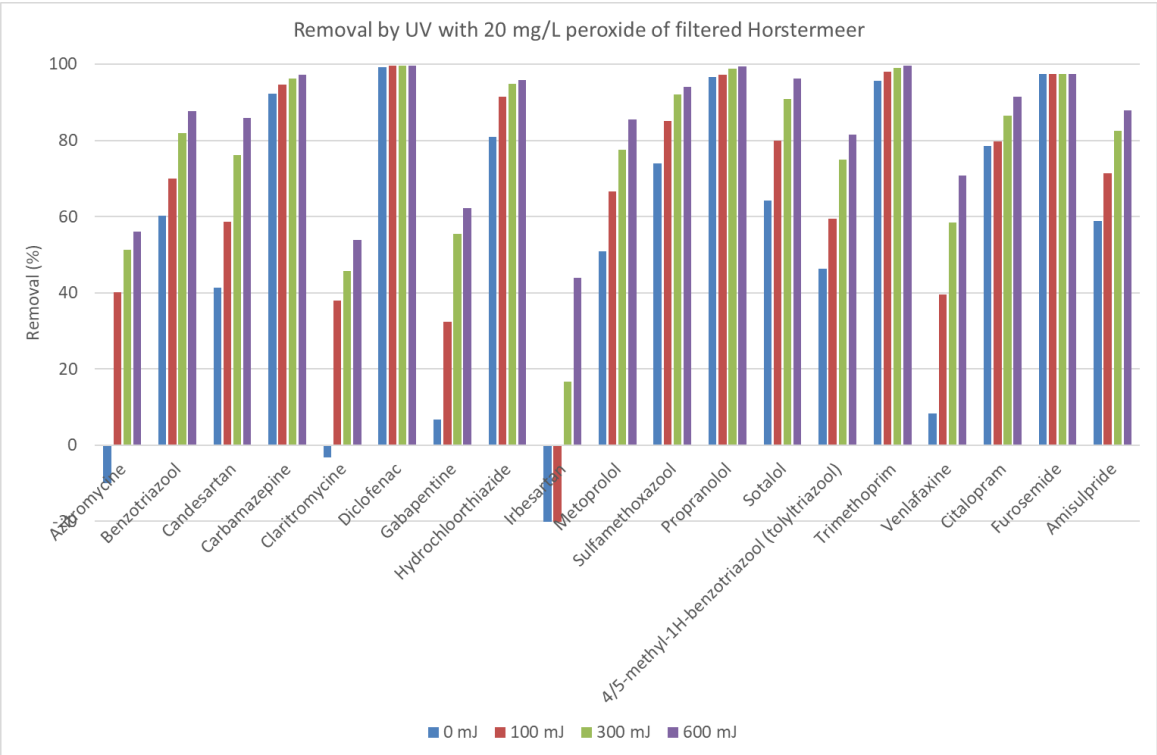

Figure 38- Removal of the compounds by UV with 20 mg/L peroxide in filtered Horstermeer WWTP effluent

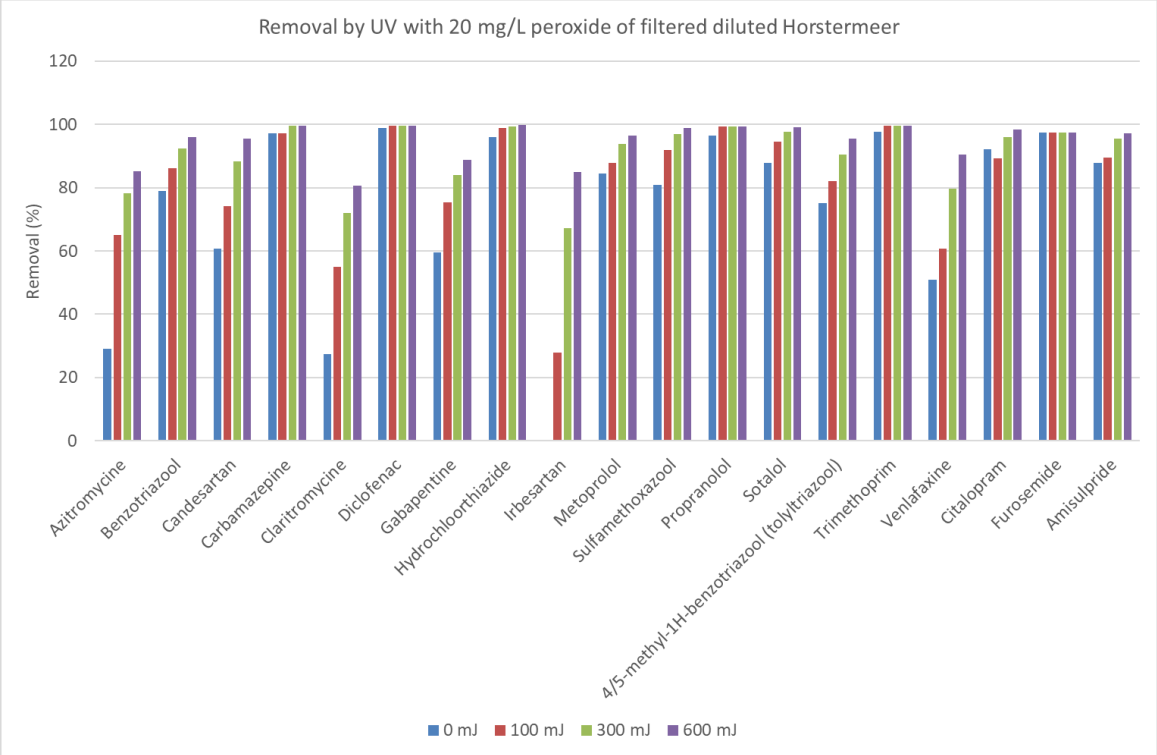

Removal of the compounds by UV with 20 mg/L peroxide in filtered diluted Horstermeer WWTP effluent

Ozone laboratory results

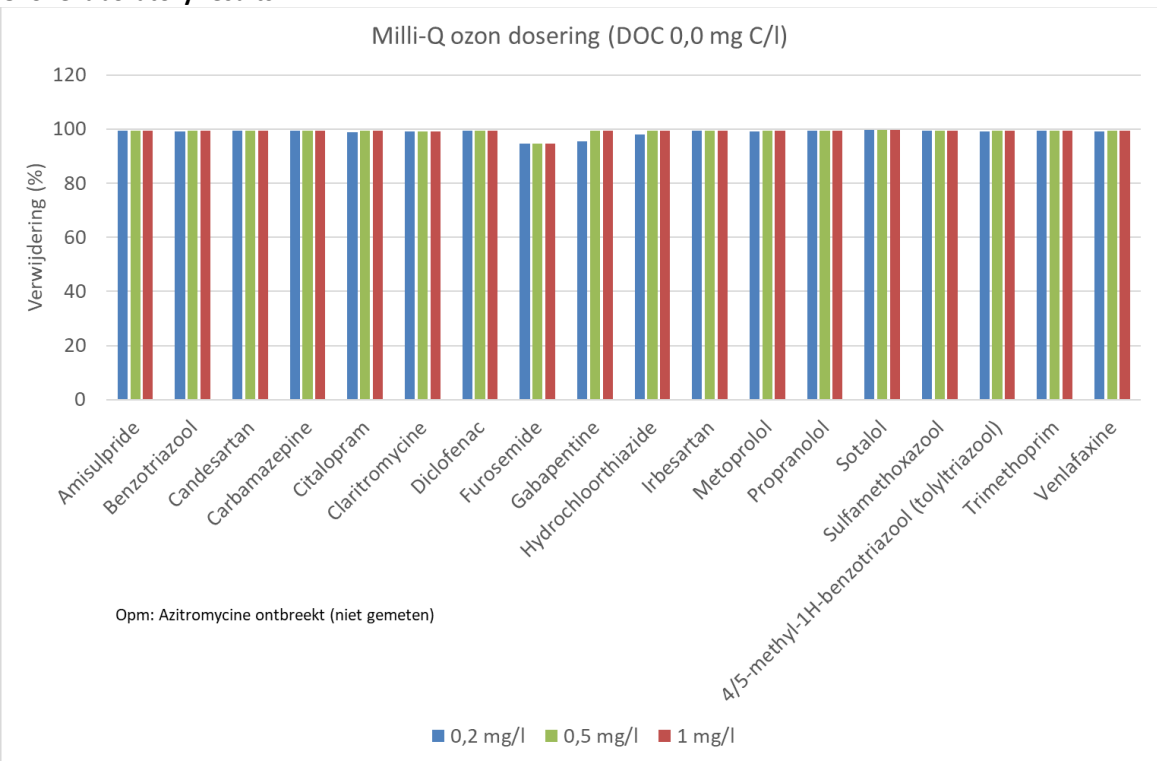

Removal of compounds by ozone with Milli-Q water

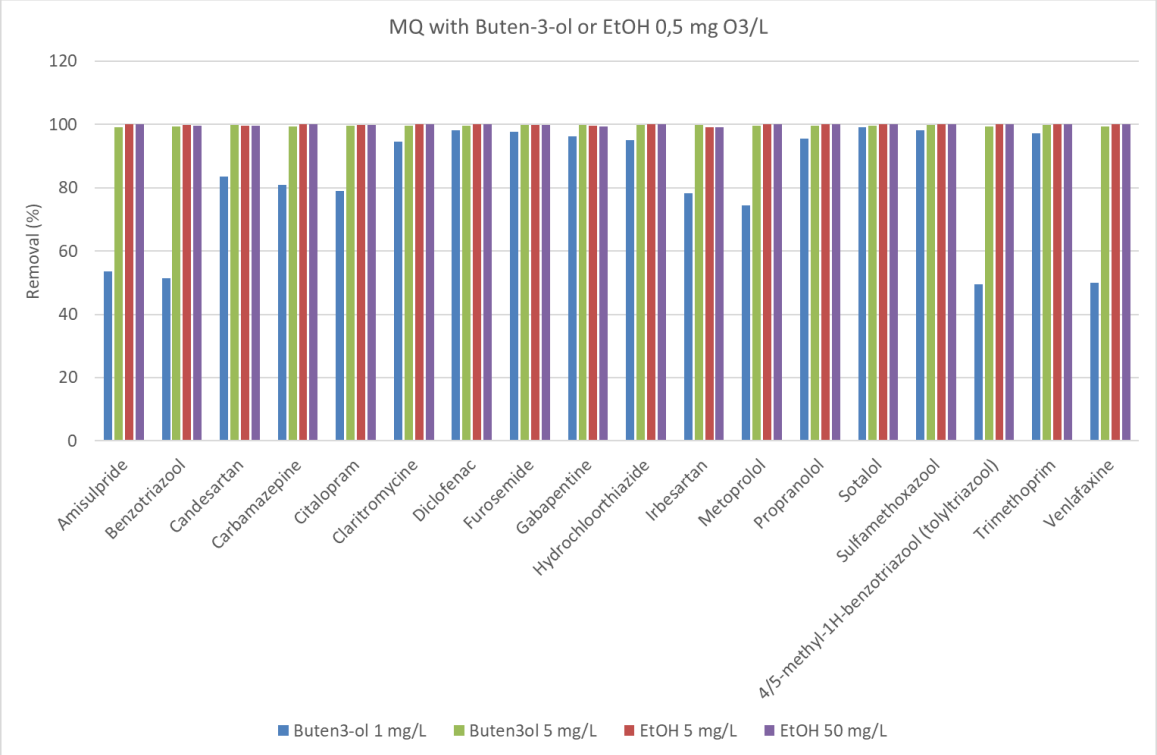

Removal of compounds by ozone with Milli-Q water with Buten-3-ol or EtOH with 0,5 mg O_3/L

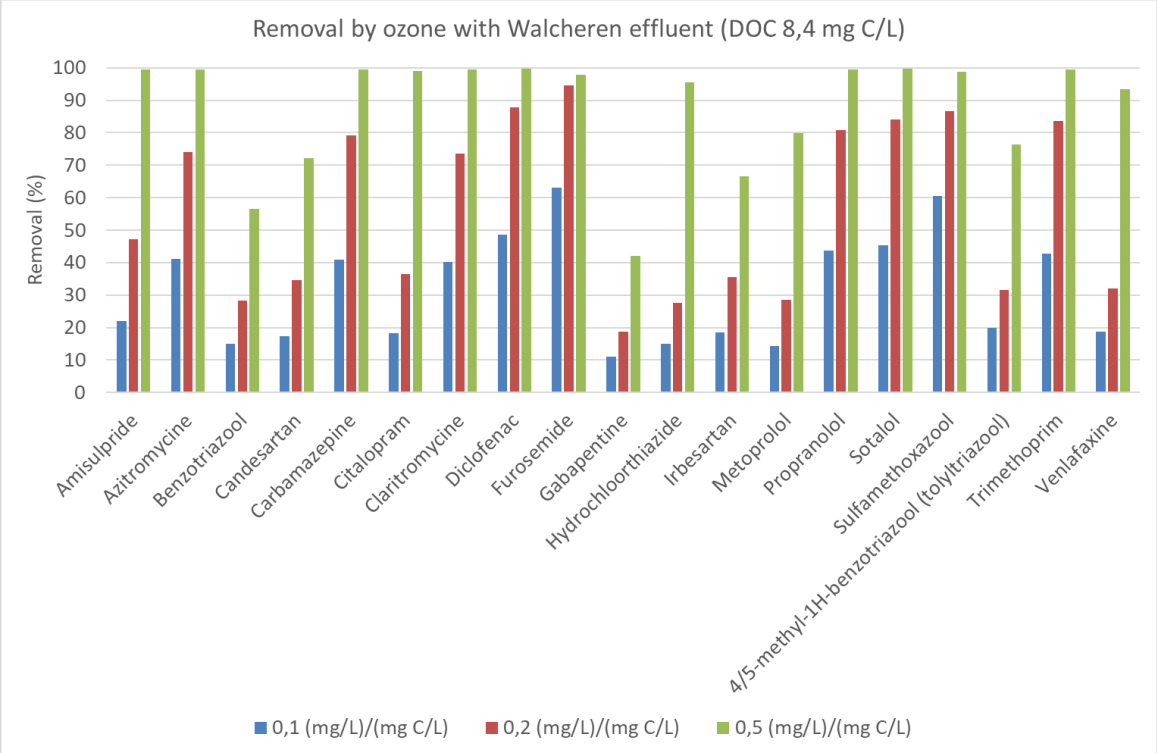

Removal of compounds by ozone with Walcheren WWTP effluent

In the figure below the decline of ozone by the water type is given, which was used for the validation of the ozone model. In Milli-Q water the ozone decline takes a longer time than in Walcheren effluent and Milli-Q with ethanol because of the absence of organic matter.

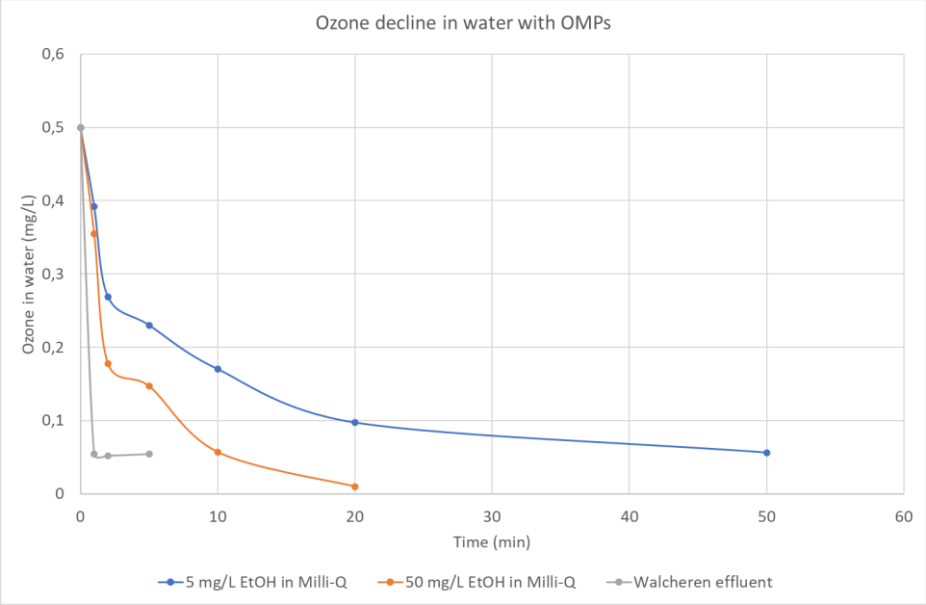

Figure: Decline of ozone in water

VI Annex – Influent concentrations of AOP pilots

UV/H_2O_2 pilot experiments

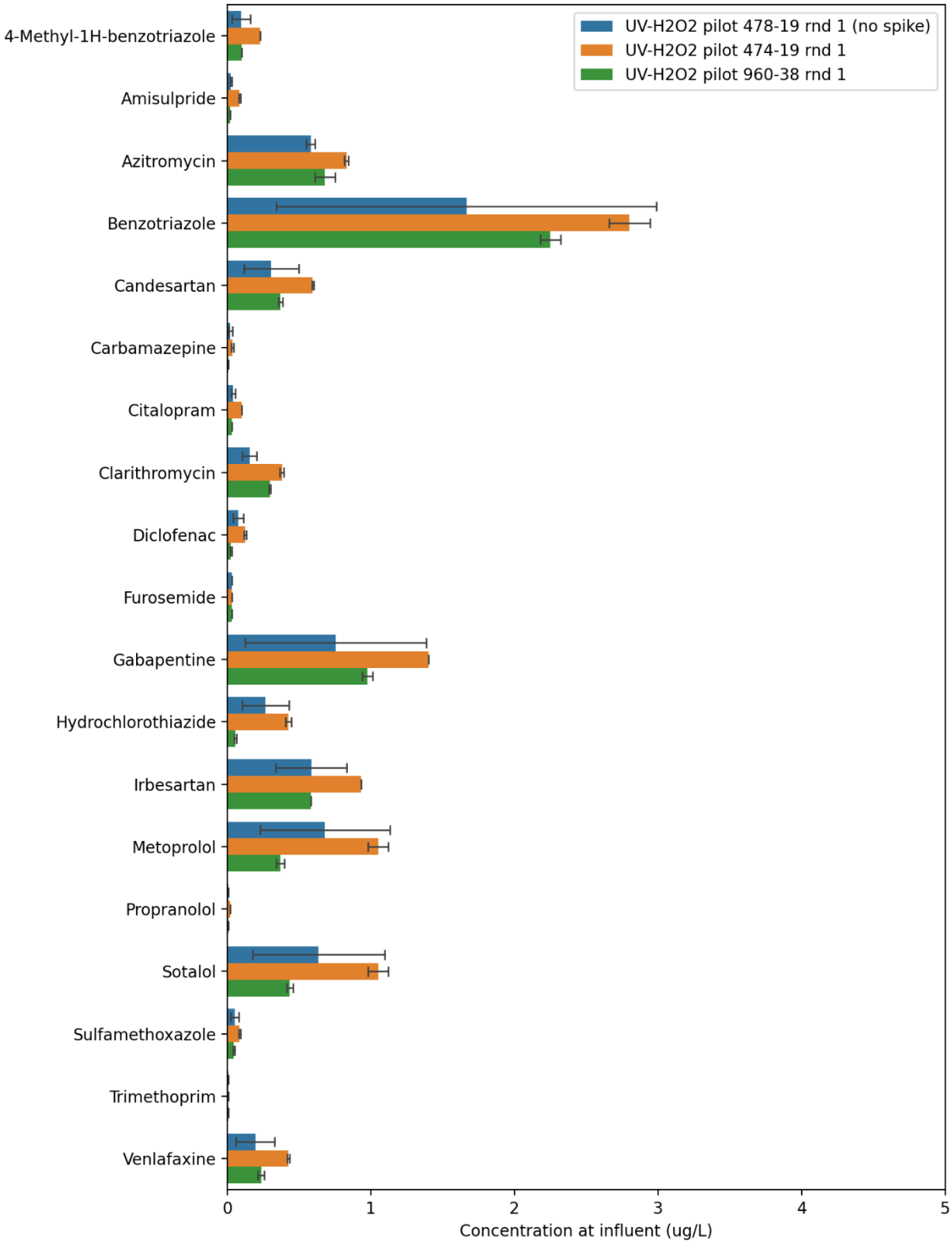

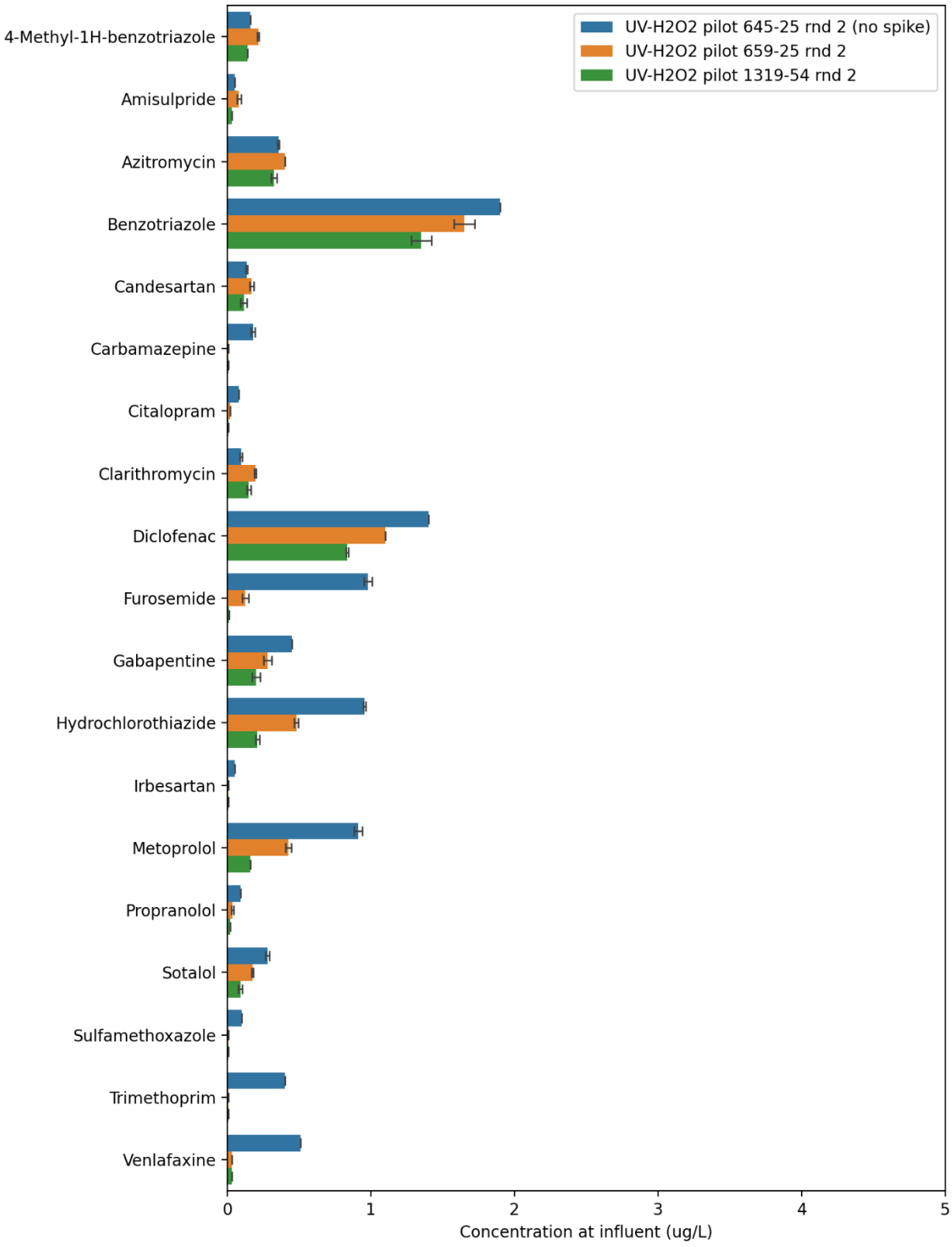
UV-H2O2 pilot 645-25 rnd 2 (no spike)
UV-H2O2 pilot 659-25 rnd 2
UV-H2O2 pilot 1319-54 rnd 2
4-Methyl-1H-benzotriazole
Amisulpride
Azitromycin
Benzotriazole
Candesartan
Carbamazepine
Citalopram
Clarithromycin
Diclofenac
Furosemide
Gabapentine
Hydrochlorothiazide
Irbesartan
Metoprolol
Propranolol
Sotalol
Sulfamethoxazole
Trimethoprim
Venlafaxine
0
1
2
3
4
5
Concentration at influent (ug/L)

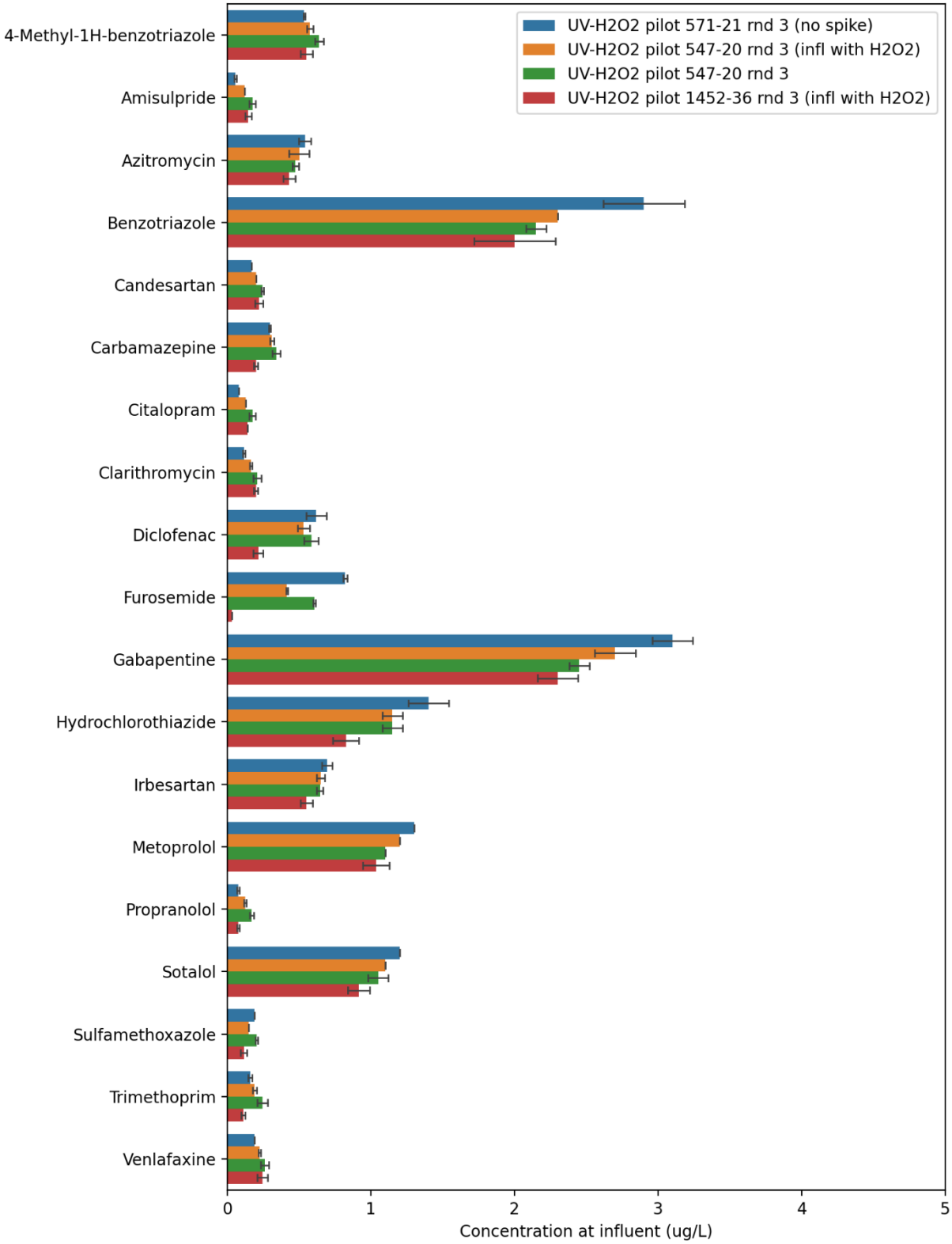
UV-H2O2 pilot 571-21 rnd 3 (no spike)
UV-H2O2 pilot 547-20 rnd 3 (infl with H2O2)
UV-H2O2 pilot 547-20 rnd 3
UV-H2O2 pilot 1452-36 rnd 3 (infl with H2O2)
4-Methyl-1H-benzotriazole
Amisulpride
Azitromycin
Benzotriazole
Candesartan
Carbamazepine
Citalopram
Clarithromycin
Diclofenac
Furosemide
Gabapentine
Hydrochlorothiazide
Irbesartan
Metoprolol
Propranolol
Sotalol
Sulfamethoxazole
Trimethoprim
Venlafaxine
0
1
2
3
4
5
Concentration at influent (ug/L)

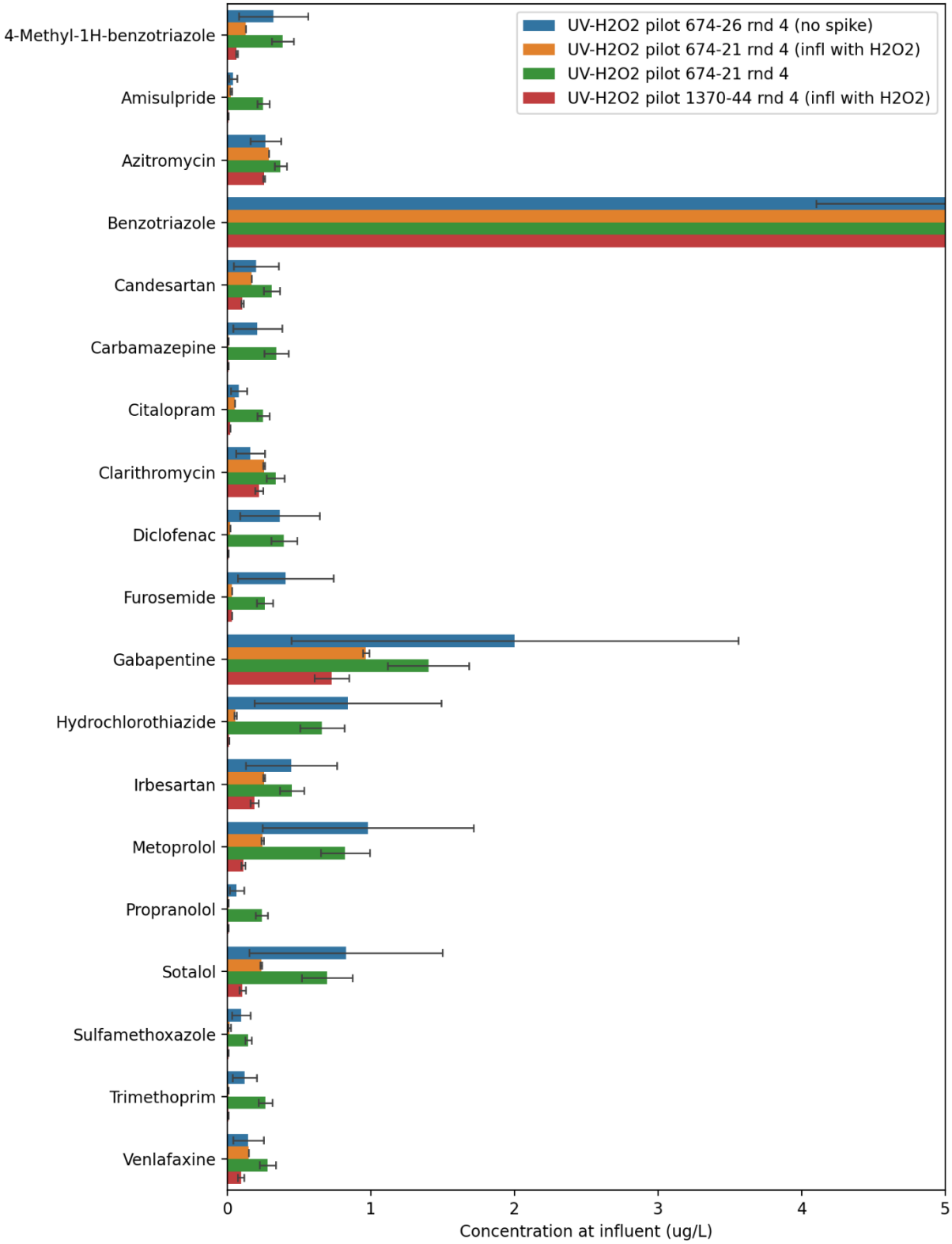
UV-H2O2 pilot 674-26 rnd 4 (no spike)
UV-H2O2 pilot 674-21 rnd 4 (infl with H2O2)
UV-H2O2 pilot 674-21 rnd 4
UV-H2O2 pilot 1370-44 rnd 4 (infl with H2O2)
4-Methyl-1H-benzotriazole
Amisulpride
Azitromycin
Benzotriazole
Candesartan
Carbamazepine
Citalopram
Clarithromycin
Diclofenac
Furosemide
Gabapentine
Hydrochlorothiazide
Irbesartan
Metoprolol
Propranolol
Sotalol
Sulfamethoxazole
Trimethoprim
Venlafaxine
0
1
2
3
4
5
Concentration at influent (ug/L)

Ozone pilot experiments

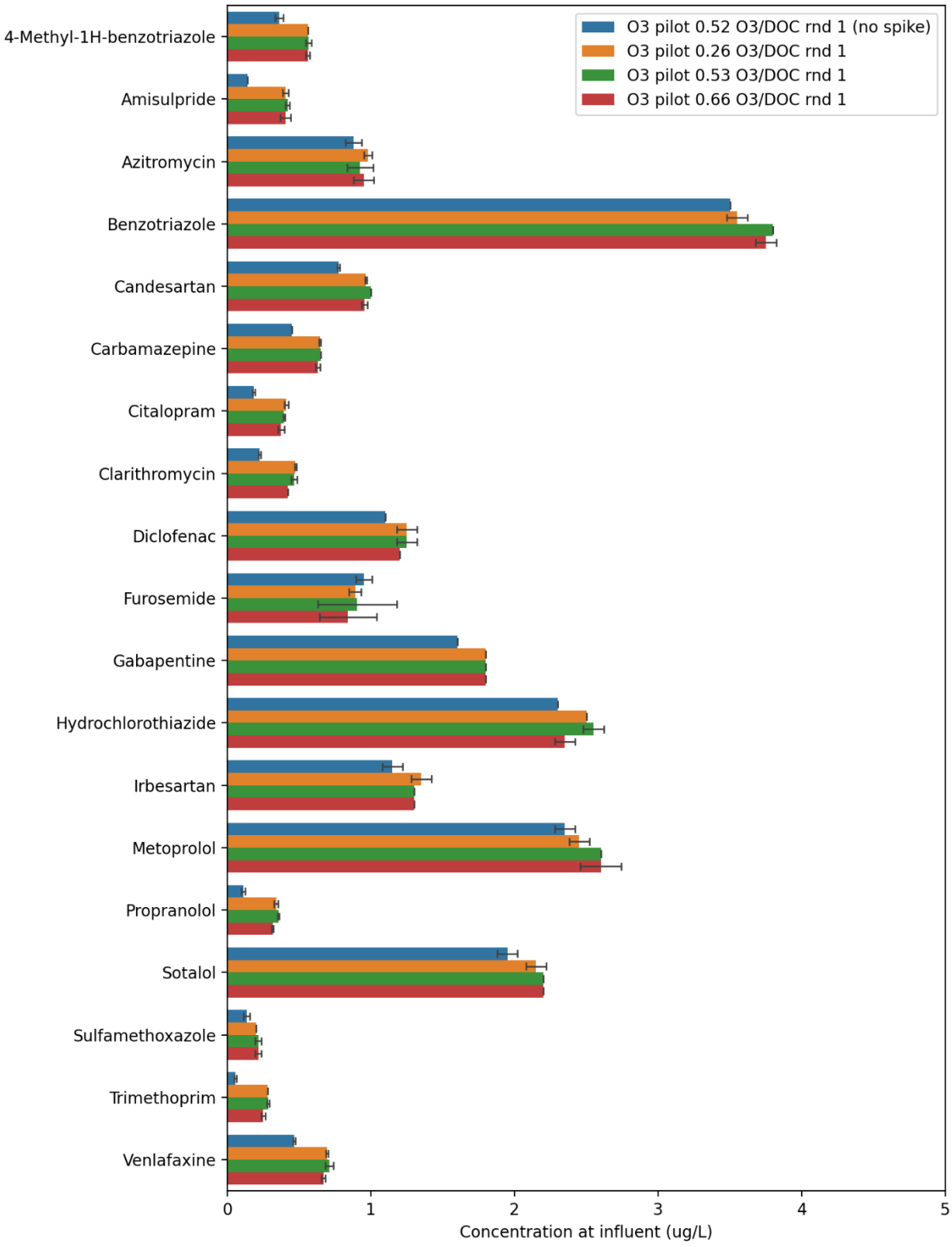

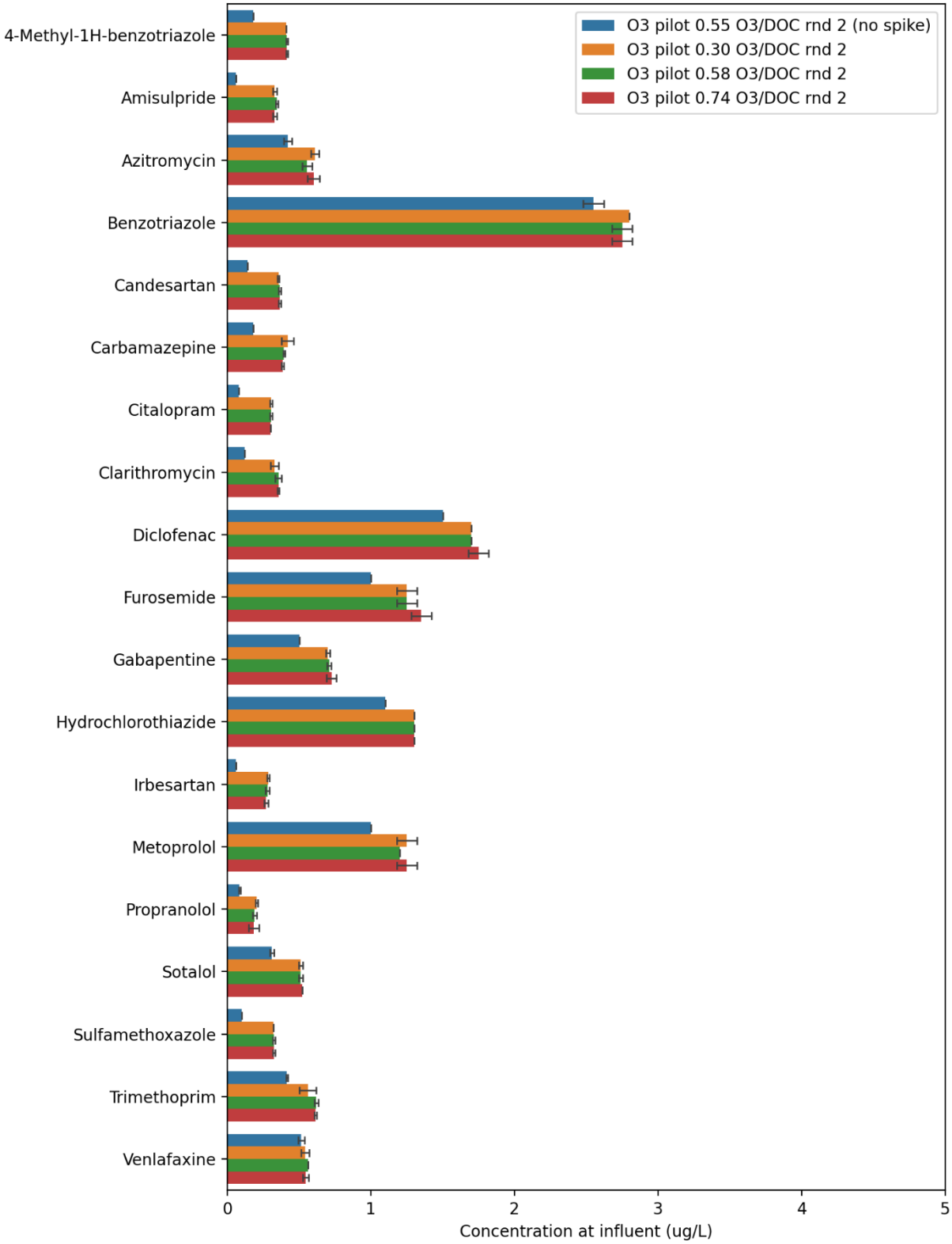
O3 pilot 0.55 O3/DOC rnd 2 (no spike)
O3 pilot 0.30 O3/DOC rnd 2
O3 pilot 0.58 O3/DOC rnd 2
O3 pilot 0.74 O3/DOC rnd 2
4-Methyl-1H-benzotriazole
Amisulpride
Azitromycin
Benzotriazole
Candesartan
Carbamazepine
Citalopram
Clarithromycin
Diclofenac
Furosemide
Gabapentine
Hydrochlorothiazide
Irbesartan
Metoprolol
Propranolol
Sotalol
Sulfamethoxazole
Trimethoprim
Venlafaxine
0
1
2
3
4
5
Concentration at influent (ug/L)

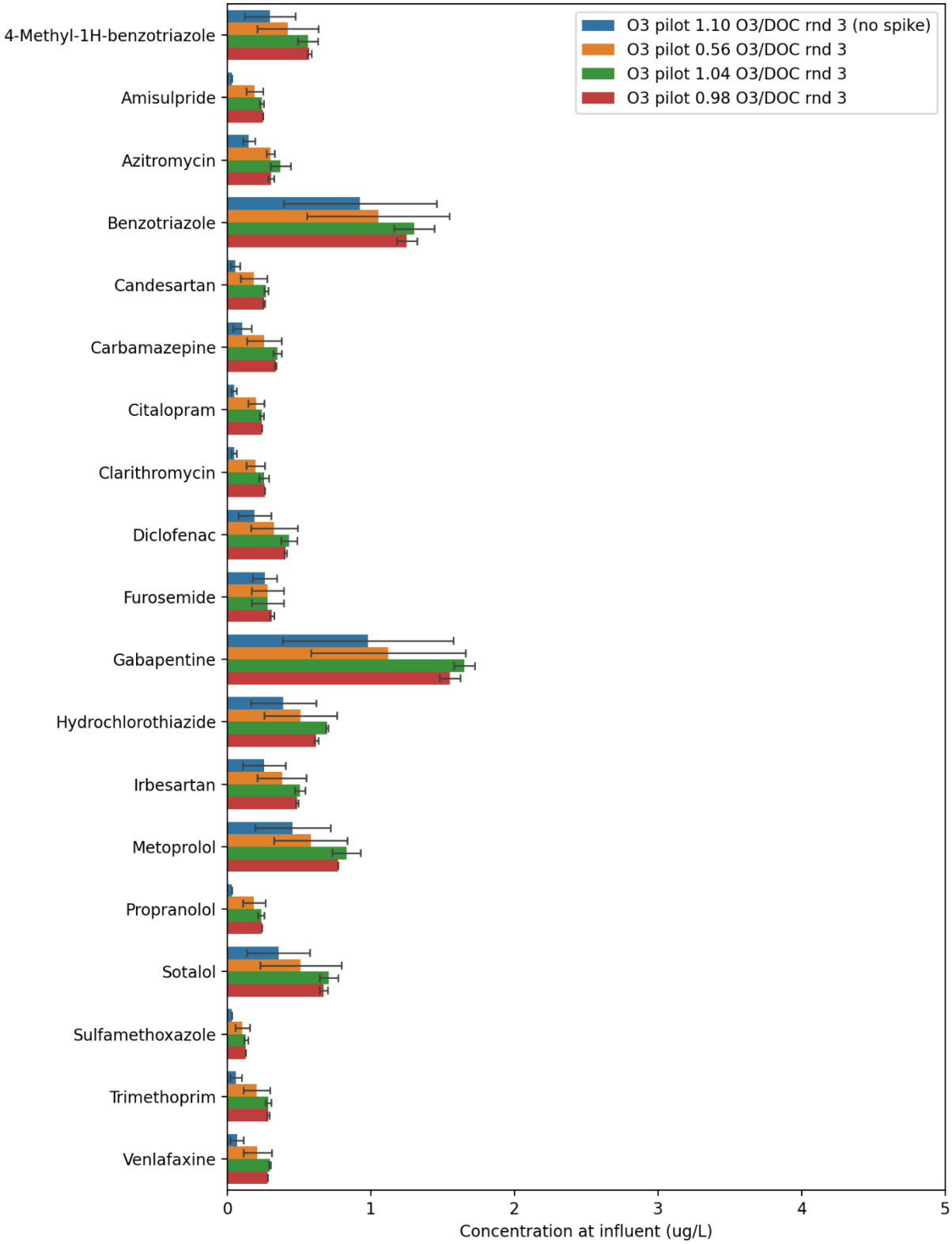
O3 pilot 1.10 O3/DOC rnd 3 (no spike)
O3 pilot 0.56 O3/DOC rnd 3
O3 pilot 1.04 O3/DOC rnd 3
O3 pilot 0.98 O3/DOC rnd 3
4-Methyl-1H-benzotriazole
Amisulpride
Azitromycin
Benzotriazole
Candesartan
Carbamazepine
Citalopram
Clarithromycin
Diclofenac
Furosemide
Gabapentine
Hydrochlorothiazide
Irbesartan
Metoprolol
Propranolol
Sotalol
Sulfamethoxazole
Trimethoprim
Venlafaxine
0
1
2
3
4
5
Concentration at influent (ug/L)

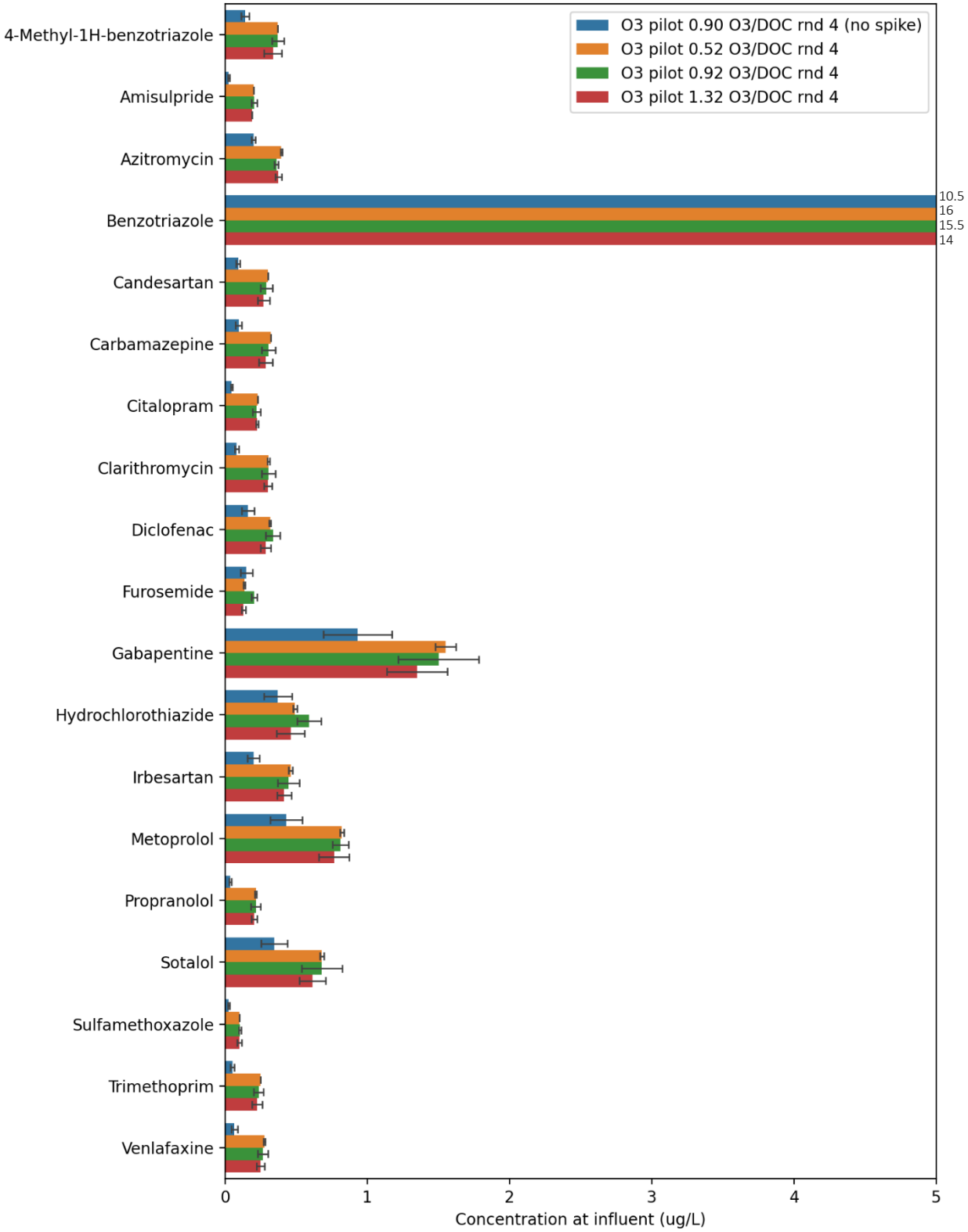
O3 pilot 0.90 O3/DOC rnd 4 (no spike)
O3 pilot 0.52 O3/DOC rnd 4
O3 pilot 0.92 O3/DOC rnd 4
O3 pilot 1.32 O3/DOC rnd 4
4-Methyl-1H-benzotriazole
Amisulpride
Azitromycin
Benzotriazole
Candesartan
Carbamazepine
Citalopram
Clarithromycin
Diclofenac
Furosemide
Gabapentine
Hydrochlorothiazide
Irbesartan
Metoprolol
Propranolol
Sotalol
Sulfamethoxazole
Trimethoprim
Venlafaxine
10.5
16
15.5
14
0
1
2
3
4
5
Concentration at influent (ug/L)

VII Annex – AOP pilot experimental results

UV/H_2O_2 pilot experiments

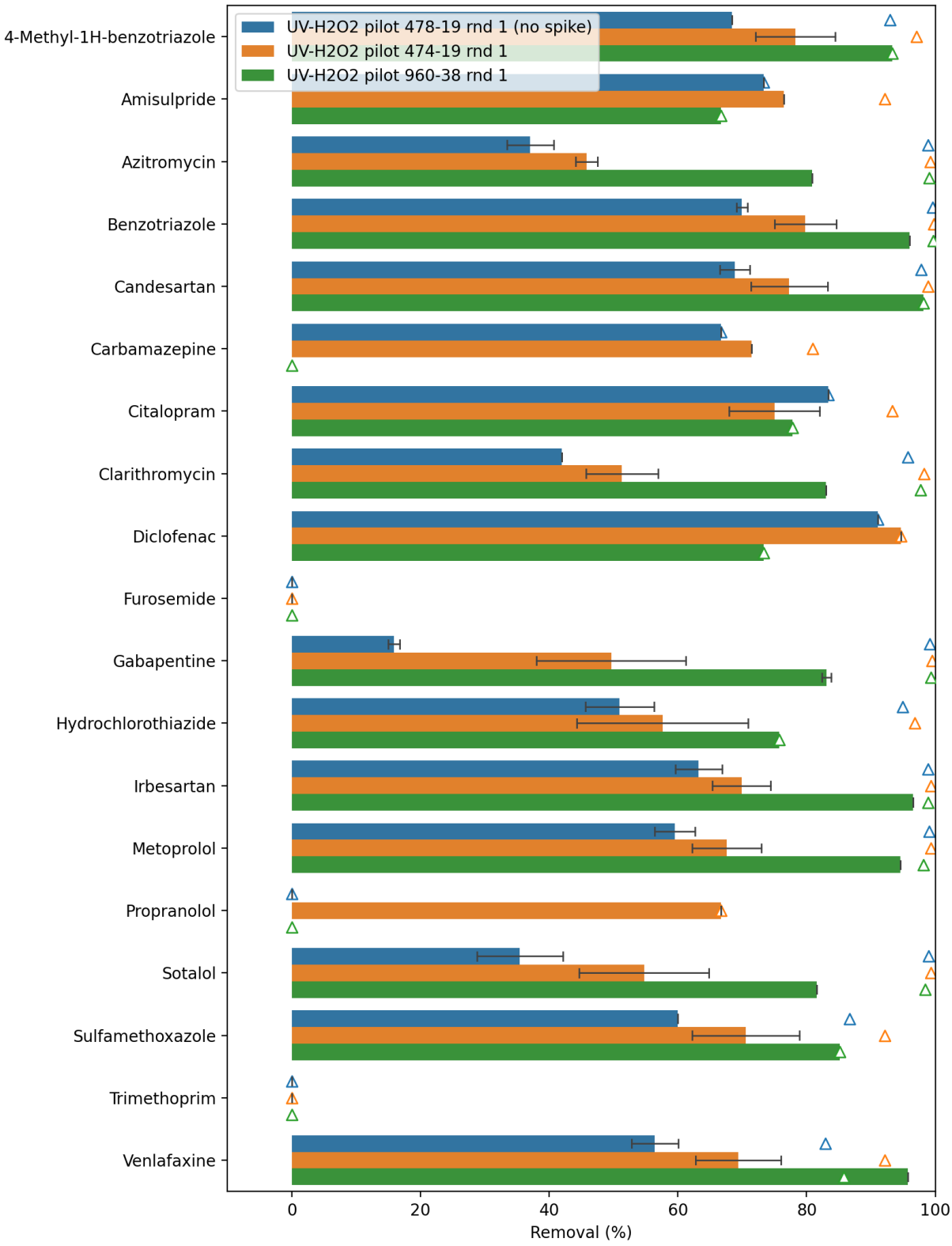

Removal percentages of micropollutants during UV/H_2O_2 treatment for round 1. The first number in the legend represents the UV dose (mJ/cm^2), the second number represents the H_2O_2 concentration (mg/L). The triangles show the maximum degradation that can be demonstrated given the influent concentration and limit of detection. The error range is calculated from the standard deviation of the duplicate samples.

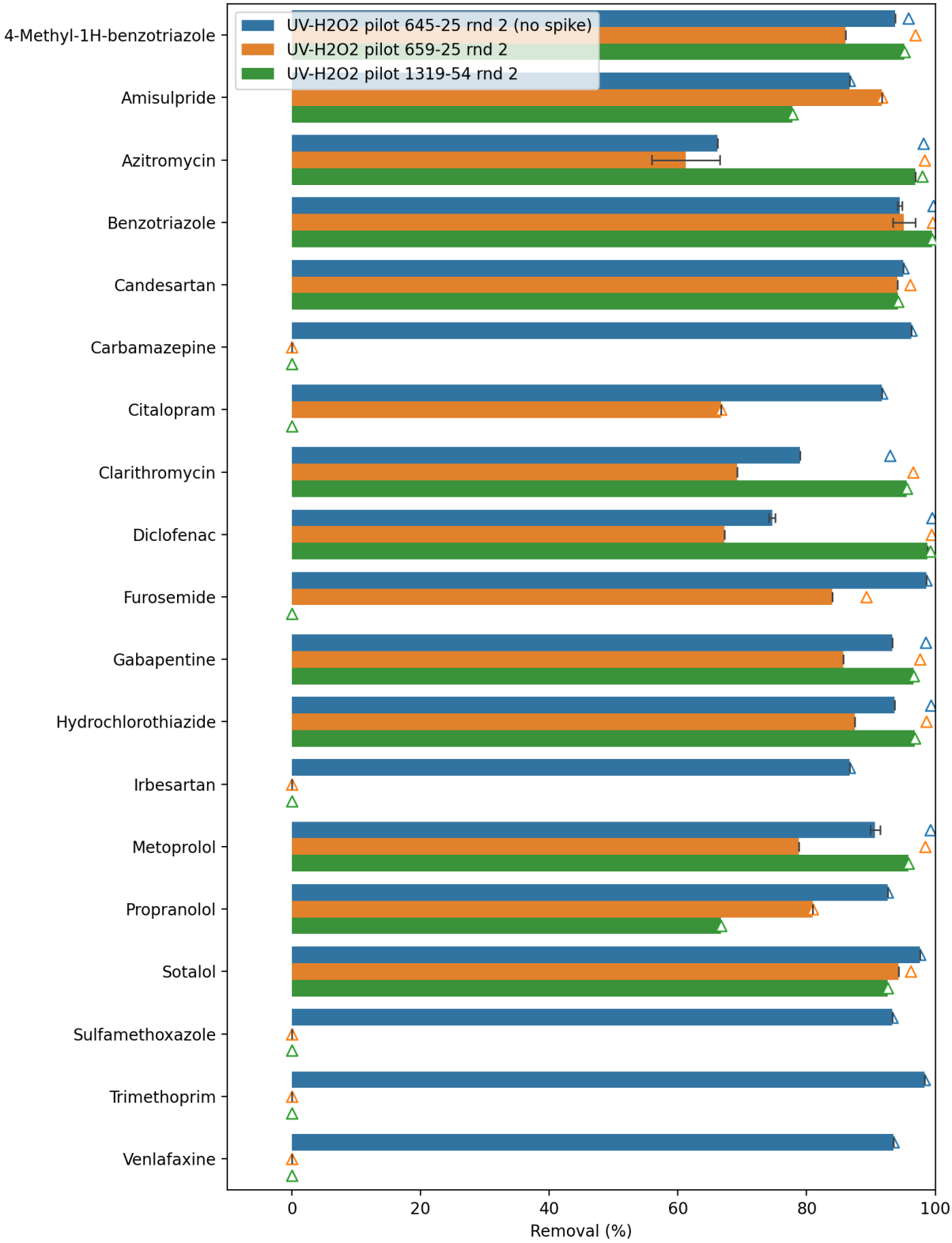

Removal percentages of micropollutants during UV/H_2O_2 treatment for round 2. The first number in the legend represents the UV dose (mJ/cm^2), the second number represents the H_2O_2 concentration (mg/L). The triangles show the maximum degradation that can be demonstrated given the influent concentration and limit of detection. The error range is calculated from the standard deviation of the duplicate samples.

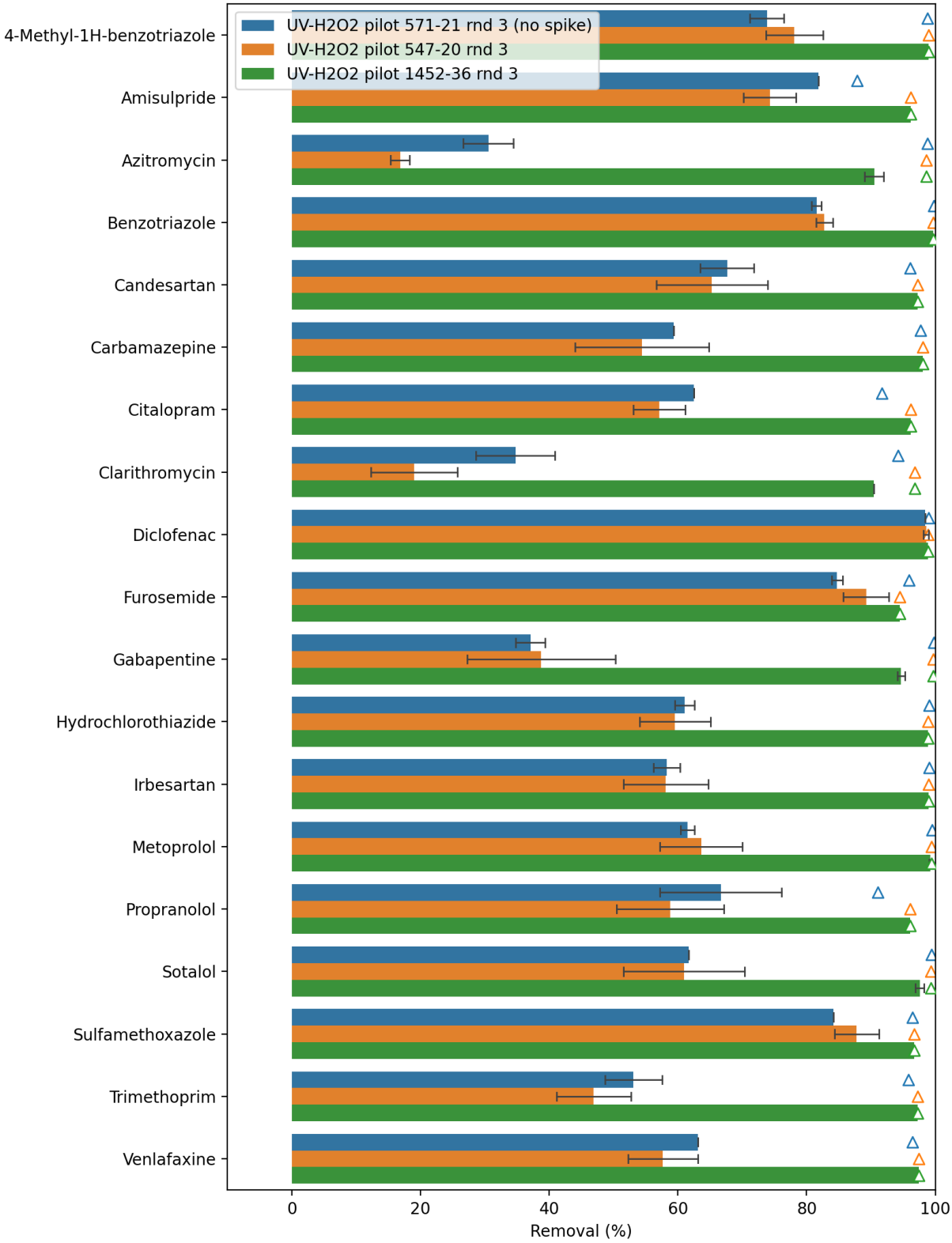

Removal percentages of micropollutants during UV/H_2O_2 treatment for round 3. The first number in the legend represents the UV dose (mJ/cm^2), the second number represents the H_2O_2 concentration (mg/L). The triangles show the maximum degradation that can be demonstrated given the influent concentration and limit of detection. The error range is calculated from the standard deviation of the duplicate samples.

Ozone pilot experiments

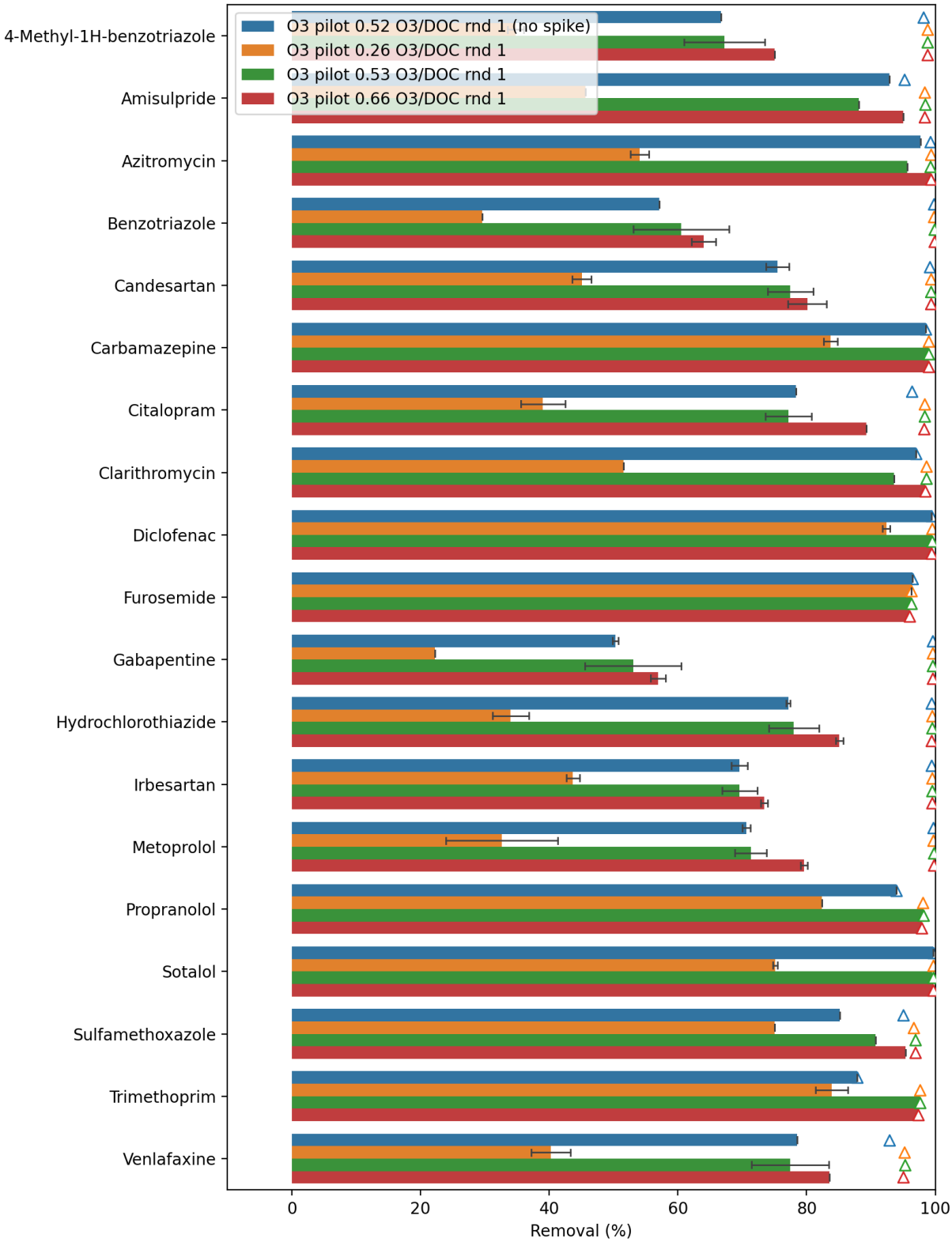

Removal percentages of micropollutants during ozone treatment for round 1. The triangles show the maximum degradation that can be demonstrated given the influent concentration and limit of detection. The error range is calculated from the standard deviation of the duplicate samples.

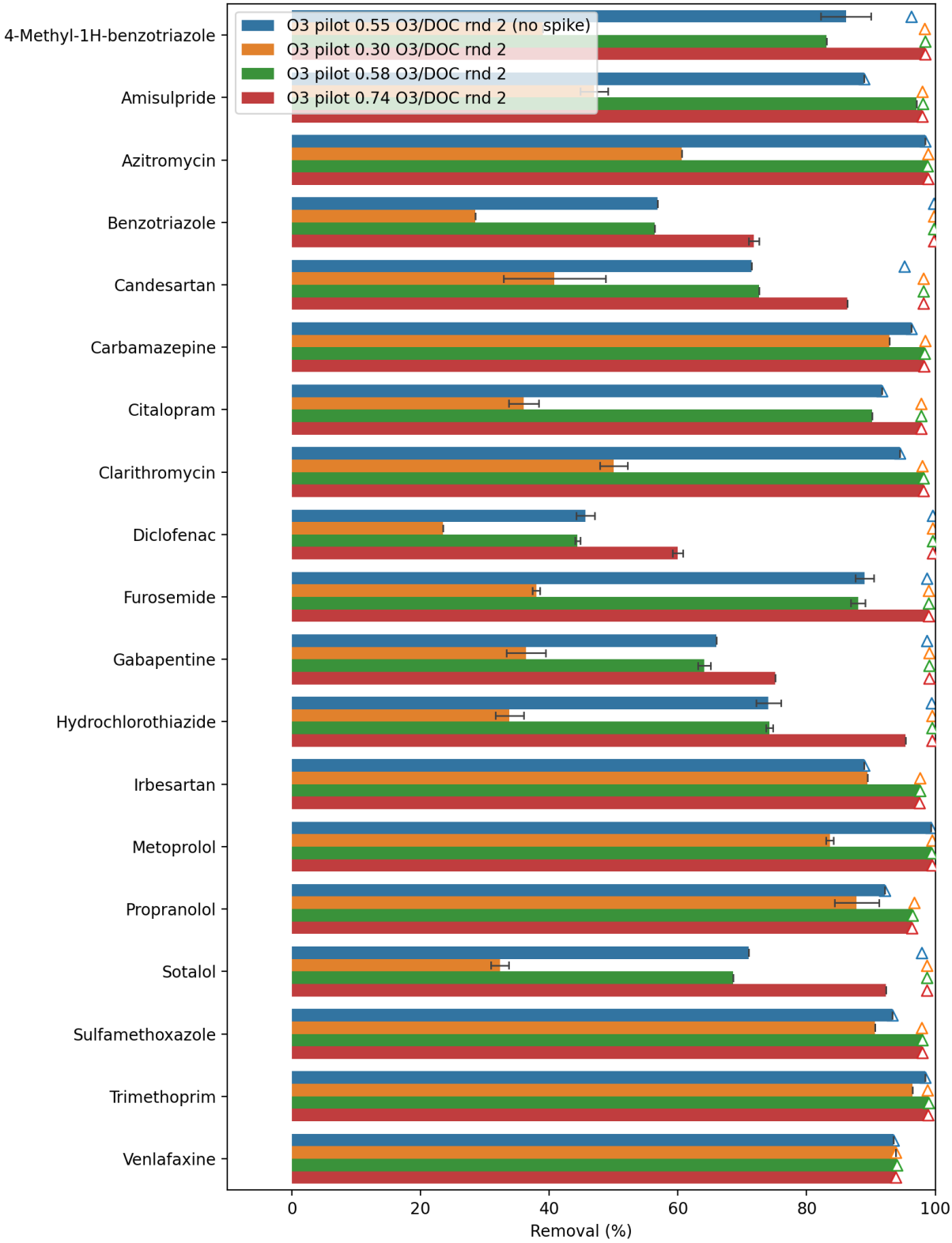

Removal percentages of micropollutants during ozone treatment for round 2. The triangles show the maximum degradation that can be demonstrated given the influent concentration and limit of detection. The error range is calculated from the standard deviation of the duplicate samples.

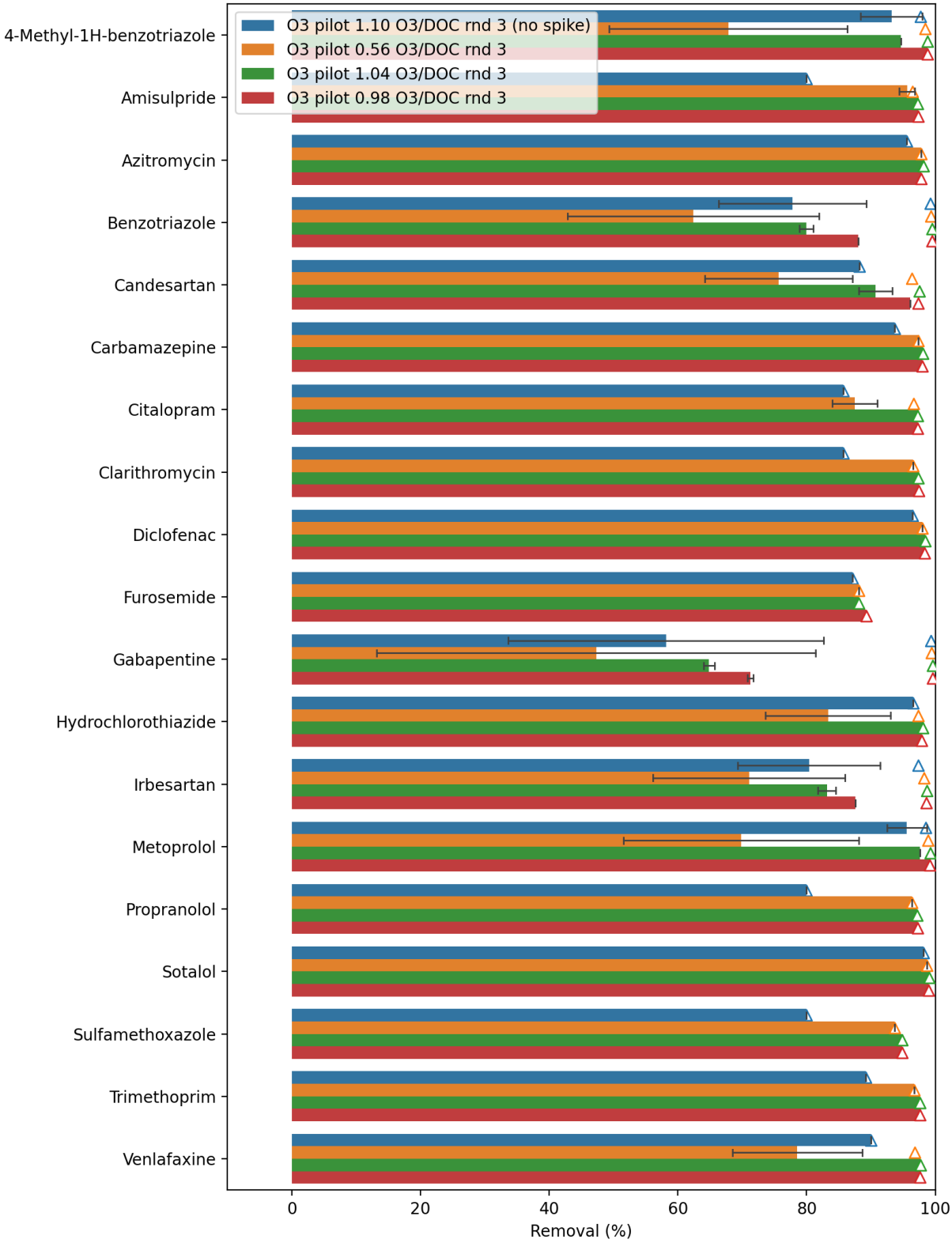

Removal percentages of micropollutants during ozone treatment for round 3. The triangles show the maximum degradation that can be demonstrated given the influent concentration and limit of detection. The error range is calculated from the standard deviation of the duplicate samples.

VIII Annex – Model validation of laboratory AOP tests

This Annex shows the figures of measured and modelled degradation for the laboratory tests. The blue bars show the model and the orange bars the experiments. The origin of the constants used in the model is shown as text in the bar. If no reliable measurement was possible, the text no data is shown in the bar of the measurement.

UV/H_2O_2 laboratory experiments

UV/H_2O_2 Horstermeer effluent 20 mg/L H_2O_2

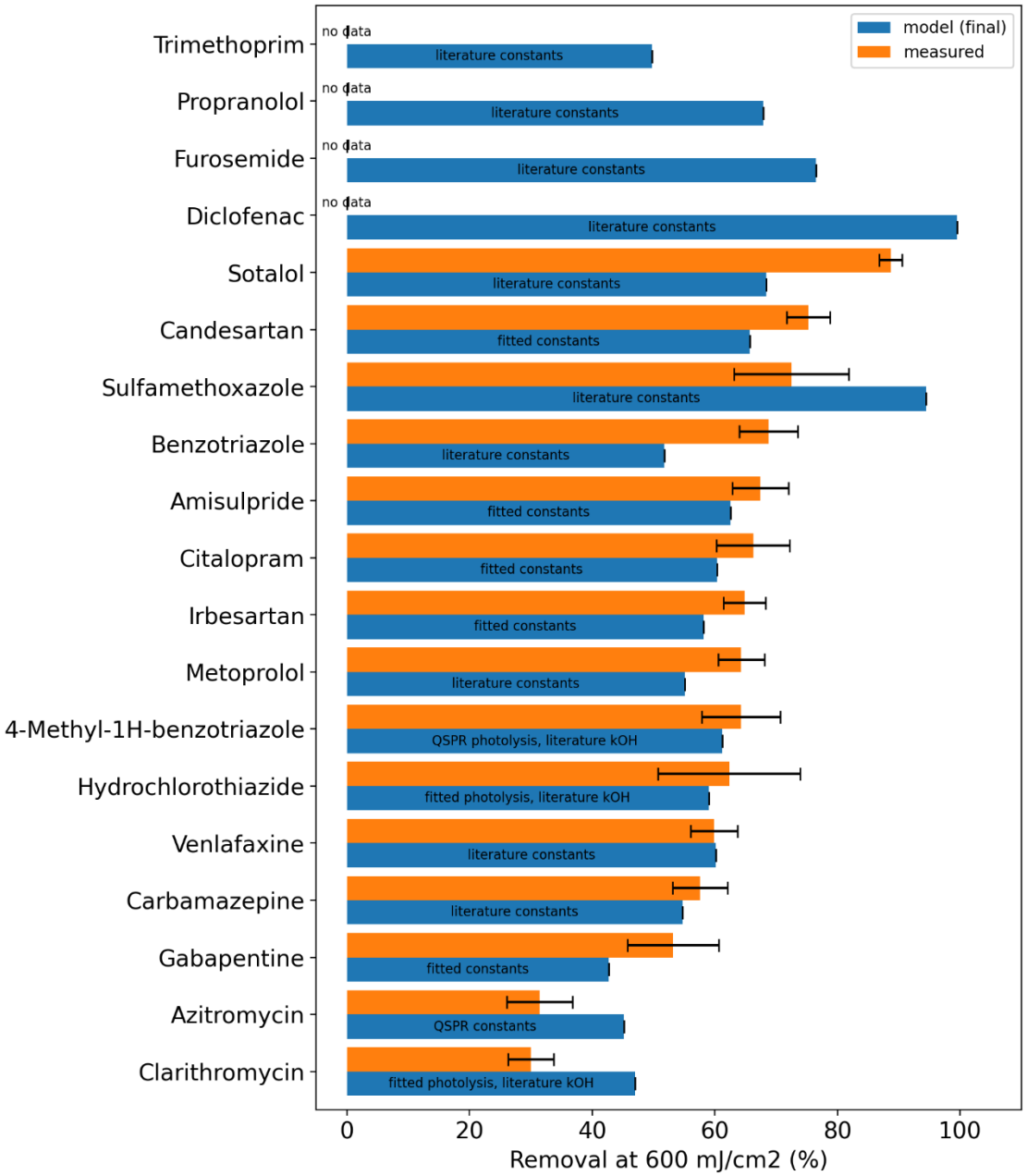

UV/H_2O_2 Horstermeer diluted effluent 20 mg/L H_2O_2

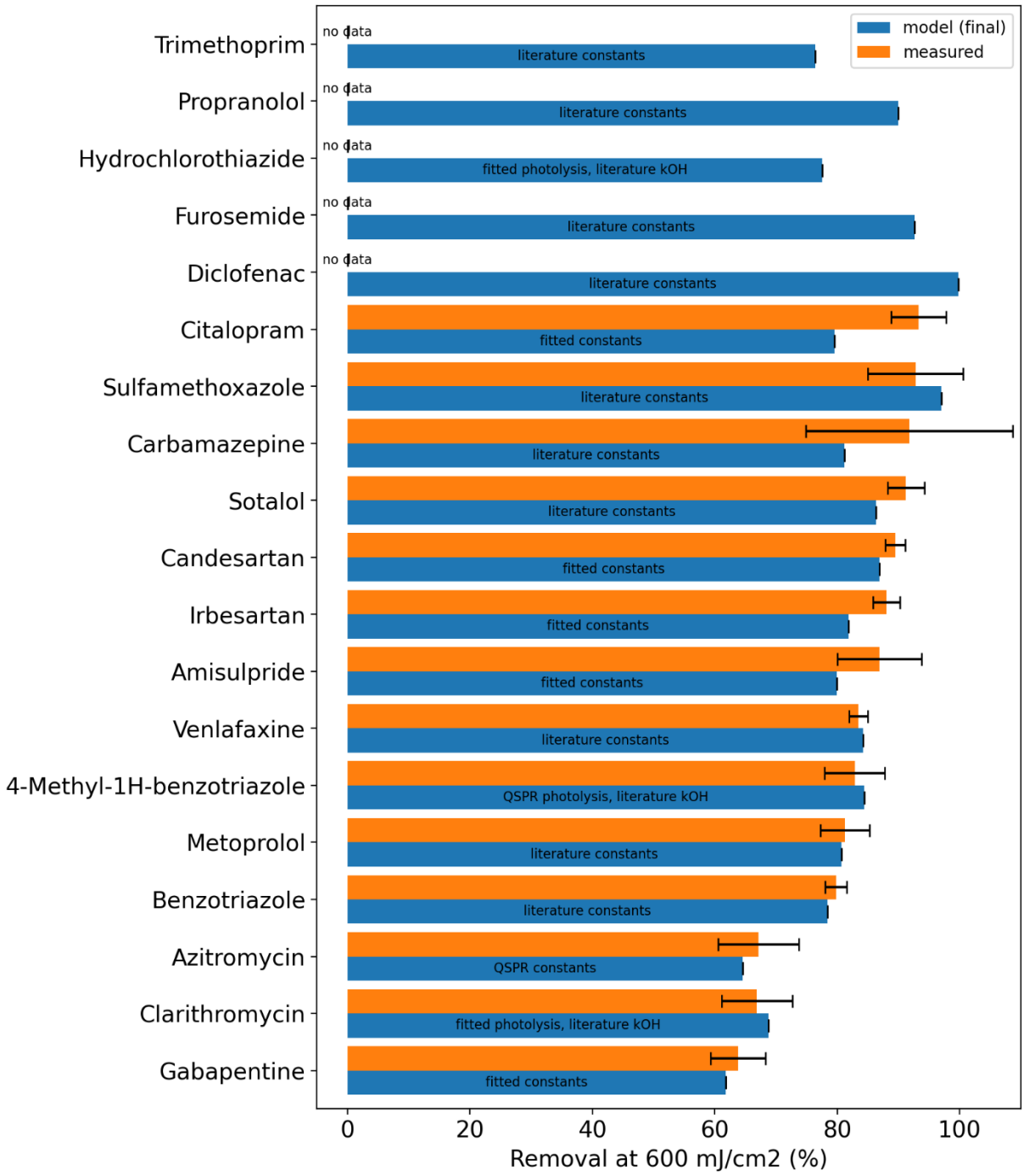

UV/H_2O_2 MQ 0 mg/L H_2O_2

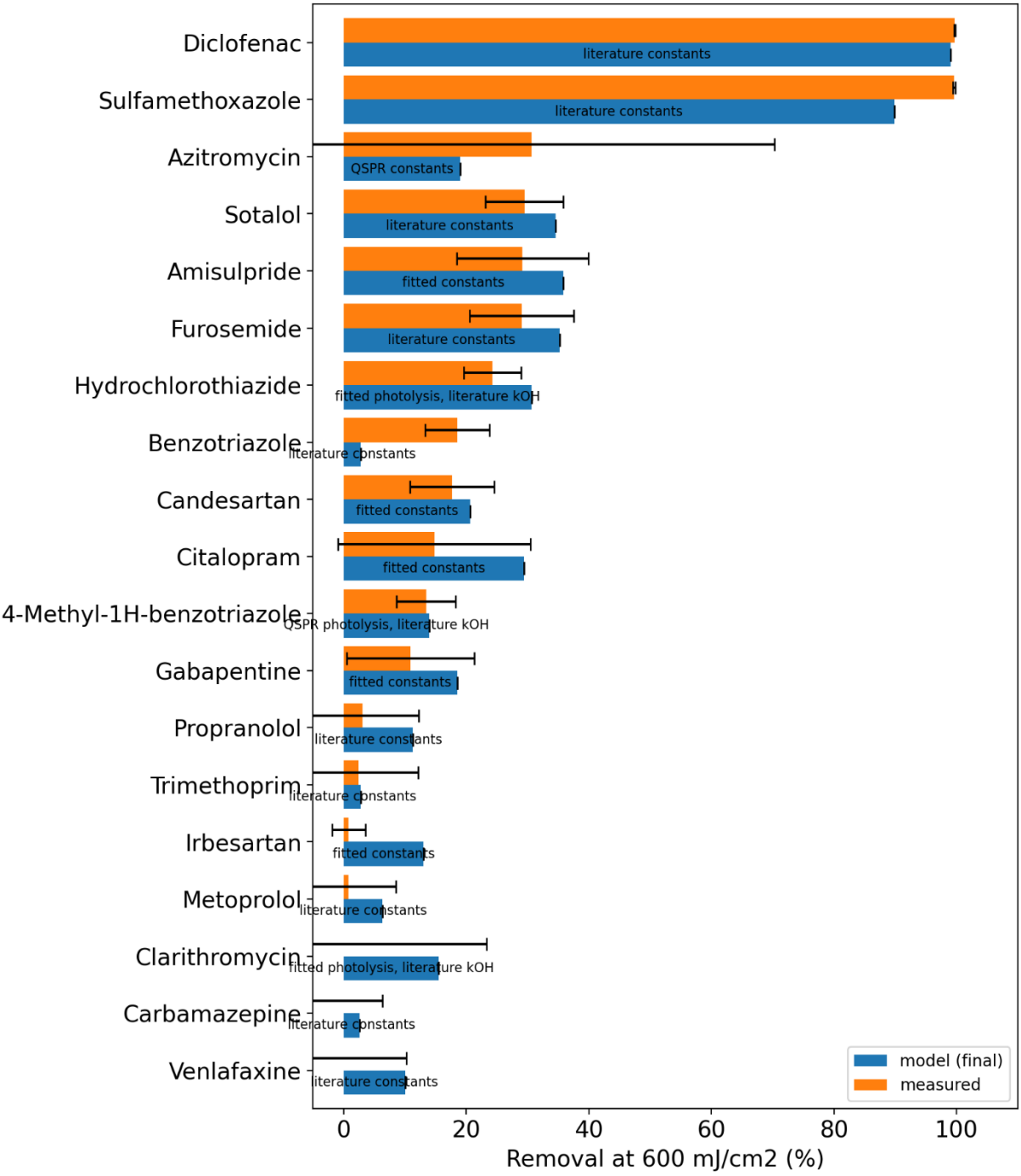

UV/H_2O_2 MQ 10 mg/L H_2O_2

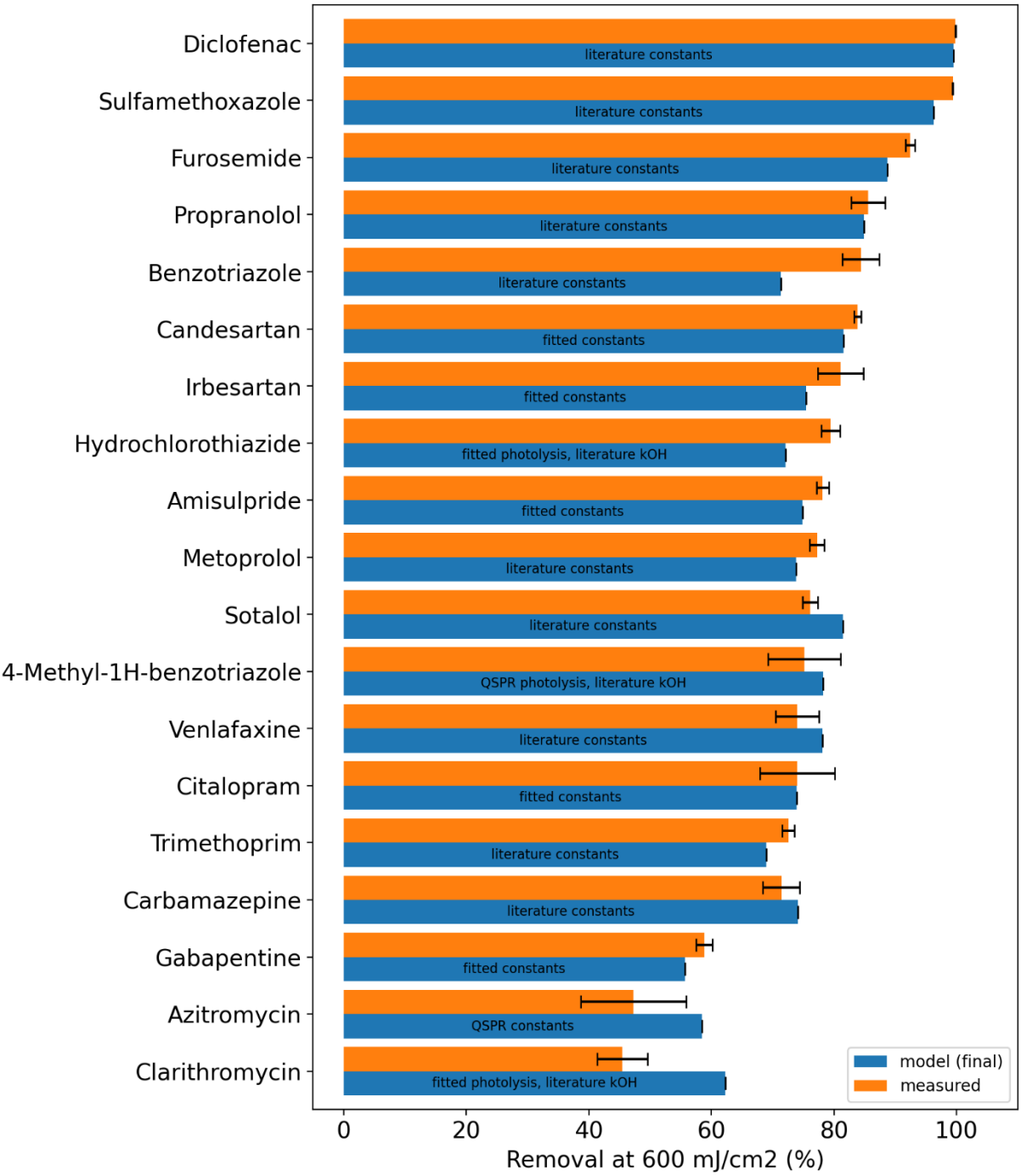

UV/H_2O_2 MQ 20 mg/L H_2O_2

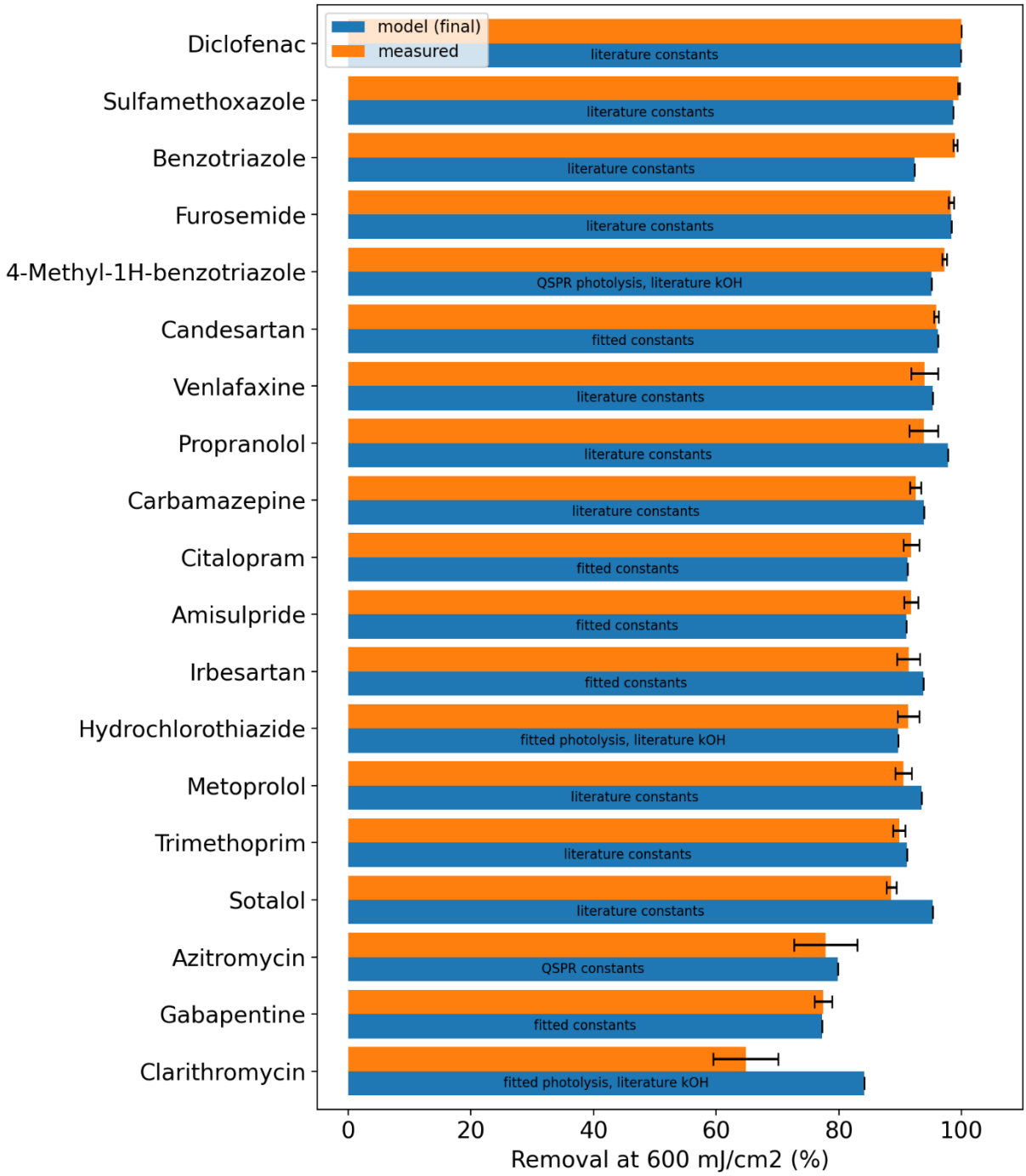

UV/H_2O_2 Walcheren effluent 0 mg/L H_2O_2

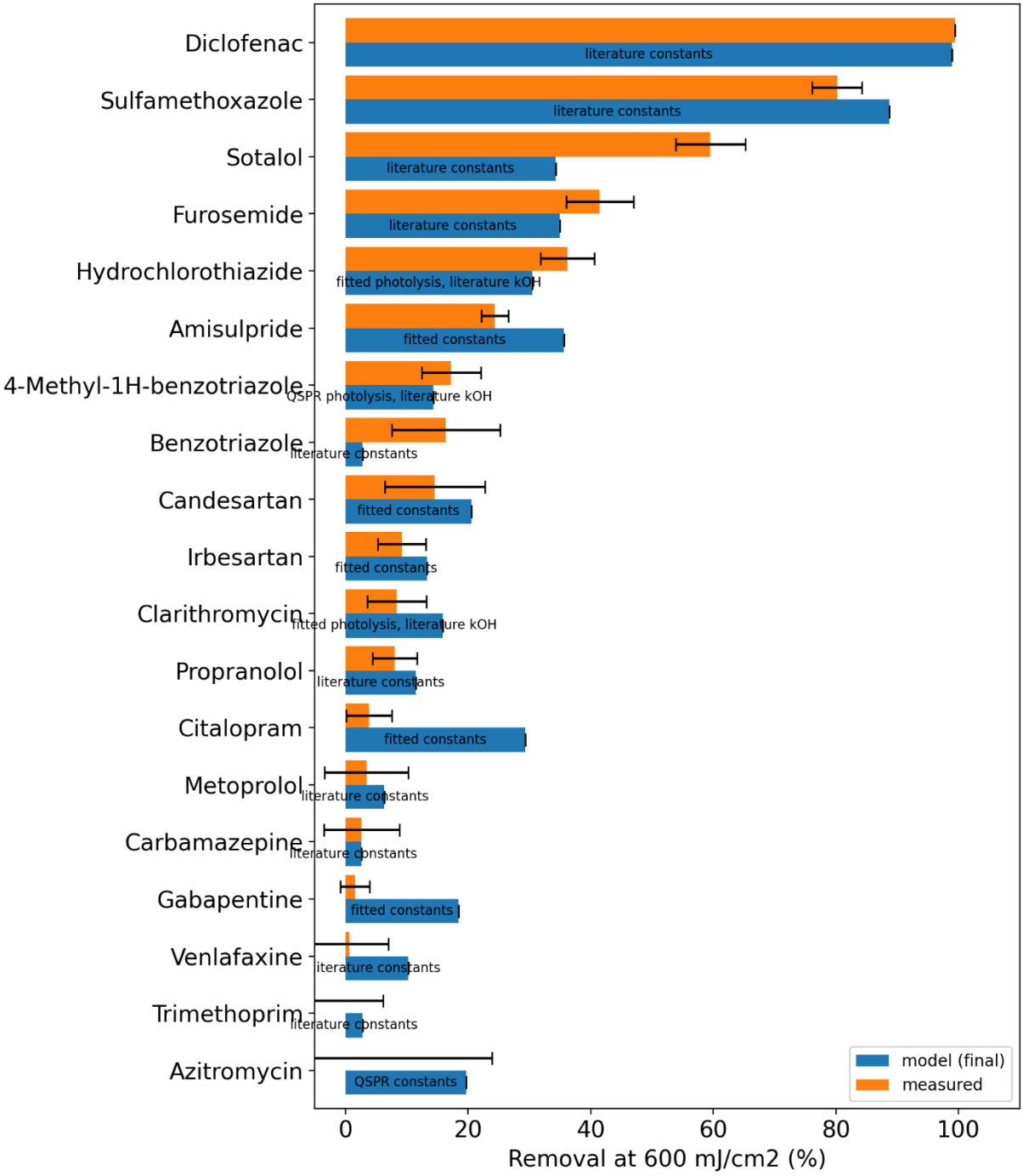

UV/H_2O_2 Walcheren effluent 20 mg/L H_2O_2

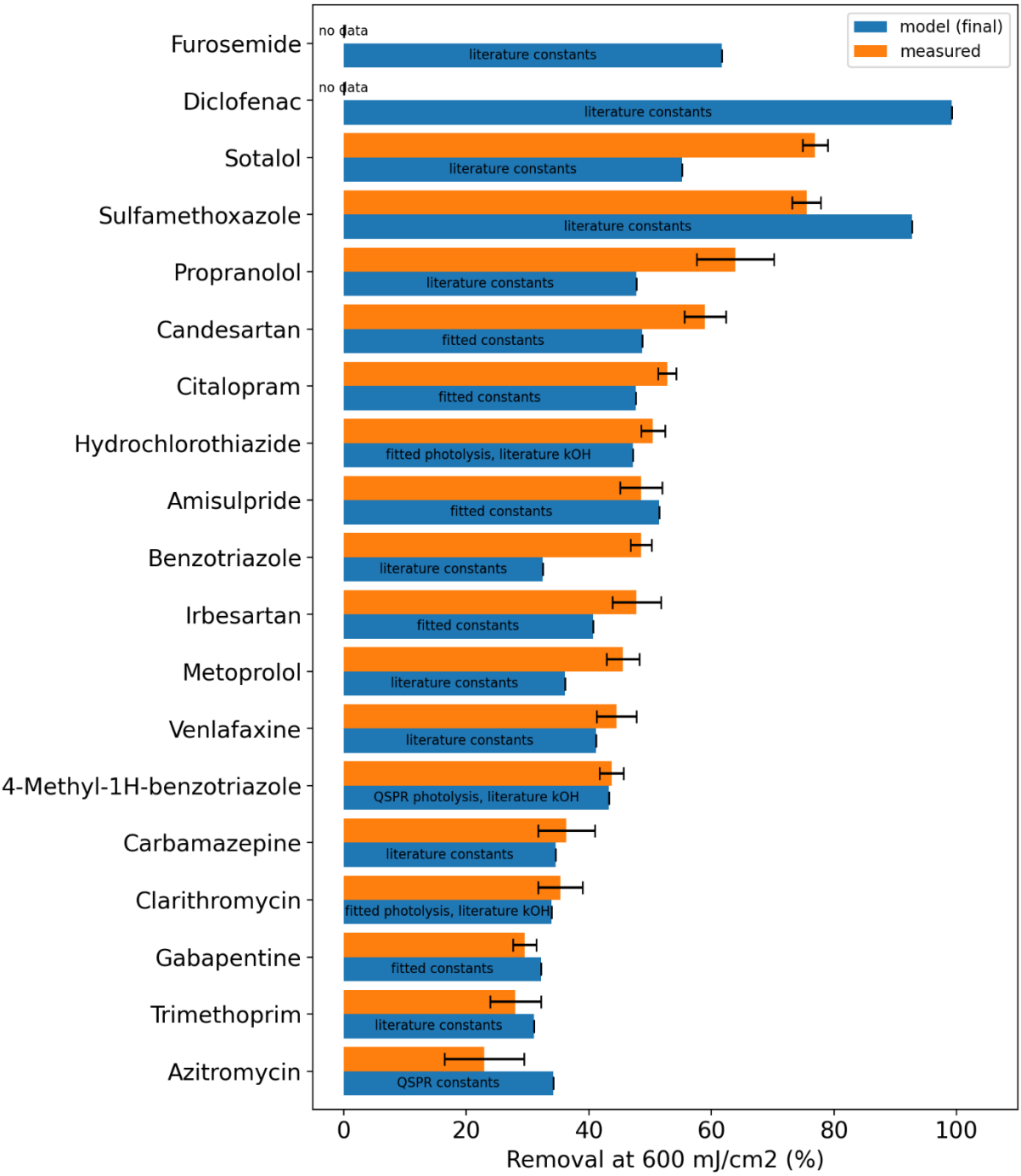

UV/H_2O_2 Walcheren effluent 40 mg/L H_2O_2

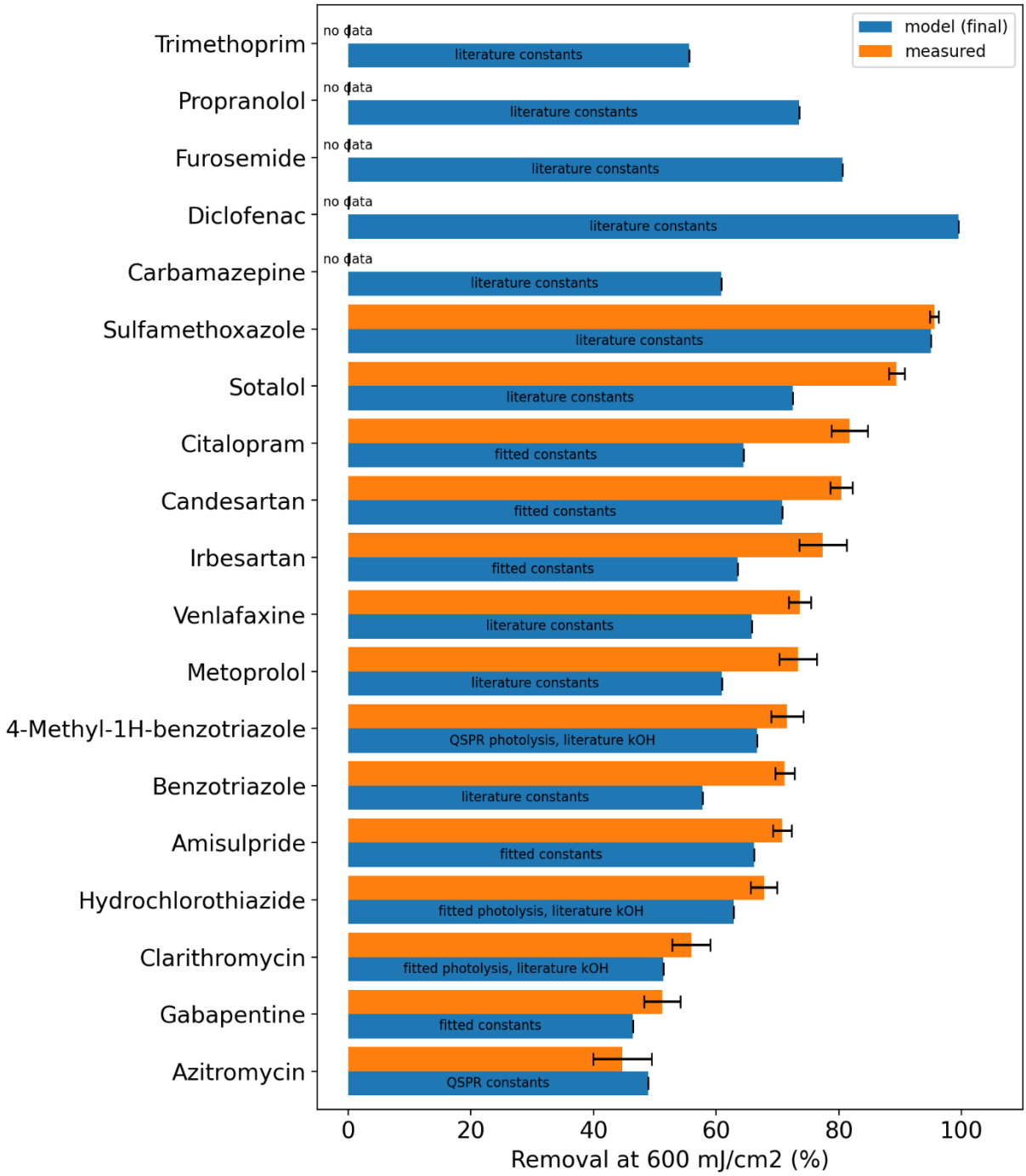

UV/H_2O_2 Walcheren effluent unfiltered 0 mg/L H_2O_2

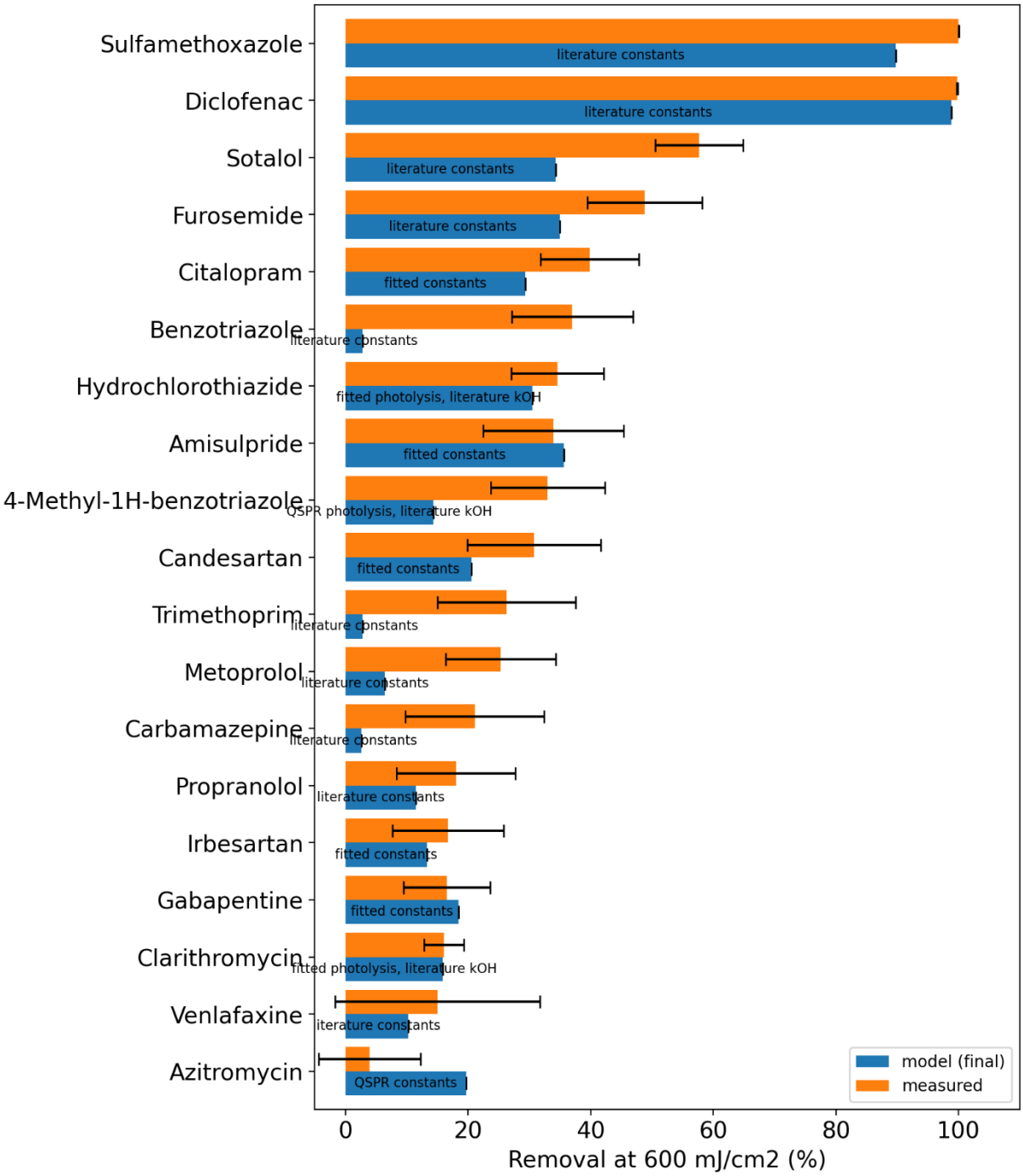

UV/H_2O_2 Walcheren effluent unfiltered 20 mg/L H_2O_2

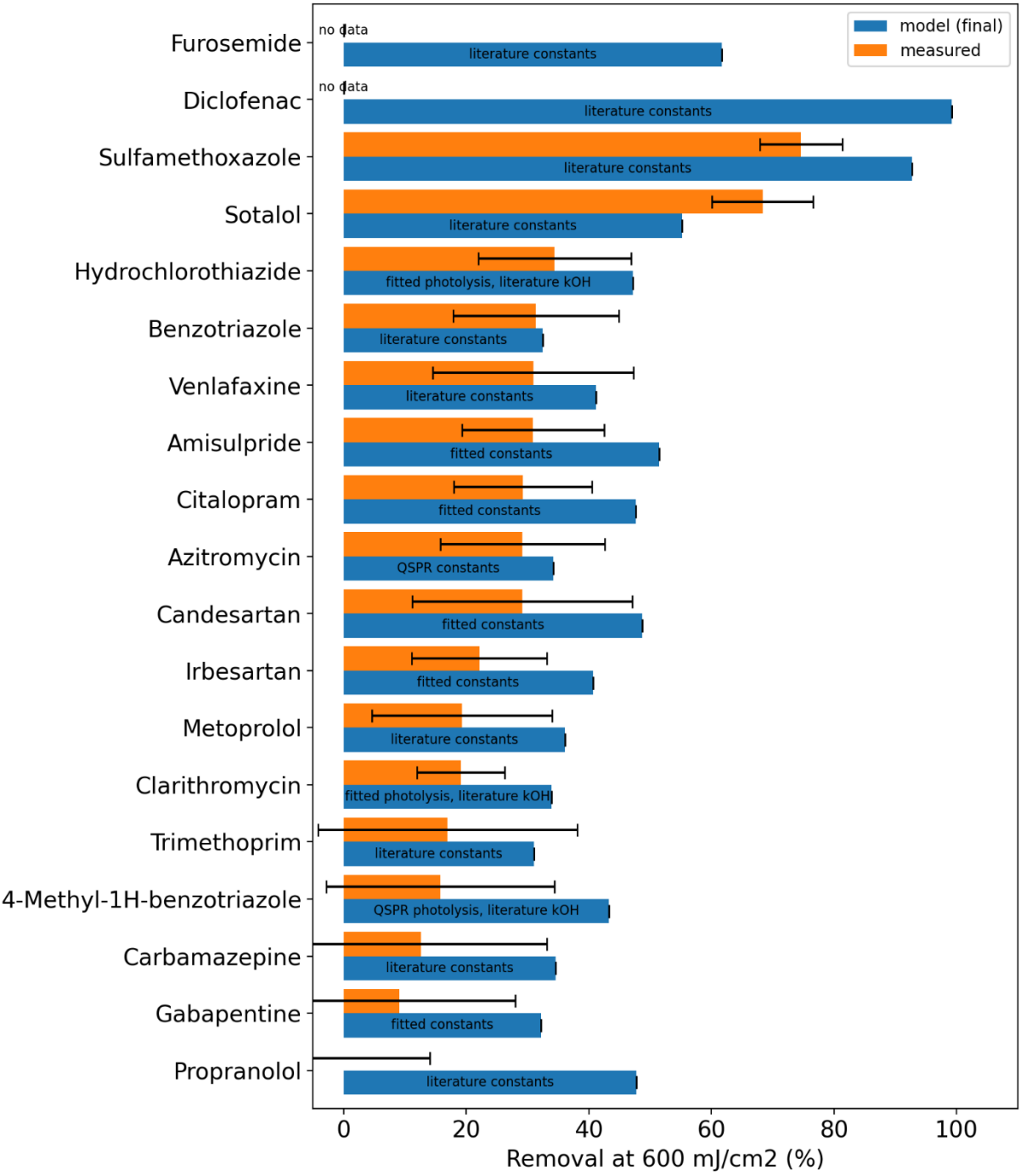

UV/H_2O_2 Walcheren effluent diluted 20 mg/L H_2O_2

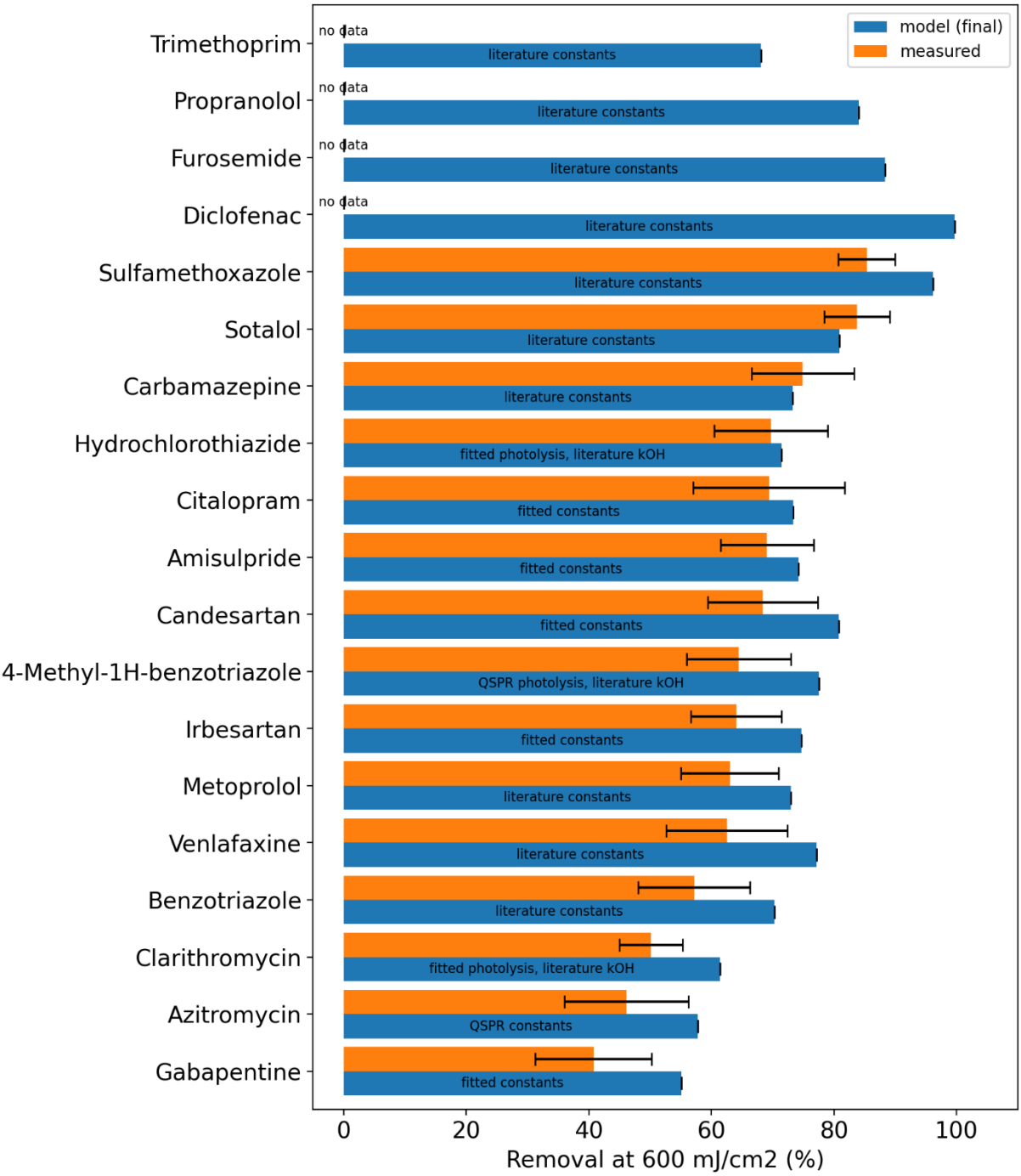

Ozone laboratory experiments

Ozone Walcheren effluent 0.84 mg/L O_3

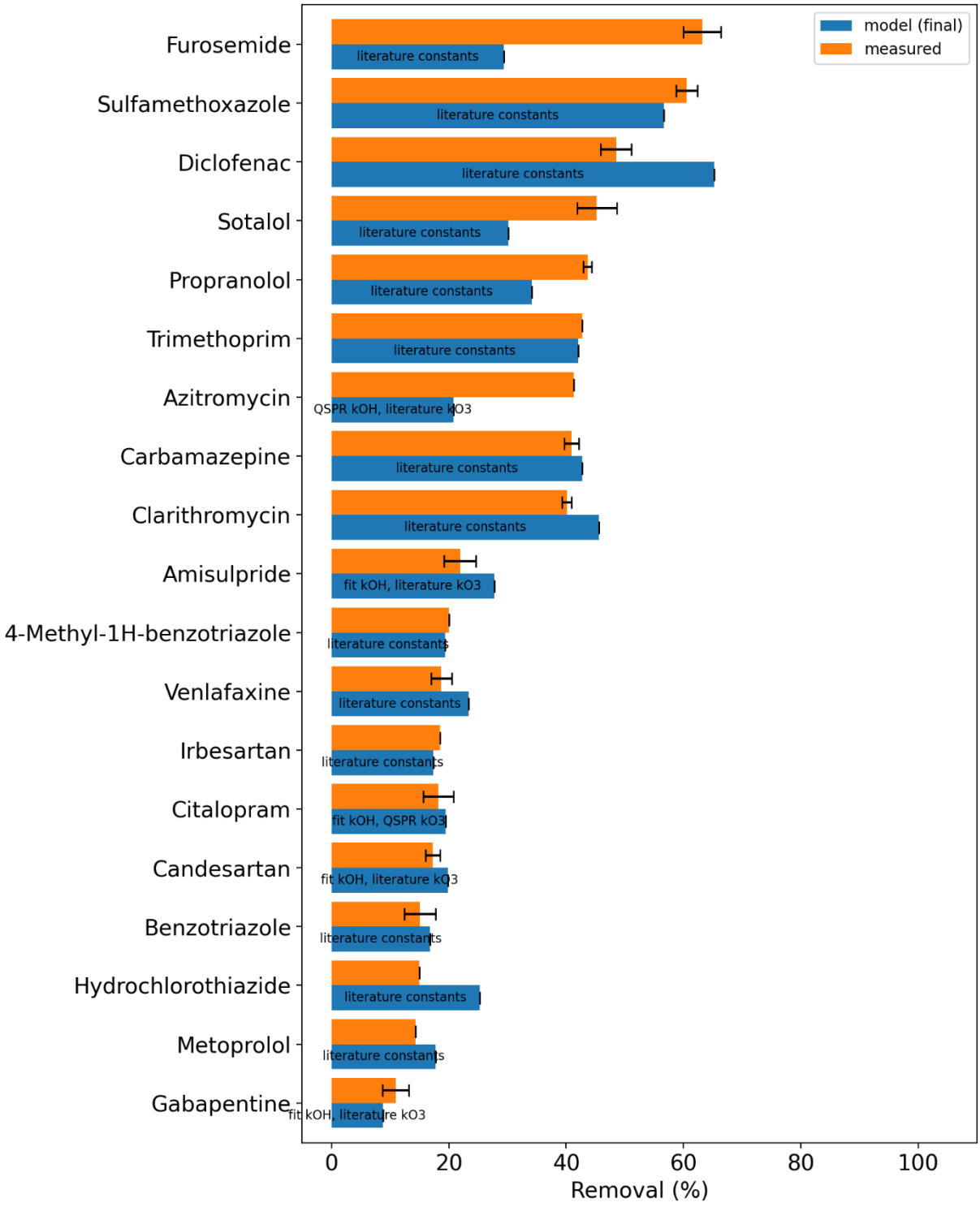

Ozone Walcheren effluent 1.68 mg/L O_3

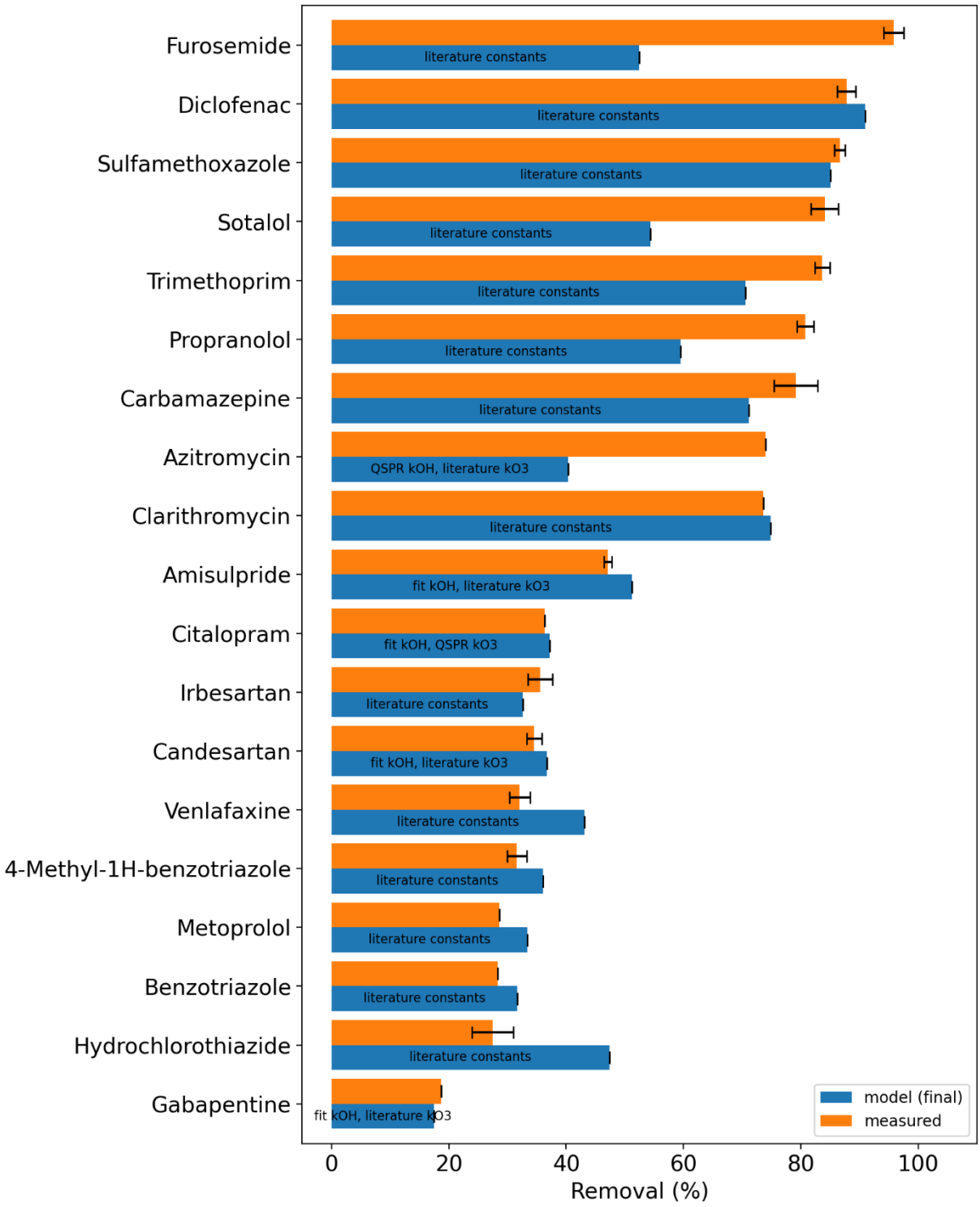

Ozone Walcheren effluent 4.2 mg/L O_3

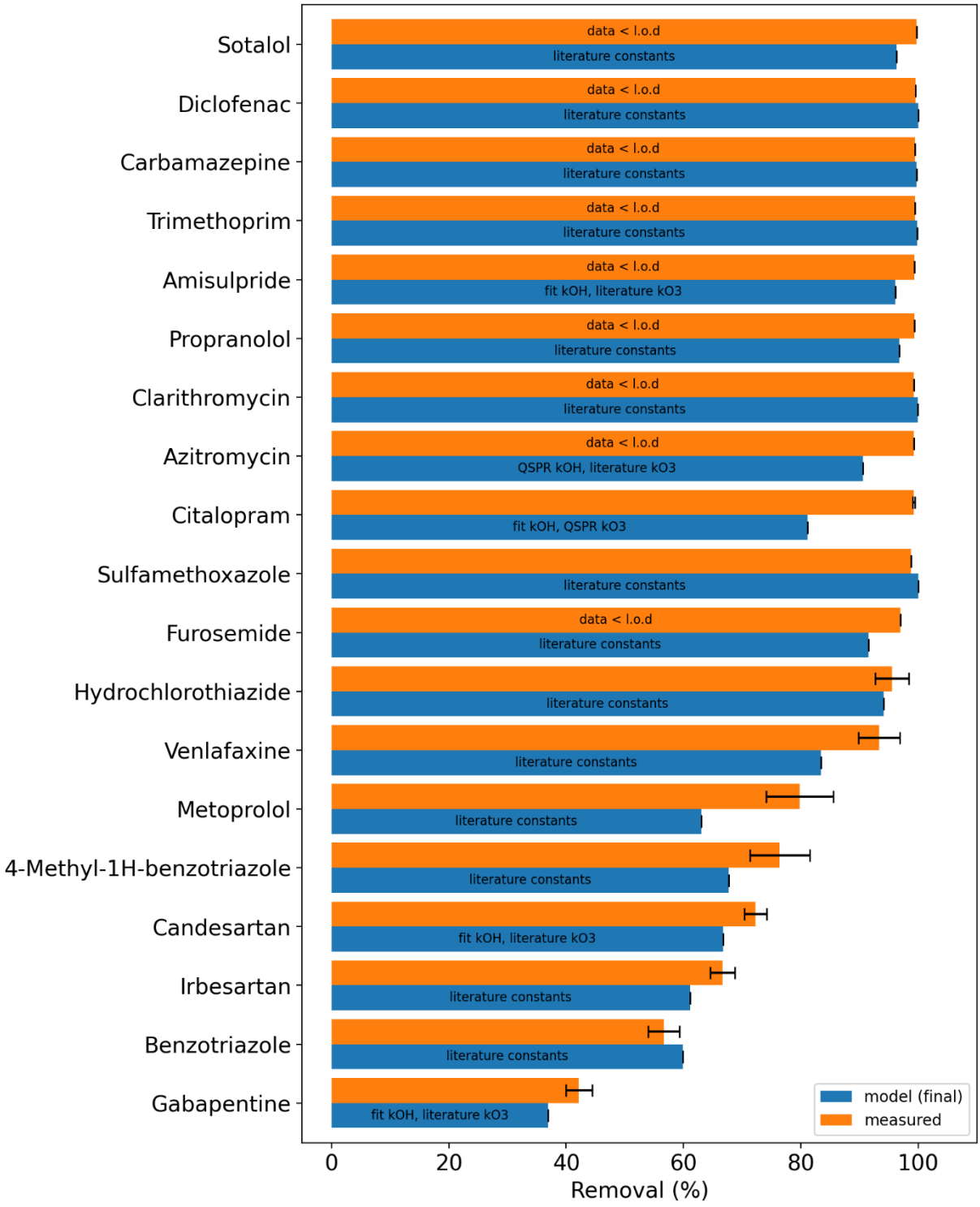

IX Annex - Model validation of pilot AOP tests

Figures of measured and modelled degradation

UV/H_2O_2 pilot experiments

UV/H_2O_2 pilot 478 mJ/cm2 and 19 mg/L H_2O_2 round 1 (without spike)

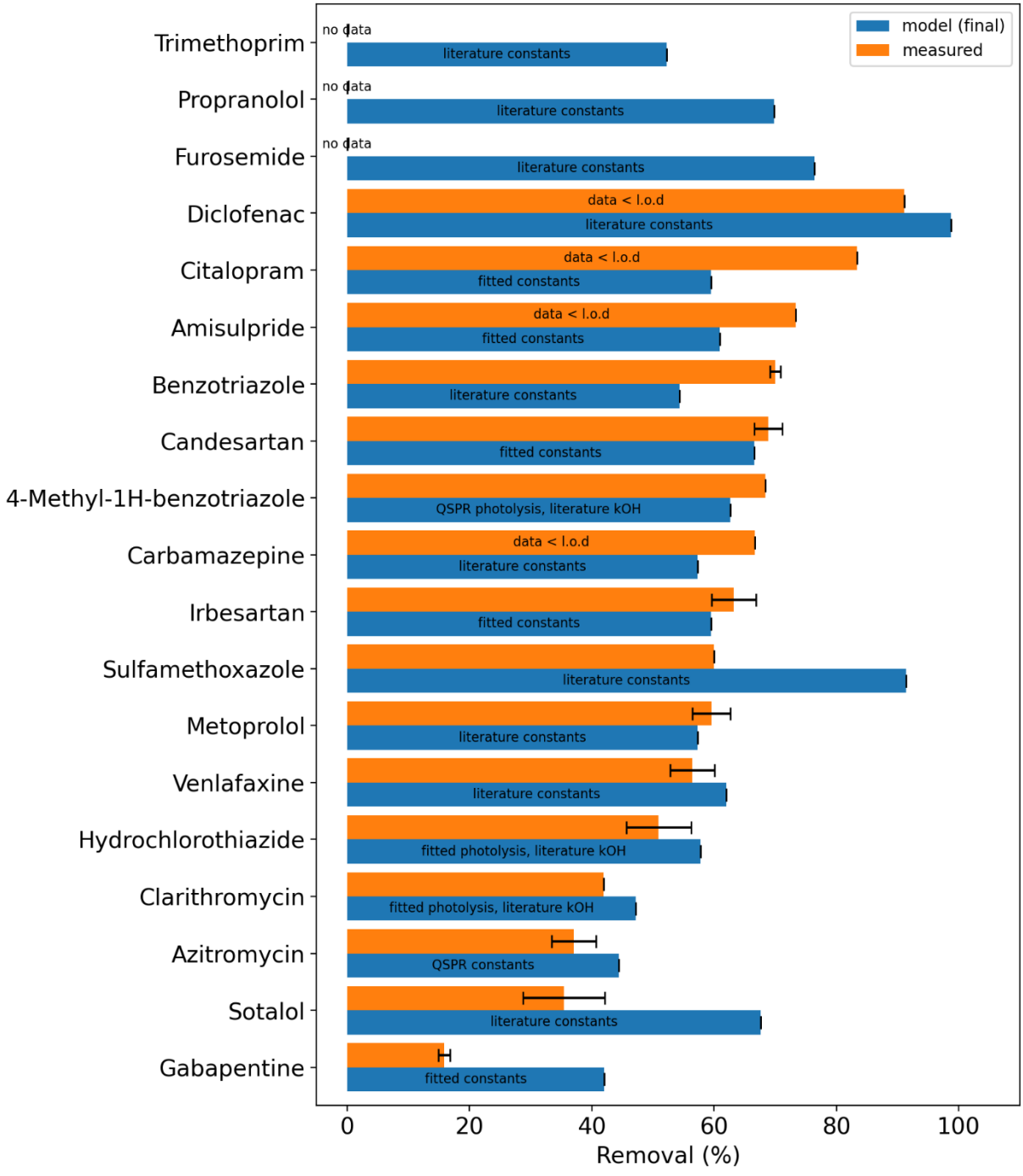

UV/H_2O_2 pilot 474 mJ/cm2 and 19 mg/L H_2O_2 round 1 (with spike)

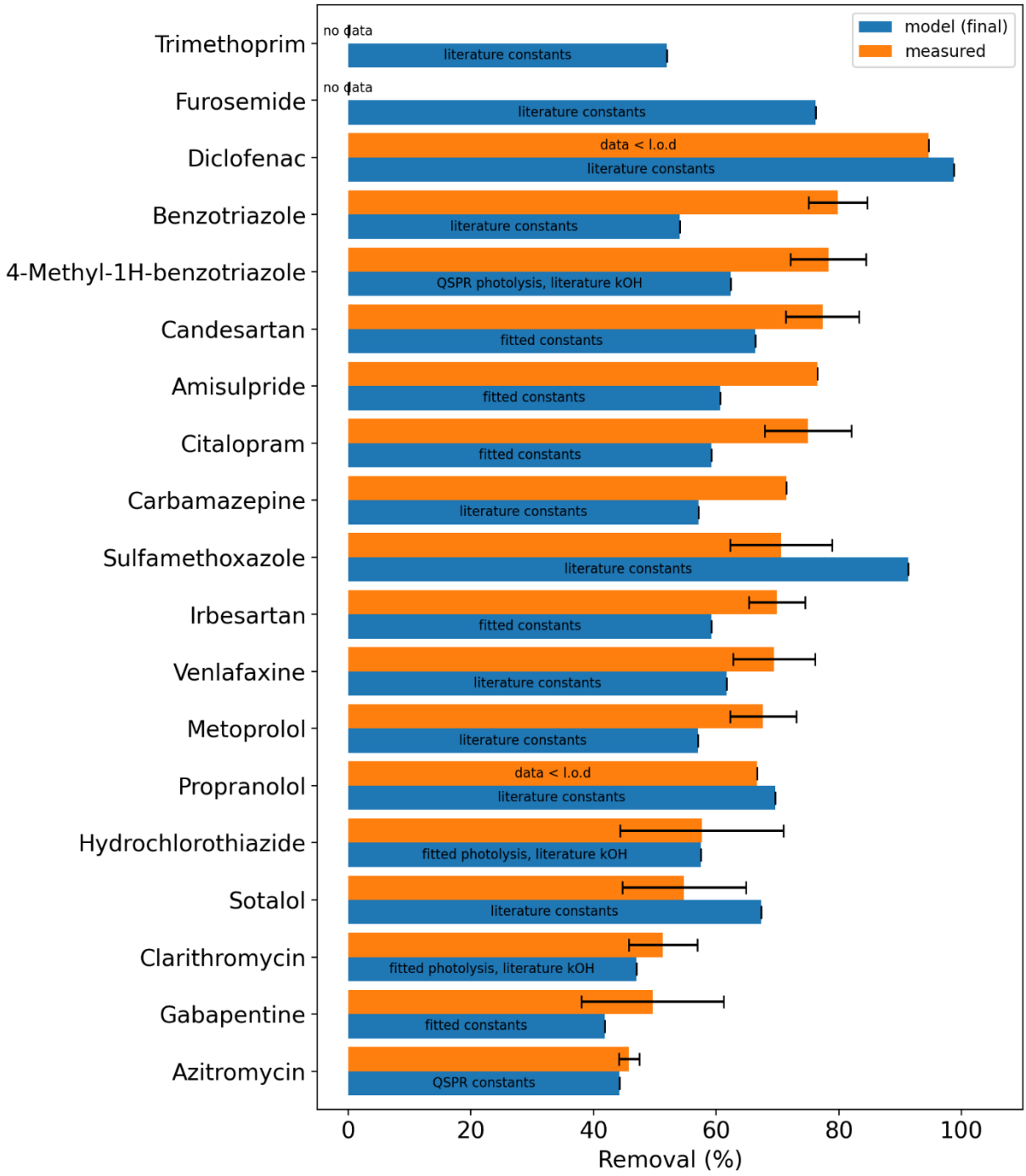

UV/H_2O_2 pilot 960 mJ/cm2 and 38 mg/L H_2O_2 round 1 (with spike)

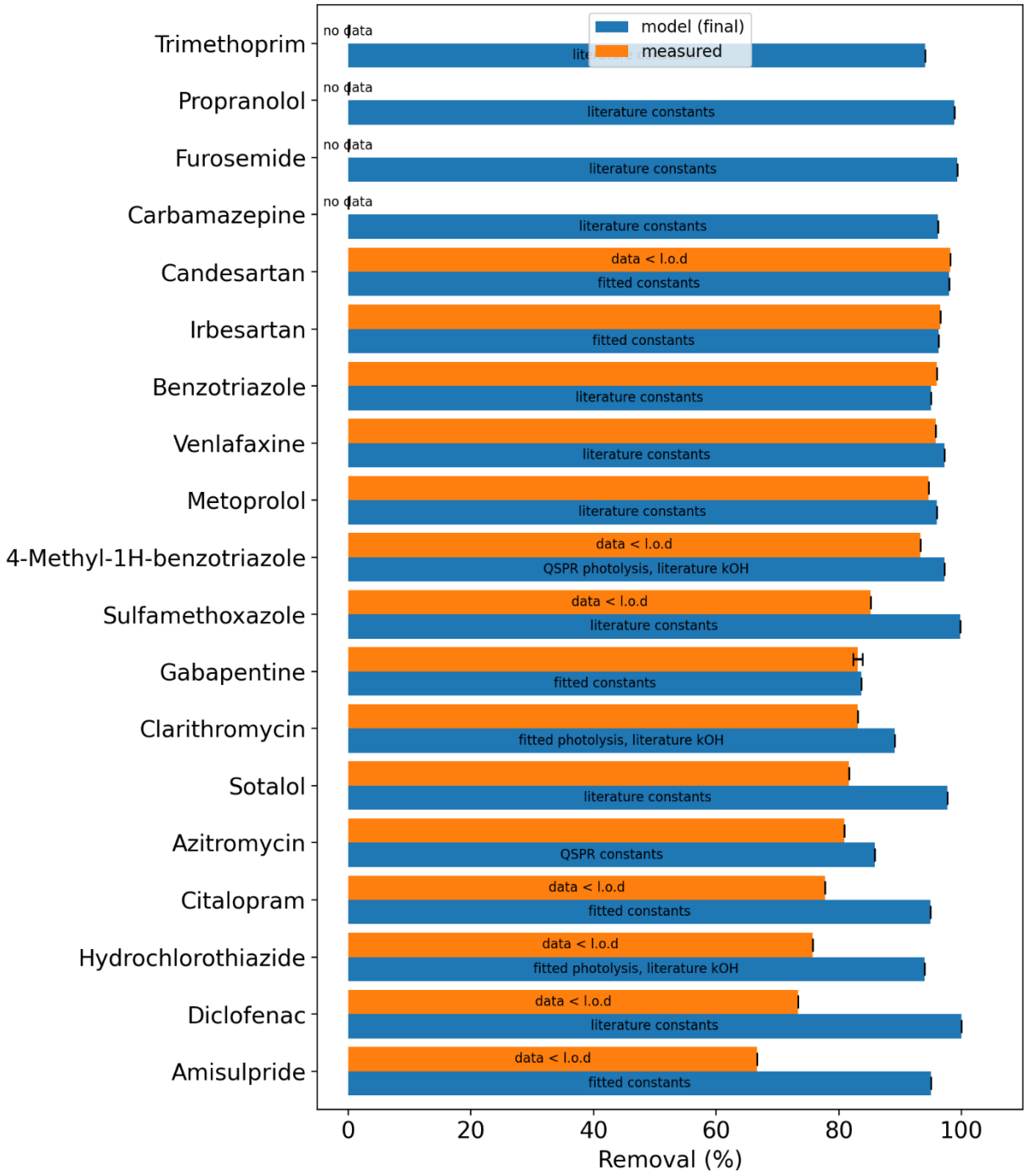

UV/H_2O_2 pilot 645 mJ/cm2 and 25 mg/L H_2O_2 round 2 (without spike)

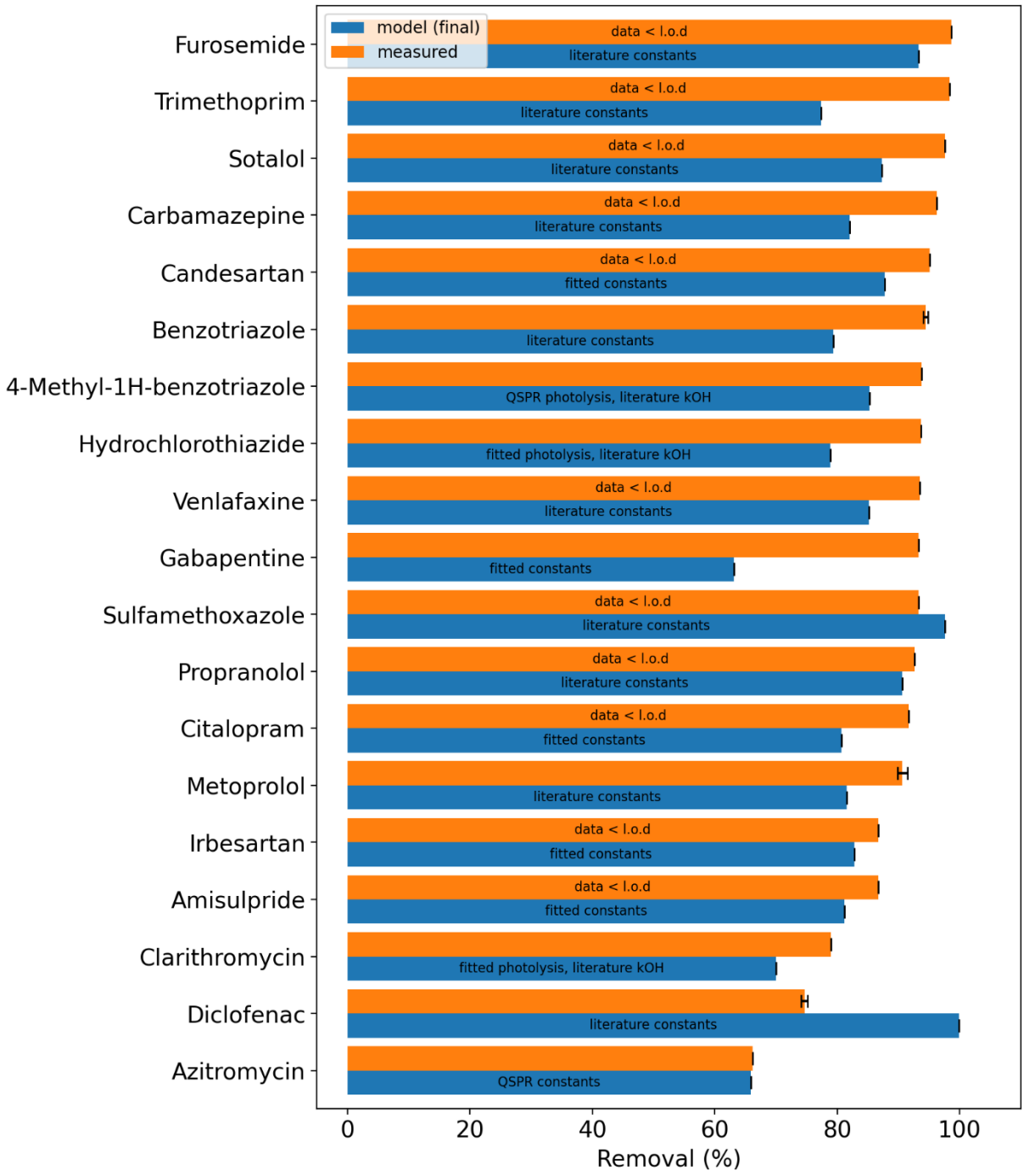

UV/H_2O_2 pilot 659 mJ/cm2 and 25 mg/L H_2O_2 round 2 (with spike)

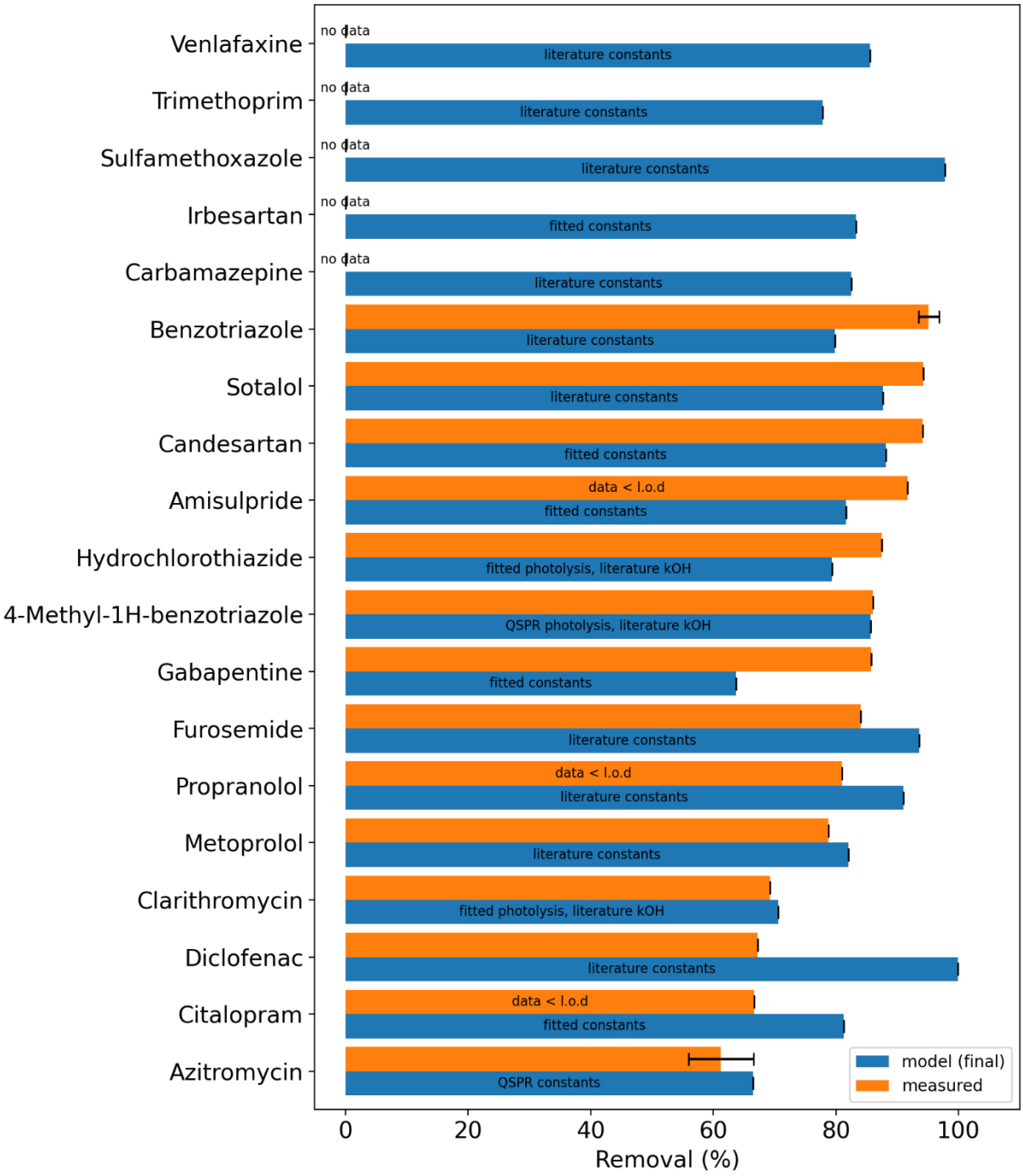

UV/H_2O_2 pilot 1319 mJ/cm2 and 54 mg/L H_2O_2 round 2 (with spike)

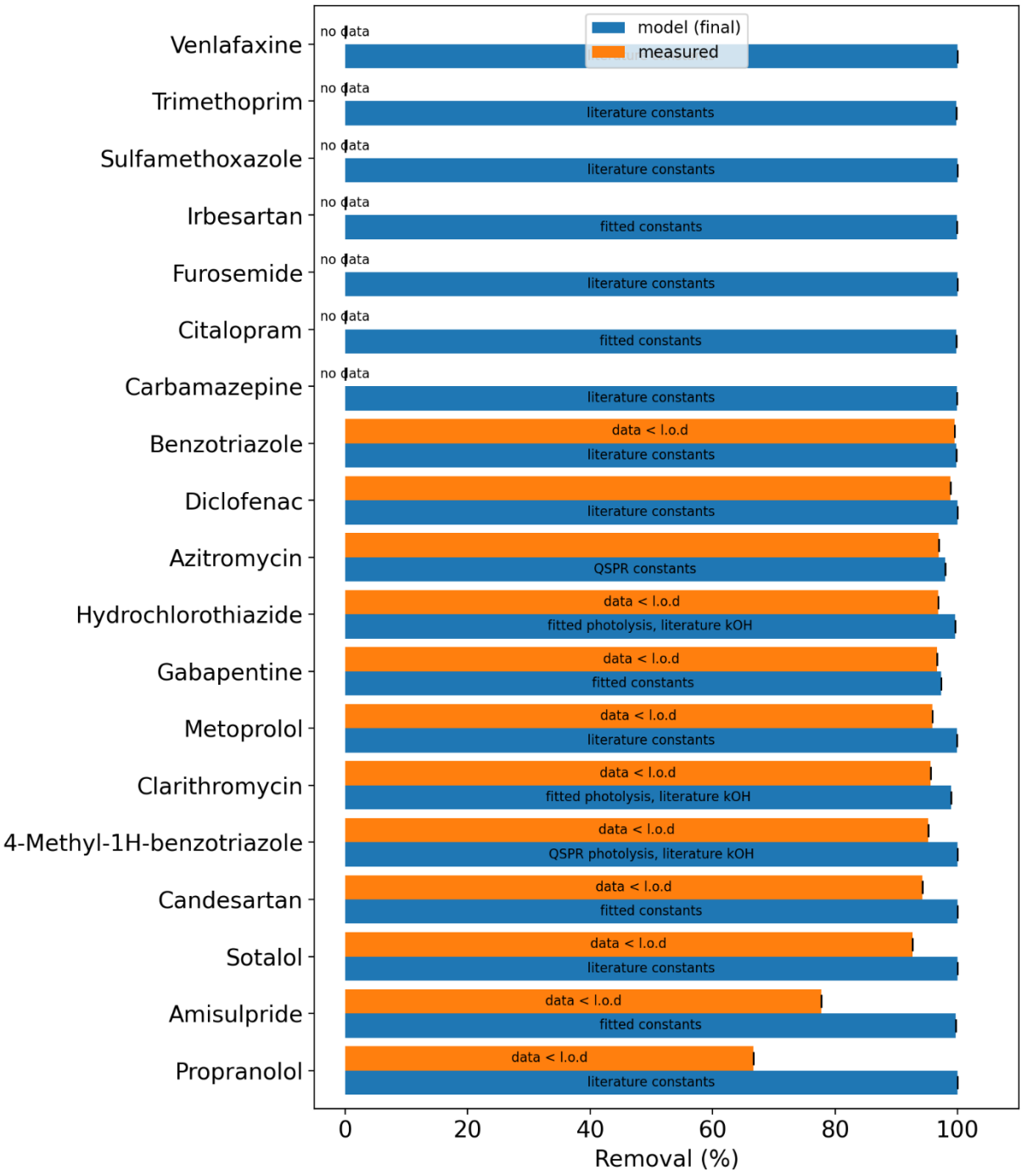

UV/H_2O_2 pilot 571 mJ/cm2 and 21 mg/L H_2O_2 round 3 (without spike)

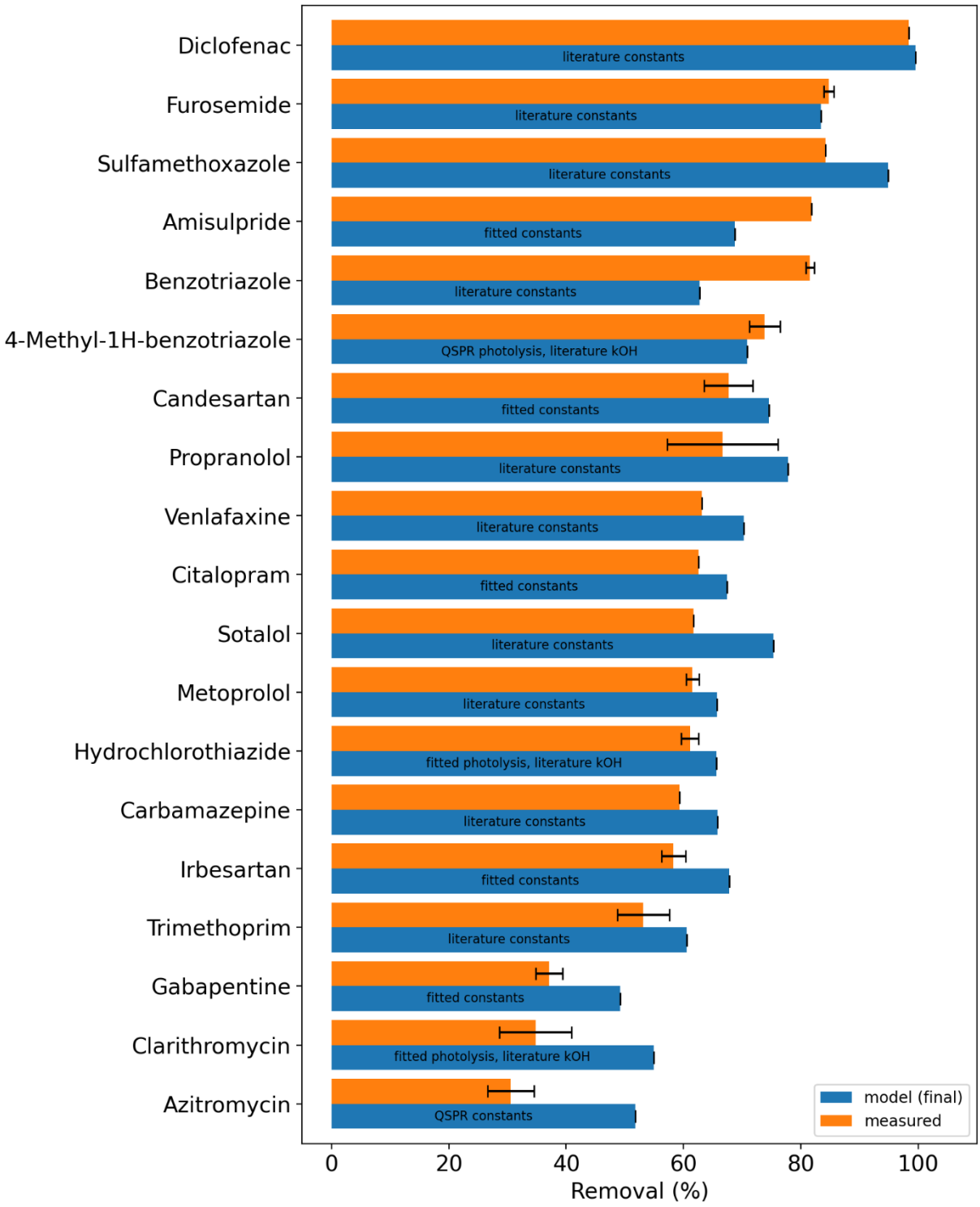

UV/H_2O_2 pilot 547 mJ/cm2 and 20 mg/L H_2O_2 round 3 (with spike)

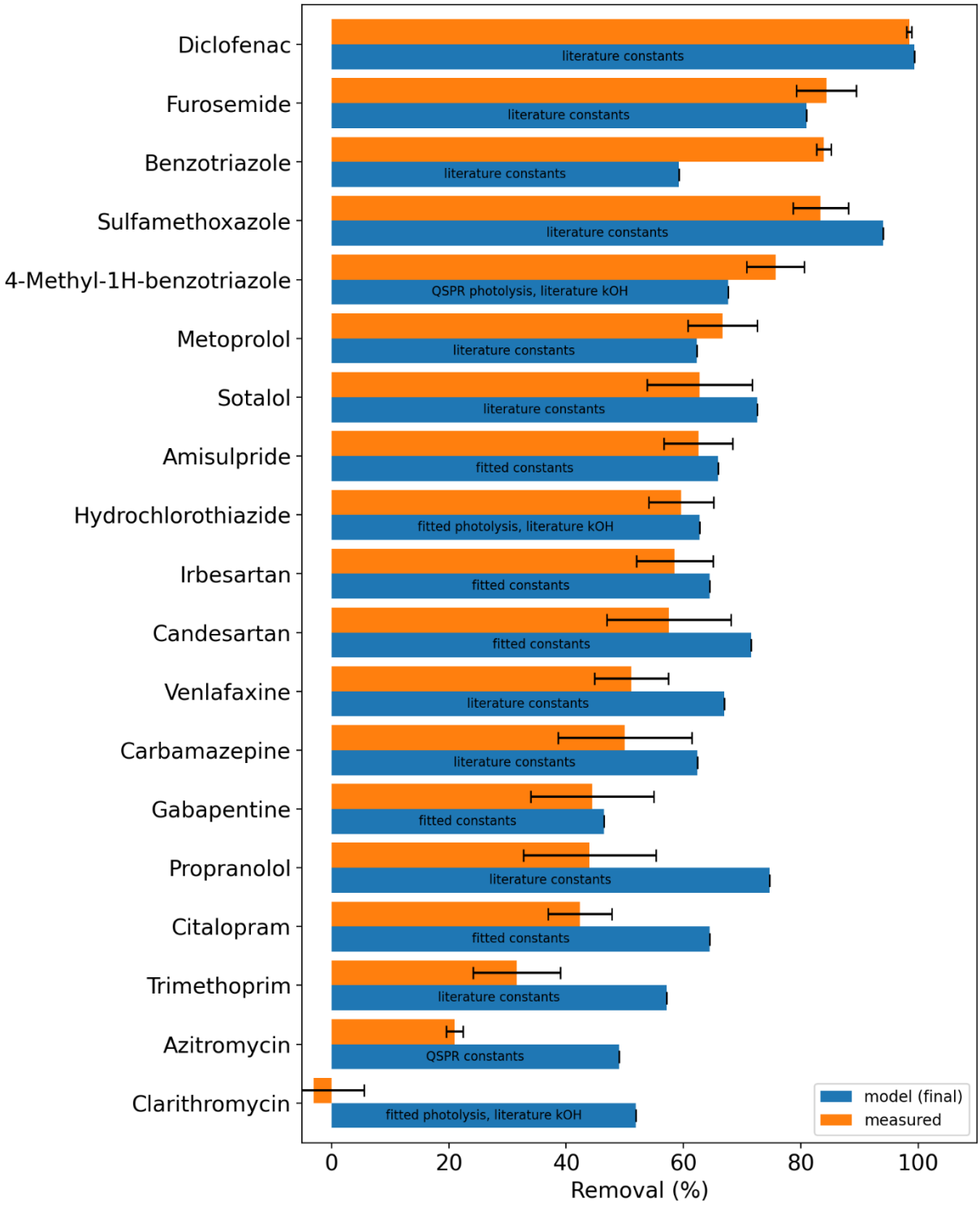

UV/H_2O_2 pilot 1452 mJ/cm2 and 36 mg/L H_2O_2 round 3 (with spike)

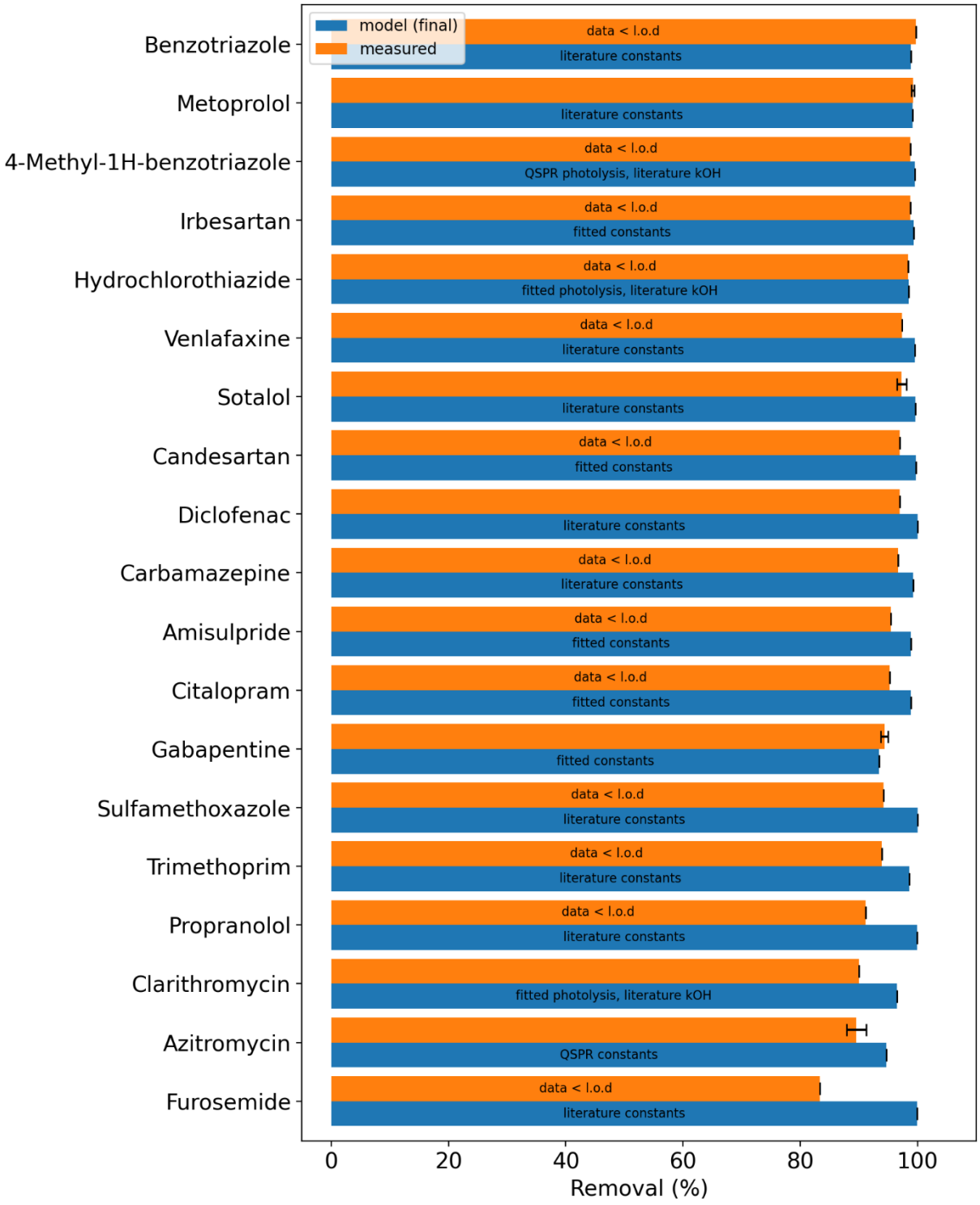

UV/H_2O_2 pilot 674 mJ/cm2 and 26 mg/L H_2O_2 round 4 (without spike)

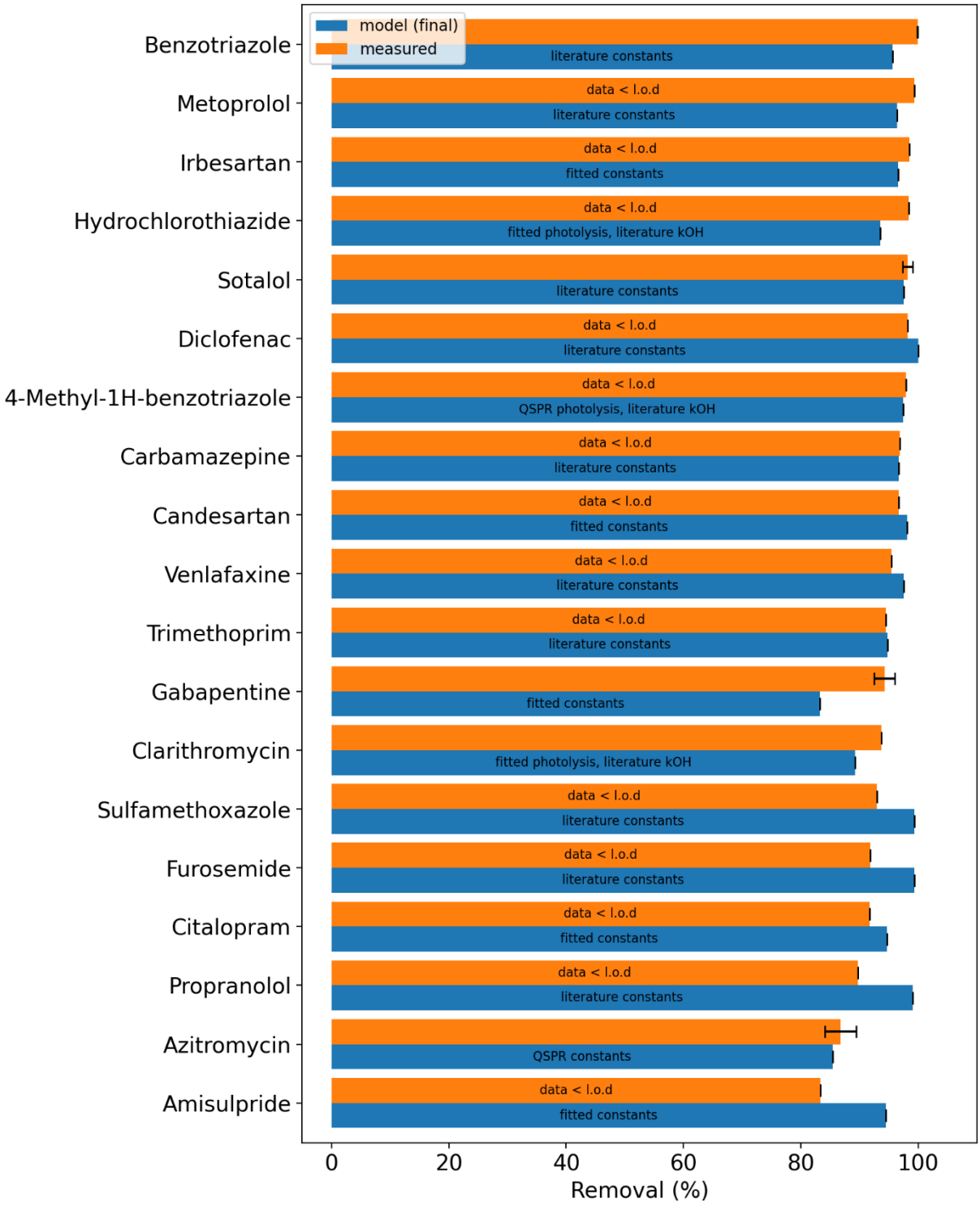

UV/H_2O_2 pilot 674 mJ/cm2 and 21 mg/L H_2O_2 round 4 (with spike)

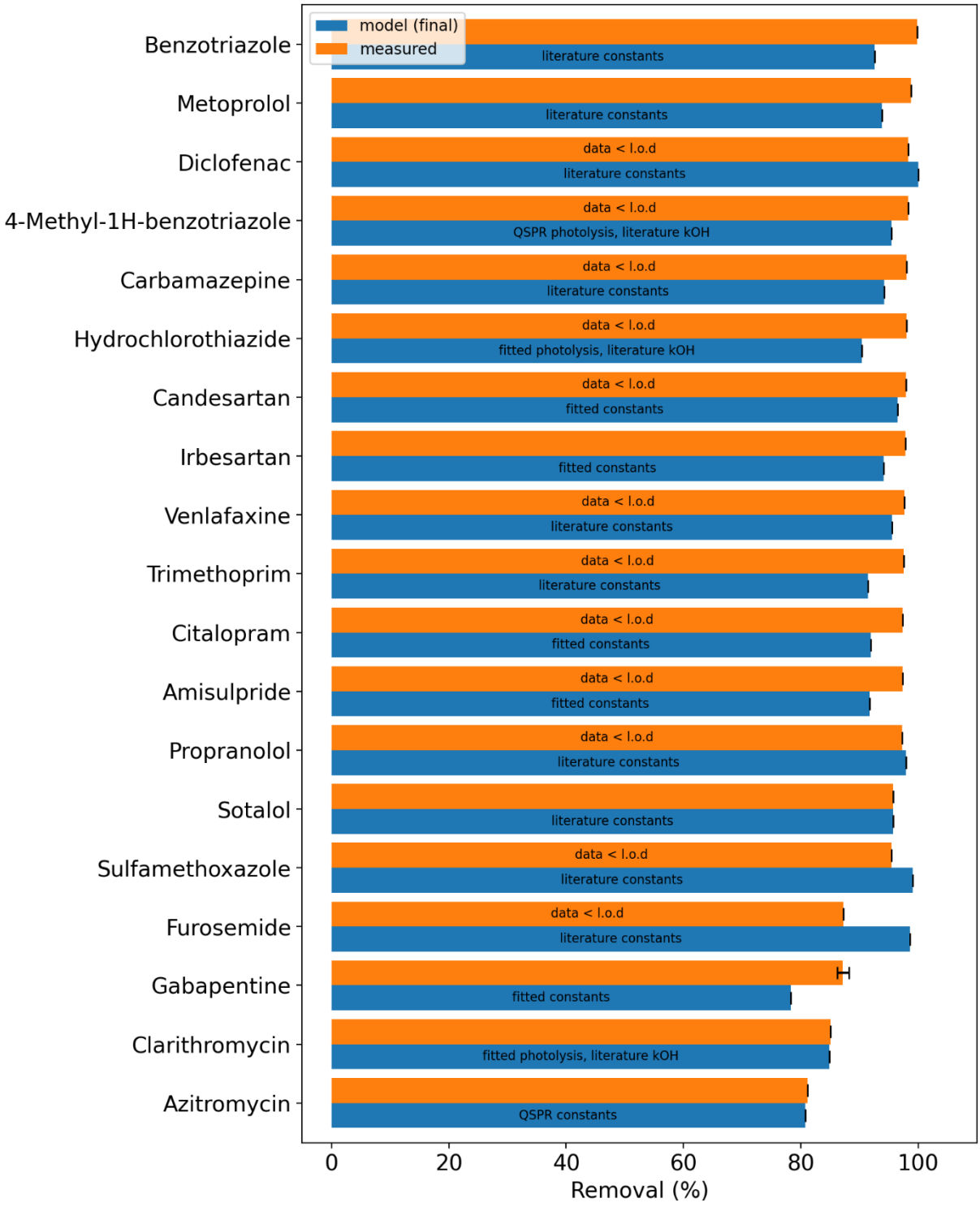

UV/H_2O_2 pilot 1370 mJ/cm2 and 44 mg/L H_2O_2 round 4 (with spike)

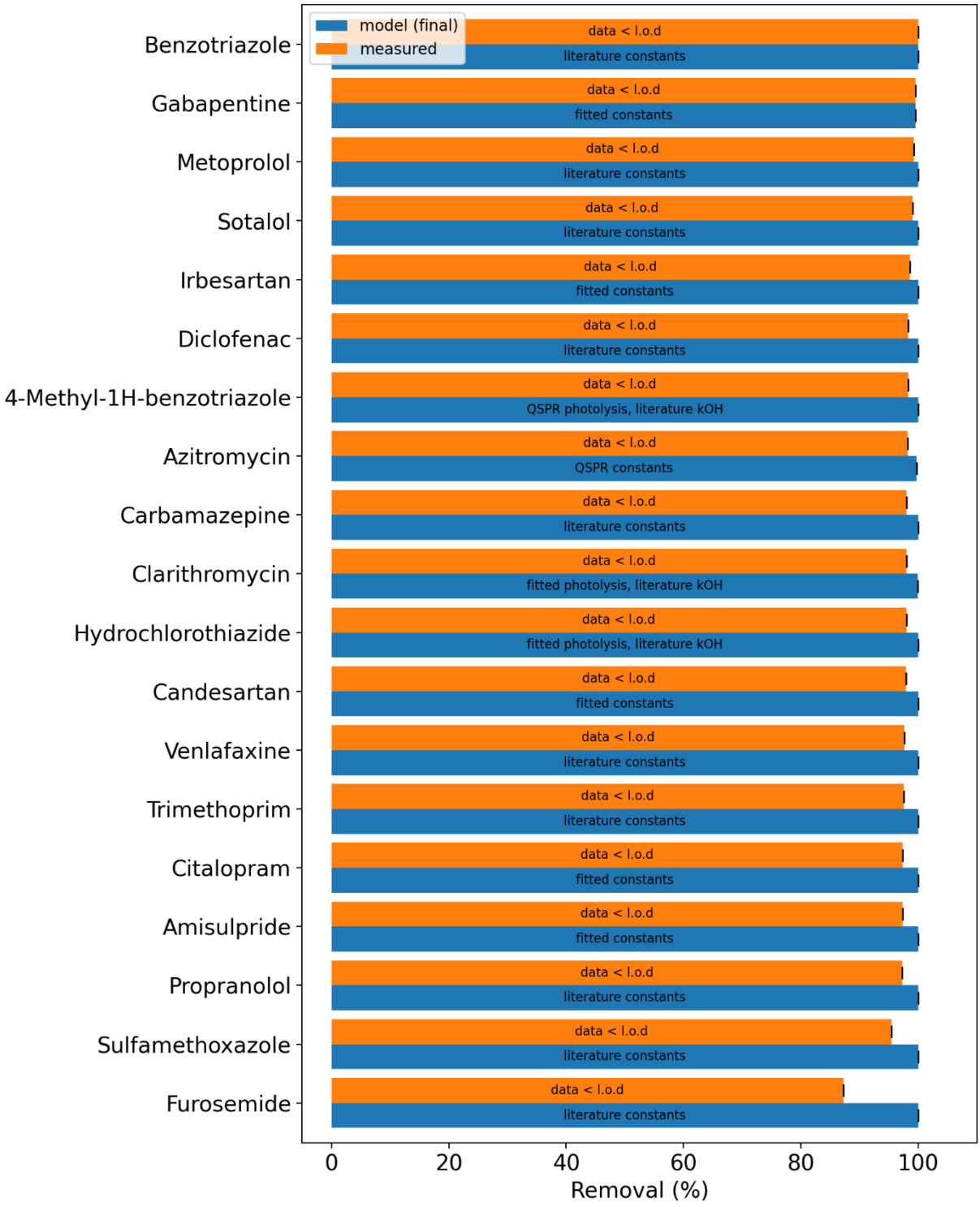

Ozone pilot experiments

Ozone pilot 6.8 mg/L O_3 (0.52 O_3/DOC) round 1 (without spike)

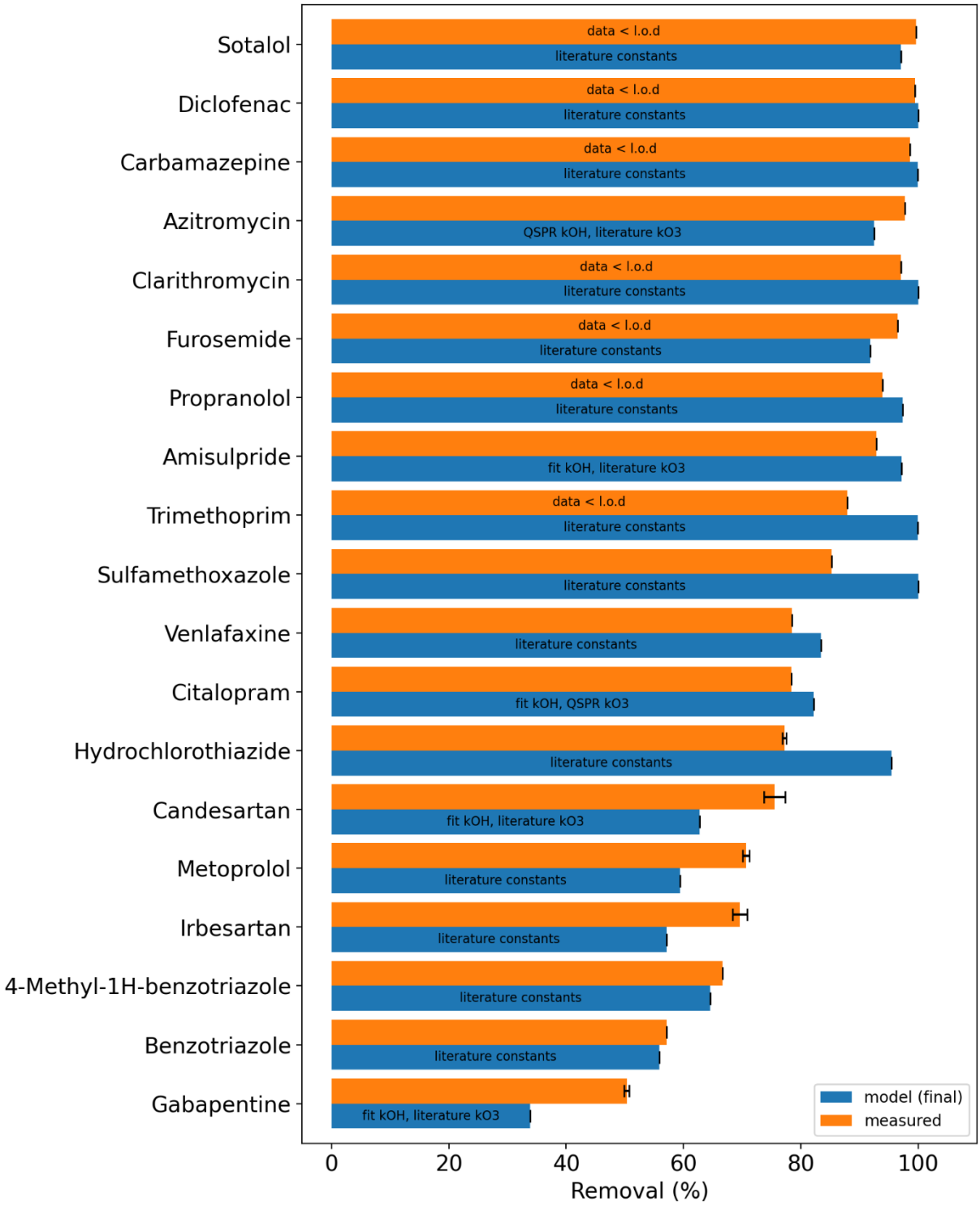

Ozone pilot 3.4 mg/L O_3 (0.26 O_3/DOC) round 1 (with spike)

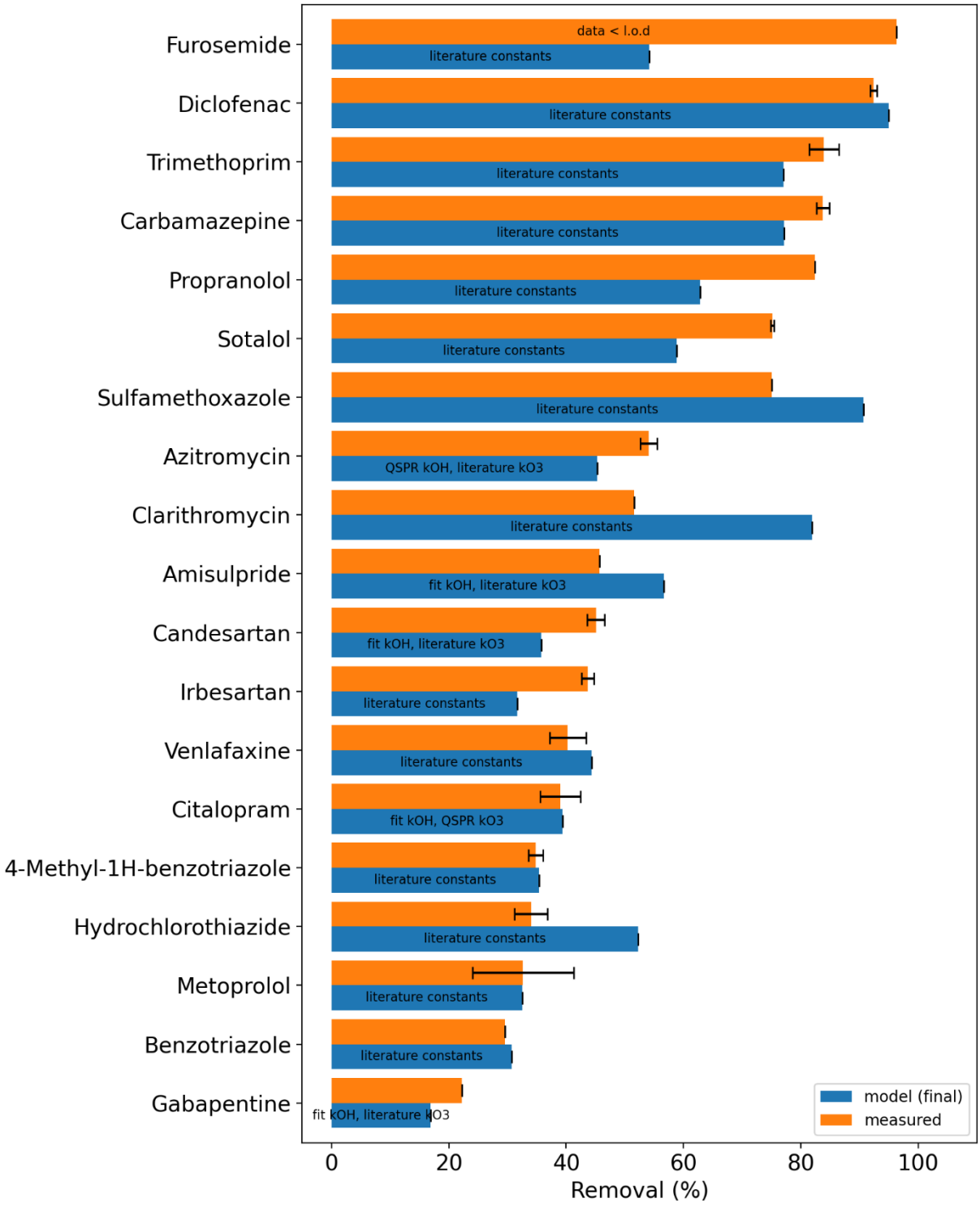

Ozone pilot 6.8 mg/L O_3 (0.53 O_3/DOC) round 1 (with spike)

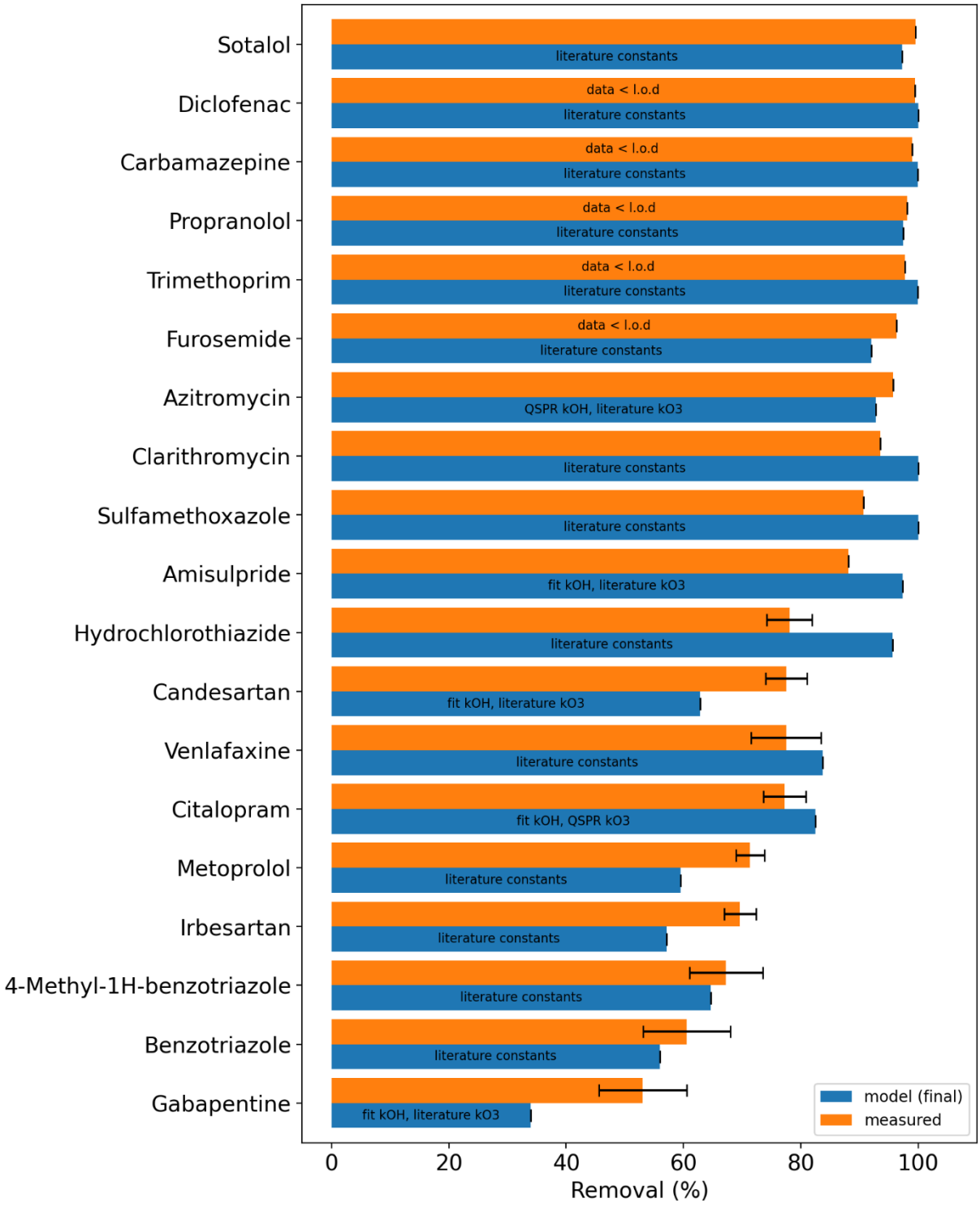

Ozone pilot 8.6 mg/L O_3 (0.66 O_3/DOC) round 1 (with spike)

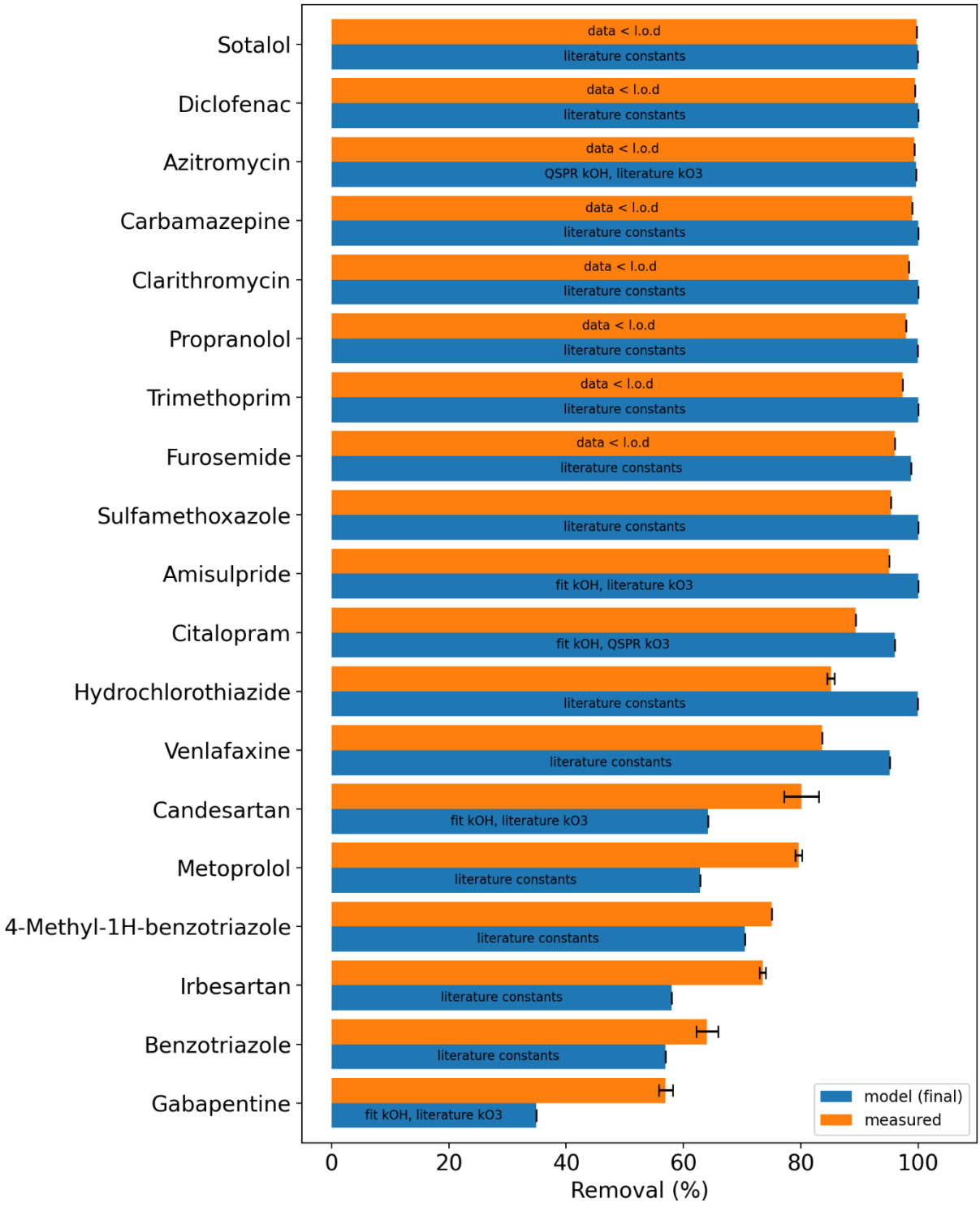

Ozone pilot 5.5 mg/L O_3 (0.55 O_3/DOC) round 2 (without spike)

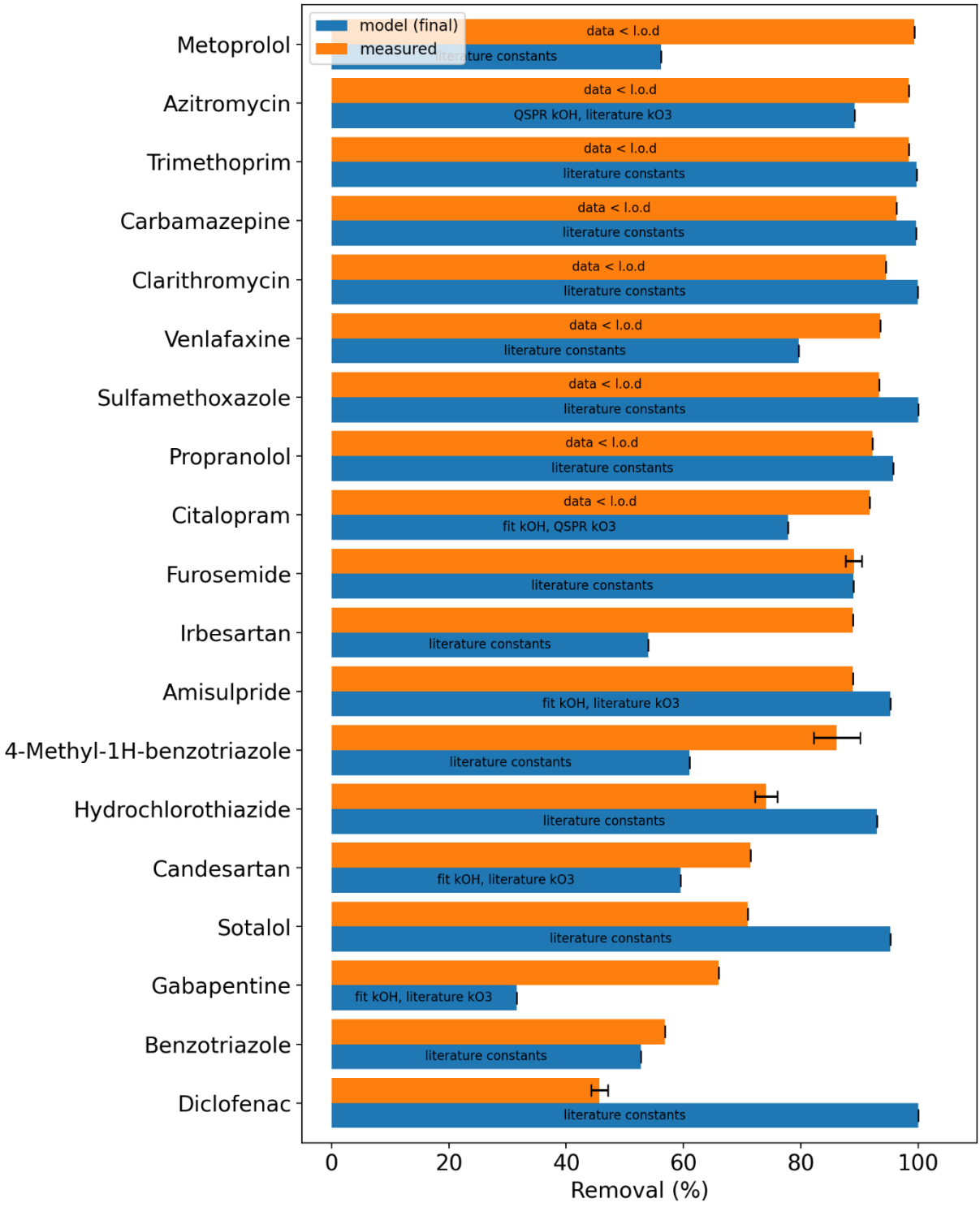

Ozone pilot 3.0 mg/L O_3 (0.30 O_3/DOC) round 2 (with spike)

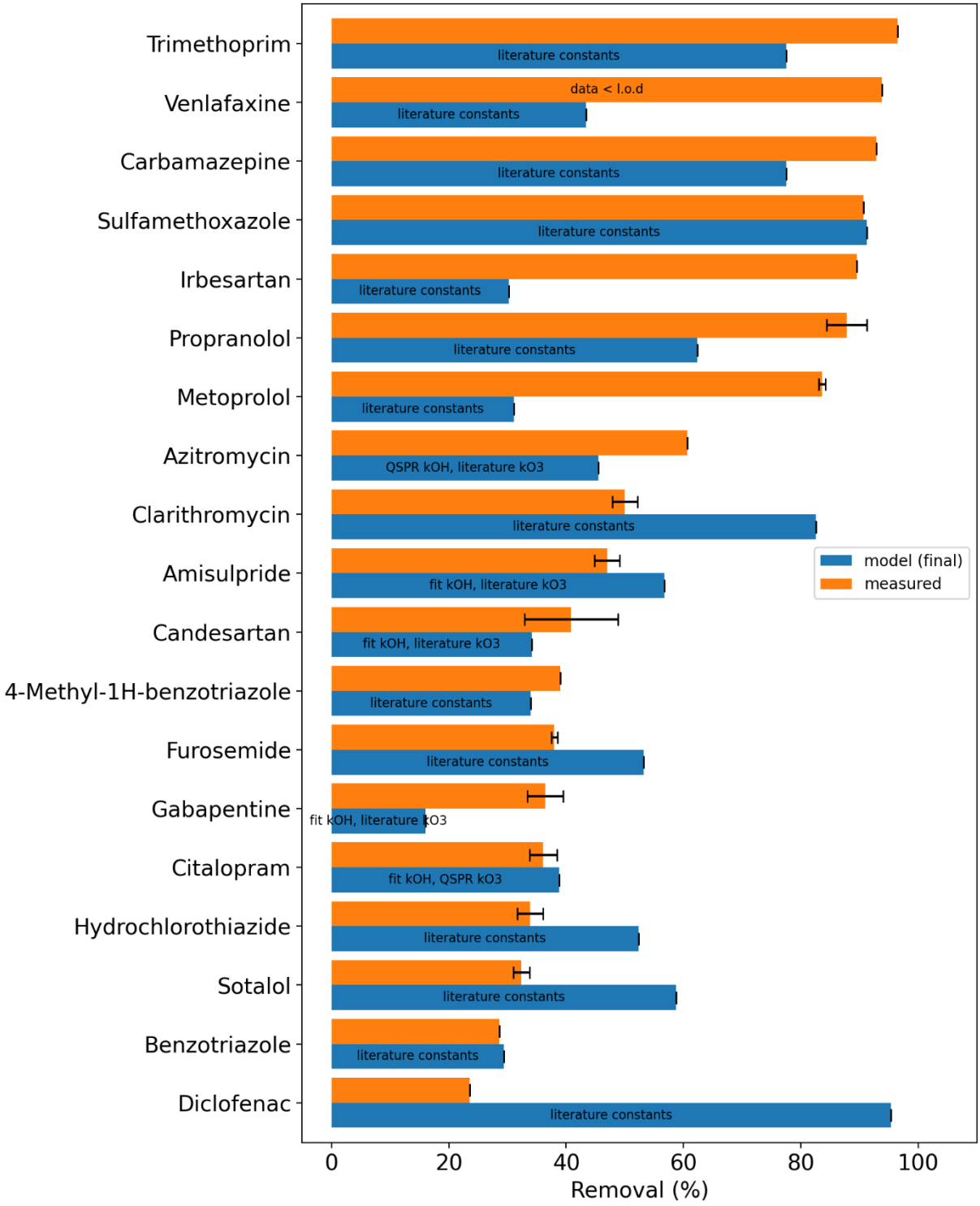

Ozone pilot 5.8 mg/L O_3 (0.58 O_3/DOC) round 2 (with spike)

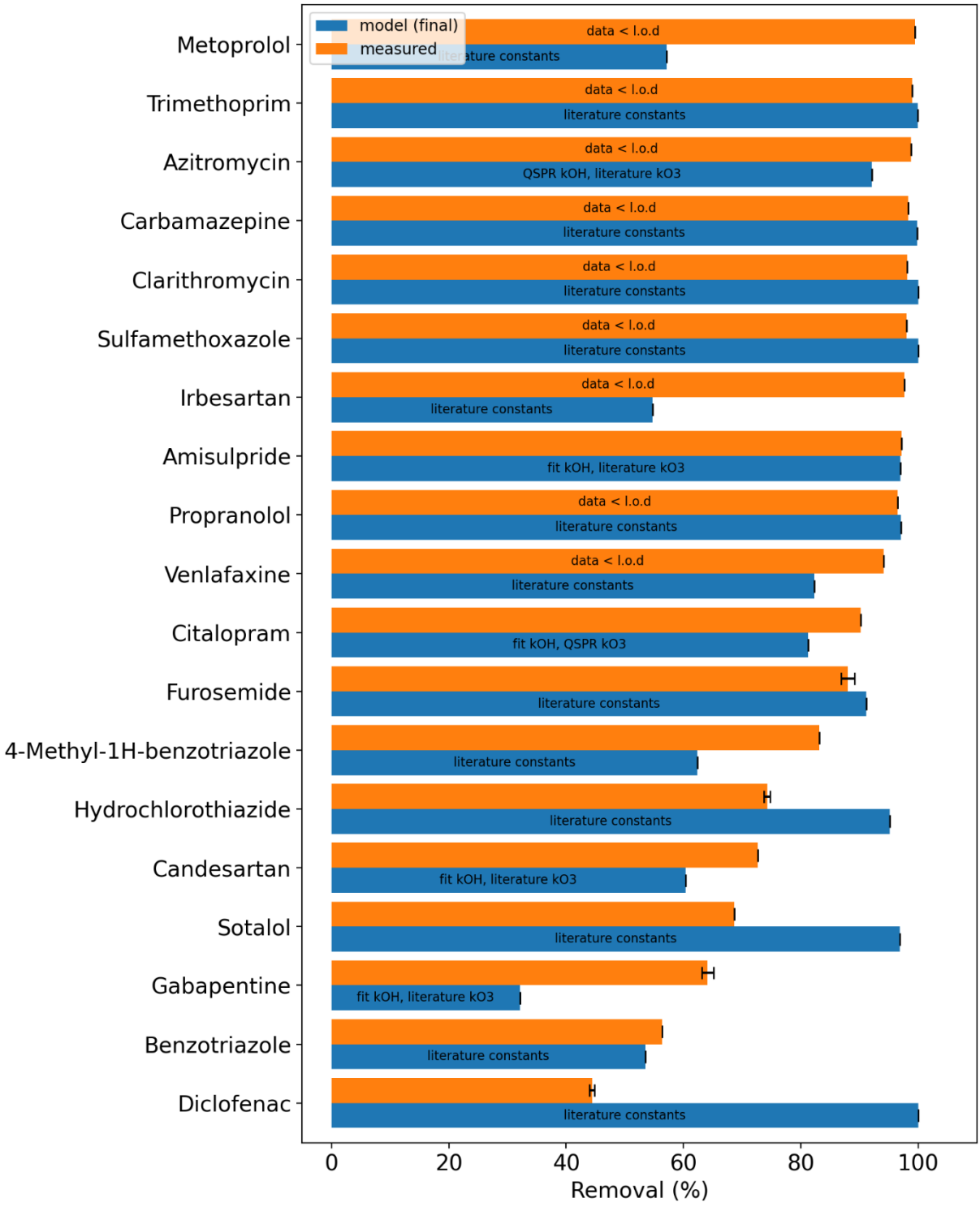

Ozone pilot 7.4 mg/L O_3 (0.74 O_3/DOC) round 2 (with spike)

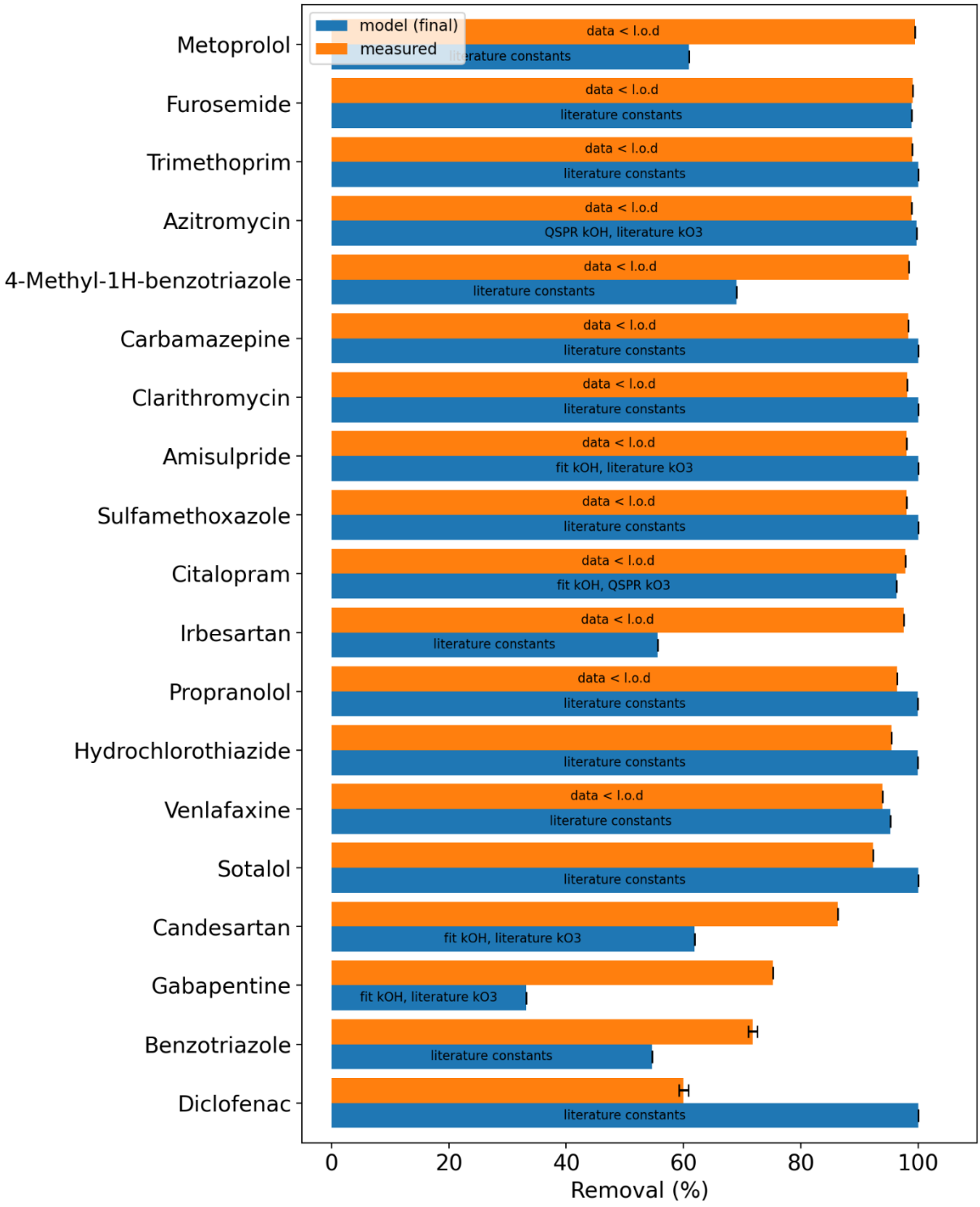

Ozone pilot 6.1 mg/L O_3 (1.10 O_3/DOC) round 3 (without spike)

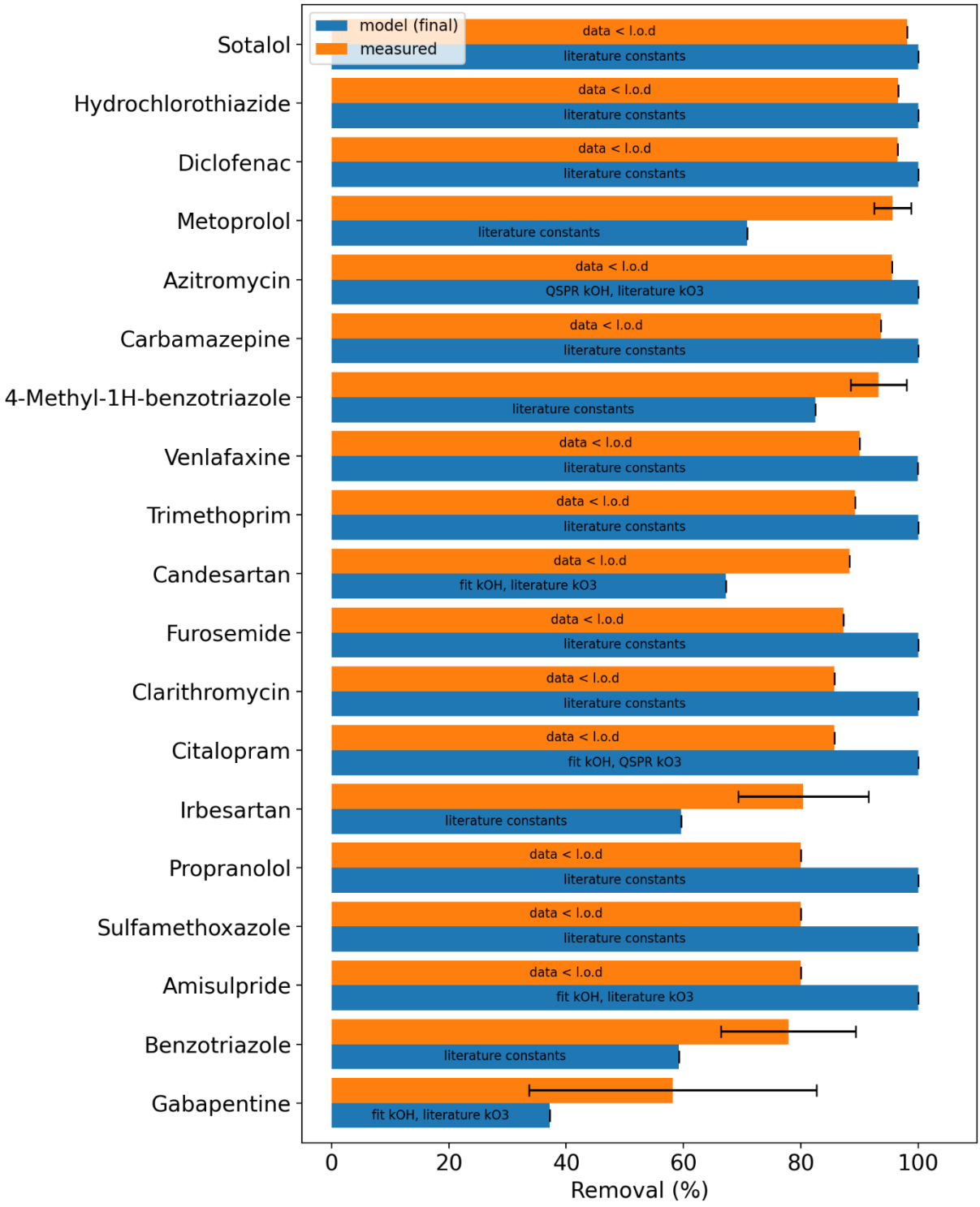

Ozone pilot 3.1 mg/L O_3 (0.56 O_3/DOC) round 3 (with spike)

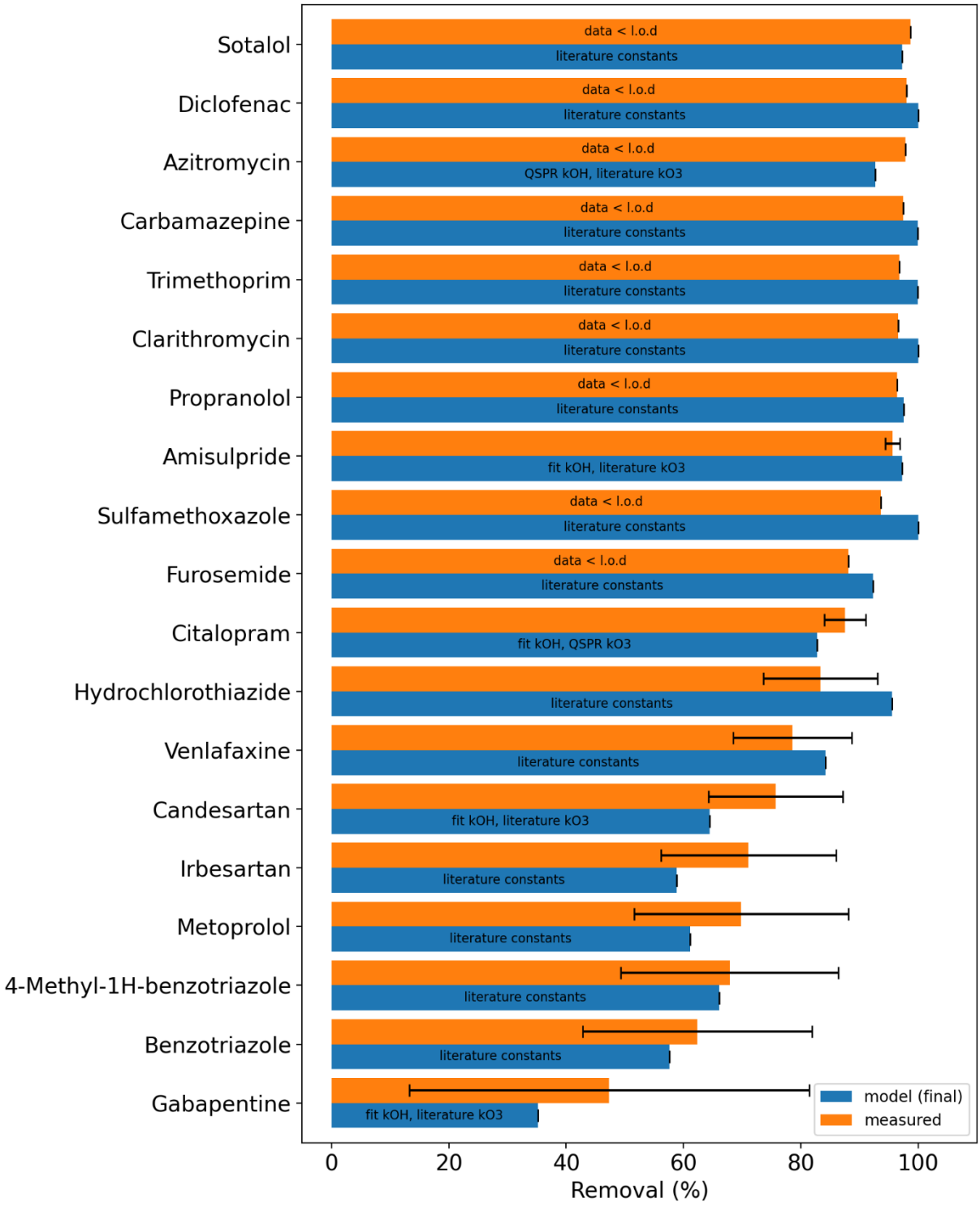

Ozone pilot 5.8 mg/L O_3 (1.04 O_3/DOC) round 3 (with spike)

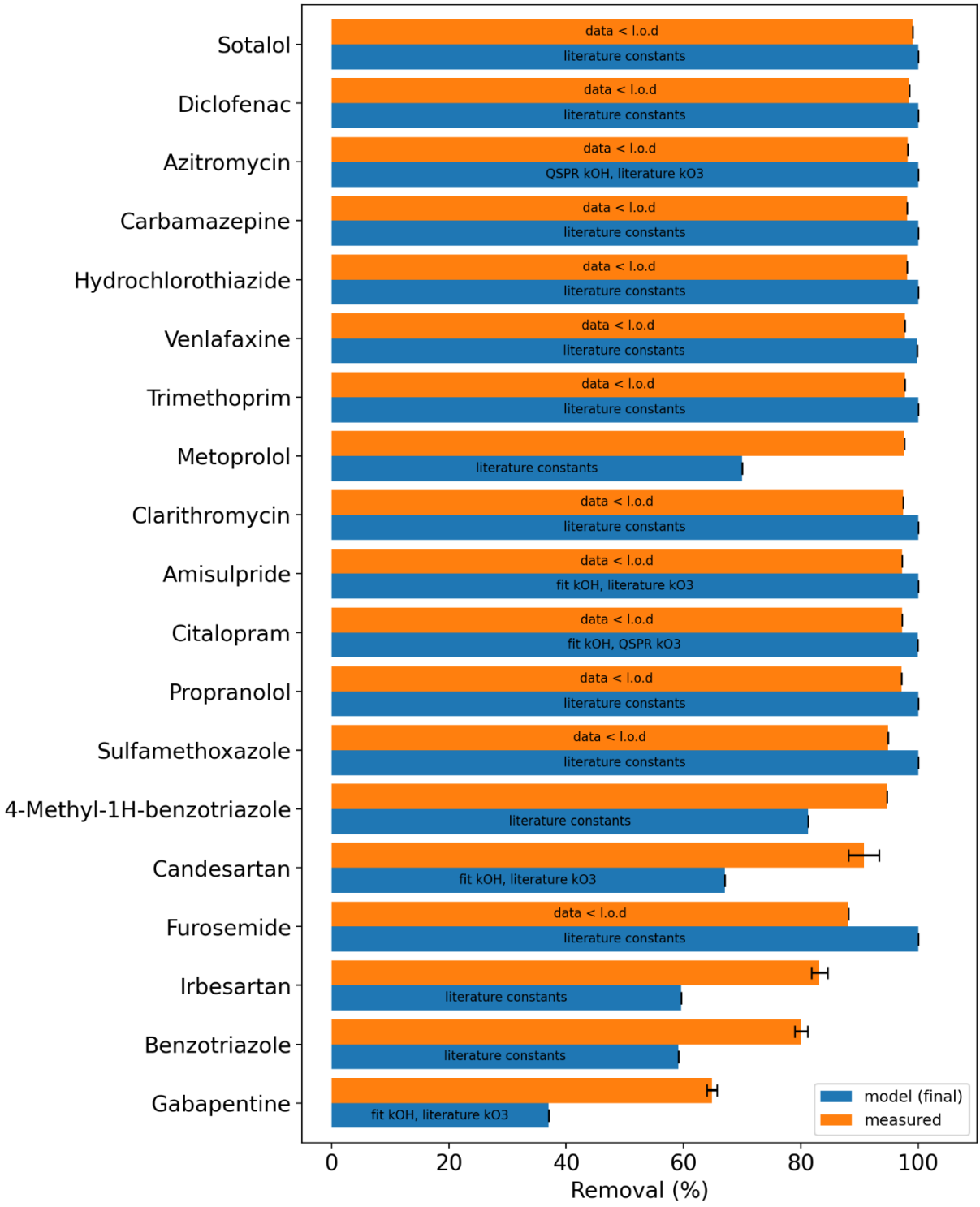

Ozone pilot 5.5 mg/L O_3 (0.98 O_3/DOC) round 3 (with spike)

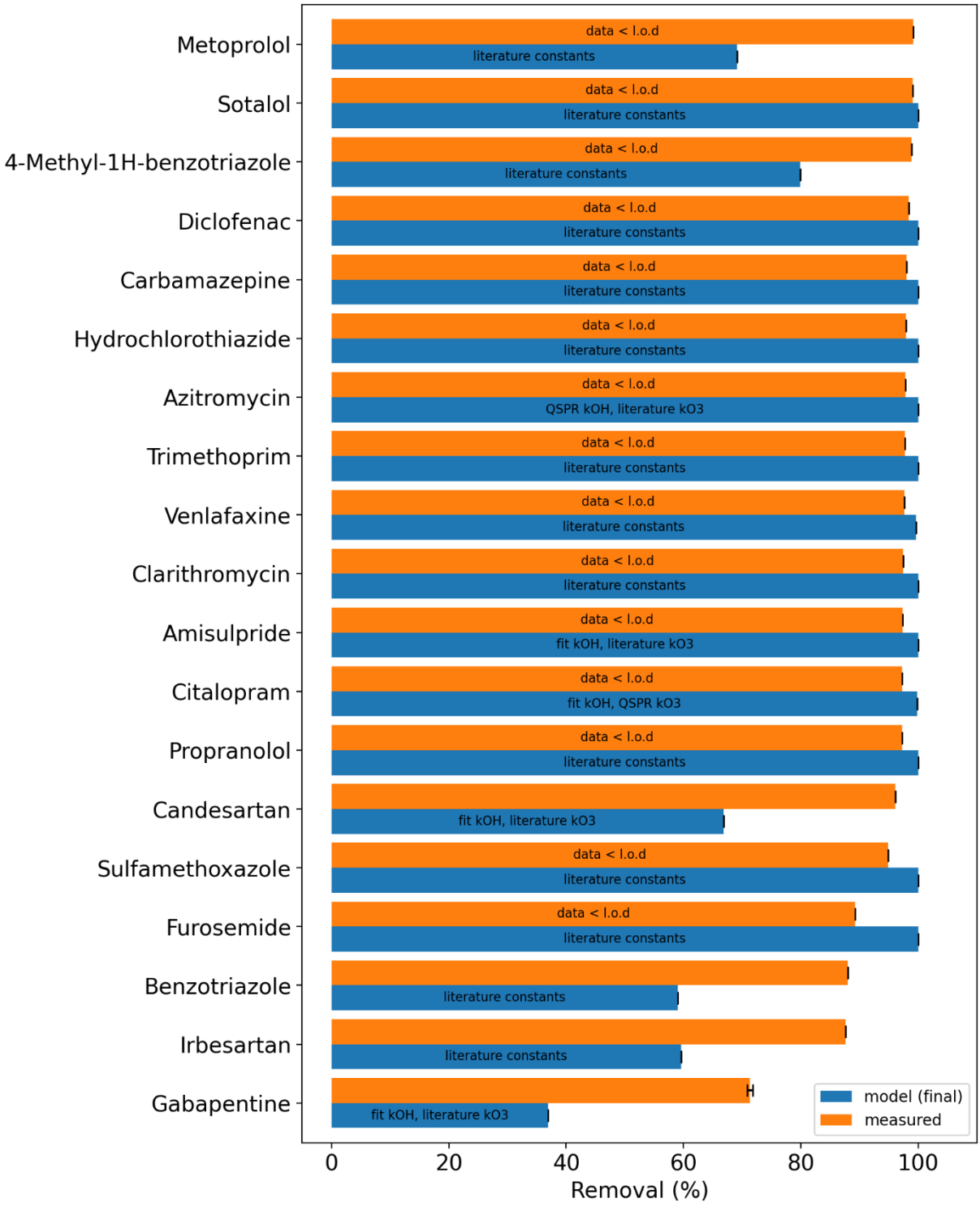

Ozone pilot 5.4 mg/L O_3 (0.90 O_3/DOC) round 4 (without spike)

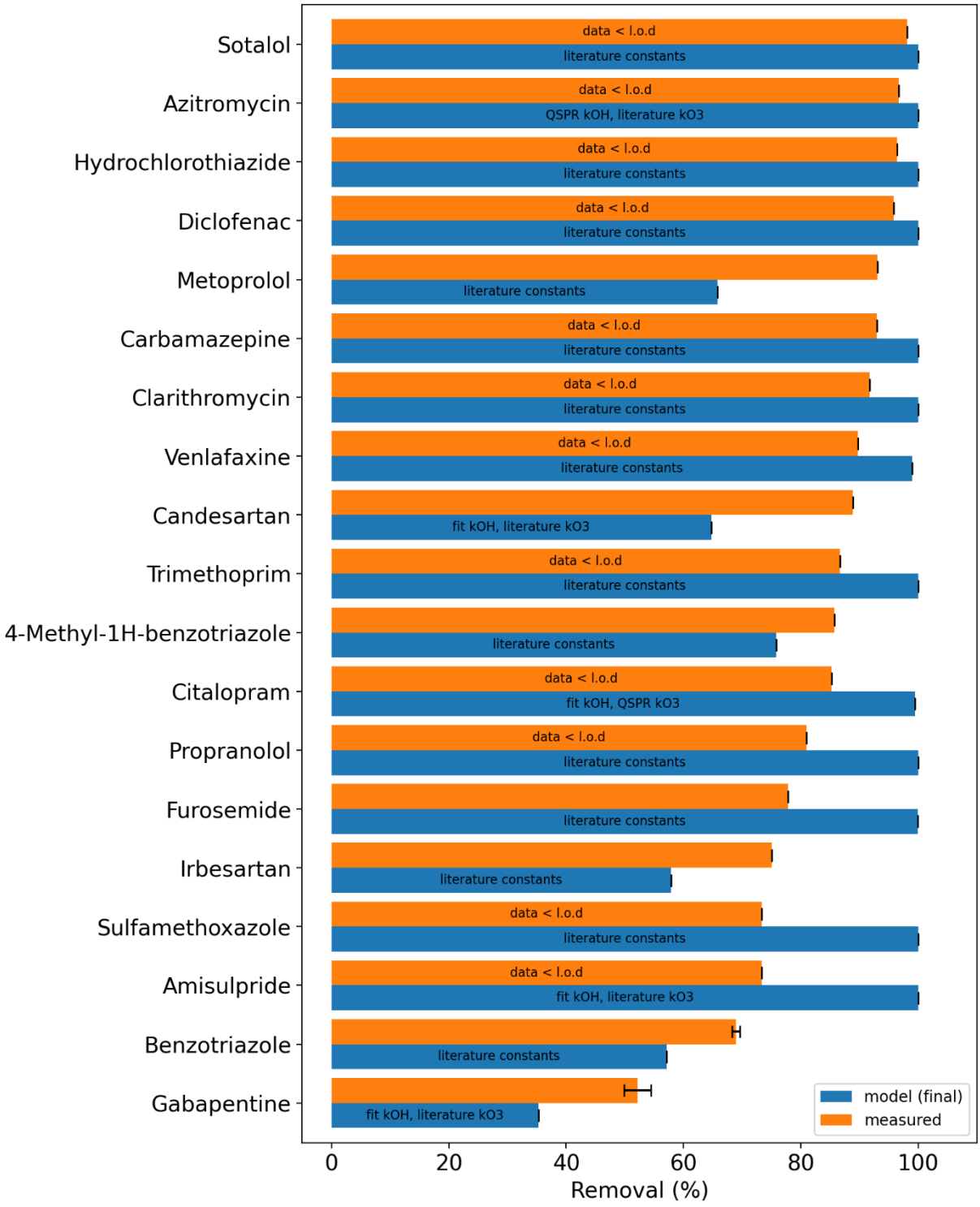

Ozone pilot 3.1 mg/L O_3 (0.52 O_3/DOC) round 4 (with spike)

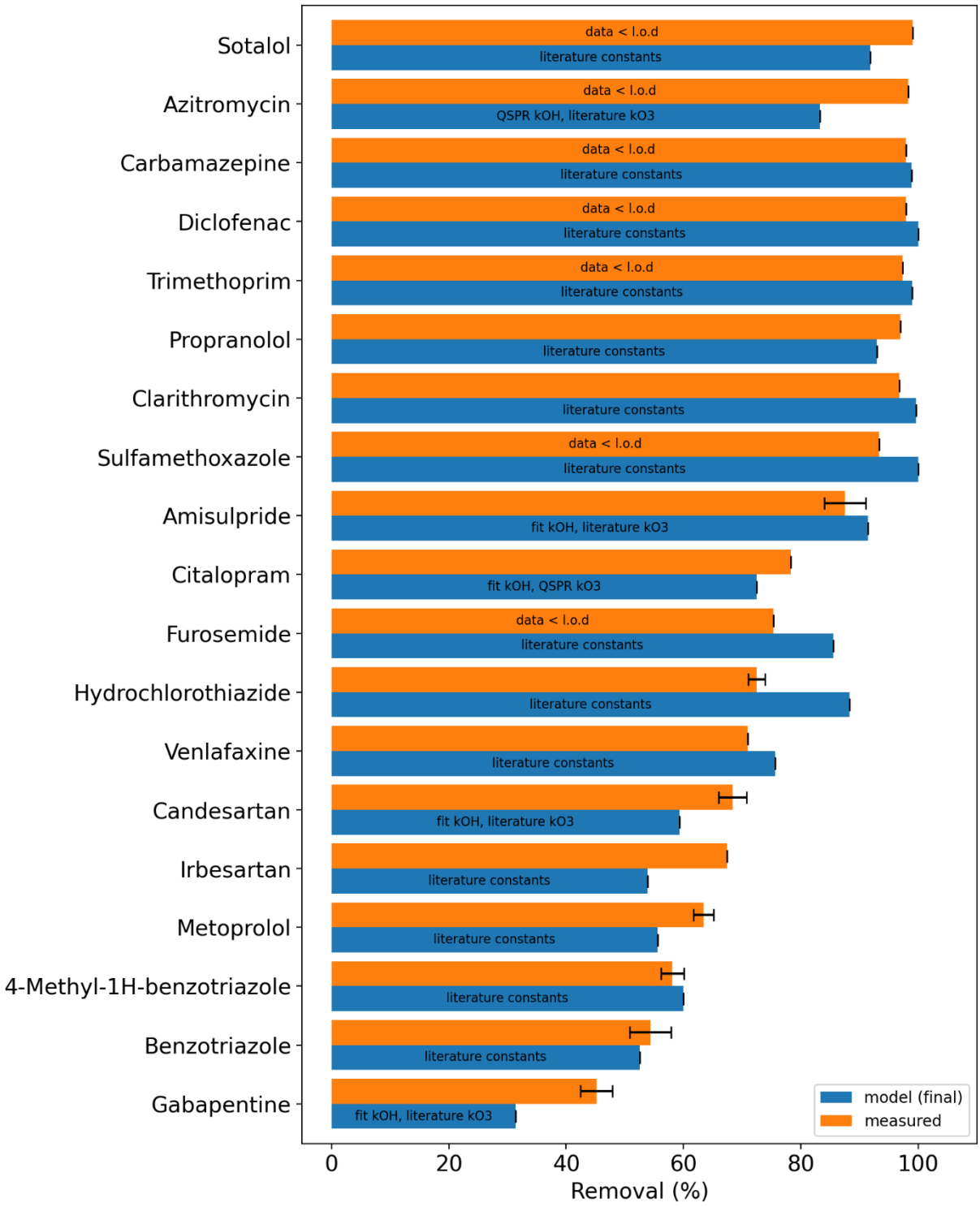

Ozone pilot 5.5 mg/L O_3 (0.92 O_3/DOC) round 4 (with spike)

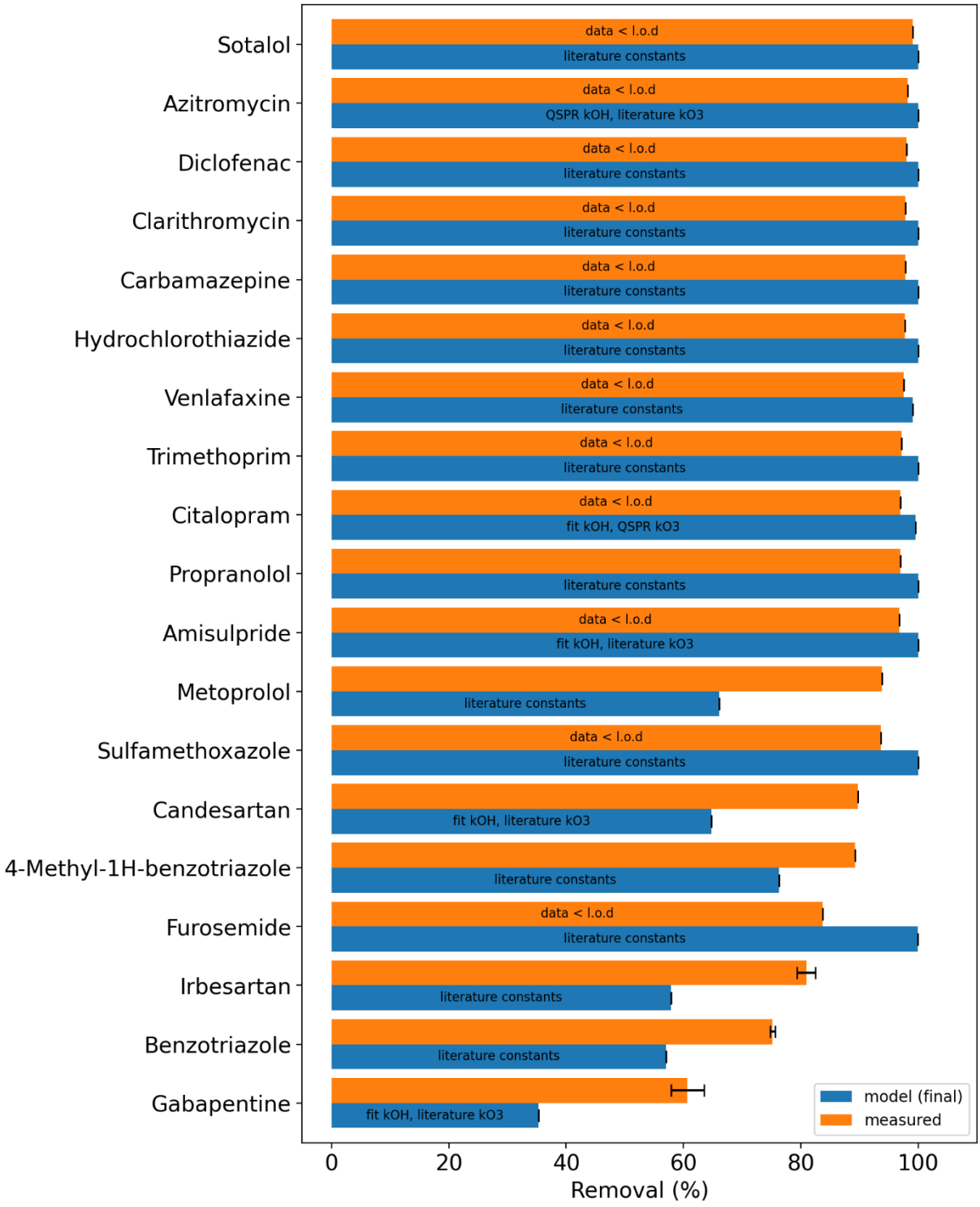

Ozone pilot 7.9 mg/L O_3 (1.32 O_3/DOC) round 4 (with spike)